Process development for upgrading low value α C8-olefin from Fischer-Tropsch to 2-hexyl-nonanal

by

Simbarashe Fidelis Denhere (BEng. Chemical)

Thesis presented in partial fulfilment
of the requirements for the Degree

of

MASTER OF ENGINEERING
(CHEMICAL ENGINEERING)

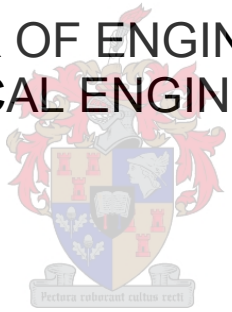

in the Faculty of Engineering
at Stellenbosch University

Supervisor

Dr. Percy Van der Gryp

Co-Supervisor/s

Professor Manie Vosloo

December, 2016

DECLARATION

By submitting this thesis electronically, I declare that the entirety of the work contained therein is my own, original work, that I am the sole author thereof (save to the extent of explicitly stated), that reproduction and publication thereof by Stellenbosch University will not infringe any third party rights and that I have not previously in its entirety or in part submitted for any publication.

Signature:……..

S. F Denhere,

Date:……

ABSTRACT

A wide variety of specialty chemicals are now available from technology based on the olefin metathesis reaction. This versatile reaction allows the conversion of simple, relatively inexpensive olefins into specialty, high-purity olefins which are useful intermediates in the fragrance, agricultural, and many other specialty chemical industries.

Literature has shown that low value (C5-C9) olefins produced from a Fischer-Tropsch reaction can be used as important feedstocks for the manufacture of high value, detergent range linear internal alkenes (C10-C18). These detergent range internal alkenes could then be subsequently functionalised during hydroformylation to asymmetric aldehydes, which can be used as intermediates for manufacturing *Guebert-type* surfactants. The *DST-NRF Centre of Excellence in Catalysis* (change) have investigated the efficacy of homogeneous catalysts towards upgrading low value, unique olefinic feedstocks from a Fischer-Tropsch product stream through the RSA Olefins programme. The homogeneous catalysts are reported to be highly selective and reactive but are not employed industrially because they are expensive and decompose as the high boiling products are distilled from the reaction medium. Hence, the RSA Olefins programme of the *DST-NRF Centre of Excellence in Catalysis* has been active in developing organic solvent nanofiltration (OSN) membrane technology to allow for efficient separation and subsequent recycling of the homogeneous catalysts.

Using literature sources and industrial catalogues, an initial screening of catalyst systems was done to select candidate catalytic systems for the metathesis of low value 1-octene (C8) and the subsequent hydroformylation of 7-tetradecene (C14) to detergent range products. The criteria such as catalyst cost, selectivity (product distribution), turnover number (TON) together with economic potential (*EP)* values determined at five levels of design were used to develop candidate processes using the Douglas hierachichal method. The Hoveyda-Grubbs 2 **(HGr-2)** precatalyst and water-soluble **Rh-TPPTS** were selected for the metathesis of 1-octene and

hydroformylation of 7-tetradecene respectively. Two process scenarios A (liquid multiphase system) and B (OSN membrane) were developed and evaluated using a techno-economic analysis (TEA) model. The viewpoints of design and performance were developed by integrating the technical and economic information through Aspen Plus™ process simulation and sensitivity analysis of the key operating parameters. The goal was to detect promising process concepts as early as possible and to single out the crucial parameters such that experimental and modelling work can be focused on those alternatives that most likely will lead to an economic process.

The discounting cash flow (DCF) method was used to evaluate the two process scenarios A (liquid multiphase system) and B (OSN membrane process) producing 10 000 tonnes per annum of 2-hexyl-nonanal at a purity of 99 wt. %. The feedstock to be used is low value 1- octene a Fischer-Tropsch Synthol product stream. The performance criterion is to maximise the net present value (NPV) of the process. The NPV included revenues, total capital investment and depreciation costs was determined based on interest rate of 15 % and the lifetime of 15 years. Economic parameters such as internal rate of return (IRR %) and payback period (PBP) were calculated for each scenario. The results were then used to determine the configuration with the most favourable economic indicators. The two process scenarios studied proved to be profitable with IRR % ranging between 58 % and 83 % with scenario B having the highest NPV and IRR %. The NPV for scenario A and scenario B were $ 439 M and $ 563 M respectively at the end of project life of 15 years. The IRR % for process scenario A was 59 % compared to scenario B of 83 % for the same pay back period of 3 years. Sensitivity analysis were performed on the two process scenarios. The parameters investigated were: 2-hexyl-nonanal selling price; **Rh-TPPTS** catalyst cost; 1-octene feed cost; **HGr-2** catalyst cost and tax rate %. Their impact on NPV and IRR % was evaluated. Curve diagrams were constructed to illustrate the effect of variation of different cost parameters on NPV and IRR %. The most effective input variables for the two process scenarios were 2-hexyl-nonanal selling price, **Rh-TPPTS** and **HGr-2** catalyst cost on both NPV and IRR. The

process scenario B which considers OSN membrane technique for catalyst recovery was the most profitable configuration and the NPV was 22 % better than the liquid multi phase system.

Keywords: Low value olefins, metathesis, hydroformylation, functionalized hydrocarbons, OSN membrane, techno-economic evaluation, DCF, NPV, IRR %.

OPSOMMING

Proses ontwikkeling vir die opgradering van lae waarde alpha-C8 olefiene vanaf die Fischer-Tropsch proses na 2-heksiel nonaal.

'n Groot verskeidenheid gespesialiseerde chemikalieë is hedendaags beskikbaar te danke aan tegnologie wat gebaseer is op die olefiene-metathesis reaksie. Hierdie veelsydige reaksie laat die omskakeling van eenvoudige en relatief goedkoop olefiene toe na meer gespesialiseerde, suiwer olefiene. Hierdie meer gespesialiseerde olefiene, is bruikbare oorbrugging chemikalieë vir die parfuum, landbou en verskeie ander chemiese industrieë.

Literatuur wys daarop dat lae-waarde (C5-C9) olefiene, wat geproduseer word vanaf die Fisher-Trospch reaksie, gebruik kan word as belangrike roumateriale vir die vervaardiging van waardevolle, lineêre interne skoonmaakmiddel-reeks alkene (C10-C18). Hierdie reeks internerne skoonmaakmiddel alkene, kan gevolglik gefunctionaliseer word tydens hidroformilasie tot asimmetriese aldehiede, wat gebruik kan word as intermediêre middels vir die vervaardiging van *Geubert*-tipe benatters. Die doeltreffendheid van homogene katalisators om lae waarde, unieke olefiene voerstowwe van die Fischer-Tropsch synthol produkstroom op te gradeer, is ondersoek deur die olefiene program *DST-NRF Centre of Excellence in Catalysis*. Dit word gerapporteer dat die homogene katalisators hoogs selektief asook reaktief is, maar dat dit nie industrieel in werking gestel word nie, omdat dit baie duur is en ontbind tydens die distillasie proses, wanneer die produkte gedistilleer word vanaf die reaksie medium. Daarom is die olefiene program van die *DST-NRF Centre of Excellence in Catalysis* aktief besig om organiese oplosmiddel-nanofiltrasie (OSN) membraan tegnologie te ontwikkel, wat effektiewe skeiding en daaropvolgende herwinning van die homogene katalisator, toe te laat.

'n Aanvanklike keuring van katalisators is gedoen, om kandidaat katalisator sisteme te identifiseer deur die gebruik van literatuur bronne en industriële katalogusse, vir die metatesis van lae waarde 1-okteen (C8) en daaropvolgende hidroformilasie van skoonmaakmiddels

7-tetradekeen (C14) produk alkene. Katalisator koste, selektiwiteit (produk distribusie), *TON* tesame met *EP* waardes (teen 5 ontwerpsvlakke) is gekies vir die kriteria om katalisator sisteme te skep. Hierdie sisteme is geskep deur die hiërargiese metode soos gestipuleer in Douglas (1988). **HGr-2** voor-katalisator en water oplosbare **Rh-TPPTS** was gekies vir die metatesis van 1-okteen en daaropvolgende hidroformilasie van 7-tetradekeen, onderskeidelik. Twee proses scenario's, scenario A (vloeistof multi-fase sisteem) en scenario B (OSN membraan) was ontwikkel en deur 'n tegno-ekonomiese analise (TEA model) te ondersoek. Die ontwerp en prestasie oogpunte was ontwikkel deur die tegniese en ekonomiese inligting in die simulasie program (Aspen Plus™) te integreer, asook deur die sensitiwiteitsanalises van die kern bedryf parameters. Die doel was om belowende proses konsepte so vroeg as moontlik te identifiseer, en dus ook die kern parameters, sodat eksperimentele en modelleringswerk só opgestel kon word om te lei na die mees belowende ekonomiese prosesse.

Die verdiskontering kontantvloei (DCF) metode was gebruik om die twee proses scenario's, A (vloeistof multifase sisteem) en B (OSN membraan proses), te evalueer teen 10 000 ton per jaar 2-heksiel-nonanal, met 'n massa suiwerheid van 99% vanaf die lae waarde 1-okteen Fischer-Tropsch Synthol produkstroom. Die Ekonomiese parameters, soos die internerne opbrengskoers (IRR %), terugbetalingstydperk (PBP) en netto huidige waarde (NPV), was bereken vir elke scenario. Die resultate is gebruik om die opset met die mees gunstige ekonomiese aanwysers te bepaal. Dit is gevind dat die twee proses-scenario's (A en B), ekonomies gunstig is, met IRR % waardes wat varieer tussen 58 en 83%. Scenario B het die hoogste NPV en IRR %. Die NPV vir scenario A en B, teen die einde van die 15 jaar projek lewe, was $ 439 M en $563 M onderskeidelik. Die IRR % vir proses scenario A was 59 % in vergelyking met scenario B wat 83 % was vir dieselfde terugbetalingstydperk van 3 jaar. Die twee proses-scenario's het ook sensitiwiteitsanalises ondergaan. Die parameters wat ondersoek is sluit die verkoopsprys van 2-heksiel-nonanal, **Rh-TPPTS** katalisator koste, 1-okteen voerstof koste, **HGr-2** katalisator koste en rente koerse % in. Die impak van die verkeie

parameters op die NPV en IRR % is ondersoek. Kurwe diagramme is opgestel om die invloed van die verskillende parameter kostes op die NPV en IRR % parameters aan te dui. Die mees doeltreffende inset veranderlikes vir die twee proses scenario's was die verkoopsprys van 2-heksiel-nonanal en die prys van die Rh-TPPTS en HGr-2 katalisators op die NPV en IRR % parameters. Proses scenario B, wat die OSN membraan tegniek insluit vir katalisator herwinning, is gevind om die mees ekonomiese winsgewende opset te wees. Die NPV was 22 % beter as scenario A, wat die multifase sisteem gebruik het.

Sleutelwoorde: Lae waarde olefiene, Metatesis, Hidroformilasie, gefunksionaliseerde koolwaterstowwe, OSN membraan, Tegno-ekonomiese evaluasie, DCF, NPV, IRR %

ACKNOWLEDGEMENTS

To God be the honour, glory and praise!

I would like to appreciate the following individuals and organisations for their assistance and support.

First, Dr. Percy Van der Gryp and Professor Manie H.C Vosloo for their assistance and feedback in preparing this work.

The DST-NRF *Centre of Excellence in Catalysis* (c*change) and Stellenbosch University for their financial support in this project. I would also like to thank the Catalysis Society of South Africa (CATSA) for allowing me a myriad of opportunities to present my research at various academic forums.

Upon completion of this study, I would like to acknowledge several individuals without whom this work would not have been possible:

- Dr Mandeguiri for his generosity and kindness assistance with Aspen Plus™.
- Dr Marco Haumann from Technical University of Berlin for his insights into hydroformylation
- Dr David Muller from Technical University of Berlin for insights into catalyst recovery systems and product separation
- Dr. Frans Marx from North-West University and Professor Eric Van Steen from University of Cape Town fruitful discussions.
- My colleagues and friends at Stellenbosch University.

Finally, to Precious my fiancé who changed my life and has been supportive ever since.

TABLE OF CONTENTS

LIST OF ABBREVIATIONS

Abbreviation	Description
2-HN	2- hexyl-nonanal
APEA	Aspen Process Economic Analyser
CAPEX	Capital Expenditure
DCF	Discounted Cash Flow
EC	Equipment Cost
EPM	Economic Potential for metathesis process
EPH	Economic Potential for hydroformylation process
EOS	Equation of State
FT	Fischer-Tropsch
IRR	Internal Rate of Return
LKP	Lee-Kesler-Plocker
LMS	Liquid Multiphase System
LPO	Low Pressure Oxo-process
NPV	Net Present Value
NRTL	Non-Random Two-Liquid
OSN	Organic Solvent Nanofiltration
PBP	Pay Back Period
PC-SAFT	Perturbed Chain Statistical Associating Fluid Theory
PR	Peng-Robinson
PRBM	Peng-Robinson- with Boston-Mathias
RCH	Ruhrchemie
RCH/RP	Ruhrchemie Rhone-Poulenc Process
RKSBM	Redlich-Kwong-Soave with Boston-Mathias
RKS	Redlich- Kwong-Soave

SARS	South African Revenue Services
SRK	Soave-Redlich-Kwong
TEA	Techno economic analysis
TDC	Total Direct Costs
TFCI	Total Fixed Capital Investment
UNIFAC	UNIQUAC Functional-group Activity Coefficients
UNIQUAC	UNIversal QUAsiChemical

NOMENCLATURE

Symbol	Description	Unit
S	Percent selectivity	%
X	percentage conversion	%
Y	percentage yield	%
W_{cat}	Weight of catalyst	g
PMP	primary metathesis products	-
IP	Isomerisation products	-
SMP	secondary metathesis products	-
Gr-2	Grubbs second generation catalyst	
Gr-1	Grubbs first generation catalyst	-
TMS	Thermomorphic multicomponent solvent	-
TPPTS	Trisulfonated triphenylphosphine	
RRP	Ruhrchemie-Rhone-Poulenc process	-
DMF	dimethylformamide	-
Syngas	synthesis gas (CO+ H_2)	-
PC-SAFT	Perturbed chain statistically associating fluid theory	
n-Aldehydes	normal aldehydes	-
iso-Aldehydes	isomeric aldehydes	-
Subscripts		
C8	octene	-
C9	nonene	-
C10	decene	-
C11	undecene	-
C12	dodecene	-
C13	tridecene	-
C14	tetradecene	

CHAPTER 1: INTRODUCTION

"When you don't know where you are going all roads will take you there"

Yiddish Proverb

Overview

Chapter 1 gives an introduction to the work carried out to solve the challenge of upgrading low value olefins from a Fischer-Tropsch Synthol product stream to Guerbet-type surfactants. The chapter is subdivided into four sections namely; Section 1.1 (discusses the background and motivation towards development of this work), Section 1.2 (objectives set out to map direction towards the solution to this challenge), Section 1.3 (gives an outline of the scope of this work) and finally, Section 1.4 (an outline of the thesis).

1.1 Background and motivation

The DST-NRF Centre of Excellence in Catalysis (c*change) RSA Olefins program is focused primarily on upgrading low value olefins (C5-C9 alkenes) from a Fischer-Tropsch product stream to detergent range long chain internal alkenes (C10-C18). These alkenes can then be functionalized and subsequently converted to surfactants of the Guerbet-type, a specialty chemical. Guerbet-type alcohols are normally synthesized through a 4-step process, oxidation of alcohol to aldehyde, aldol condensation, dehydration of the aldol product and hydrogenation of the allylic aldehyde (Lubrizol Advanced Chemical, 2012). The reactions selected to achieve these conversions are the homogeneous self-metathesis of shorter chain 1-alkenes to long chain internal alkenes followed by the hydroformylation of the internal alkenes into aldehydes (Figure 1.1). According to Mills and Chaudhari (1997), Guerbet-type aldehydes typically serve as intermediates and building blocks for alcohols, other derivatives, which have applications in pharmaceuticals, fine chemicals and perfumery chemicals.

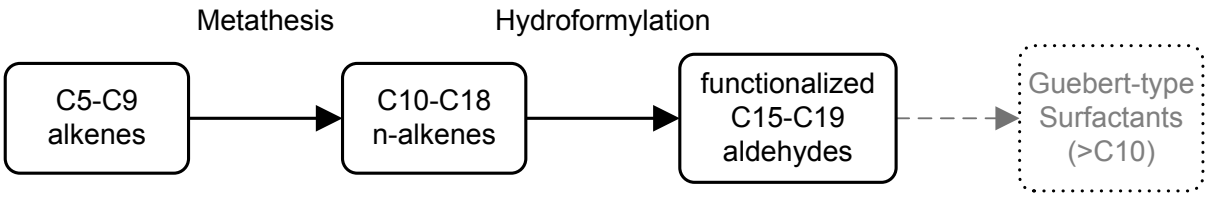

Figure 1.1.: Proposed upgrading of low value olefins to high value surfactants

Challenges of separation of homogeneous catalysts from their post reaction mixtures particularly due to low thermal stability of the metal-based complexes have been reported in literature (Maynard and Grubbs, 1999, Sharma and Jasra, 2015). These challenges have been identified as a major hindrance towards commercialization of such processes. Losses as low as 1 ppm have been reported in previous hydroformylation studies but economics depends on quantity of Rh loss and cost of metal (Sharma, 2008). The leaching of 1 ppm Rh during 1-octene hydroformylation in a 400 000 ton per year plant may result in the financial loss of

US $ 500 000 per year (Wiese and Obst, 2006). According to Sharma (2008), a loss of 1 ppm Rh for 100 000 tons per year plant will result in a loss of US $ 400 000 per year.

In many catalytic transformations, the post-treatment of the reaction product for catalyst/product separation is an important concern in particular when products formed have higher boiling points (Huang et al., 2015). The higher boiling point of these products means higher temperatures for their volatilization, hence separation problems due to the narrowing differences in product and catalyst solution volatilities (Schmidt et al., 2014). More importantly, the catalyst's thermal stability range is encroached at these higher distillation temperatures and degradation significantly increases (Beller et al., 1995, Dreimann et al., 2015). Irreversible destruction of the sensitive catalyst during thermal separation of the reaction products is a serious challenge towards catalyst recycle (Wiese et al., 2006). Michrowska and Grela (2008) identified finding a subtle balance between the stability of the catalyst, and its high activity as one of the "Holy Grails" of catalysis. The challenge is especially visible in the field of olefin metathesis, a fairly old reaction that has long remained a laboratory curiosity without significance for advanced organic chemistry (Michrowska and Grela, 2008). According to Westhus et al. (2004), removal of the metal-containing by-products upon completion of the metathesis reaction is a serious drawback which affects subsequent synthetic reactions.

The low reactivity of long chain olefins due to poor solubility in aqueous catalyst media have also been identified as a major challenge in aqueous rhodium-catalyzed hydroformylation processes (Herrmann and Cornils, 1997; Haumann et al., 2002a; Haumann et al., 2002b; Porgzeba et al., 2015; Hentschel et al., 2014; Muller et al., 2013; Muller et al., 2014; Muller et al., 2015; Zagajewski et al., 2016). Herrmann and Cornils (1997) have reported that the solubility of propylene in water is 1 000 times more than that of 1-octene. According to Haumann et al. (2002b), the reactivity of linear terminal alkenes is about four times that of linear internal alkenes e.g. 7-tetradecene.

Several novel techniques especially aimed at an efficient combination of reaction and catalyst separation have been reported for homogeneous metathesis and also hydroformylation of long chain olefins. Behr et al. (2007), Zagajewski et al. (2014), Brunsch and Behr (2013), Schafer et al. (2012) and Hentschel et al. (2014) propose thermomorphic multicomponent solvent systems (TMS) as a possible solution to reaction and catalyst separation in hydroformylation process. Muller et al. (2013), Muller et al. (2014), Haumann et al. (2002a) and Haumann et al. (2002b) have demonstrated successful application of liquid multiphase system (LMS) in Rh-catalyzed hydroformylation of long chain olefins. The use of organic solvent nanofiltration (OSN) membrane to recover homogeneous catalysts has been reported in literature (Bhanushali, 2002; Vankelecom et al., 2002; Schmidt et al., 2014). Bhanushali (2002) and Van der Gryp et al. (2012) have demonstrated the successful use of novel organic solvent nanofiltration (OSN) technique in separation and reuse of homogeneous Ru-based catalysts. Schmidt et al. (2014) and Seifert et al. (2013) have developed models to investigate OSN membrane technique as a potential solution towards reduction of Rh-catalyst losses during hydroformylation process.

According to the author's knowledge, no open source data or publication is currently available for a process of upgrading low value (C5-C9) olefins from a Fischer-Tropsch Synthol product stream to functionalized Guebert-type aldehydes. It is therefore the aim of this study to develop a conceptual process of upgrading low value terminal C8 from a Fischer-Tropsch Synthol product stream to 10 000 tonnes per annum 2-hexyl-nonanal at 99 wt.% purity. 2-hexyl-nonanal can be is a reactive intermediate which can be used to manufacture especially expensive personal care products due to its low irritational potential and low volatility. The viewpoints of this study will contribute to the *DST-NRF Centre of Excellence in Catalysis* RSA Olefins programme's knowledge base and will help focus research on development of more efficient catalysts and or catalytic systems.

1.2 Objectives

The aim of this study is to develop a conceptual process for upgrading low value terminal C8 olefins from Fischer-Tropsch Synthol product stream to 2-hexyl-nonanal (C15-aldehyde). In order to achieve the main aim of this study the following sub-objectives are set:

Objective 1:

- Investigate current technologies for C5-C9 olefin metathesis
- Investigate current technologies for C10-C18 olefin hydroformylation
- Investigate current technologies for recovering homogeneous catalysts from post reaction mixtures.

Objective 2:

- Propose and develop several conceptual processes for upgrading low value C8 olefins to C15 functionalised hydrocarbons

Objective 3:

- Develop Aspen Plus™ simulation models for the various process scenarios as proposed in objective 2
- Validate Aspen Plus™ models with literature data
- Propose possible optimized operating conditions for the process

Objective 4:

- Compare and evaluate from both a techno-economic and energy viewpoint the various proposed scenarios

1.3 Scope of Investigation and thesis outline

The study proposes the use of metathesis and hydroformylation reaction pathways for the upgrading of low value olefins from Fischer-Tropsch Synthol product stream to functionalised hydrocarbons using literature data. Figure 1.2 is the scope of this investigation.

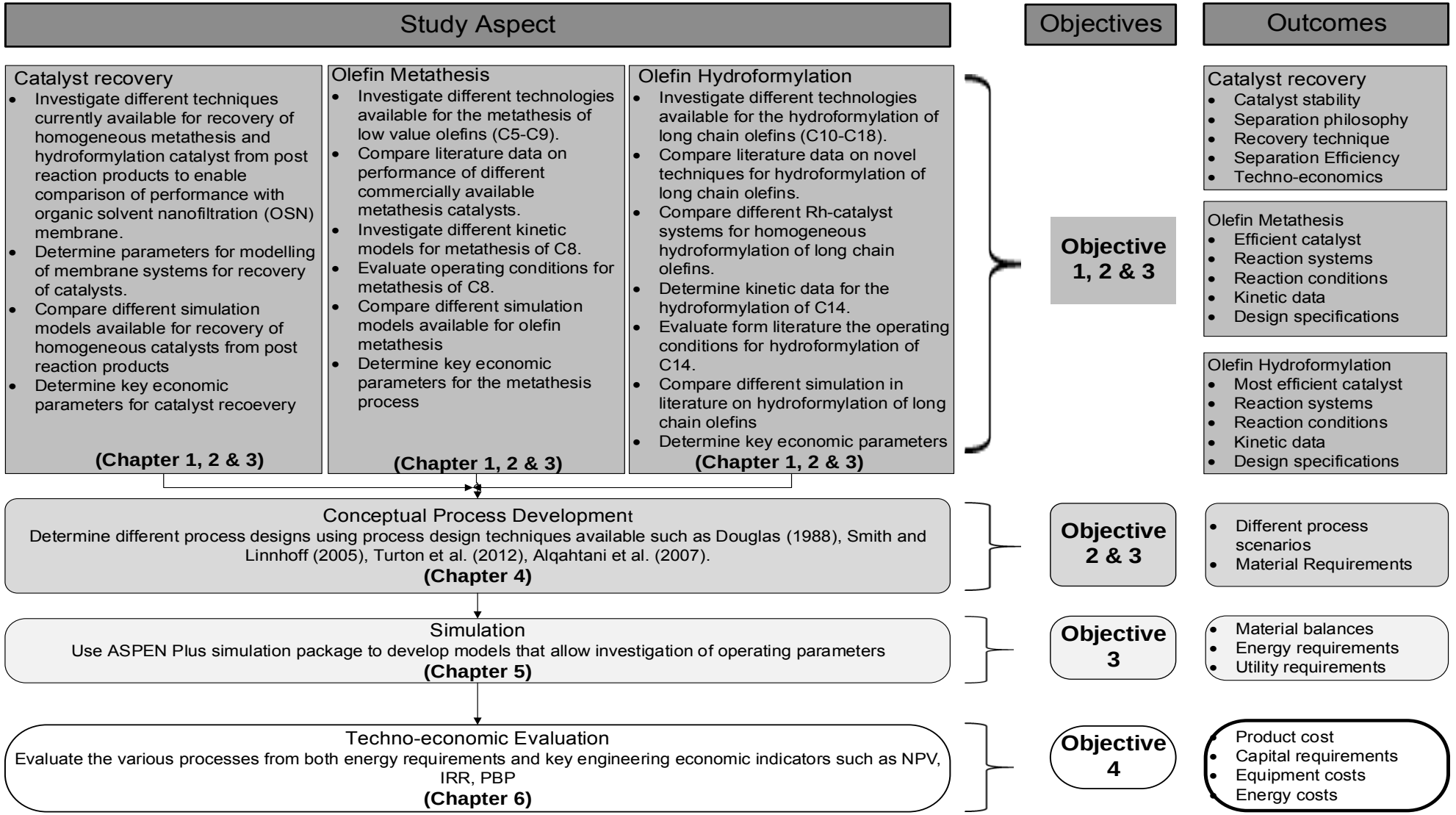

Figure 1.2.: Scope of investigation

Chapter 2: Research approach

In Chapter 2, the approach for solving the problem and methodology of evaluating a viable solution is discussed. Chapter 2 covers the conceptual framework and design approach.

Chapter 3: Literature review

Chapter 3 addresses **Objectives 1, 2** and **3**. Chapter 3 covers olefin metathesis, hydroformylation technologies and recovery of homogeneous catalysts especially focusing on OSN membrane process. A discussion of operating conditions and processes designs of commercial plants and pilot plants for metathesis and hydroformylation including homogeneous catalysts recovery technologies is presented along with the previous simulation work done by other researchers.

Chapter 4: Process Development

Chapter 4 addresses **Objectives 2** and **3**. Chapter 4 outlines how different process scenarios were developed. The chapter covers decisions and heuristics considered in development of a conceptual process for upgrading low value olefins from a Fischer-Tropsch Synthol product stream into functionalised hydrocarbons.

Chapter 5: Aspen Plus™ Simulation

Chapter 5 details how different Aspen Plus™ simulation models for the different process scenarios were developed. Chapter 5 also discusses how optimal conditions for the various processes were obtained. This chapter addresses **Objective 3**.

Chapter 6: Energy Analysis and Economic Evaluation

Chapter 6 addresses **Objective 4**. In Chapter 6, the simulation results are used to carry out a techno-economic evaluation the various process scenarios to determine the most profitable.

Chapter 7: Conclusions and recommendations for future work

In Chapter 7, the main findings of this study are discussed. A summary of the main process findings is also presented. Chapter 7 also outlines recommendations for future work.

1.4 References

Brunsch., B Behr, Y. A. Temperature-controlled catalyst recycling in homogeneous transition-metal catalysis: minimization of catalyst leaching, Angewandte Chemie International Edition **52** (2013) 1586-1589.

Huang, S, Bilel, H., Zagrouba, F., Hamdi, N., Bruneau, C., Fischmeister, C. Olefin metathesis transformations in thermomorphic multicomponent solvent systems, Applied Catalysis: A General **434** (2015) 1564-1576 http://dx.doi.org/10.1016/j.catcom.2014.09.009

Haumann, M., Koch, H., P. Hugo, P., Schomäcker, R. Hydroformylation of 1-dodecene using Rh TPPTS in a microemulsion, Applied Catalysis a General **225** (2002a) 239–249

Haumann,.M, Koch, H., Hugo, P., Schomäcker, R. Hydroformylation of 7-tetradecene using Rh-TPPTS in a microemulsion. Applied Catalysis a General **225** (2002b) 239-249

Herrmann, W. A and Boy Cornils, Organometallic Homogeneous Catalysis-Where now? Angewandte Chemie International Edition **36** (1997) 1048- 1067

Hentschel, B., Kiedorf, G, Gerlach, M, Hamel, C., Seidel-Morgenstern, A, Freund, A, Sundmacher, K. Model-Based Identification and Experimental Validation of the Optimal Reaction Route for the Hydroformylation of 1‑Dodecene. Industrial & Engineering Chemistry Research (2015) **54** 1755−1765 DOI: 10.1021/ie504388

Janssen, M, C. Muller, D. Vogt, M. Recent advances in the recycling of homogeneous catalysts using membrane separation, Green Chemistry. **13** (2011) 2247–2257.

Maynard, H.A Grubbs, R H. Purification Technique for the Removal of Ruthenium from Olefin Metathesis Reaction Products Tetrahedron Letters **40** (1999) 4137-4140

Michrowska, A., Grela, K. Quest for the ideal olefin metathesis catalyst Pure Applied Chemicals **80** (2008) 31–43. doi:10.1351/pac200880010031

Mills, P.L, Chaudhari, R.V. Multiphase catalytic reactor engineering and design for pharmaceuticals and fine chemicals, Catalysis Today **37** (1997) 367-404

Muller, D., Kasaka, Y., Muller, D., Schomacker, R., Wozny, G. Process Design for the Separation of Three Liquid Phases for a Continuous Hydroformylation Process in a

Miniplant Scale Industrial & Engineering Chemistry Research Industrial & Engineering Chemistry Research **52** (2013) 7259−7264 dx.doi.org/10.1021/ie302487

Muller, M., Muller, D., Minh, D.H, Merchan, V.A, Arellano-Garcia, H, Kasaka, Y., Muller, M, R. Schomacker, R, G. Wozny, Towards a novel process concept for the hydroformylation of higher alkenes: Mini-plant operation strategies via model development and optimal experimental design, Chemical Engineering Science **115** (2014)127–138

Muller, D., Esche, E., Pogrzeba, T., Illner, M., Leube, F., Schomacker, R., Wozny, G., Systematic Phase Separation Analysis of Surfactant-Containing Systems for Multiphase Settler Design Industrial & Engineering Chemistry Research **54** (2015) 3205−3217 DOI: 10.1021/ie5049059

Pogrzeba, D., Muller, D., Illner, M., Schmidt, M., Kasaka, Y., Weber, A., Wozny, G., Schomacker, R., Schwarze, M. Superior catalyst recycling in surfactant based multiphase systems-Quo vadis catalyst complex? Chemical Engineering and Processing **99** (2016) 155–166

Scarpello, JT., Nair, D., Freitas dos Santos, L.M., White, L.S., Livingston, A.G. The separation of homogeneous organometallic catalysts using solvent resistant nanofiltration, Journal of Membrane Science **203** (2002) 71–85.

Schmidt, P., Bednarz, E.L., Lutze, P., Gorak, A. Characterisation of organic solvent nanofiltration membranes in multi-component mixtures: process design workflow for utilising targeted solvent modifications, Chemical Engineering Science **115** (2014) 115–126.

Sharma, SK Jasra, R.V. Aqueous phase catalytic hydroformylation reactions of alkenes Catalysis Today **247** (2015) 70–81

Vankelecom, I.F.J. Polymeric membranes in catalytic reactors, Chemical Engineering Review **102** (2002) 3779-3810.

Westhus, M., Gonthier, E., Brohm, D Breinbauer, R. An efficient and inexpensive scavenger resin for Grubbs catalyst. Tetrahedron Letters **45** (2004) 3141–3142

Wiese, K.D., Obst D. Catalytic carbonylation reactions Topics in Organometallic Chemistry, **18** (2006) 1–33.

Zagajewski, M., Dreimann, J., Thones, M., Behr, A. Rhodium catalyzed hydroformylation of 1-dodecene using an advanced solvent system: Towards highly efficient catalyst recycling Chemical Engineering and Processing xxx (2015) xxx–xxx (Article in Press)

CHAPTER 2: RESEARCH APPROACH

"*Research is to see what everybody else has seen, and to think what nobody else has thought"*

Albert Szent-Gyorgyi- Biochemist

Overview

Chapter 2 provides a detailed description of the methodology and framework that was followed in this investigation. The Chapter is subdivided into three main sections, starting with Section 2.1, which gives a brief background into conceptual process design. Section 2.2 highlights current available design approaches and Section 2.3 presents the design approach used in this study. A motivation for the Douglas methodology was also given in Section 2.3.1.

2.1 Introduction: Conceptual approach

The conceptual bases to design and solving problems in chemical engineering are well known (Potier et al., 2015). The three most acknowledged models in conceptual process design according to Frillici et al. (2015) are the Pahl and Beitz (2007), Ulrich and Eppinger (2010) and Ullman (2007) models. Table 2.1 is a summary of the main steps of these design models.

Table 2.1.: Conceptual processes and related activities

Ullman (2010)	Paul and Beitz (2007)	Ulrich & Eppinger (2007)
i. Generate concepts	1. Abstract to identify essential problems	1. Identify customer needs
2. Evaluate concepts	2. Establish function structures	2. Establish target specifications
3. Make concepts decisions	3. Search for working principles	3. Generate product concepts
4. Document and communicate	4. Combine working principle	4. Select product concepts
5. Refine plan	5. Select suitable combinations	5. Test product concepts
6. Approve concepts	6. Firm up into principle solution variants	6. Set final specifications
	7. Evaluate variants against technical and economic criteria	7. Plan downstream development

Although at first sight the three models appear quite different, it is possible to identify a common path, i.e. starting from the requirement list, a set of concept variants is generated and then a selection of the preferred ones is performed by means of evaluation parameters. Curry (2010) and Frillici et al. (2015) agrees also that when it comes to generating concepts variants, all the three models proposes substantially the same steps. The steps are: (i) formulation and

decomposition of the design problem (by means of functional analysis and decomposition) (ii) definition of the solutions related to single sub-functions and (iii) combination of the solutions related to single functions.

With respect to a process conceptualisation problem, Steimel and Engell (2015) describes process synthesis as the choice of the best options from a set of promising design candidates during the early stages of process development. Hence, steps can be translated to identification of candidate processes, evaluating the processes and presenting the most viable option. Usually the decision has to be made under complete information and hence all alternatives have to be explored either in experimental work on the laboratory or pilot plant level. Steimel and Engell (2015) reiterates the need to stop laboratory or pilot plant experiments as soon as sufficient information has been gathered as one of the main challenges towards the use of such tools. Steimel and Engell (2015) confirms that the quantification of the point in time when the information is sufficient is usually difficult. Moreover, though this had an advantage of proving that the process really worked, it is costly and not very flexible with regard to major changes in the process especially for processing challenges such as metathesis and hydroformylation where expensive catalysts are involved. However, evaluation of candidate processes can be done using process simulators which allow virtually all options to be explored using computer tools such as FLOWTRAN, PROII™, GPROMS, HYSYS and Aspen Plus™ (Mizsey and Fonyo, 1990).

Oden et al. (2006) defines simulation as application of computational models and computing power to the prediction of system behaviour. Howat (1997) states that prior to simulation, some preparatory work needs to be done in order to allow smooth flow of work and to ensure that everything is done systematically to reduce oversight. Oden et al. (2006) also pointed out that if simulation is not approached systematically, the output from the simulation might be misleading or meaningless.

2.2 Literature review: Design approach

Conceptual process design and synthesis originated from the concept of unit operation and was first introduced by Little in 1915 (Li and Kraslawski, 2004). Little (1915) pointed out that any chemical process can be represented as a series of 'unit operations' (King, 2000). Until the late 1960s, the unit operation concept was a cornerstone of process design, thanks to the works of Rudd and Watson (1968) who dealt with the synthesis problem using systematic approaches. The later 20 years saw considerable research being performed in the area of process synthesis (Johns, 2001). During that time, most of the research was related to well-defined sub-problems. It was believed that general-purpose process synthesis systems would be soon in routine use. However, until now, only limited progress has been observed in the practical application of process synthesis tools (Johns, 2001).

The task of defining appropriate process configuration requires the generation of and evaluation of many technological schemes (process flowsheets) in order to find those exhibiting better performance indicators. A series of solving strategies have been proposed being classified into two large groups i.e. knowledge-based process synthesis and optimization-based process synthesis (Cardona et al., 2012). Different types of models have been used previously for the two classes of approach as shown in Table 2.2.

Table 2.2.: Process design approach

Knowledge based	Optimization based
Douglas (1988) hierarchical approach	MINLP, LP, LGDP, QP, NLP techniques
Smith and Linnhoff (2005) onion approach	Branch and bound method
Turton et al. (2009) evolutionary approach	Outer-approximation method
Siirola and Rudd (1971) systematic heuristic approach	Generalized benders method
	Extended cutting plane methods

Optimisation based methods use not only traditional algorithmic methods, such as mixed-integer non-linear programming (MINLP), but also stochastic ones such as simulated annealing and evolutionary algorithms such as genetic algorithms (GA). Two common features of optimisation-based methods are the formal, mathematical representation of the problem and the subsequent use of optimisation.

A lot of studies (Grossmann and Tresalacios, 2013; Grossmann and Cabellero, 2000; Friedler et al., 1993) have been carried out into the optimisation based approach, and it has been widely applied in process design and synthesis. An important drawback of optimisation-based methods is the lack of the ability to automatically generate a flowsheet superstructure (Kraslawski and Li, 2004). While several tools and methods have been proposed to solve the process superstructure design problem, none has yet been established as the standard (Grossmann and Tresalacios, 2013). Especially in the early phases of process synthesis, no formalized method or tool for the screening of alternatives is available (Cardona et al., 2012). Another disadvantage is the need for a huge computational effort and the fact that the optimality of the solution can only be guaranteed with respect to the alternatives that have been considered a priori (Grossmann, 1985).

Li and Kraslawski (2004) concluded that a key topic for the advancement of conceptual process design is the “improvement of optimization and simulation techniques as well as of information management tools in order to handle more information and knowledge from various sources”.

Knowledge-based methods like heuristic methods are based on the long-term experience of engineers and researchers and combines heuristics with an evolutionary strategy for process design (Li and Kraslawski, 2004). Siirola and Rudd (1971) made their first attempt to develop a systematic heuristic approach for the synthesis of multi component separation sequences. In the subsequent years, a lot of research has been carried out (Douglas, 1988; Jaksland et al., 1995; and Grossmann et al., 2001; Sieder et al., 2004; Smith and Linnhoff, 2005; Alqahtani et al., 2007; Turton et al., 2009) into knowledge-based methodologies.

Douglas (1988) has proposed a method in which any process can be decomposed into five levels of analysis for its design as shown in Figure 2.1.

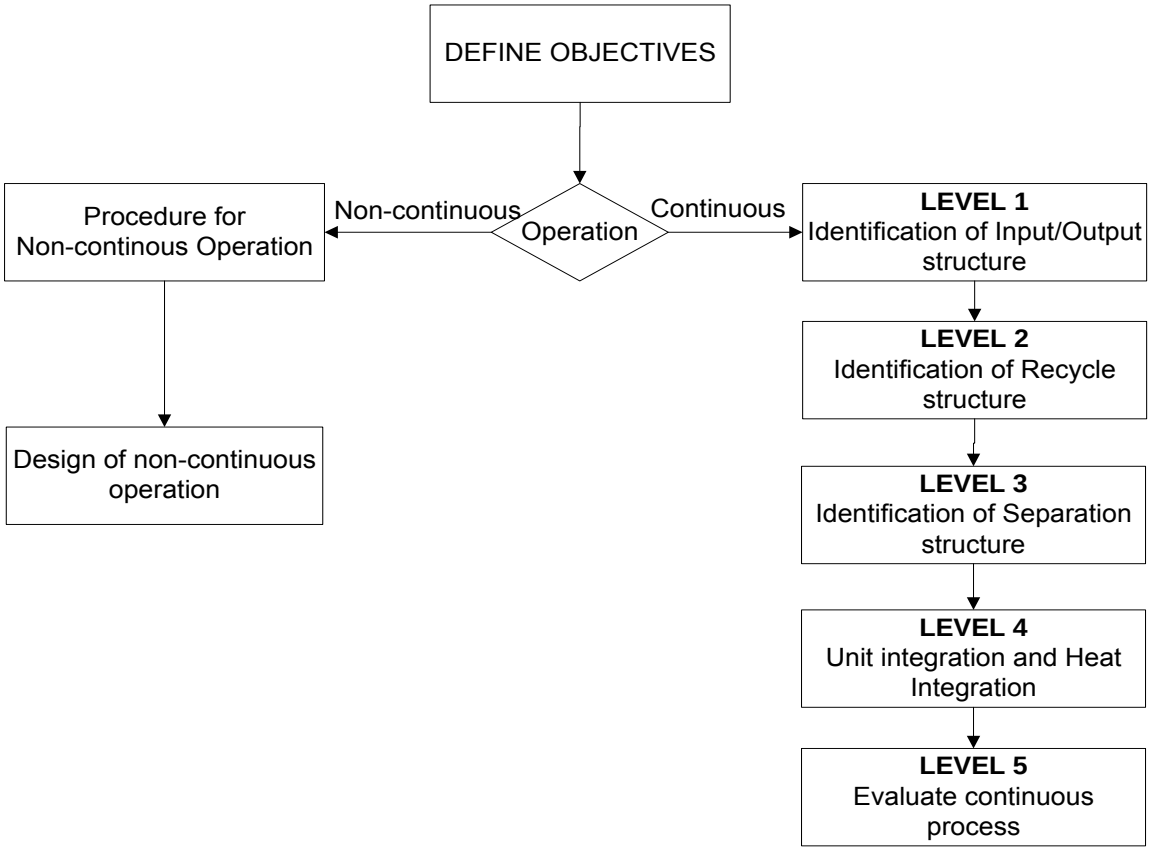

Figure 2.1.: Douglas method of design (Douglas, 1988)

Douglas' (1988) methodology has a hierarchical sequential character considering that in each level different decisions are made based on heuristic rules. Douglas' (1988) strategy allows the generation of different alternatives, which are evaluated from an economic viewpoint using short-cut methods. According to Douglas (1988), the hierarchical decomposition comprises the analysis of the process in the following levels: (i) batch vs. continuous, (ii) input–output structure of the flowsheet, (iii) recycle structure of the flowsheet, (iv) separation system synthesis, and (v) heat recovery network. The whole chemical process is taken into account at each of the five decision levels. These five levels generate a base case design that will be

used for the successive detailed engineering analysis in simulation. Each level includes new decisions and additional flowsheet structures. Heuristics are used to help the designer to make those decisions and the opposite decisions are accumulated in a list of process alternatives to be considered after a base-case design has been generated. Also at each level, the dominant design variables are identified, and both capital and operating costs are evaluated as a function of these variables. The hierarchical heuristic method emphasizes the strategy of decomposition and screening. The Douglas' (1988) methodology has been mostly applied to chemical and petro-chemical processes. Hierarchical design approach is absolutely necessary due to the inherent hierarchy nature of conceptual process design (Yang and Shi, 2000). It allows the quick location of flowsheet structures that are often 'near' optimum solutions (Li and Kraslawski, 2004).

However, the major limitation of the Douglas (1988) method is due to its sequential nature, hence, it is impossible to manage the interactions between different design levels (Yuan et al., 2013). The importance of the simultaneous optimization of various subsystems has been demonstrated (Duran and Grossmann, 1986). The same reason causes problems in the systematic handling of multi-objective issues within hierarchical design. Therefore, the hierarchical heuristic method offers no guarantee of finding the best possible design (Yuan et al., 2013).

Since the physical and chemical properties of the involved chemical system plays a very important role for the design/synthesis of a process, a thermodynamic insight based hybrid method to select the separation process was proposed by Jaksland et al. (1995).

A set of criteria to be used to evaluate the process alternatives was proposed by Turton et al. (1998). Turton et al. (1998) defined design as an evolutionary process that can be represented as a sequence of diagrams that describe the chemical process. Thus, a chemical engineer can start the design of a process with the block flow diagram, in which only the feeds and the output products are represented, then decomposes the process in basic functional elements, such as reaction and separation sections. The engineer can also identify recycle streams and

consider the use of additional units to obtain the required operating conditions (temperature and/or pressure). In order to identify these basic elements, more detailed diagrams are built. With the mass balance a preliminary block flow diagram (BFD) can be obtained. As more detailed mass and energy balances are developed, calculations of unit operations specifications can be made, resulting in a process flow diagram (PFD). Finally, when the mechanical details and instrumentation are considered, they are represented by means of a piping and instrumentation diagram (P&ID).

Hostrup et al. (2001) further developed this method by including a reverse design approach where process design variables are “back-calculated” for known design targets. Seider et al. (2004) proposed a step-by-step method for design of chemical processes. Similarly, Smith and Linnhoff (2005) have proposed an onion model for decomposing the chemical process design into several layers (Figure 2.2). The design process starts with the selection of the reactor and then moves outward by adding other layers, the separation and recycle system, it also includes the heating and cooling utilities, and wastewater and effluent treatment.

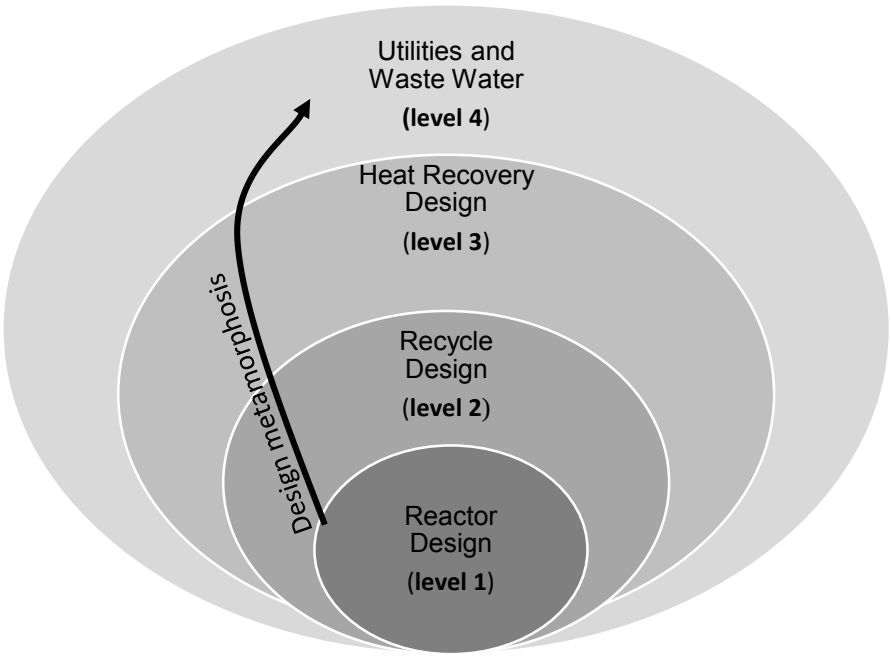

Figure 2.2.: Onion method of design (Smith and Linnhoff, 2005)

The effort to keep the system simple and not adding equipment in early stages of design may result in missing benefits of interactions between different items of equipment in a more complex system. Gani and d' Anterroches (2005) also proposed a reverse approach for process flowsheet design based on process knowledge similar to knowledge of molecular structures. Alqahtani et al. (2007) developed the design method for synthesis of reaction-separation-recycle systems similar to the onion model by Smith and Linnhoff (2005). The methods according to Gani and d' Anterroches (2005), Alqahtani et al. (2007), Smith and Linnhoff (2005) however, focus on processes with one main product for a fixed reaction-catalyst and do not consider process alternatives in terms of diversion of resources to another product within the same overall process. A systematic step-by-step methodology which considers a large number of alternative processes including all feasible separation techniques should be considered and developed for design.

2.3 This study: Design approach

The objective of this study is to develop a process of manufacturing 2-hexyl-nonanal an intermediate feedstock for the Guerbet-type surfactants by upgrading low value 1-octene feedstock from a Fischer-Tropsch Synthol product stream at Sasol Secunda. The design capacity is given in Table 2.3

Table 2.3.: A summary of the design base used in this study

Design parameter	Description	Justification
Product name	2-hexyl-nonanal (99 wt. %)	Market requirement (Hentschel et al., 2014, Steimel et al., 2014)
Desired production rate	10 000 ton per year	Petrochemical 10 000-500 000 tonnes per year attractive to investors (Arnoldy, 2000)
Feedstock	1-octene (100 % mol basis)	Feed stock purity selected was 100 % purity for academic purpose and the fact that the literature used excluded effects of feed purities.
Plant location	Secunda, SA	Proximity to raw materials (syngas, 1-octene) and developed building facilities

2.3.1 Motivation for the Douglas methodology

The "Douglas Method" is based on hierarchical decision-making using economic feasibility as a main criterion for process evaluation. A complex problem is gradually solved through completion of a number of arbitrary "stages" or levels of analysis. The Douglas' (1988) hierarchical approach is a simple but powerful methodology for the synthesis of process flowsheets. It consists of a top-down analysis organised as a clearly defined sequence of tasks grouped in levels. In applying the methodology, the designer has to identify dominant design variables and make design decisions. As a result, a number of alternatives are produced that are submitted to an evaluation from an economic viewpoint using short-cut methods, an advantage of the Douglas methodology compared to reducible methodologies such as the Smith and Linnhoff (2005). Thus, the major advantage of the hierarchical approach is that it offers a consistent frame for developing alternatives rather than a single design. Checking the projected economic potential at early stages of the design process allows for quick elimination of non-feasible design alternatives.

The hierarchical design approach of Douglas is necessary due to the inherent hierarchy nature of conceptual process design (Yang and Shi, 2000). In a chemical process, the transformation of raw materials into desired products is broken down into a number of steps that provide intermediate transformations. The transformations are carried out in reactors, separators etc. In this study, a holistical step-wise layout of the design approach based on Douglas (1988) was used as summarized in Figure 2.3. The evaluation of optimal process conditions involves examining possible process solutions developed by applying the adopted design approach, using a steady state simulator and a set of key engineering criteria. For the same reason that the design can be approached in many ways, it is necessary to consider more deeply the design approach to be used.

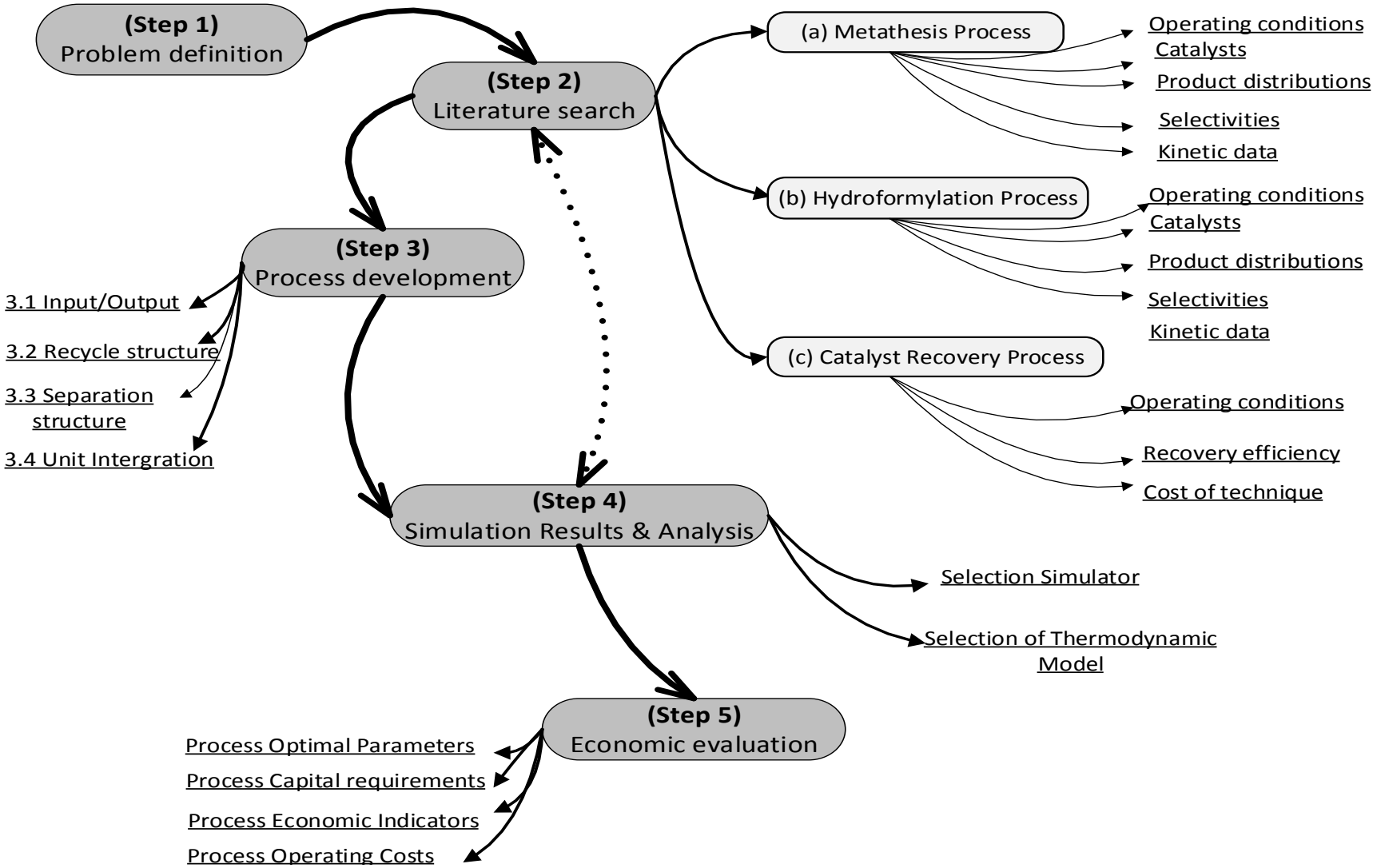

Figure 2.3.: Design approach used in this study

Step 1: Problem definition

The objective was to design a chemical process to produce 10 000 tonnes per year of 2-hexyl-nonanal at a purity of 99 wt. % which can be used as a feedstock for the manufacture of Geubert-type surfactants. The feedstock to be used is low value 1-octene from a Fischer-Tropsch product stream. The performance criterion is to maximise the net present value (NPV) of the process. The NPV included revenues, total capital investment and depreciation costs were determined based on interest rate of 15 % and the life time of 15 years. According to Miremadi et al. (2013), for preliminary economic evaluation of petrochemical plants the project life of 15 years is used. The net present value is a function of a number of process variables, such as flow rate, pressure, and temperature which determines heat and mass requirements. Decision variables such as equipment size (diameter, height etc.) define total capital investment and material costs such as 1-octene, syngas, and catalysts will determine revenues.

Step 2: Search literature

The second step involved literature search (**Chapter 3**) on the properties of the chemicals involved in order to develop alternatives of conceptual process for upgrading low value 1-octene from Fischer-Tropsch product stream to 2-hexy-nonanal a feedstock to Geurbet-type surfactants. The objectives of **Chapter 3** were to:

2.1 Understand the field of olefin metathesis, hydroformylation and catalyst recovery in detail

2.2 Acquire relevant input information

2.3 Review of what others did in the process simulation (previous Aspen Plus™ simulations etc.)

2.4 Review previous membrane simulations

2.5 The missing data was also estimated based on thermodynamic models. Information on raw materials, main products, side products, reactions, catalysts, reaction

conversion and operating conditions was also gathered. Information on all available flowsheets was also considered as alternative heuristics in process development.

Step 3: A hierarchical approach to process development

In the third step (**Chapter 4**) the hierarchical decomposition method of Douglas (1988) was applied to develop a continuous process to manufacture 10 000 tons per year of 2-hexy-nonanal at a purity of 99 wt. % as shown in Figure 2.4.

3.1 Input-output information

3.2 Recycle structure

3.3 Separation structure

3.4 Unit and Heat integration

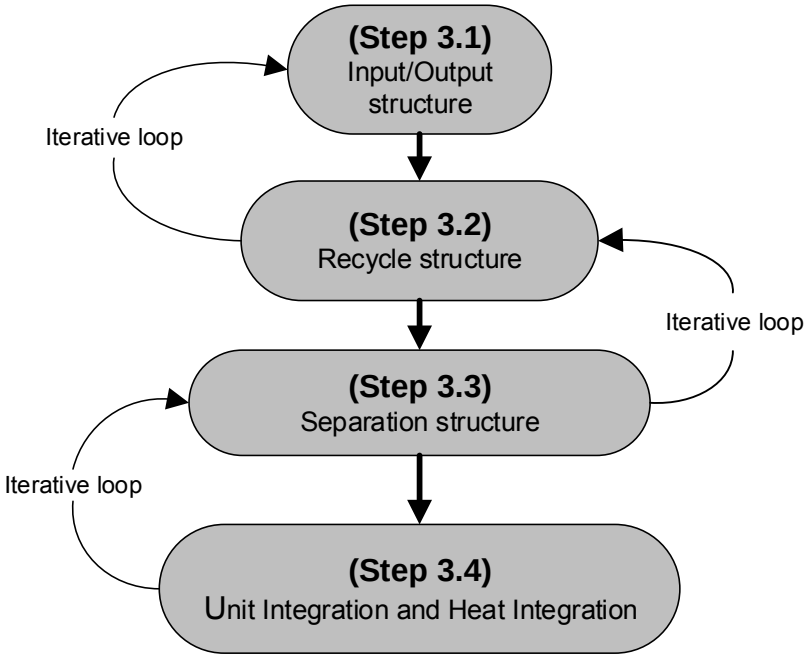

Figure 2.4.: Adopted design approach based on Douglas' (1988) methodology

The approach considered also aspects of Turton et al. (2009) evolutionary method to conceptual process development for developing process flow diagrams (PFDs) for the various process scenarios. Thermodynamic insights and a simple mass balance is used to generate

possible process alternatives by considering alternative separation techniques and different reaction catalysts together with a list of decision variables that will need to be determined. The alternatives were screened by considering design constraints in a hierarchical manner with conventional techniques applied first. The high costs of the catalyst and problem of separation of catalyst from product stream was the criteria behind selection of separation technique.

Step 4: Aspen Plus™ simulation development

After some process alternatives are eliminated the remaining alternatives that include feasible unit operations such as reactors, flash operators, distillation, membrane separators and decanter within flowsheets, are simulated by using Aspen Plus™ (**Chapter 5**) before corresponding performance criteria are computed in the next step for economic analysis and final process selection. The general approach for simulation by using Aspen Plus™ has been described elsewhere by Quintero et al. (2008) and Aspen Tech Pvt Ltd. etc.

Step 5: Economic evaluation of process scenarios

Finally, an energy requirement and economic analysis of the process alternatives was performed in **Chapter 6**. The alternative process configurations are analysed through profitability indicators such as a net present value (NPV). The following assumptions were adopted to determine NPV; interest rate is 15 %, a linear depreciation and project life of 15 years. According to Miremadi et al. (2013), for preliminary economic evaluation of petrochemical plants, the project life of 15 years is used. A sensitivity analysis was carried out to determine key economic parameters. Finally, an optimal process was selected.

.

2.4 References

Alqahtani, A., Hellgardt, K., Holdich, R., Cumming, I., Integrated knowledge based system for process synthesis. Computers and Chemical Engineering **24** (2007) 437–442.

Conti, G.A.P., Paterson, WR., Chemical Reactors in Process Synthesis. Chemical Engineering Science **115** (1985) 92-105

Chitrao, S.P., Govind, R., Synthesis of Optimal Serial Reactor Structures for Homogeneous Reactions, American Institute of Chemical Engineers Journal., (1985) **31** 185-193

Cardona, C.A., Sanchez, O.J., Fuel ethanol production: process design trends and integration opportunities. Bioresources Technology **98** (2007) 2415–2457

Cardona, C.A, Sanchez, O.J, Conceptual design of cost effective and environmentally-frendly configurations for fuel production from sugar can by knowledge based process synthesis Bioresources Technology **104** (2012) 305-314

Douglas, J.M. Conceptual Design of Chemical Processes, McGraw-Hill. New York. (1988).

Duran, M.A., Grossmann, I.E., Simultaneous Optimization and Heat Integration of Chemical Processes American Institute of Chemical Engineering Journal **32**, (1986) 123-138

Eppinger, S. D., Ulrich, K. T., Product Design and Development, 4th ed. Mc Graw HIll. (2007).

Frillicia, F.S., Fiorineschi, L., Cascini, G. Linking TRIZ to Conceptual Design Engineering Approaches, Procedia Engineering **131** (2015) 1031 – 1040

Grossmann. I.E., Mixed-integer programming approach for the synthesis of integrated process flowsheets, Computational Chemical Engineering **9** (1985) 463–482

Grossmann, I. E., Trespalacios, F., Systematic modeling of discrete-continuous optimization models through generalized disjunctive programming. American Institute of Chemical Engineering Journal **59** (2013) 3276–3295

Grossmann, I. E., Caballero,, J. A., Yeomans, H. Advances in mathematical programming for the synthesis of process systems. Latin American Applied Research, **30** (2000) 263-284.

Hentschel, B., Peschel, A., Xie, M., Vogelpohl, C., Sadowski, G., Freund, H., Sundmacher, K., Model-based prediction of optimal conditions for 1-octene hydroformylation, Chemical Engineering Science **115** (2014) 58-68

Howat, S.C., Analysis of Plant performance. In: Green, D., W (ed.) Perry's Chemical Engineer's Handbook. New York: Mc Graw-Hill. (1997)

Hostrup, M., Harper, P. M., Gani, R., Design of environmentally benign processes: Integration of solvent design and process synthesis. Computers and Chemical Engineering **23** (1999). 1395–1414.

Hostrup, M., Gani, R., Kravanja, Z., Sorsak, A., Grossmann, I. Integration of thermodynamic insights and MINLP optimization for the synthesis, design and analysis of process flowsheets. Computers and Chemical Engineering **25** (2001). 73–83.

Jabareen, Y., Building a Conceptual Framework: Philosophy, Definitions, and Procedure. Interanational Journal of Qualitative methods **8** (4) (2009) 49-62. (http://creativecommons.org/licenses/by/2.0)

Jaksland, C., Gani, R., Lien, K. Separation process design and synthesis based on thermodynamic insights. Chemical Engineering Science **50** (1995) 511–530.

Johns, W.R, Process synthesis: poised for a wider role, American Institute of Chemical Engineers (2001) 59–65

King, J.C. From unit operation to separation processes, Separation Purification Methods **29** (2000) 233–245.

Lapkina, A., Voutchkova, A., Anastas, P. A conceptual framework for description of complexity in intensive chemical processes, Chemical Engineering and Processing **50** (2011) 1027– 1034

Li, X., Kraslawski, A. Conceptual process synthesis: past and current trends. Chemical Engineering Process. **43** (2004) 589–600.

Mizsey, P., Fonyo., Z. Toward a More Realistic Overall Process synthesis-The Compined Approach, Computers in Chemical Engineeering, **14** (1990) 1213-1236,

Motard, R.L., Westerberg, A. W. Process Synthesis, American Institute of Chemical Engineers Advanced Seminar Lecture Notes, New York, (1978)

Oden, J. T., Belytschko, T., Fish, J., Hughes, T., J. R., Johnson, C., Keyes, D., Laub, A., Petzold, L., Srolovitz, D., Yip, S. 2006. Simulation Based Engineering Science. Computers in Chemical Engineeering **25** (2006) 1-63.

Pahl, G., Beitz, W. Engineering Design: a Systematic Approach, (3rd Edition) London Springer-Verlag; (2007)

Perkins, J., Education in process systems engineering: past, present and future. Computational Chemical Engineering **26** (2002) 283–293.

Rudd, D.F., Watson, C.C., Strategy of Process Engineering, Wiley, New York, 1968

Siirola, J.J., Rudd, D.F., Computer-aided synthesis of chemical process designs, Industrial Engineering Chemical Fundamentals **10** (1971) 353.

Steimel, J., Haumann, M., Schembecker, G., Engell, S., Model-based conceptual design and optimization tool support for the early stage development of chemical processes under uncertainty, Computers and Chemical Engineering **59** (2013) 63– 73

Steimel, J., Haumann, M., Schembecker, G., Engell, S., A framework for the modelling and optimization of process superstructures under uncertainty, Chemical Engineering Science **115** (2014) 225–237

Steimel, J., Engell, S., Conceptual design and optimization of chemical processes under uncertainty by two-stage programming, Computers and Chemical Engineering **81** (2015) 200–217

Seider, W.D., Seader, J.D., Lewin, D.R. Process Design Principles. Synthesis, Analysis and Evaluation, (First Edition) John Wiley & Sons, New York. (1999)

Seider, W. D., Seader, J. D., Lewin, D. R. Product and process design principles. New York: Wiley. (2004).

Turton, R., Bailie, R., Whiting, W., Shaeiwiz, J. Analysis, synthesis and design of chemical processes (3rd Edition.) Printice Hall (2009).

Ullman, D.G. The Mechanical Design Process (4th Edition) Mc Graw Hill; 2010.

Yuana, Z., Chen, B., Gani, R. Applications of process synthesis: Moving from conventional chemical processes towards biorefinery processes Computers and Chemical Engineering **49** (2013) 217– 229 (Review)

CHAPTER 3: LITERATURE REVIEW

"*In great literature, I become a thousand different men but still remain myself*."

C.S. Lewis

Overview

Chapter 3 is a detailed study of the properties of chemicals and reactions involved in this investigation, which enabled the development of various conceptual processes. The chapter is subdivided into three main sections, starting with Section 3.1 which introduces Centre of Excellence in Catalysis background. Section 3.2 and Section 3.3 highlights current technologies in metathesis and hydroformylation. Section 3.4 details conventional as well as novel technologies for homogeneous catalyst recovery. Section 3.5 is a review of previous studies on process development. Finally, a summary of the findings is given in Section 3.6.

3.1 Introduction: Centre of excellence in catalysis

Within the RSA Olefins programme of the DST-NRF Centre of Excellence in Catalysis, the efficacy of homogeneous catalysts for upgrading low value olefinic feedstocks (C5-C9) to higher value functionalized hydrocarbons (C10-C19) is investigated. Fundamental research is focused primarily on selection of catalysts and maximizing productivity using product selectivity and substrate conversion as catalyst performance indicators and process conditions as optimization parameters. Over 90 % of the world's industrial processes are dependent on catalysis and homogeneous catalysts are usually preferred due to their high activity and selectivity since they remain in the same phase as the substrate (Mao and Yu, 2013).

One important unit operation for an economic process is the separation and recovery of reagents, products, solvents, catalysts and intermediates from each other. Separation techniques, which are increasingly evident in chemical catalysis, have proven to be challenging in hydrocarbon processes due to catalyst instability at operating conditions. Therefore, when migrating from proof of concept stage to industrial application, catalyst efficiency cannot be the only deciding factor in identifying the most productive route, as this does not necessarily translate to an economically viable solution.

Low value olefins (C5-C9), especially in the case of alpha olefins, can readily be subjected to metathesis reactions to produce longer chain internal olefins (C10-C18) (Mol, 2001). The internal alkenes can then be further functionalized through hydroformylation to the Guerbet-type aldehydes (C11-C19). The oligomerisation route normally produces a full range of products hence the challenge of a lack of selectivity and higher costs incurred in separation of products into individualistic products. In the detergent industry, the perennial balancing act is between surfactant chain length, biodegradability and solubility.

Traditionally linear alpha-olefins in the C12 to C15 range are used in the manufacture of alcohol sulphates. Longer chain linear alcohol sulphate surfactants leads to higher surfactancy and performance but is offset by low hardness tolerance and limited cold water solubility. The

branching in Guerbet-type surfactants allows the use of chain lengths as long as C16 and C17 without incurring the historical negatives such as lack of biodegradability (Sasol, 2008). Asymmetric hydroformylation is a very promising catalytic reaction that produces chiral aldehydes from inexpensive feedstock (alkenes, syngas) in a single step under essentially neutral reaction conditions (Gual et al., 2010). Even though asymmetric hydroformylation offers great potential for the fine chemical industry the reaction has not yet been utilised on an industrial scale due to several technical challenges (Gual et al., 2010).

The overall aim is to develop a substantial body of knowledge regarding the application of catalyst technologies in various forms of “small production platforms” so as to reduce the requirement for huge initial capital investments.

3.2 Metathesis

Olefin metathesis is increasing becoming an established valuable synthetic tool, which is providing increasing access to numerous specialty chemical markets (Banks et al., 1982 and Grubbs, 2003). According to Mol (2004), the technology allows the conversion of simple, relatively inexpensive olefins into specialty, high purity olefins which are intermediates in the fragrance, and many other specialty industries. Olefin metathesis is one of the few fundamentally novel organic reactions discovered in the last 60 years (du Toit et al., 2013, Balcar and Cejka, 2013, Tomasek and Jürgen Schatz, 2013). The first catalysts for the olefin metathesis reaction were ill-defined, multicomponent initiators consisting of transition metal halides or oxides with alkylating co-catalysts, such as WCl6-SnMe4 or MoCl5-EtAlCl2 (Irvin and Mol, 1999). The advantages of well-defined, single-component catalysts over ill-defined initiators is that they provide control over reaction initiation and functional group compatibility (Grubbs et al., 2003). Richard Schrock and Robert Grubbs pioneered homogeneous metathesis catalysts (du Toit et al., 2014). Yves Chauvin proposed the metallacycle mechanism for metathesis involving carbenes long before any stable carbenes had been detected (Vougioukalakis, 2012). Grubbs, Schrock and Chauvin were awarded the Nobel Prize for Chemistry in 2005 for their work in the field of olefin metathesis (Vougioukalakis,

2012). The metathesis reaction involves the reaction of two olefins in a disproportionation reaction via a metallacyclobutane intermediate **1** as depicted in Figure 3.1.

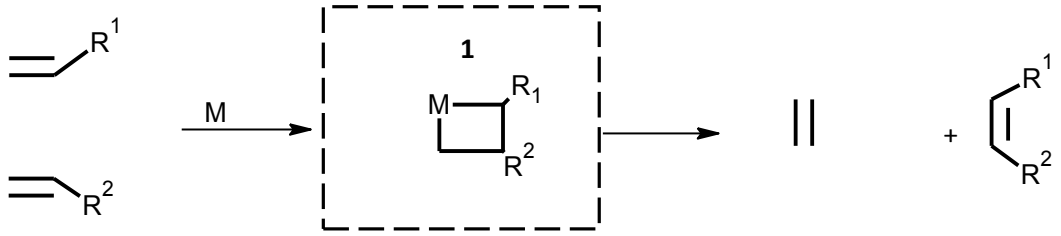

Figure 3.1.: General olefin metathesis reaction

Homogeneous metathesis has become an extremely useful tool in organic synthesis due to well-defined metathesis catalysts. Grubbs based and Hoveyda-Grubbs based precatalysts were introduced by the groups of Grubbs in the mid 1990s and Hoveyda in 1999 respectively. According to Mol (2004), homogeneous metathesis reaction has already found application in the production of pharmaceutical products. In small volumes, high value products the cost of the catalyst is not a major factor in the process economics (Mol, 2001). In pharmaceutical processes, the catalyst is not recycled, and decomposition of the catalyst is not a serious issue (Mol, 2004). The major industrial scale uses of metathesis are the production of propene via the reaction of ethylene and 2-butene over a heterogeneous catalyst (OCT process), and the Shell Higher Olefin Process (SHOP) (Leeuwen, 2004) which involves homogeneous ethylene oligomerisation followed by metathesis over a heterogeneous catalyst (Mol, 2004) and polymerization reactions.

3.2.1 Olefins Conversion Technology (OCT^{TM})

An alternative route to propene is by applying the metathesis reaction for the conversion of a mixture of ethene and 2-butene into propene (Mol 2004). OCT^{TM} uses the Phillips Triolefin Process in reverse, (i.e. the conversion of ethylene and 2-butene to propene) and this process is now offered for licence by ABB Lummus Global, Houston (USA) (Mol, 2004). The feed (a mixture of C4s and high purity ethylene) is heated prior to introducing into the metathesis

reactor. The reaction takes place in a fixed-bed reactor over a mixture of WO_3/SiO_2 (the metathesis catalyst) and MgO (an isomerization catalyst) at >260 °C and 30−35 bar (Mol, 2004). 1-Butene in the feedstock is isomerized to 2-butene as the original 2-butene is consumed in the metathesis reaction. The conversion of butene is above 60 % per pass and the selectivity for propene is >90 %. The catalyst is retained in the reactor and is regenerated on a regular basis (Mol, 2004). Figure 3.2 shows a simple process flow diagram of the OCT process.

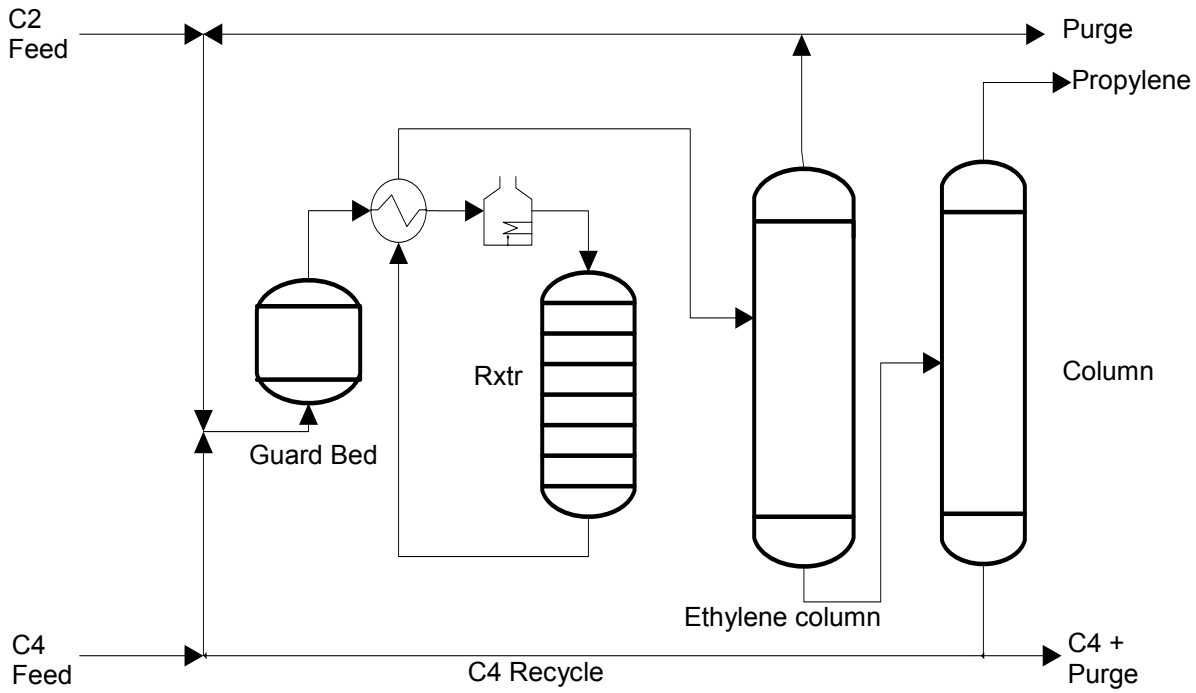

Figure 3.2.: The OCT™ process (Mol, 2004)

3.2.2 The Shell Higher Olefins Process (SHOP)

The Shell (SHOP) process according to Leeuwen (2004) includes a heterogeneous metathesis reaction step for the production of α-olefins. In the first step, ethylene is oligomerised in the presence of a homogeneous catalyst and a polar solvent, giving even-numbered α-olefins with a Schultz-Flory distribution. In the second stage, these alkenes undergo double bond isomerization over a solid alkali-metal based isomerization reactor to an

equilibrium mixture of terminal alkenes (Mol, 2004). In the third stage, the mixture is upgraded by metathesis to detergent range internal olefins (C11-C14). The desirable C11 to C14 olefins are separated by distillation and fractionated into individual compounds for use as co-monomers for further processing into plasticizer and detergent alcohols, or synthetic lubricants. Shell Chemicals units at Geismar, USA, produces 920 000 tonnes per year of higher alkenes using this technology (Singh, 2006). The olefins formed are immiscible with the solvent, product and catalyst phases are thereby readily separated so that the Ni catalyst can be recycled repeatedly (Mol, 2004).

3.2.3 The Meta-4 process

The Institute of Petroleum in France and the Chinese Petroleum Corporation have jointly developed a process for the production of propene, called Meta-4 (Mol, 2004). In their process, ethylene and 2-butene react with each other in the liquid phase in the presence of a Re_2O_7/Al_2O_3 catalyst at 35 ^oC and 60 bar. The process is not yet commercialized mainly because of the cost of the catalyst and the requirement of a high purity of the feed stream (Mol, 2004).

3.2.4 The Polynorbornene process

The first commercial metathesis polymer according to Banks et al. (1982) was polynorbornene, which was put on the market in 1976 by CdF-Chimie in France, and in 1978 in the USA and Japan, under the trade name Norsorex^{TM}. The polymer is obtained by ROMP of 2-norbornene (bicyclo [2.2.1]-2-heptene), the Diels-Alder product of dicyclopentadiene and ethylene, and gives a 90 % trans-polymer with a very high molecular weight (>3×10^6 g/mol) and a glass transition temperature (T_g) of 37 °C. The process uses a $RuCl_3$/HCl catalyst in butanol, operates in air, and produces a useful elastomer. Due to the difference in density between the catalyst phase and product, it is possible to achieve lower than ppm losses of catalyst in product stream.

3.2.5 Polydicyclopentadiene

The technology using the well-defined Grubbs ruthenium catalyst is made available for poly-DCPD production by Materia (Pasadena, CA, USA) (Van Arnum, 2003). Cymetech also uses the technology of DCPD polymerization based on ruthenium catalysis to produce polymers under the trade name Prometa™. The difference in weight between the polymer product and the catalyst allows the recovery and reuse of the catalyst without significant losses.

3.2.6 Metathesis of 1-octene

Although metathesis reaction has been investigated for producing long chain alkenes (C10-C18) from low value alkenes (C5-C9) (Ivin and Mol, 1997, Mol, 2004, Sanford, 2003, Jordaan et al., 2006, Boeda et al., 2008, du Toit et al., 2014, Lehmann et al., 2003, Van der Gryp et al., 2012, Vougioukalakis, 2012, du Toit et al., 2013) none have yet been implemented and commercialised. Major obstacles to the commercialisation of homogeneous metathesis technology for bulk chemical products include the relatively short lifetime of the catalysts, and side reactions (such as isomerisation and cross metathesis) that take place concurrently with self-metathesis.

Homogeneous metathesis precatalysts including Grubbs (1^{st}, 2^{nd}) generation, Hoveyda-Grubbs (1^{st}, 2^{nd}), and ruthenium allenylidene catalyst precursors have been investigated extensively for 1-octene metathesis. According to Stark et al. (2006), many of these reactions feature high selectivities and high reaction rates in the first run which then decrease upon recycling or deactivation of the catalysts. Jordaan et al. (2006) investigated the catalytic activity and selectivity of the Grubbs 1^{st} generation precatalyst, (**Gr-1**) towards the primary metathesis products, in the 1-octene metathesis reaction. Grubbs 1^{st} generation precatalyst, (**Gr-1**) is active for the metathesis of 1-octene at 25 ^{o}C yielding 7-tetradecene as the major product even at 1-octene/Ru molar ratio of 10 000. However, the product mixture consisted of three groups of products, i.e. primary metathesis products (PMP), isomerisation products (IP) and secondary metathesis products (SMP). Jordaan et al. (2006) observed that using **Gr-1** precatalyst, 1-octene was converted to approximately 62 % 7-tetradecene (PMP)

and 5 % SMP due to simultaneous double bond isomerisation and cross metathesis. This indicates that Grubbs first generation precatalyst (**Gr-1**), has a high selectivity towards PMP (94%). Similar conclusions could be drawn for Hoveyda-Grubbs first (**HGr-1**) and second generation (**HGr-2**) pre-catalyst reported by different authors. Several authors (Jordaan et al., 2006, Boeda et al., 2008, du Toit et al., 2014, Lehmann et al., 2003, Van der Gryp et al., 2012) have confirmed that temperature has a strong influence towards product distribution in olefin metathesis. Table A.1 in Appendix A summarises some of the best catalysts results of 1-octene metathesis reactions from the reviewed literature.

3.2.6.1 Effect of temperature on product distribution

During metathesis reaction, temperature significantly affects the product distribution. As the reaction temperature increases from 30 to 100 °C, the percentage of PMP products decreases, while IP and SMP formations becomes significant (Lehmann et al., 2003, Jordaan et al., 2006, Du Toit et al., 2014). Van der Gryp et al. (2012), Van der Gryp et al. (2010), and Du Toit et al. (2013) have observed that when the temperature is increased above 50 °C, the formation of IP started to increase rapidly and PMP formation decreases. du Toit et al. (2014) also observed that at temperatures ≥ 80 °C, an increase in SMP formation was visible for all the pre-catalysts due to possible precatalyst decomposition or reversible allyl-hydride formation. Van der Gryp et al. (2010) have also shown that, when the temperature increases above 50 °C, IP and SMP increases exponentially (from 11 % to 40 %). It can be seen again from Table A.1 in Appendix A.3 for all precatalysts, that within the observed optimal temperatures, the selectivity towards PMP was highest at low temperatures (< 60 ^{o}C) and low for high temperatures especially >80 ^{o}C although catalytic activities (TON) increased with temperature. In reaction engineering, the optimal temperature is normally that which minimises formation of by-products (IP, SMP) therefore decreasing separation costs and loss of yields but also ensuring shorter reaction times so as to minimise reactor sizes.

3.2.6.2 Catalyst activity and extent of reaction

A number of authors have investigated the effects of several process parameters on catalysts activity and extend of reaction. Boeda et al. (2008) investigated the activity of Phoban-based

Ru precatalyst in the self-metathesis reaction of 1-octene at different temperatures ranging from 40 to 60 °C and 1-octene/Ru molar ratio of 9 000 in different solvent systems and noted that higher final conversions were obtained at higher temperatures. According to Boeda et al. (2008), higher conversions were obtained when the catalyst was introduced as is, rather than in toluene solution. Motoboli (2010) also confirms that second generation Grubbs catalysts has a high activity than first generation Grubbs (**Gr-1**) catalysts. The overall efficiency of the pre-catalyst (TON) defined as the number of 1-octene molecules that are converted to metathesis products by one molecule of a pre-catalyst, was found to be 2756 for **Gr-2** and 1429 for Gr1. Van der Gryp et al. (2012) also observed that 1-octene/precatalyst molar ratio have a little effect on TON up to 1-octene/precatalyst molar ratios of 10 000. The TON only started to drop as 1-octene/precatalyst molar ratio increases above 10 000.

3.2.6.3 Catalyst stability and alkene isomerisation

Olefin isomerization reaction is responsible for cross metathesis reactions, which leads to loss of yield and low selectivity. Schrock et al. (2003) conducted a model study to determine the extent to which olefin isomerization occurs during olefin metathesis of simple 1-octene with Grubbs ruthenium catalysts and Schrock's molybdenum catalyst. It was found that the N-heterocyclic carbene ligated ruthenium complex promotes extensive isomerization of both internal and terminal olefins at temperatures of 50-60 ^{o}C, whereas the bisphosphine ruthenium complex and Schrock's molybdenum complex do not. Schrock molybdenum did not promote significant isomerization of 1-octene or 2-octene at 30 or 45 ^{o}C. The latter kinetic situation would be expected to yield a distribution of products typically classified under primary metathesis products.

First and second generation precatalyst were found to promote olefin isomerization to a very small extent after long reaction times although temperature played a significant role towards isomerization (Schrock et al., 2003). According to Lehmann et al. (2003), simultaneous metathesis and isomerization could easily describe the formation of a product mixture (PMP, IP, SMP) during the reaction of 1-alkenes. The current conceivable pathway for the formation of these olefins by isomerization and metathesis is illustrated in Scheme 3.1.

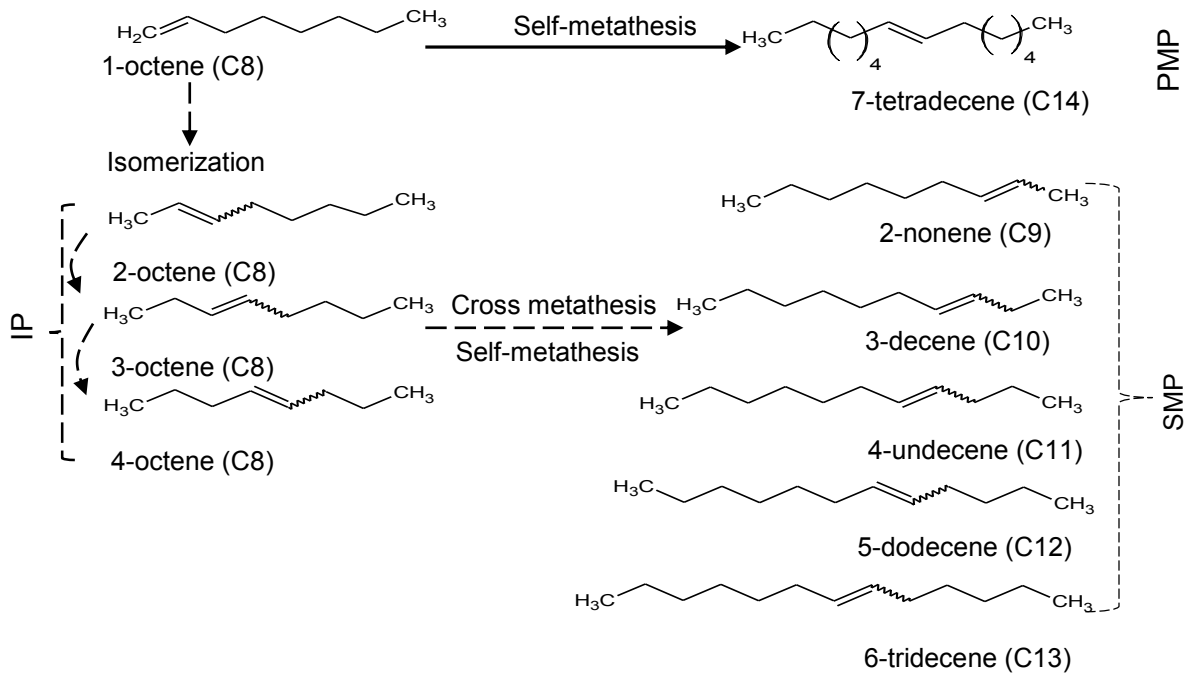

Scheme 3.1.: Typical reactions and pathways leading to PMP, IP and SMP olefins by olefin isomerization and metathesis (adapted from Lehman et al., 2003, Van der Gryp, 2009).

3.2.6.4 Selection of operating conditions

Jordaan et al. (2006) and Lehmann et al. (2003) confirmed the mechanistic viewpoint suggested by Van der Gryp et al. (2012) which states that two competing mechanisms which are temperature dependent are responsible for the product distribution in metathesis reaction systems. One mechanism is towards the selective formation of PMPs and SMPs (metathesis active mechanism) and the other is selective towards the formation of IP's (isomerization active mechanism). According to Van der Gryp et al. (2012), the isomerization active mechanism starts to occur at temperatures above 50 °C, while the metathesis active mechanism is observed for the whole temperature range. du Toit et al. (2014) concluded that at temperatures above 80 °C, the precatalysts starts to decompose, lose activity for metathesis and possibly deactivates and promotes isomerisation reactions. Reaction engineering identifies a small reactor size and maximization of PMP products as the two extremely important requirements in designing a reactor. For designing multi-reaction reactors such as this reaction system, the objective must be to minimize the formation of undesired products

and to maximize the formation of the desired product, because the greater the amount of undesired product formed, the greater the cost of downstream separation processes. A reactor must therefore be designed in such a way that the selectivity and TON are maximized. From an economic standpoint, maximizing selectivity and TON will maximize profits.

3.2.6.5 Selection of optimal precatalyst loading

In separate experimental investigations by Van der Gryp et al. (2012), Huijsmans et al. (2009), and du Toit et al. (2014) using different metathesis precatalysts, the TON generally increased with 1-alkene/precatalyst molar ratios. The optimal 1-octene/**HGr-2** molar ratio according to Van der Gryp et al. (2012) was found to be 10 000 as further increase in 1-octene substrate resulted in a significant drop in TON. However, catalyst load did not show any significant effect on selectivity with relatively constant values of 96 % at 1-octene/precatalyst molar ratios of 5 000 and 10 000 respectively. Hence, from economic and environmental point of view it is important to operate the reactor at high 1-octene/precatalyst loadings.

3.2.6.6 Selection of catalyst

Grubbs' "first-generation" ruthenium catalyst possesses in general a remarkable application profile combining satisfactory activity with an excellent tolerance for a variety of functional groups and moisture but unfortunately, its lifetime in the reaction medium is limited (Grubbs and Chang, 1998, Schrock, 1998, Furstner, 2000, Trnka and Grubbs, 2001, Hoveyda and Schrock, 2001). The more expensive but more stable and active "second-generation" catalysts are gaining popularity (Vougioukalakis, 2012). Despite general superiority offered by modern homogeneous Grubbs and Hoveyda–Grubbs catalysts, they share some disadvantages. The most undesirable feature of these complexes is the formation of ruthenium by-products which are difficult to remove from the reaction products, presenting a problem when the olefin metathesis reaction is used in pharmaceutical processes (Bhanushali et al., 2013). However, most of these undesirable characteristics can be minimised by operating the reactor at <60 °C (Lehmann et al., 2003, Jordaan et al., 2006, Du Toit et al., 2014. Van der Gryp et al., 2012 and Du Toit et al., 2013). Table 3.1 is a comparison of some commercial metathesis catalysts.

Table 3.1.: Comparison of different commercial catalysts (du Toit et al., 2014)

Precatalyst	Optimum temperature[a]	Formation of IPs[b]	Formation of SMPs[b]	Relative activity[c]	Relative life-time[d]
Gr-1	Low (30 °C)	>70 °C	X	2801	≈ 2
Gr-2	Low(30 °C)	>60 °C	>60 °C	5337	≈ 3
HGr-1	Low(30 °C)	>50 °C	X	4458	≈ 8
HGr-2	Medium (50 °C)	>60 °C	>60 °C	6448	≈ 10

[a] Temp which gives highest selectivity to PMP at catalyst load 7 000

[b] temperature where > 35 starts to format catalyst load 7000 (molar ratio)

[c] TON at optimum temperature and catalyst load of 10 000

[d] time in hrs measured of catalyst activity for PMP formation with consecutive separation and reuse

3.2.6.7 Effect of solvent

According to Van der Gryp (2009), the addition of organic solvents had a significant effect on the metathesis, and is mostly detrimental. Table 3.2 shows the influence of different solvents towards the metathesis reaction of 1-octene with precatalyst **HGr-2** was investigated at 50 °C and a precatalyst load of 7000.

Table 3.2.: Effect of different organic solvents on the metathesis of 1-octene at 50 °C using HGr-2 (Van der Gryp, 2009)

Solvent	C8	PMP %	IP %	SMP %	S %	TON
(-) neat	30.16	68.60	0.24	1.01	98.22	4802
Toluene	57.25	41.25	0.25	0.98	96.50	2887
Acetic Acid	94.53	2.23	3.09	0.15	40.77	156
Phenol	87.40	11.01	1.50	0.10	87.36	771
Ethanol	90.05	2.52	6.73	0.71	25.33	177

PMP = Primary metathesis produsts (%)

IP = Percentage of isomeric products (%)

SMP = Percentage of secondary metathesis products (%)

S = Selectivity to PMP = $\frac{PMP}{PMP+IP+SMP}$ %

3.2.7 Summary of olefin metathesis

Olefin metathesis is an organic reaction that entails the redistribution of fragments of alkenes (olefins) by the scission and regeneration of carbon-carbon double bonds. Catalysts for this reaction have evolved rapidly for the past few decades. Because of the relative simplicity of olefin metathesis, it often creates fewer undesired by-products and hazardous wastes than alternative organic reactions. Olefin metathesis was first commercialized in petroleum reformation for the synthesis of higher olefins from cross metathesis products (alpha-olefins) from the Shell Higher Olefin Process under high pressure and high temperatures.

To the author's knowledge, the simulation and operation of a commercial plant for the self-metathesis of low value olefins (C5-C9) from a Fischer-Tropsch Synthol product stream is not reported in literature. The low activity of commercially available catalysts and challenges of recovery and separation of the homogeneous catalysts from the reaction product have hampered commercialization.

3.3 Hydroformylation

One of the most important applications of homogeneous catalysis according to Zagajewski et al. (2013) is the hydroformylation of unsaturated hydrocarbons. The hydroformylation or oxo-reaction is the transition metal mediated addition of carbon monoxide and dihydrogen to the double bond of an alkene. It is one of the most versatile methods for the functionalization of C=C bonds and can be considered consequently as a very robust synthetic tool (Kegl, 2015). The primary products of the exothermic reaction are aldehyde isomers. Like many landmark discoveries, hydroformylation was discovered serendipitously. In 1938, while investigating the intermediacy of alkenes in Fischer-Tropsch reaction, Otto Roelen discovered that a formyl group is added to the olefinic double bond by the use of synthesis gas (CO/H_2) in the presence of a homogeneous transitional catalyst (Roelen 1934, 1964).

According to Sharma and Jasra (2015), the development of hydroformylation, which originated within the German coal-based industry, is considered one of the premier achievements of 20th century industrial chemistry. According to Kohlpaintner et al. (2001), the 60 years of oxo-syntheses has experienced at least five quantum leaps of development (1) “Diaden process” with heterogeneous cobalt catalysts; (2) high pressure process with homogeneous Co catalyst; (3) introduction of Rh as the central atom of complex catalysts and (4) of ligand-modified Rh or Co catalysts (5) the two-phase catalysis. Sharma and Jasra (2015) defined the process as inspired by three phases of catalytic developments namely first generation (Co-metal), second generation (Rh-modified by PPh_3) and the third generation (Rh-modified by TPPTS).

The developments are all inspired by the need to achieve high catalysts activity, moderate operating conditions and more significantly the need to minimize leaching of the highly expensive Rh-based catalyst. Ever since, this clean and mild method for the functionalization of hydrocarbons has grown to be among the most important homogeneously catalysed reactions in industry (Kohlpaintner et al., 2001).

Industrial processes generally use Rh-based catalysts for lower olefins and cobalt (Co)-based catalysts for C5+ olefins (Billig and Bryan, 2000). However, Co-based catalysts require rather harsh conditions. For example, the most common cobalt catalyst, cobalt carbonyl hydrides, requires pressures of 200−350 bar and temperatures of 150−180 °C in order to prevent decomposition of the catalyst and avoid syngas starvation (Frohning et al., 2002). Cobalt-based catalysts require more forcing conditions than their rhodium counterparts, a consequence of their lower catalytic activity, and although separation technologies have been developed for Co systems, they are by no means simple (Frohling and Kohlpaintner, 1996). Recycling of the Co-catalyst is usually accomplished in a series of unit operations that are not only energy intensive but also require significant amounts of acid and base resulting in sizable waste streams (Cornils, 1980). On the other hand, Rh-based catalysts are known to provide higher activity and better product selectivity toward the linear aldehydes at much milder operating conditions (40−130 °C, 10−40 bar).

The annual production and consumption of aldehydes is 12 million tons per year with expected growth rate of 4.0 % of various aldehydes for the manufacture of detergents, soaps, and plasticiser alcohols and speciality chemical industry (Sharma and Jasra, 2015). Current technology for the synthesis of detergent range alcohols (C11-C20), which produces over 1 million tons per annum, is based on less efficient cobalt catalysts, often modified with tertiary phosphines (Webb et al., 2003). According to Franke et al. (2012), hydroformylation also has some potential for removing unsaturated compounds from the refinery cracking process. Commonly these undesired olefins, which might produce viscous polymers or solids capable of blocking the carburettors and injectors of vehicles, are converted into harmless alkanes by hydrogenation (Franke et al., 2012).

In general, the *n*-aldehyde is desired product due to biodegradability of linear carbon chains (Wiese and Obst 2006) but highly branched products are often desirable for their properties (Marray et al. 1998) e.g. as lubricating oil additives in order to depress the freezing point of the oil. This has led to the key parameter for regioselectivity in hydroformylation, which is specified by the l/b-ratio (Van Leeuwen and Claver, 200, Behr et al., 2012; Cornils and

Hermann, 2002). Figure 3.3 shows a basic process flowsheet depicting the main steps of hydroformylation process.

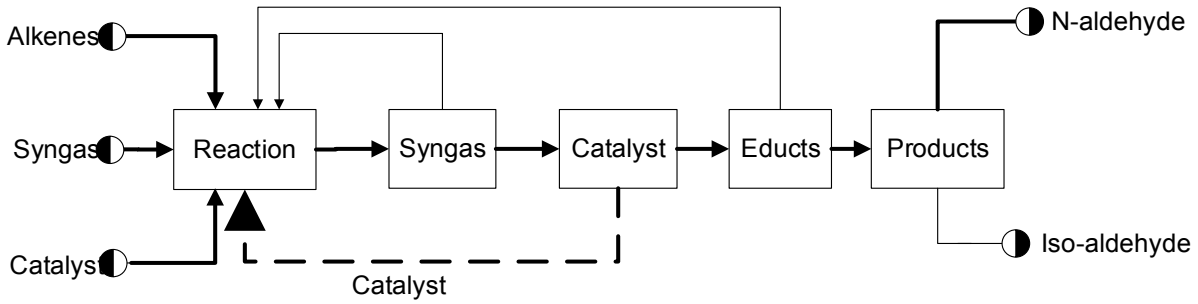

Figure 3.3.: Basic flowsheet of the hydroformylation process (redrawn, Steimel et al., 2013)

The most important oxo products are in the range C3 – C19. The economic importance of oxo synthesis is mainly based on *n*-butanal with a share of 73 % of overall hydroformylation capacity (Subramanian et al., 2014). The *n*-butanal is converted to 2-ethyl-hexanol which is used in the production dioctyl phthalate (DOP), a plastic used in polyvinyl chloride (PVC) applications.

Industrially important oxo-processes can be divided into four main catalytic systems (Mol, 2003). Table 3.3 gives an overview of these catalyst system and reaction conditions. The most important of the rhodium based process on an industrial scale uses so-called phosphine modified catalyst system. The unmodified rhodium carbonyl complex is used for the reaction of special olefins (Ruhrchemie Process).

Table 3.3.: List of industrial important oxo processes and process parameters (Mol, 2003)

Catalyst Metal Variant	Cobalt Process		Rhodium Process	
Ligand	Non	Modified Phos	Non	Modified Phos
Process	BASF	Shell	Ruhrchemie	RHC/RP
Active Catalyst	**$HCo(CO)_4$**	**$HCo(CO)_8/(L_3)$**	**$HRh(CO)(L)_3$**	**$HRh(CO)(L_3)$**
Phosphine: metal ratio	-	02:01	50:1	50:1-100:1
Pressure (bar)	200-300	50-100	15-25	40-60
Temperature (°C)	110-160	160-200	80-120	110-130
Cat conc.(%metal/Olefin)	0.1-1.0	0.6	0.01-0.06	0.001-1
Products	Aldehydes	Alcohols	Aldehydes	Aldehydes
n/iso-Product ratio	80:20	88:12	50:50	92:8
Olefin hydrogenation (%)	<2	15	5	<2
By-products amounts	High	High	Low	Low
Catalyst recovery	difficult	Simpler	for C_3 and C_4	Facile

Up until the mid-1970's cobalt was used as catalyst metal in commercial processes e.g., by BASF, Ruhrchemie, Kuhlmann (Mol, 2003). Although the activity of rhodium catalysts is about 1 000 times higher than cobalt, the application of cobalt catalysts in technical hydroformylation of long chain olefins was widely spread due to the lower Co-metal price (Zagajewski et al. 2015, Xie et al., 2014). However, Rh-metal is highly promising for technical usage, because of milder reaction conditions (lower temperature and pressure). The ligand modification introduced by Shell researchers was a significant progress in hydroformylation as it allowed separation, recovery and reuse of expensive Rh-catalysts (Sharma and Jasra, 2015).

3.3.1 Rhodium based hydroformylation processes

Rh-based hydroformylation processes are also known as low pressure oxo-processes (LP Oxo) due to comparatively low operating pressures than Co-based processes (Beller et al.,

1999). The highly sophisticated RCH/RP process, which together with Union Carbide's Mark IV process represents the state-of-the-art in today's oxo technology in terms of the variable and fixed costs per ton of product (Kohlpaintner et al., 2001). Major factors attributing for the reduction in the overall manufacturing costs are a highly efficient catalyst and energy recovery system and minimum capital requirements for an RCH/RP oxo unit. According to Gursel et al. (2015), the Rh-catalysed process is an environmental benign and green process. Cole-Hamilton and Tooze (2006) have also confirmed that the environmental (E) factor for conventional cobalt catalyzed hydroformylation processes is about 0.6–0.9. This factor falls below 0.1 for the RCH/RP process due to conservation of resources and minimization of waste (Cole-Hamilton and Tooze, 2006).

The lifetime of Rh catalyst charge may exceed 1 year under the condition that sufficient purity of the feed and careful process control is guaranteed (Franke et al., 2012). According to Beller et al. (1999), for plants operating the LP Oxo^{TM} process, the variable cost contribution from rhodium is often barely US $1 per ton of product, which is extremely modest but however, the rhodium price can have a large impact on the working capital needed for a new plant investment. Rhodium is currently 25 times more expensive in U.S. dollar terms than it was when the strong economic drivers for rhodium oxo-synthesis first emerged in the early 1970s while the price of aldehydes has only increased to four times (Market and Marketers, 2016). The increase in the rhodium price have caused concerns among companies contemplating investing in TPP/rhodium-based technology. The main problem of rhodium is its high, very volatile price over the years. The price on the world market is dictated by the automotive industry, which uses ~80 % of the metal in catalytic converters. In July 2008, rhodium broke the $220.000 per kg barrier for the first time (Kitco, 2016). Because of the global financial crisis, which began in the last quarter of 2008, the rhodium price fell from this level to about $40,000 per kg within a few months. The Volkswagen scandal of 2015 has also seen rhodium prices falling to $ 100,000 per kg in December of the same year (Infomine, 2015).

The higher price of rhodium is offset by mild reaction conditions, simpler and therefore cheaper equipment, high efficiency, and high yield of linear products and easy recovery of the catalyst

(Beller et al., 1999). The reactions are usually carried out at a temperature range of 120−190°C and a syngas pressure of 10−30 bar in large industrial companies, such as BASF, Exxon, Sasol, and Shell (Franke et al., 2012). In addition, with respect to raw material utilization and energy conversation, the LP Oxo™ processes is more advantageous than the cobalt technology, thus leading to their rapid growth (Dreimann et al., 2015). One of the main differences between large-scale Rh-catalysed hydroformylation processes according to Franke et al. (2012) is the technology used to separate the product and the catalyst with the aim of catalyst recycle.

3.3.1.1 The Union Carbide Corporation (UCC) process

The process of hydroformylation of propylene was developed by a joint venture between Union Carbide Corporation (UCC), Johnson Matthey and Co. and the former Davy Powergas Ltd. (today Davy McKee) (Beller et al., 1999). Several modifications predominantly aimed at improvements in the product/catalyst separation led to the emergency of two process versions, which were later on named the gas recycle process and liquid recycle process (Dreimann et al., 2015). The gas phase recycle, aimed at removal of the product aldehydes from the catalyst solution by applying a large gas recycle in order to evaporate the aldehydes (Pruett and Smith, 1969). The catalyst solution consisted of high boiling aldehyde condensation products (dimers, trimers and various other aldehyde consecutive products) in which an excess of triphenylphosphine and Rh complex itself was dissolved (Morrel and Sherman, 1978).

However, according to Brewester and Pruett (1977) requirements for constant reaction mixture, temperature and pressure conditions, gas flux for continuous evaporation of the aldehyde product resulted in the process being a fairly complex one. To avoid these drawbacks and following RCH/RP's excellent experiences with liquid recycles, the gas recycle was replaced by the liquid recycle variant Figure 3.4, which is in use in most modem LPO plants.

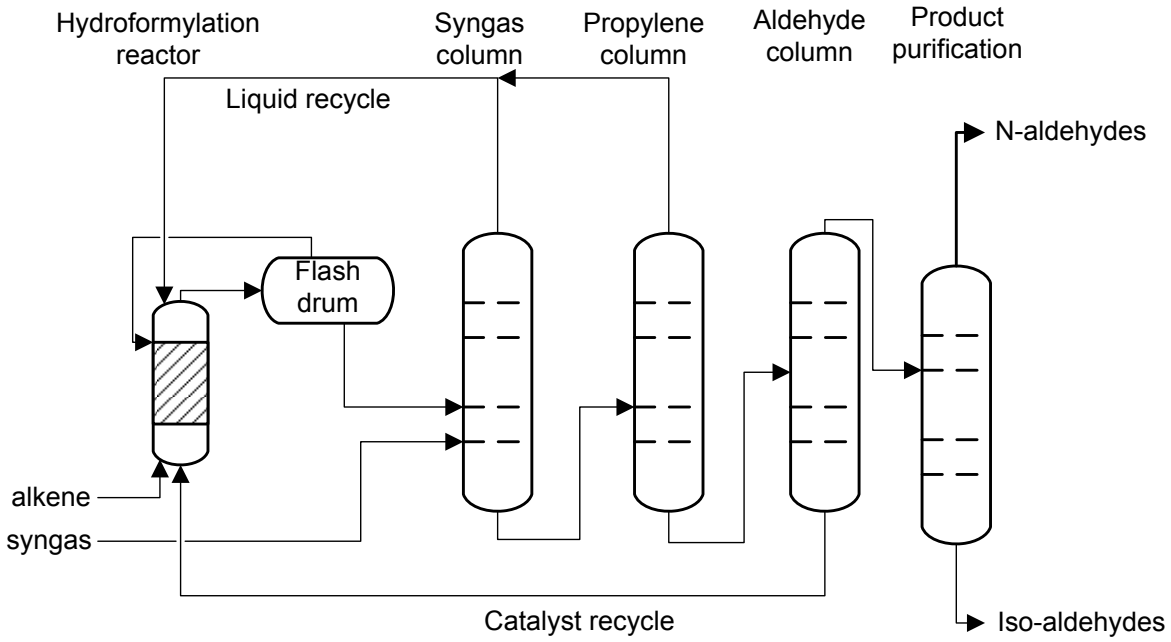

Figure 3.4.: UCC liquid recycle process (Beller et al., 1999)

3.3.1.2 The Ruhrchemie/Rhone-Poulenc (RCH/RP) process

The idea of E. Kuntz (Rhone-Poulenc) to apply water-soluble rhodium complexes as catalysts for the hydroformylation reaction was taken up and commercialized by Ruhrchemie AG for the hydroformylation of propylene. After only two years of development on the laboratory scale the first plant was erected in 1984 followed by rapid further increases in capacity to more than 11 million tonnes per year today (European Chemical News, 2012). According to Obrecht et al. (2013), the operational simplicity, robustness and the excellent economics of the process (loss of rhodium by leaching into the organic phase lies in the ppb range) make the RCH/RP a benchmark process in the field of aqueous biphasic transition metal catalysis.

The RCH/RP unit is essentially a continuous stirred tank reactor (R1), followed by a phase separator (FD) and a strip column (C1 & C2) as shown in Figure 3.5. The reactor (R1) which contains the aqueous catalyst, is fed with propylene and syngas. The crude aldehyde product passes into decanter (FD) where it is degassed and separated into the aqueous catalyst solution and the organic aldehyde phase.

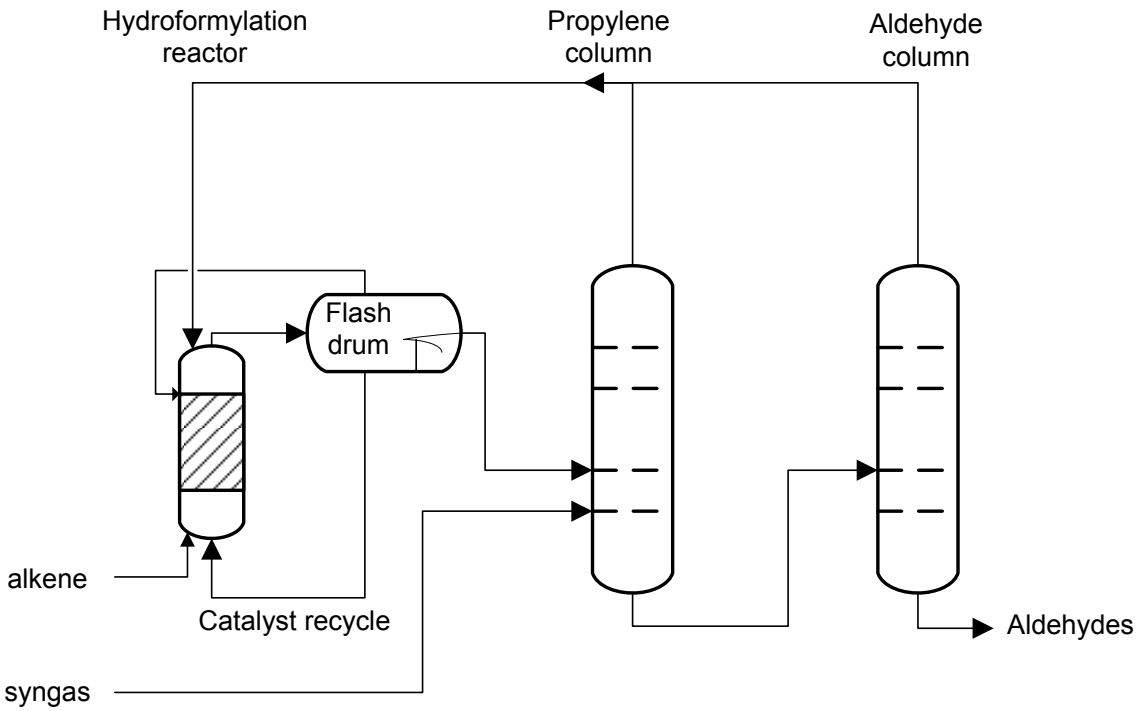

Figure 3.5.: The Rhuhiechemie/Rhone Poulenc process (adapted from Wise and Obst, 2006)

In aqueous phase hydroformylation, slightly higher concentration of catalyst (150-500 ppm rhodium) at reaction temperature (120-130 ^{o}C) and pressure (40-60 bar) are used to achieve the satisfactory levels of space time yields (Sharma and Jasra, 2015). Due to the use of a water soluble catalyst system the catalyst can be considered to be 'heterogeneous' hence very simple recycling of the homogeneous oxo-catalyst by immobilization in "mobile support" water (Dreimann et al., 2015). Accordingly, excellent economics owing to minimal losses of the catalyst metal rhodium, low purity demands on the reactants, excellent process potential from safety and environmental points of view (Sharma and Jasra, 2015).

The process is very energy efficient as the reaction heat from the exothermic hydroformylation is recovered and used in the reboiler of the distillation column that separates the organic phase into *n*- and *iso*-butyraldehyde (Cole-Hamilton and Tooze, 2006). Therefore, during its lifetime less than 1 ppb of Rh-catalyst is lost reflecting high economy of the process (Baerns et al., 2006). The high selectivity, yields and high-energy efficiency achieved with this RCH/RP process enable it to have about 10 % lower manufacturing costs compared to other Rh

catalyzed hydroformylation processes that do not use aqueous phase operation (Wiebus and Cornils, 1994).

3.3.1.3 The BASF process

Developed nearly in parallel to UCC's LP Oxo^{TM} process, the BASF process also makes use of a gas recycle to separate aldehydes and catalyst solution (Schwirten and Kummer, 1983). Propylene and synthesis gas (CO/H_2= 45/55) are fed to a stainless steel tank reactor with intense mixing. While the catalyst remains in the reactor, aldehydes are withdrawn by a recycle gas stream, condensed by partial cooling and freed from dissolved gases in a stabilizer column (Fischer et al., 1981). The combined gaseous streams from these operations are recompressed and sent to the reactor.

3.3.1.4 The Mitsubishi process

Mitsubishi uses a modification of the Rh-catalyzed high-pressure hydroformylation of long-chain olefins octene and nonenes (Onada, 1993, Sato et al., 1994). Hydroformylation is carried out in the presence of the weakly complexing triphenylphosphine oxide (TPPO) as ligand at pressures up to 200 bar. It is claimed that the activity of rhodium is diminished less by TPPO than by TPP, thus reducing the rhodium inventory in comparison to TPP as ligand (Beller et al., 1999). According to Beller et al. (1999), TPP is added to stabilize rhodium catalyst before conventional distillation is used to separate catalyst from the organic product. TPP is then oxidized to TPPO before re-use of the catalyst solution by a non-disclosed oxidation procedure (OX) as shown in Figure 3.6. Part of the catalyst solution is purged for external upgrading.

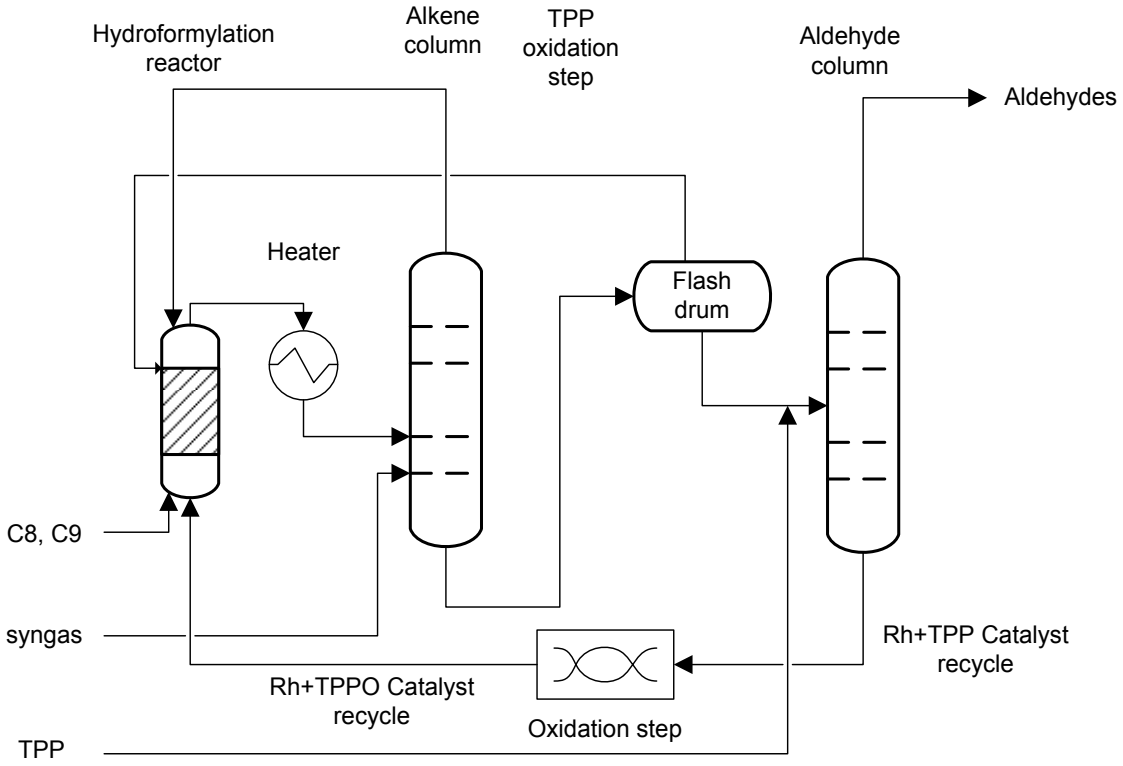

Figure 3.6.: Mitsubishi process (adapted from Beller et al., 1999)

3.3.1.5 The Technische Universitat Berlin (TUB) mini-plant

In the field of homogeneous catalysis, miniplants are often useful for the analysis and verification of new recycling concepts for catalysts. A continuously operated miniplant has been designed and investigated by Professor Schomacker's group at Technische Universitat Berlin, with special focus on the catalyst activity and recycling in the hydroformylation of 1-dodecene. According to Behr et al. (2012), experiments in a continuously operated miniplant allows a comprehensive optimization of the selectivity based on the entire process including all recycling streams. The results show that optimal reaction conditions of 110 °C and 50 bar and a mass fraction of surfactant of between 8 % is required to achieve yields above 50 % at the same time attaining low catalysts losses of close to 1 ppm.

Figure 3.7 shows the miniplant flowsheet diagram for **$Rh(acac)(CO)_2$**, and a Water/Marlipal solvent system for hydroformylation of long chain olefins at the miniplant conditions at TUD Dortmund, Germany.

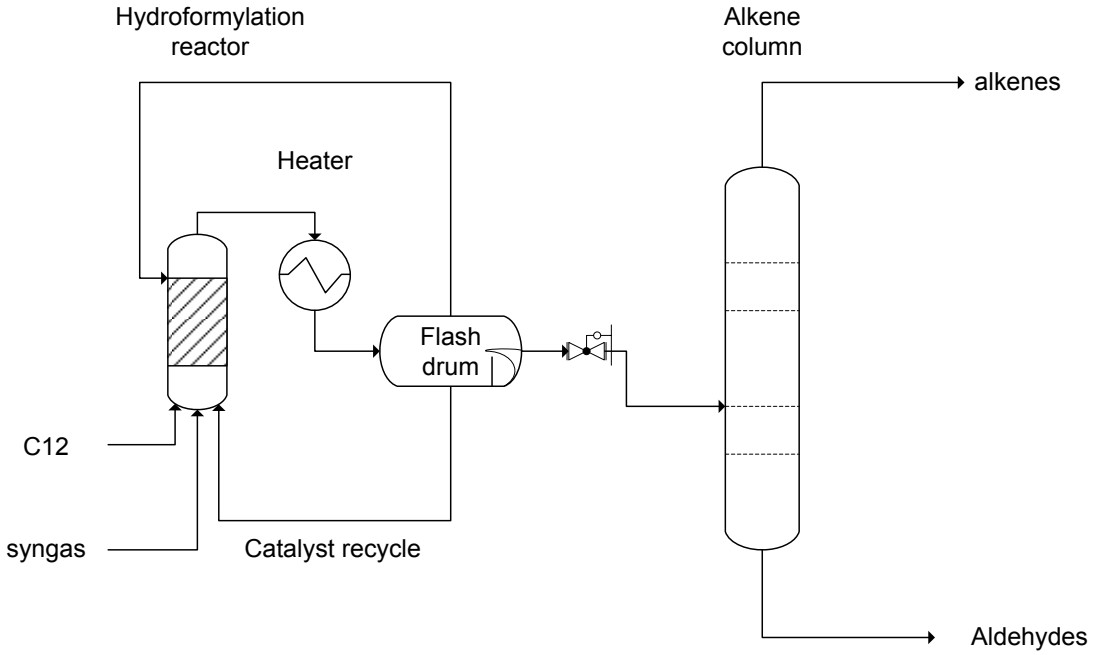

Figure 3.7.: Miniplant hydroformylation of 1-dodecene (redrawn Muller et al., 2013)

3.3.2 Hydroformylation of long chain alkenes

In the case of short chain olefins (Cn<C6) an efficient process, namely the Ruhrchemie-Rhone/Poulenc (RCH/RP) process has been developed to minimize the rhodium losses (Zagajewski et al., 2014, Hentschel et al., 2014, Porgzeba et al., 2015, Muller et al., 2014). Kohlpaintner et al. (2001) also confirmed that with the RCH/RP process it is possible to hydroformylate propene up to pentene with satisfying space time yields (STY). The rate of aqueous phase hydroformylation of alkenes depend upon the alkene solubility in water which makes process practicable at commercial scale (Sharma and Jasra, 2015). The gaseous olefins and the co-reactants hydrogen and carbon monoxide can be solved in an aqueous catalytic phase, where the liquid product directly forms a separate organic phase.

The solubility of long chain olefins in an aqueous phase is not sufficient, for example, C8 olefins are typically 1 000 times less soluble in water than propylene (Cornils, 1999). Zagajewski et al. (2016) observed the decrease in the olefin conversion rate with the increase in its chain length which he describes as due to the reduction of its reactivity. Previous work by Vogelpohl et al. (2013), Markert et al. (2013), Zagajewski et al. (2014) and Hentschel et al.

(2014), Sharma and Jasra (2015) have confirmed that reaction times are long and conversions are low and hence the concept is not applicable for these reactants (Cn ≥ C6).

3.3.2.1 The hydroformylation reaction system

Different media solutions have been proposed to enhance the solubility of higher olefins and hence reactivity during hydroformylation reactions. Hentschel et al. (2014), Steimel et al. (2014), Peschel et al. (2012), Kierdorf et al. (2014) and Hentschel et al. (2015) have confirmed successful results of hydroformylation of 1-dodecene and 1-octene in different thermomorphic solvent and liquid multiphase systems. According to Kierdorf et al. (2014), in order to ensure a fast reaction and ensure an efficient recycling of the precious catalyst-ligand complex, the reaction system must maintain a certain composition of the components.

Kierdorf et al. (2014) observed that the reaction solution must contain 20 wt. % 1-dodecene, 32 % of the polar solvent DMF and 48 % of decane in order to achieve high conversions and minimise catalyst leaching in the organic product. The TMS system was characterised as homogeneous above 85 ^{o}C and heterogeneous at lower temperatures allowing reaction mixture to be separated into organic product and aqueous catalyst phases. According to Kierdorf et al. (2014), conversions of 1-dodecene around 70 % and selectivities around 98 % towards the linear aldehyde products were observed in a CSTR reactor at 105 ^{o}C, 30 bar. Hentschel et al. (2014) used experimental results by Kierdorf et al. (2014) to develop a technoeconomic model. The results of technoeconomic study concluded that conversion and recycle rates affected the sizes of compressors and reactant recovery columns indirectly.

According to Porgzeba et al. (2015), a non-ionic surfactant is able to solubilize the hydrophobic substrate in an aqueous environment and thus supports the catalytic reaction and facilitates catalyst recycling in its active form. Rost et al. (2013) observed that the hydroformylation in a microemulsion solution started at 80 ^{o}C giving a conversion of about 50 %. According to Rost et al. (2013), an appropriate temperature has to be chosen in order to achieve a desired catalyst separation and that to ensure economic feasibility of overall process a further extraction step is needed to reduce catalyst losses to lower than 1 ppm. Muller et al. (2014) have reported hydroformylation results of 1-dodecene in CSTR reactor over a mini-plant

developed for the hydroformylation at 85 °C and 30 bar. Haumann et al. (2002a) investigated the **Rh-TPPTS** catalysed hydroformylation of 1-dodecene in a microemulsion using Marlipal O13/aqueous biphasic phase system and found out that the reaction rate was a function of the microemulsion concentration of the surfactant.

The use of surfactant with **Rh-TPPTS** catalyst in an aqueous solution resulted in reasonable TOF of 440 h^{-1} which is almost half the TOF of the RCH/RP (700 h^{-1}) process for the hydroformylation of propylene (Haumann et al., 2002a). Relatively poor selectivities for the *n:iso* ratio of between 70/30 and 80/20 was reported and thus lower than the ones obtained for propylene conversion in the two-phase RCH/RP process (95/5) (Haumann et al., 2002). Rost et al. (2013) investigated bidentate water-soluble ligands, like SulfoXantPhos in the hydroformylation reaction of 1-dodecene together with alkyl-phenol-ethoxylates (like Marlophen NP-9 from Sasol) as surfactants in N,N-dimethylformamide/*n*-decane system. High activities and selectivities of *n:iso* 98:2 % were observed.

Literature study have shown that no conversion of long-chain olefins was detected without addition of surfactant, but fast reaction rates are obtained when surfactants are used to formulate a multiphase system (Porgzeba et al., 2015). Schwarze et al. (2015) suggest that the selection of an appropriate surfactant for a reaction is crucial and has to be done carefully. Markert et al. (2013) investigated the hydroformylation of 1-dodecene using **$Rh(acac)(CO)_2$** and a ligand in a TMS system of N,N-dimethylformamide/*n*-decane system. According to Markert et al. (2013), overall aldehyde yields exceeding 95 % were reported with **Rh-TPPTS**. Homogeneity was observed above 90 °C and catalyst recycling was investigated and successful reused in a series of 30 runs. Steimel et al. (2013) observed high selectivities of n:iso of 98:2 % in homogeneous hydroformylation of 1-dodecene in liquid multiphase system (LMS) and thermomorphic solvent systems N,N-dimethylformamide/*n*-decane/methanol (TMS).

According to Muller at al. (2013), phase separation of the microemulsion after the reaction is very much dependent on the conversion as well as on the composition. Li et al. (2002) studied the hydroformylation of 1-dodecene in biphasic catalytic system containing mixed micelle

using a water-soluble rhodium phosphine complex, **$RhCl(CO)(TPPTS)_2$** in the presence of various micelles. High conversion and regioselectivities were observed in mixed micellar solutions than in single micelle. However, Li et al. (2002) model did not consider the recovery of the catalyst from the organic product which is an important aspect of the economical process.

3.3.2.2 Reaction scheme

The corresponding reaction network for the hydroformylation of 7-tetradecene (Scheme 3.2) was developed according to Leeuwen et al. (2000) and Koeken et al. (2011) models. The yield of 2-hexyl-nonanal can be enhanced by reducing the isomerization using an optimal process trajectory manipulating the process variables (T,p_{CO}) during the reaction (Market et al., 2013). From experimental investigations by Markert et al. (2013), Haumann et al. (2002a) and Muller et al. (2013) consecutive hydrogenation of the aldehydes leading to corresponding alcohols is not observed in hydroformylation of long chain olefins with Rh-catalysed systems at the typical reaction conditions. Scheme 3.2 shows the possible reactions during hydroformylation of 7-tetradecene.

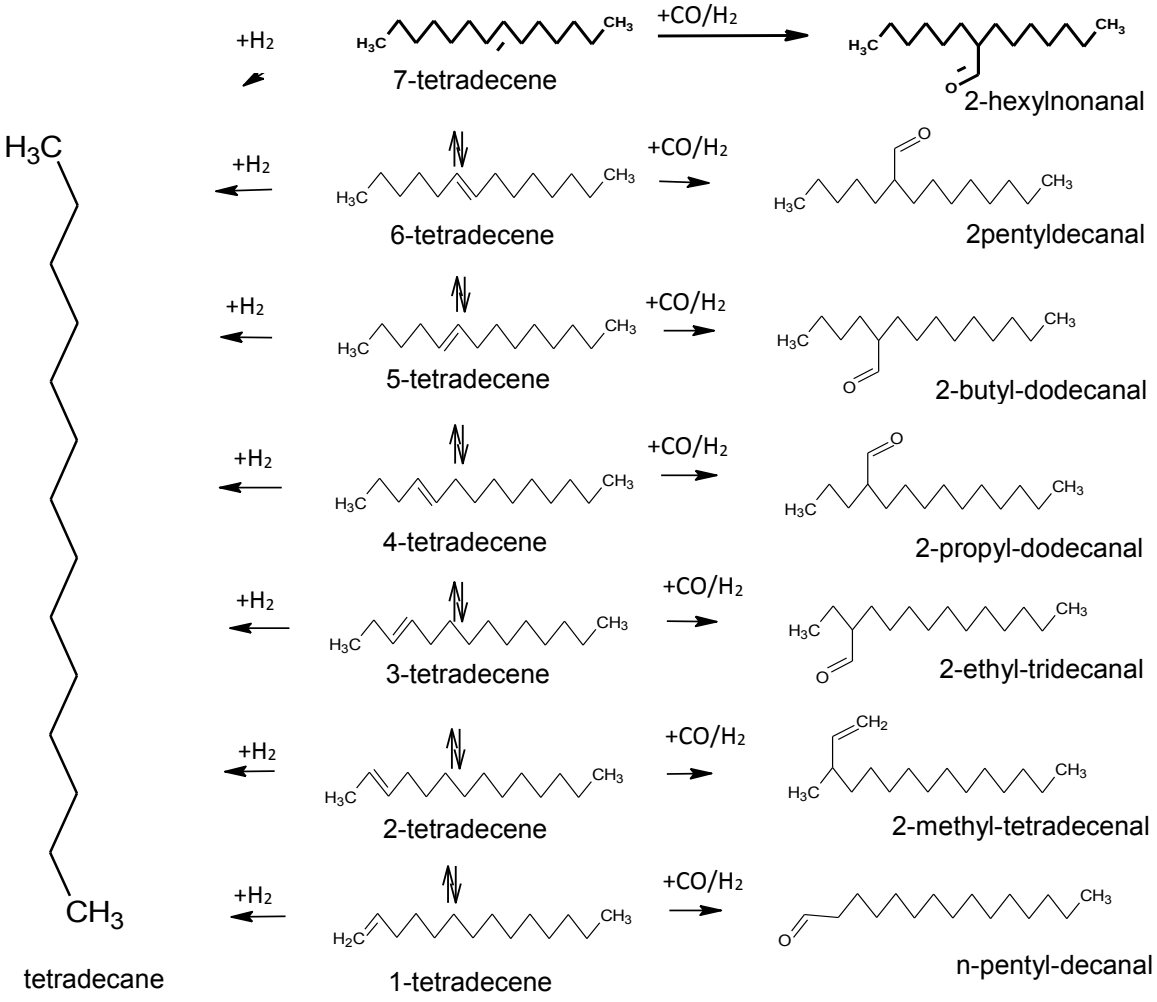

Scheme 3.2.: Illustration of main reaction and possible side reaction patterns during hydroformylation of 7-tetradecene (adapted from Markert et al., 2013)

3.3.2.3 Selectivity and product distribution

According to Dabbawala et al. (2011), interests in selective formation of the branched aldehydes in the case of linear alkenes have increased recently due to their use in the preparation of polyols and plasticizers. The production of branched aldehydes already represents 9 % of the world consumption of oxo-chemicals and is expected to increase steadily in the near future (Dabbawala et al., 2011). The catalytic systems which give branched aldehydes regioselectivity in linear alkene are limited. Literature has indicated that branched aldehydes are mostly formed during hydroformylation of internal alkenes. Of note is an investigation conducted by Haumann et al. (2002b) into the hydroformylation of 7-tetradecene

in a microemulsion solution. Haumann et al. (2002b) observed that the product distribution is predominantly 2-hexyl-nonanal. Albers et al. (2008) investigated the hydroformylation of 4-octene at syngas pressures ranging from 7 to 50 bar with a ratio of CO/H_2 of 1:1 and found that yield and conversion increased with increasing pressure. High syngas pressure favours hydroformylation over the isomerization of the starting olefin. Albers et al. (2008) concluded that, at a high pressure and with 4-octene used as a substrate, mainly internal aldehydes were formed. Table A.2 in Appendix A3 shows the different models and reactions conditions for the hydroformylation of long chain alkenes.

3.3.2.4 Effect of temperature

Generally, rhodium catalysed systems are run at moderate temperatures (80-190 °C) compared to cobalt catalysed processes mainly because rhodium catalyst is more reactive than cobalt catalyst (Beller et al., 1995). However, the optimum temperature will also be determined by the upper critical temperature of the solvent system which will determine extent of homogeneous mixture and how much reactant is in contact with the catalyst and ability to separate catalyst and product phases after reaction.

3.3.2.5 Effect of hydrogen partial pressure

The rhodium catalyst equilibrium depends on reaction conditions (T, C_{H2}, C_{CO}) and hence also the selectivity (Peschel et al., 2013). Hydrogen has a linear influence on the reaction rate and according to results of Peschel et al. (2013), the catalyst agglomerates if the hydrogen concentration is too low. Hence, a high CO/H_2 ratio will increase the activity of the hydroformylation system, which was proved experimentally to be between 0.8 and 1.2 for 1-dodecene by Haumann et al. (2002). However, if the hydrogen concentration is too high, the hydrogenation of the reactants and products will be promoted (Kiedorf et al., 2014, Peschel et al., 2013).

3.3.2.6 Effect of CO partial pressure

High CO partial pressures inhibited all reactions especially isomerisation (Kiedorf et al., 2014) indicating formation of inactive Rh-dimers and Rh-dicarbonyl complexes at high carbon

monoxide partial pressures. According to the Wilkinson cycle, a high CO concentration leads to the formation of an inactive species in the catalyst cycle. Therefore, a high CO concentration will reduce the activity of the hydroformylation system (Peschel et al., 2012) which is in accordance to Wilkinson cycle Figure 3.8.

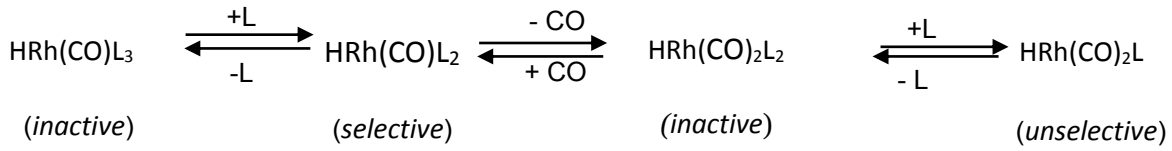

Figure 3.8.: Catalyst equilibrium of the TPPTS modified rhodium

3.3.2.7 CO: H2 stoichiometric ratio

According to Kierdorf et al. (2014), the CO/H_2 ratio affects the n/iso ratio and for the hydroformylation of 1-dodecene, the maximum amount of desired product tridecanal formed was observed for the stoichiometric ratio CO/H_2 = 1:1. It was observed that if CO partial pressure is increased the conversion of 1-dodecene was decreased, which decreased extent of the reaction. According to Haumann et al. (2002b), the formation of the unmodified rhodium species should result in an increased activity as well as decreased selectivity towards linear aldehydes.

3.3.2.8 Agitation on reaction rate

According to Haumann et al. (2002b), no significant influence on the rate of reaction was observed for stirrer speeds between 500 and 2000 rpm and experimental investigations can be conducted at 1500 rpm. Bhanage (1997) concurred that all reactions should be conducted at agitation speeds above 900 rpm to ensure that reactions occurred in kinetic regime.

3.3.2.9 Effect of catalyst concentration

The effect of the concentration of the catalyst precursor **$Rh(CO)_2$*(acac)*** (with the P:Rh ratio constant) was investigated by different authors (Bhanage et al., 1997, Hentschel et al., 2008, Haumann et al., 2002, Kiedorf et al., 2013) at constant partial pressures of H_2 and CO and

octene concentration. Haumann et al. (2002) confirmed that the rate of the reaction increased with an increase in the catalyst concentration with a first order dependence. This type of behaviour is expected since an increase in the catalyst concentration will enhance the concentration of active catalytic species and the rate of the reaction.

3.3.2.10 Ligands for special applications

A crucial point in the workup of a hydroformylation reaction is the separation of product and catalyst (Franke et al., 2012). In aqueous biphasic hydroformylation system, excellent water-soluble ligands are usually used to “fix” the metal complex catalysts in the aqueous phase. The immobilization of the noble rhodium catalyst in aqueous phase is crucial to the potential scale-up of this technique (Fu et al., 2008). When a surfactant is used to promote the aqueous biphasic hydroformylation of higher olefin, the addition of surfactant indeed can break the mass transfer barrier, and therefore accelerate the reaction. However, the surfactant can also lead to the leaching of the catalyst from aqueous phase to organic phase.

According to Fu et al. (2008), experimental results showed that increasing the amount of water-soluble ligand could significantly mitigate the catalyst leaching when surfactant was used. However, there exists a critical value for the mole ratio of TPPTS to surfactant, which is important for catalyst ‘fixation’. A lower mole ratio of TPPTS to surfactant will lead to catalyst leaching, whereas a higher ratio will cause the catalyst to be fixed in the aqueous phase (Fu et al., 2008). Different critical values exist for different surfactants. In best-case scenarios, the latter can be recycled and used for subsequent runs.

A breakthrough was the use of the sulfonated phosphine ligand TPPTS (trisodium salt of 3,3,3″-phosphinidyne tris(benzenesulfonic acid) in the Ruhrchemie/Rhone-Poulenc process for hydroformylation of propene, which, to the best of the author’s knowledge, is the only aqueous two-phase hydroformylation used in industry to date. TPPTS exhibits excellent solubility in water (~1.1 kg/L) and is in general insoluble in most organic solvents used for two-phase catalytic reactions (Franke et al., 2013).

3.3.3 Product purification

The purified aldehydes are essential intermediates for bulk and fine chemicals like diluents or odorants in the flavour and fragrance industry (Beierling et al., 2013). According to Hentschel et al. (2014) and Steimel et al. (2014) downstream processing require purities above 98 wt. %. Distillation is still the most commonly used separation technology in the chemical industry. However, due to close physical properties, the separation of close boiling mixtures is generally difficult due to low driving forces (Beierling et al., 2013, Micovic et al., 2012). Examples of close boiling mixtures are mixtures of isomers that are formed in some non-regiospecific reactions, such as hydroformylation.

According to Hentschel et al. (2014), the investment costs during hydroformylation of 1-dodecene to *n*-tridecanal are dominated by the product separation column, followed by compressor and reactor. The costs of the n/iso-column arise from the comparably difficult separation of the two very similar aldehydes; hence, a high number of stages is required (Hentschel et al., 2014). The separation process requires a large number of theoretical stages and a high reflux ratio, which lead to high investment and operating costs. According to Micovic et al. (2012), the distillation separation of long-chain isomers tends to be more costly or even technically infeasible due to the decreasing difference in boiling points with increasing chain length.

Several methods have been described for the separation of isomeric long-chain aldehydes. One separation technique combines a precipitation of the aldehydes with hydrogen sulfite compounds and a subsequent extraction (Beierling et al., 2013). Since amongst others the aldehydes are used as flavours, no impurities are allowed to remain in the aldehydes that affect the odour or smell, therefore this method is not favourable. Furthermore, hydrogen sulfite compounds catalyze a polymerization of aldehydes to cyclic trimers. Another method is the supercritical CO_2 ($scCO_2$) extraction of aldehydes from a reaction medium containing ionic liquids. Therefore, $scCO_2$ works as a carrier, which inserts the educts into the reaction media and extracts the products. Since less than 100 % conversion can be realized in a continuous

process, the $scCO_2$ takes amongst the product also not converted educt out of the reaction media. Therefore, an additional subsequent separation after the reaction step is required.

Layer melt crystallization, in contrast, is a technically-proven and selective method for separating isomeric compounds. Micovic et al. (2012) and Steimel et al. (2014) have recommended hybrid processes of melt crystallisation and distillation. The combination of melt crystallisation and distillation in an integrated hybrid process may lead to enormous benefits through the synergetic effects of the high capacity of distillation and the high selectivity of melt crystallisation (Steimel et al., 2014). Such hybrid separations have found industrial application for the separation of isomers. Stepanski and Haller (2000) have described the recovery of xylenes from isomeric mixtures using combination of crystallization and distillation. Ruegg (1989) have described the use of distillation plus crystallization for purification of dichlorobenzenes. Bastiaensen (2002) have demonstrated use of crystallization and distillation in purification of acrylic acids or methycrylic acid.

All contributions have demonstrated that the use of stand-alone distillation presents challenges of high operating costs as a result of high energy demand and investment costs as a result of packaging height.

3.4 Catalyst recovery from metathesis and hydroformylation systems

Commercialisation of metathesis and hydroformylation reactions in fine-chemical/specialty chemical/pharmaceutical product transformation is hindered by the high costs of catalysts and problems of recovery of homogeneous catalysts (Huang et al., 2014). Vougioukalakis (2012) states that pharmaceutical processes and medical regulation requires ruthenium complexes in post reaction products to be less than 9 ppm. Due to high boiling points of long chain olefins and crude aldehyde products the catalysts cannot be separated from reaction mixtures by conventional distillation due to thermal instability of catalysts at the operating temperatures (Hentschel et al., 2014, Muller et al., 2013, Huang et al., 2014). Hence, it is evident from these shortcomings that one must look at different separation processes for the recovery of catalysts.

An arsenal of techniques in homogeneous catalyst recovery has offered remarkable progress in recent years. Above all, these improvements concentrate on the modification and the handling of homogeneous catalysts in general and the removal and subsequent recycling of catalysts in particular. Among the possibilities considered so far include multiphase operation of homogeneous catalysis and are not limited to; processes with organic/organic, organic/aqueous, or “fluorous” solvent pairs (solvent combinations), nonaqueous ionic solvents, supercritical fluids, systems with soluble polymers and OSN membrane processes. Figure 3.9 shows the progress of homogeneous catalyst recovery using multiphase operation of homogeneous catalysis.

According to Cornils et al. (2005), the advent of multiphase system at Ruhrchemie/Rhone-Pouenc’s oxo plant at Oberhausen gave an enormous impetus to the homogeneous catalysis community. The use of liquids in homogeneous catalysis means not only a liquid support from the basic handling of the catalyst but also a modern separation technique. However, because of high catalyst costs requirements for close to 100 % catalyst recovery have often prompted the need for a second separation step to reduce the catalyst loss. According to Schmidt et al. (2014), multistage OSN membrane set can be used to

achieve > 99,9 % rejection of catalyst. Figure 3.9 shows the techniques currently applied for homogeneous catalyst recovery from post reaction mixtures.

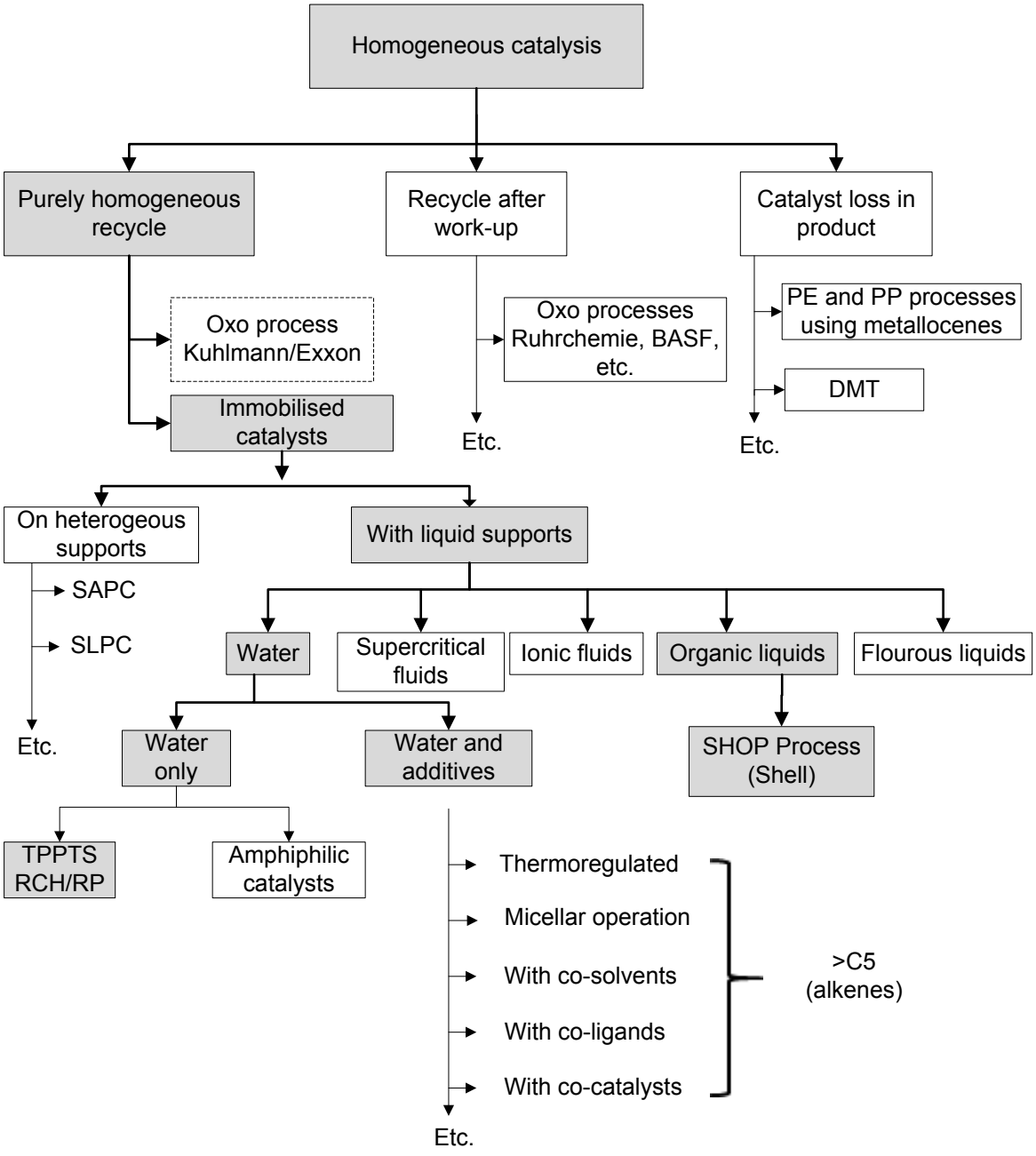

Figure 3.9.: Schematic of homogeneous catalysis utilising 2-phase catalyst recovery system

Concerning two-phase systems, only two processes (Ruhrchemie/Rhône-Poulenc and Shell SHOP) are operative industrially so far (Wiese and Obst, 2006). Sections 3.4.1 to Section

3.4.4 herein discuses some of the potential techniques to address the challenge of recovery and recycle of homogeneous catalyst.

3.4.1 Liquid multiphase systems (LMS)

Different solution systems have been proposed to enhance the solubility of higher olefins (Cn>C5) and separation of catalyst from product stream. According to Kohlpaintner et al. (2001), a liquid multiphasic system would solve the problem of product/catalyst separation in a very elegant manner. A liquid multiphase system consists of two immiscible solvents A and B to promote solubility of reaction substrates and or catalyst during reaction and allows separation of reactants and products from the catalyst when allowed to settle in a decanter (Beller et al., 1999). The principle behind this technique is that the catalyst is dissolved in the solvent B and the product is separated within the solvent A while reactants are soluble in both phases, so that good mass transfer between the two phases in the reactor ensures good reaction performance (Dreimann et al., 2014). However, a good phase separation and catalyst recovery has to be ensured (Hentschel et al., 2014) in order to minimize loss of the valuable Rh-catalyst.

Dreimann et al. (2016) owes the excellent catalyst recovery of the Ruhrchemie/Rhone-Poulenc (RCH/RP) process, one of the most important industrial applications of homogeneous catalysts to the successful application of the liquid multiphase system. According to Liu et al. (2015), the RCH/RP process was a milestone for liquid/liquid biphasic catalysis and greatly promoted the development of aqueous/organic biphasic catalysis. However, adopting this process to more complex substrates (higher olefins) leads either to poor catalyst activity, due to mass transport limitations or to the loss of precious metal catalysts (Muller et al., 2013, Dreimann et al., 2016). Behr and Brunsch (2013) investigated the effect of the chain length of the product on the catalyst leaching as dissolved in the product phase. Table A.3 in Appendix A summarises different solvent reaction systems used in hydroformylation of long chain alkenes to maximise solubility of long chain alkenes.

According to Porgzeba et al. (2016), microemulsion systems are ternary mixtures consisting of a non-polar compound (oil), a polar compound (water), and a surfactant (often non-ionic

surfactants are chosen in this context). Figure 3.10 shows the schematic diagram of the liquid multiphase system for the promotion of reaction and recovery of catalysts. Figure 3.10 illustrates the enormous importance of the biphasic technique for homogeneous catalysis: the catalyst solution is charged into the reactor together with the reactants A and B, which react to form the solvent-dissolved reaction products C and D. The products C and D have different polarities than the catalyst solution and are therefore simple to separate from the catalyst phase (which may be recycled in a suitable manner into the reactor) in the downstream phase separation unit.

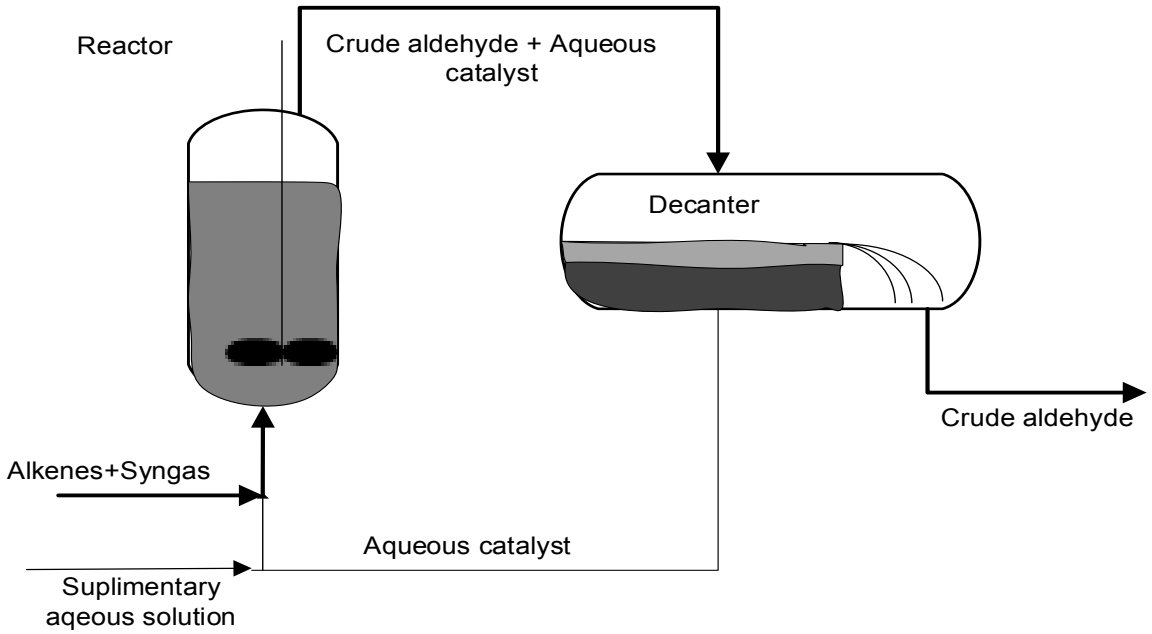

Figure 3.10.: Principle of two-phase catalysis (Cornils et al., 2005)

A number of advantages of the aqueous/organic biphasic catalysis system, such as environment benignity and facile catalyst recovery have stimulated researchers to extend the system to the hydroformylation of higher olefins. In using surfactant systems as part of an integrated reaction and separation process, the surfactant will have a huge impact on the phase behaviour of the mixture and the distribution of catalyst and reactants between the aqueous and organic phase (Muller et al., 2013). Rhodium losses after phase separation as low as 1 ppm have been reported for biphasic post reaction systems of 1-dodecene (Muller et

al., 2013, Hentschel et al., 2014). However, for a 100,000 ton per year production plant this value would result in catalyst costs of 40 million US $ per year (2002) which is far too high for an economical process based on microemulsion (Sharma et al., 2002). The concept of catalyst recycling based on the specific properties of the surfactant system gave an efficiency for catalyst recycling of >97 % with minor loss in activity (Schwarze at al., 2015).

3.4.2 Thermomorphic multicomponent solvent systems (TMS)

Liquid multiphase techniques for recycling of homogeneous catalyst typically suffer from mass transfer problems of the product into the catalyst phase or vice versa (Dreimann et al., 2015). Literature (Hentschel et al., 2014, Muller et al., 2011, Kierdorf et al., 2014, and Zagajewski et al., 2014) have recommended an integrated setup of reaction and phase separation developed in terms of thermomorphic multicomponent solvent (TMS) systems as a novel solution to improved mass transfer and greater degree of certainty in expensive catalyst recovery in hydroformylation of long chain olefins.

The method is based on the temperature-dependent miscibility gap of two or three solvent components hence, at least two of the selected components must be immiscible at low temperatures and must form a single phase at reaction temperatures to overcome mass transport limitations (Dreimann et al., 2016). Cooling below the critical solution temperature leads to a biphasic system, then the catalyst phase can be separated from the extract phase and can be used again (Figure 3.11).

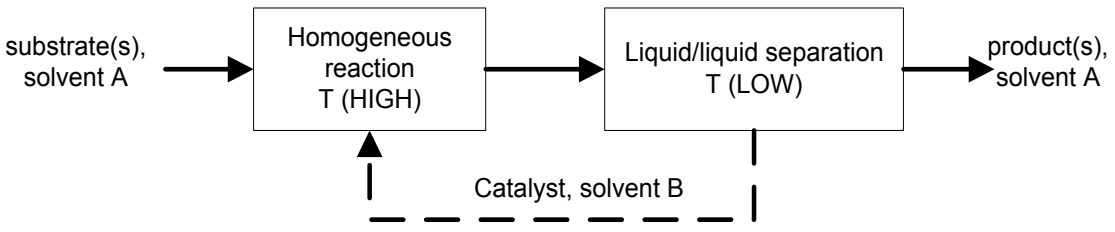

Figure 3.11.: Novel process concept for reaction and separation of catalyst (TMS)

According to Behr and Brunsch (2013), the solubility of the polar solvent (for example DMF) in the product phase increases with increasing chain length and therefore catalyst leaching.

Hence the shorter the chain length of the substrate or product, the lower the undesirable leaching of the rhodium catalyst. Zagajewski et al. (2014) and Kiedorf et al. (2014) quantified the rhodium concentration between 4 and 7 ppm, while phosphorous lies between 7 and 17 ppm and concluded that lower catalyst leaching could be achieved at low temperatures of up to 5 ^{o}C.

3.4.3 Distillation

Distillation has remained an important technique for the separation of liquid mixtures into its components (Kooijman and Taylor, 2014, Fraser, 2014). The driving force of this separation technique are different volatilities of involved species. During the distillation process, the more volatile component is enriched in the vapour phase and the less volatile component is enriched in the liquid phase. In contrast to membrane distillation, the membrane acts as a porous barrier providing the interfacial area between gas and liquid. The separation is still based on the different volatilities as in distillation; however, through the use of phobic materials towards the liquid solvent, the membrane hinders the liquid to enter the membrane (Kooijman and Taylor, 2014).

Advantages towards the use of distillation systems are the provision of high specific surface area, the potential use of milder conditions at lower pressures while disadvantages are large pressure drops as well as the identification of suitable and stable membrane materials as well as fouling (Beller et al., 1999). Distillation has been used in the Low-Pressure-Oxo process (e.g. Ruhrchemie/Rhone Poulenc Process) to recover a high boiling solvent, used in hydroformylation to dissolve the homogeneous catalyst. Figure 3.12 shows the schematic representation of distillation process to recover catalyst.

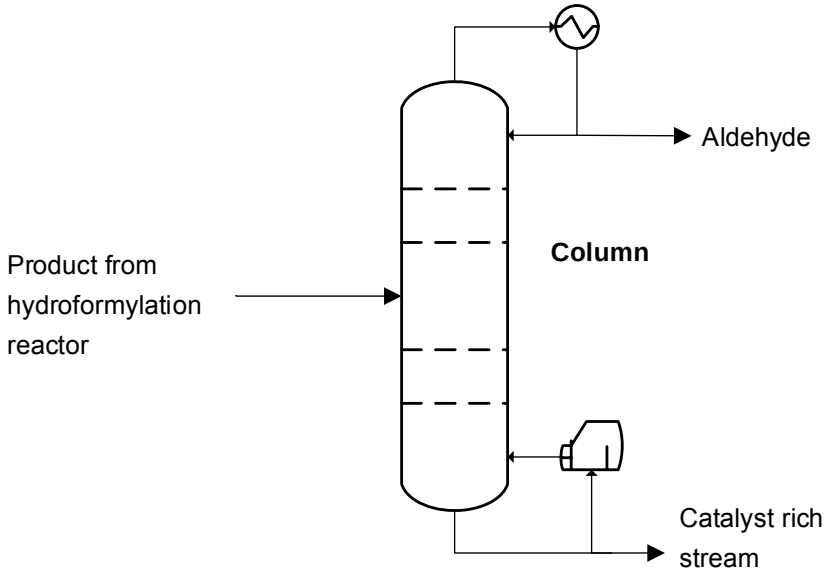

Figure 3.12.: Distillation system for catalyst recovery

Distillation is not suitable in the hydroformylation of long chain olefins due to their low vapour pressures. Evaporating the products may lead to degradation of the aldehydes and the catalyst complex due to high temperatures.

3.4.4 Organic solvent nanofiltration (OSN) membrane process

Nanofiltration in non-aqueous media, denoted as organic solvent nanofiltration (OSN) is a recent membrane process, which can replace traditional separation systems in the chemical, pharmaceutical and biotechnology industry where organic solvents are used in production (Vandezande et al., 2008, Livingston et al., 2003). An increasing number of successful applications has been reported in catalysis (Janseen et al., 2011) the petrochemical industry (White, 2006) and the pharmaceutical industry (Sheth et al., 2003).

In comparison to conventional unit operations like distillation, OSN is less energy consuming (Dreimann et al., 2015, Schmidt et al., 2013, Seifert et al., 2014) due to low separation temperatures. Both, the rejection coefficient, R and the flux, J are useful parameters to evaluate the efficiency of a membrane process. Rejection is defined as a function of the concentration of a specific component in the feed (F) compared to concentration in the

permeate (P) and represents the selectivity of the membrane. The flux, J, represents the liquid volume flowing through a specific membrane area during a specific time (L/m²h) or (kg/m²h).

To recycle homogeneous catalysts, organic solvent nanofiltration (OSN) has been investigated in the last 10 to 15 years with the development of membranes stable in organic solvents (Ormerod et al., 2013). Although initial attempts on catalyst recovery by Wijkens et al. (2000), were unsuccessful, Vougioukalakis, (2012) and Vogt et al., (2011) have demonstrated that OSN approach has great potential in homogeneous catalysis. Livingston et al. (2013) also confirmed that organometallic catalysts recycling can be performed by OSN technology as an alternative route.

Only a few large scale applications of OSN exist. Mobil's MAX-DEWAX™ process installed at Beaumont refinery in 1998 is the largest with a design feed rate of 11 500 m^3/day (White and Nirsch, 2000). It is used for solvent recovery from the dewaxed oil filtrate stream. The Max-Dewax™ process is used for solvent recovery in lube dewaxing and allowed 20 % energy savings and 3–5 % increased yield (White, 2000,2006).

Several patent applications have been made by companies on the use of membranes for homogeneous catalyst separation, e.g. DSM (Borman et al., 2003, Vries et al., 2013), Evonik (Wiese et al., 2007, Priske et al., 2007) and BASF (Peter et al., 2004). Reliable membranes possessing long term resistance to a wide range of organic solvents are now being commercially available (Schmidt et al., 2014). One example of the pilot plant application of this technique is given by Evonik (Franke et al., 2010) (Figure 3.13). In the test plant for OSN, they used as a model the Rh-catalyzed hydroformylation of 1-octene and 1-dodecene. In OSN, a pressurised liquid feed stream (transmembrane pressure (TMP) around 20-60 bar) is split into a liquid retentate and liquid permeate (Schmidt et al., 2014).

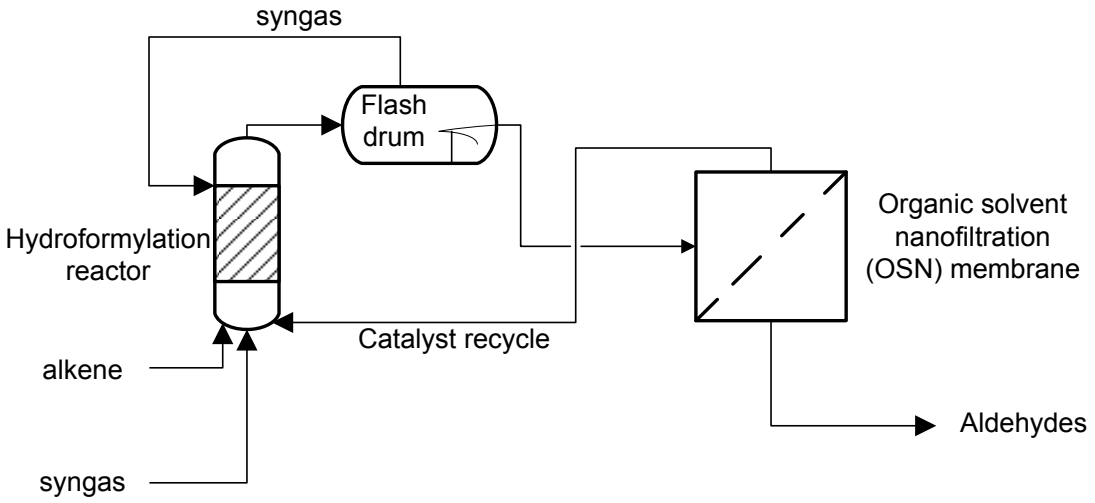

Figure 3.13.: Continuous reaction integrated separation for hydroformylation of higher olefins using OSN at Evonik (redrawn from Franke et al., 2010).

Janssen et al. (2010) operated a pilot scale combining two separate loops, the reaction loop containing a CSTR and the membrane loop containing the membrane unit in a continuous process for 13 days. The results showed that 99.96 % of the **Rh-TPPTS** can effectively be retained by the nanofiltration membrane, thus tremendously simplifying the workup as the Rh concentration in the product is extremely low. Priske et al. (2010) reported an efficient separation of a homogeneous Rh-catalyst in the hydroformylation of *n*-dodecene.

Using the Starmem-240 membrane by Grace Davison, high rhodium rejections were achieved and the preservation of the catalyst activity was shown on the basis of the *n*-dodecene conversion. According to Priske et al. (2010), Starmem™ membranes are phase inversion polyimide membranes that contains nanopores which under pressure, are mechanically deformed to a smaller cross-section which leads to better rejection. The main part of this deformation is reversible, i.e. as soon as the pressure is lowered the primary membrane structure will be recaptured hence can be reused in consecutive separation cycles.

Membrane separations are also low energy and thus often considered green separations. However, the prerequisite being that the membranes are stable in organic solvents. Van der Gryp et al. (2012) presented a solution to overcoming the challenge of separating and reusing homogeneous Ru catalysts from postreaction products using OSN in the metathesis reaction

of 1-octene to 7-tetradecene and ethylene using **HGr-2** precatalyst. Various precatalyst loadings from 340 to 1400 ppm were successfully retained by the Starmem™ 228 membrane. Different precatalyst loadings and transmembrane pressures were also investigated for different metathesis precatalysts (**Gr-1, Gr-2, HGr-1, HGr-2**) using Starmem™ 228 membrane from post reaction mixtures and gave rejections as high as 99.9 %. According to Van der Gryp et al. (2012) the process of coupling reaction, separation, and catalyst recycling increased the turnover number to 4 times for the overall consecutive reaction−separation steps of four cycles investigated. Peeva and Livingston (2012) investigated the recovery of Ru catalyst using Starmem™ 228 and PuraMem™ 280 membranes in toluene. The catalyst was successfully retained by the OSN membranes, and its high reactivity upon reuse was demonstrated by 84 % conversion. Nair et al. (2009) also demonstrated the feasibility of OSN catalyst recycle on the homogeneous, asymmetric hydrogenation of dimethyl itaconate (DMI) to dimethyl methylsuccinate (DMMS) with Ru-BINAP. The optimization of the process allowed 5 times higher substrate to catalyst ratio as well as 10 reaction cycles to be carried out with only 20 % addition of the initial catalyst while still maintaining a high reaction rate, conversion, and selectivity (Nair et al., 2009).

3.4.4.1 Effect of OSN step on catalyst activity

Apart from demonstrating that it is possible to recover homogeneous precatalysts **Gr-1**, **Gr-2**, **HGr-1** and **HGr-2** using the Starmem series of membranes at optimal reaction conditions Van der Gryp (2009) also confirmed that the catalysts could also be recovered in their “active” form contrary to previous reports by Wijkens et al. (2000) and Vorfalt et al. (2008). Van der Gryp et al. (2012) concluded that it is not the lack of stability of organic solvent nanofiltration membrane, although stability is highly sought after, but the short catalyst lifetimes that prevent the successive re-use of Grubbs type catalysts after separation.

Van der Gryp (2009) established that catalyst stability with respect to reaction lifetime with OSN process for the metathesis of 1-octene with different precatalysts are in the order **Gr-1<Gr-2<HGr-1<HGr-2** with the life of **HGr-2** estimated at close to 10 hrs. The coupled reaction-separation and recycling process increased the turnover number from 1 400 for a

single pass reaction to 5 500 for the overall consecutive reaction–separation steps (Van der Gryp, 2009).

3.4.4.2 Effect of precatalyst concentration on catalyst recovery

Rabiller-Baudry et al. (2013) studied the effect of precatalyst concentration on catalyst recovery at 40 bar in cross-flow mode with different initial pre-catalyst concentrations ranging from 0.05 x 10^{-3} to 1.40 x 10^{-3} mol/L. The pre-catalyst retention increased from 94.8 % to 99.5 % when the concentration was increased from 0.05 x 10^{-3} mol/L to 1.40 x 10^{-3} mol/L. However, an important limitation of the investigation was that the membrane was first selected on a single criterion ‘‘to have a high retention of the precatalyst’’. It should be probably better adapted to look for a compromise between the high retention of the pre-catalyst and the high transmission or flux of the product in order to limit nanofiltration stages or total membrane area. However, Van Der Gryp (2009) established that hydrophobic type membranes such as MPF-50 and Starmem^{TM} series give higher fluxes for non-polar components and that Starmem^{TM} 228 with a MWCO of 280g/mol gives high recoveries greater than 99 % and fluxes up to 15L/m^{2}h for 1-octene and 7-tetradecene mixtures.

3.5 Previous studies on simulation of metathesis and hydroformylation systems

No information for previous olefin metathesis is available from open source literature and articles. Hentschel et al. (2014) developed an Aspen Plus^{TM} model of hydroformylation of 1-dodecene in a thermomorphic multicomponent solvent system (TMS) Figure 3.14. The reactor was developed using the identified reaction network given by (Markert et al., 2013 and Kierdorf et al., 2014). The solubilities of CO and H_2 in neat solvents (decane, DMF), 1-dodecene and n-tridecanal were also modelled with PC-SAFT. Results of 10 000 tonnes per annum Aspen Plus^{TM} simulation for this system concluded that a residence time of 16,3 minutes, a volume of 11,5 m^3 could give 65.4 % conversion of 1-dodecene and a selectivity of 91,4 % n-tridecanal and optimum parameters for the reactor being100 ^{o}C, 30 bar.

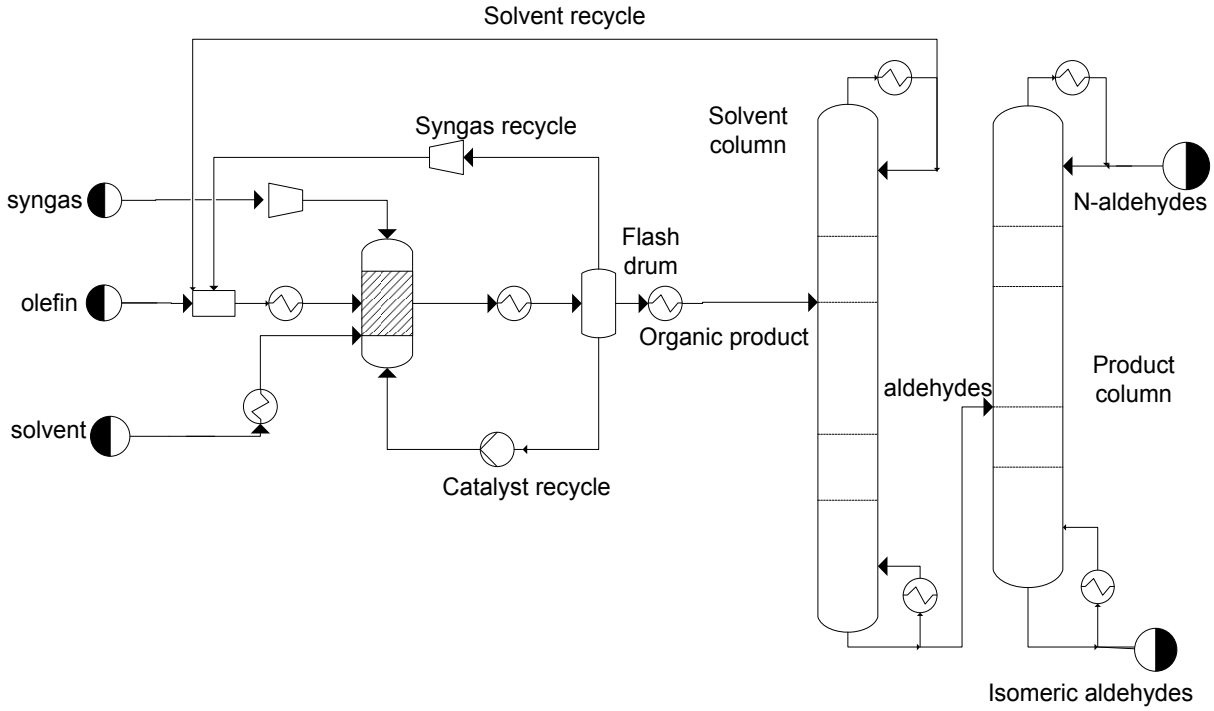

Figure 3.14.:1-dodecene hydroformylation Process (redrawn, Hentschel et al., 2014)

3.5.1 Aspen Plus™ custom models on OSN separation in hydroformylation

Schmidt et al. (2014) presented results of Aspen Custom Modeller to simulate and optimize the recovery of Rh-catalyst in hydroformylation. Triphenylphosphine was selected to represent the catalyst complex. Triphenylphosphine stage rejections of 90 %, 80 % and 70 % corresponding to three, four and five stages respectively gave overall rejections of 99.99 % for Puramem™ 280 membrane at transmembrane pressures (TMP) of 50 bar with appreciable permeate fluxes per unit membrane area. However, the methodology used for model interfacing is not revealed.

3.5.1.1 Cascade membrane systems

Vanneste et al. (2011), Vanneste et al. (2012) and Caus et al. (2009a & 2009b) extrapolated single-stage experimental data to multi-stage membrane cascades. The simple filtration unit can be arranged in multistage membrane cascades, to overcome the selectivity limit intrinsic to a single filtration stage. Marchetti et al. (2015) and Caus et al. (2009a) studied the applicability of integrated counter current cascades for the separation of individual organic components (xylose and maltose) in aqueous solutions. Caus et al. (2009a) concluded that

membranes with a low rejection for the desired component are preferred to obtain a high product recovery, whereas membranes with a much higher rejection for the undesired component are preferred to obtain a high product purity or a high selectivity product purity or a high selectivity.

3.6 Summary

From the findings of the literature study carried out, it is apparent that the process of upgrading 1-octene to functionalised hydrocarbons through a sequence of reactions namely metathesis and hydroformylation is a high potential candidate. Organic solvent nanofiltration (OSN) membrane process is attractive because of high catalyst retentions and stability of Starmem membranes (Priske et al., 2010). Specific opportunities could lie in the optimization study of the multiphase reaction system to improve the solubility of long chain olefins in aqueous catalyst media and efficient catalyst recovery and recycle. Previous simulation of hydroformylation of 1-dodecene by Hentschel et al. (2014) exposes challenges of separation of catalyst and purification of products.

Hence, using the data as obtained from literature it is possible to conduct a techno-economic study of producing 10 000 tonnes per annum of 2-hexyl-nonanal (99 wt. %) by upgrading low value 1-octene form a Fischer-Tropsch product stream. Kinetic data for self-metathesis of 1-octene as given by Van der Gryp (2009) and hydroformylation of 7-tetradecene as given by Haumann et al. (2002b) will be used to develop reactor models. In order to develop the reaction system design specifications for solvent and alkene mixtures by Haumann et al. (2002a, 2002b) and Muller et al. (2013) will be used. The species permeability data by Van der Gryp (2009) together with Bhanushali et al. (2002) model will be used to develop OSN membrane units in Aspen Plus™. Figure 3.15 shows a block flow diagram for some identifiable process units.

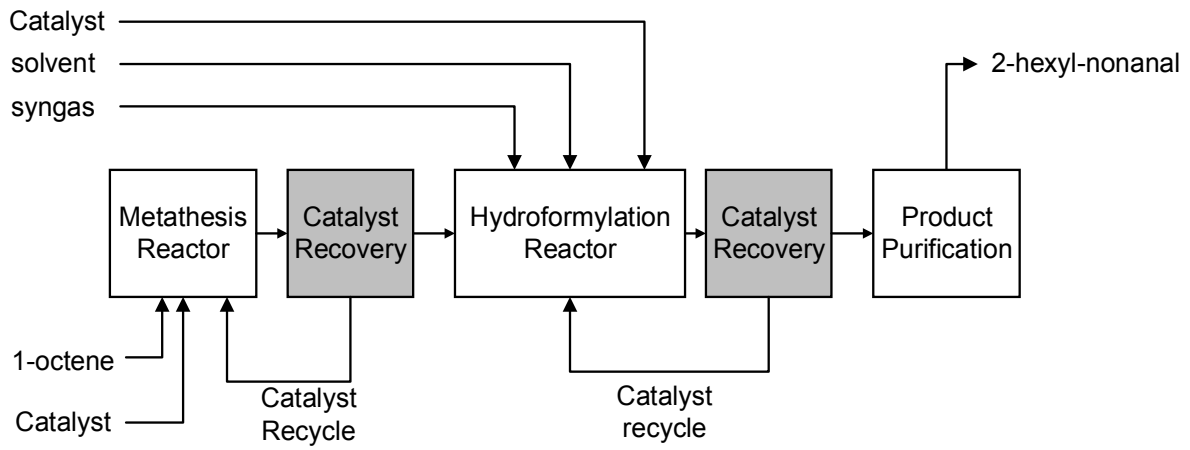

Figure 3.15.: Block flow diagram for the process

3.7 References

Baerns, M, A. Behr, A., Brehm, J. Gmehling, H., Hofmann, O. Ulfert and A. Renken, Process Development, New recycling methodology for homogeneous noble metal catalysts Technische Chemie, Wiley-VCH, (2006).

Balcar, H., Cejka, J. Mesoporous molecular sieves as advanced supports for olefin metathesis catalysts, Coordination Chemistry Reviews **257** (2013) 3107– 3124

Bhanage, B. M., Divekar, S.S., Deshpande, R.M, Chaudhari, R.V. Kinetics of hydroformylation of 1 -dodecene using homogeneous HRh(CO) (PPh,)3 catalyst, Journal of Molecular Catalysis A: Chemical **115** (1997) 247-257

Behr, A., Henze, G., Obst, O., Turkowski, B. Selection process of new solvents in temperature-dependent multi-component solvent systems and its application in isomerising hydroformylation, Green Chemistry **7** (2005), 645–649

Behr, A, G. Henze, G., Johnen, L., Awungacha, C. Advances in thermomorphic liquid/liquid recycling of homogeneous transition metal catalysts, Journal of Molecular Catalysis A: Chemical **285** (2008) 20–28

Behr, A., Brunsch, Y. Temperature-Controlled Catalyst Recycling in Homogeneous Transition-Metal Catalysis: Minimization of Catalyst Leaching, Angewandte Chemie. Interanational Edition **52** (2013), 1586 –1589

Billig, E., Bryan, D. R. Oxo Process. In Kirk-Othmer Concise Encyclopedia of Chemical Technology; Wiley-Interscience: Hoboken, NJ, (2000)

Boeda, F., Clavier, H., Jordaan, W., Meyer, H., Steven, Nolan, P. Phosphabicyclononane-Containing Ru Complexes: Efficient Pre-Catalysts for Olefin Metathesis Reactions Journal of Organic Chemistry **73** (2008) 259-263

Cole-Hamilton, D. J., Tooze, R.P. Springer Netherlands, Dordrecht, Catalyst Separation, Recovery and Recycling The Netherlands, vol. 30. (2006)

du Toit, C.G., van Sittert, E., Vosloo, H.C.M. Metal carbenes in homogeneous alkene metathesis: Computational investigations, Journal of Organometallic Chemistry **738** (2013) 76-91

Du Toit, C. G., Jordaan, Huijsmans, C. A. A., Jordaan, J. H. L van Sittert, C G. C. E., Vosloo, H. C. M., Improved Metathesis Lifetime: Chelating Pyridinyl-Alcoholato Ligands in the Second Generation Grubbs Precatalyst, Molecules **19** (2014) 5522-5537; doi:10.3390/molecules19055522

Evonik Membrane Extraction Technology Limited http://www.design-meets-polymers.com/sites/dc/Downloadcenter/Evonik/Product/DuraMem-PuraMem/brochures/duramem-and-puramem---general-brochure.pdf (2014)

Gorak, A., Schoenmakers, R. Distillation: Operation and Applications, Academic Press, Boston, 2014, pp. 155–190 (by Fraser, S Chapter 4 – Distillation in Refining)

Frohling, C. D.; Kohlpaintner, C. W. In Applied Homogeneous Catalysis with Organometallic Compounds; Cornils, B., Herrmann, W. A., Ed.; VCH: Weinheim, **1** (1996) pp 27-104

Grubbs, R.H., Trnka, M.T., Sanford, M.S. Transition Metal-Carbene Complexes in Olefin Metathesis and Related Reactions, Current Methods in Inorganic Chemistry, **3** (2003) Elsevier Science B.V

Gual, A., Godard, C., Castillón, S., Claver, C. Highlights of the Rh-catalysed asymmetric hydroformylation of alkenes using phosphorus donor ligands; Tetrahedron: Asymmetry **21** (2010) 1135–1146

Haumann, M., Koch, H., Hugo, P., Schomäcker, R. Hydroformylation of 1-dodecene using Rh-TPPTS in a microemulsion, Applied Catalysis A: General **225** (2002a) 239–249

Haumann, M., Koch, K., Hugo, P., Schomäcker, R. Hydroformylation of 7-dodecene using Rh-TPPTS in a micro emulsion. Applied Catalysis A: General **225** (2002b) 239–249

Hentschel, B., Kiedorf, G, Gerlach, M, Hamel, C., Seidel-Morgenstern, A, Freund, A Sundmacher K. Model-Based Identification and Experimental Validation of the Optimal

Reaction Route for the Hydroformylation of 1‐Dodecene. Industrial Engineering Chemistry Reserach **54**, (2015), 1755−1765 DOI: 10.1021/ie504388t

Hentschel, B., Peschel, A., Xie, M., Vogelpohl, C., Sadowski, G., Freund, H., Sundmacher, K. Model-based prediction of optimal conditions for 1-octene hydroformylation. Chemical Engineering Science **115** (2014) 58–68

Huijsmans, C. A. A. Modelling and synthesis of Grubbs type complexes with hemilabile ligands, North-West University (Potchefstroom campus), MSc Dissertation, (2009)

Ivin, K.J., Mol, J.C. Olefin Metathesis and Metathesis Polymerization, Academic Press, London, (1997)

Janssen, M., Muller, C., Vogt, D. Recent advances in the recycling of homogenous catalyst using membrane separation, Green Chemistry **13** (2011) 2247–2257

Jordaan, M., van Helden, P., van Sittert, C.G.C.E., Vosloo, H.C.M. Experimental and DFT investigation of the 1-octene metathesis reaction mechanism with the Grubbs 1 precatalyst, Journal of Molecular Catalysis A: Chemical **254** (2006) 145–154

Jorke, A., Seidel-Morgenstern, A., Hamel, C., Isomerization of 1-decene: Estimation of thermodynamic properties, equilibrium composition calculation and experimental validation using a Rh-BIPHEPHOS catalyst, Chemical Engineering Journal **260** (2015) 513–523

Kegl, T., Computational aspects of hydroformylation, (Review). The Royal Society of Chemistry **5** (2015) 4304–4327

Kiedorf, G., Hoang, D.M, Muller, M., Jorke, A., Markert, J. Arellano-Garcia, A., Seidel-Morgenstern, A., Hamel, C. Kinetics of 1-dodecene hydroformylation in a thermomorphic solvent system using a rhodium-biphephos catalyst. Chemical Engineering Science **115** (2014) 31–48

Koeken, A.C.J., van den Broeke, L.J.P., Benes, N.E., Keurentjes, J.T.F. Triphenylphosphine modified rhodium catalyst for hydroformylation in supercritical carbon dioxide. Journal of Molecular Catalysis A: Chemical **346** (2011) 94–101

Kohlpaintner, CW, Fischer, R.W., Cornils, B. Aqueous biphasic catalysis: Ruhrchemie/Rhone-Poulenc oxo process Applied Catalysis A: General **221** (2001) 219–225

Kooijman, H. A., Taylor, R. Operation and Applications, Academic Press, Boston, (2014), pp. 191-253.

Lehman, J., Schwendeman , J.E., O'Donnell, M.O, Wagener, K.B, Olefin isomerization promoted by olefin metathesis catalysts, Inorganica Chimica Acta **345** (2003) 190-198

Li, X., Y Li, Y., Chen, H., He, Y., Li, M. Studies on 1-dodecene hydroformylation in biphasic catalytic system containing mixed micelle, Journal of Molecular Catalysis A: Chemical **194** (2003) 13–17

Livingston, A., Szekely, G., Maria, F. Solomon, J., Marchetti, P., Kim, J.F., Sustainability assessment of organic solvent nanofiltration: from fabrication to application, Green Chemistry **16** (2014) 4440–4473.

Marchetti, P., Maria, F., Jimenez Solomon, S., Szekely, G., Livingston, A.G. Molecular Separation with Organic Solvent Nanofiltration: A Critical Review, Chemical Review **114** (2014) 10735−10806 dx.doi.org/10.1021/cr500006

McBride, K., Gaide, T., Vorholt, V., Behr, A., Sundmacher, K. Thermomorphic Solvent Selection for Homogeneous Catalyst Recovery based on COSMO-RS, Chemical Engineering & Processing: Process Intensification **25** (2015), http://dx.doi.org/10.1016/j.cep.2015.07.004

Motoboloi, M.P. Synthesis and modelling of imine derivatives as ligands for Grubbs type pre-catalysts, , North-West University (Potchefstroom campus), MSc Dissertation, (2010)

Muller, D., Minh, D.H., Merchan, V.A., Arellano-Garcia, H., Kasaka, H, Muller, M., Schomacker, R., Wozny, G. Towards a novel process concept for the hydroformylation of higher alkenes: Mini-plant operation strategies via model development and optimal experimental design, Chemical Engineering Science **115** (2014)127–138

Peschel, A., Hentschel, B., Freund, H., Sundmacher, K. Design of optimal multiphase reactors exemplified on the hydroformylation of long chain alkenes. Chemical Engineering Journal 1**88** (2012) 126– 141

Priske, M, Wiese, K.D., Drews, A., Kraumec, M., Baumgarten, G. Reaction integrated separation of homogenous catalysts in the hydroformylation of higher olefins by means of organophilic nanofiltration, Journal of Membrane Science **360** (2010) 77–83

Pogrzeba, D., Muller, M., Illner, M., Schmidt, Y., Kasaka, A., Weber, G., Wozny, R., Schomäcker, M., Schwarze, M. Superior catalyst recycling in surfactant based multiphase systems –Quo vadis catalyst complex? Chemical Engineering and Processing **99** (2016) 155-166

Rabiller-Baudry, M., Nasser, G., Renouard, T., Delaunay, D., Camus, M., Comparison of two nanofiltration membrane reactors for a model reaction of olefin metathesis achieved in toluene. Separation and Purification Technology **116** (2013) 46–60

Rost, A., Muller, M., Hamerla, T., Kasaka, Y., Wozny, G., Schomäcker, R. Development of a continuous process for the hydroformylation of long-chain olefins in aqueous multiphase systems, Chemical Engineering and Processing **67** (2013) 130– 135

Schafer, A., Brunsch, Sadowski, G., Behr, A., Hydroformylation of 1‑Dodecene in the Thermomorphic Solvent System Dimethylformamide/Decane. Phase Behaviour−Reaction Performance−Catalyst Recycling, Industrial Engineering Chemistry Research **51** (2012) 10296−10306 dx.doi.org/10.1021/ie300484q

Shahane, S., Toupet, L., Fischmeister, C, Bruneau, C. Synthesis and charactorization of Sterrically Enlarged Hoveyda-Type Olefin Metathesis Catalysts, European Journal of Inorganic Chemistry, **45** (2013) 54-60

Steimel, J., Harrmann, M., Schembecker, G., Engell, S. A framework for the modelling and optimization of process superstructures under uncertainty, Chemical Engineering Science **115** (2014)225–237

Steimel, J., Harrmann, M., Schembecker, G., Engell, S. A framework for the modelling and optimization of process superstructures under uncertainty. Chemical Engineering Science **115** (2014) 225–237

Tomasek, J., Schatz, J. Olefin metathesis in aqueous media, The Royal Society of Chemistry (Review) Green Chemistry **15**, (2013), 2317–2338

Vandezande, P., Lieven, E. M., Gevers, M., Ivo, F., Vankelecom, J., Solvent resistant nanofiltration: separating on a molecular level, Chemistry Social Review **37**, (2008) 365–405

Van der Gryp, P., Barnard, A., Cronje, P.J., de Vlieger, D., Marx ,S., Vosloo, H.C.M., Separation of different metathesis Grubbs-type catalysts using organic solvent nanofiltration, Journal of Membrane Science **353** (2010) 70–77

Van der Gryp, P, Separation of Grubbs-based catalysts with Nanofiltration, (PhD Thesis), North-West University, (2009).

Van der Gryp, P., Marx S., Vosloo, H.C.M. Experimental, DFT and kinetic study of 1-octene metathesis with Hoveyda–Grubbs second generation precatalyst, Journal of Molecular Catalysis A: Chemical **355** (2012) 85– 95

Van Leeuwen, P.W.N.M., Claver C., Rhodium Catalysed Hydroformylation, Kluwer Academic Publishers, Dordrecht (2000).

Vougioukalakis, G.C. Removing Ruthenium Residues from Olefin Metathesis Reaction Products, Chemistry a European Journal **18** (2012), 8868 – 8880

Webb, M., Sellin, M.F., Kunene, T.E., Williamson, S., Alexandra, M., Z. Slawin, Z., Cole-Hamilton, D.J., Continuous Flow Hydroformylation of Alkenes in Supercritical Fluid-Ionic Liquid Biphasic Systems Journal of American Chemical Society. **125** (2003), 15577-15588

Wiebus, E., Cornils, B. Organic Solvent Nanofiltration (OSN), Chemical Ingineering Technology **66**, (1994) 916–923.

White, L. S. Development of large-scale applications in organic solvent nanofiltration and pervaporation for chemical and refining processes, Journal of Membrane Science **286** (2006) 26–35.

White, L.S, Nitsch, A.R. Solvent recovery from lube oil filtrates with a polyimide membrane, Journal of Membrane Science **179** (2000) 267–274

Xaba, M. S., Synthesis and modelling of Tungsten catalysts for alkene metathesis; North-West University (Potchefstroom campus), MSc Dissertation, (2010)

Zagajewski, M., Behr, A., Sasse, P., Wittmann, J. Continuously operated miniplant for the rhodium catalyzed hydroformylation of 1-dodecene in a thermomorphic multicomponent solvent system (TMS), Chemical Engineering Science **115** (2014) 88-94

CHAPTER 4: PROCESS DEVELOPMENT

"Engineers like to solve problems. If there are no problems handily available, they will create their own problems."

Scott Adams

Overview

Chapter 4 provides a detailed procedure for developing a process of upgrading low value 1-octene from a Fischer-Tropsch Synthol product stream to 2-hexyl-nonanal an important intermediate for the manufacture of Guerbet-type surfactants at Sasol Secunda. This chapter is subdivided into four sections which are, Section 4.1 (Introduction), Section 4.2 (Douglas methodology for process development), Section 4.3 (Overall process development of the process section), Section 4.4 (Overall process integration) and finally Section 4.5 (A summary of the chapter).

4.1 Introduction

The process to be developed can be defined as the homogeneous metathesis of 1-octene from a Fischer-Tropsch product stream to produce 7-tetradecene (*n*-alkene) and the subsequent hydroformylation of 7-tetradecene to 2-hexyl-nonanal. The process will produce 10 000 tonnes per annum of 2-hexyl-nonanal at a purity of 99 wt. % from raw materials and feedstocks such as 1-octene, syngas, solvents and utilities purchased on site at Sasol Secunda, South Africa. According to Arnoldy (2000), annual design capacities for petrochemical process of 10 000-500 000 tonnes are more attractive to investors. The required product purity for 2-hexyl-nonanal is 99 wt. %. According to Hentschel et al. (2014) and Steimel et al. (2014), downstream processing requires aldehyde purities above 98 wt. %. Table 4.1 is a summary of the process requirements.

Table 4.1.: A summary of basic process requirements

Design parameter	Description	Justification
Product name	2-hexyl-nonanal (99 wt. %)	Market requirement (Hentschel et al., 2014; Steimel et al., 2014)
Desired production rate	10 000 ton per annum	Petrochemical 10 000-500 000 tonnes per year attractive to investors (Arnoldy, 2000)
Feedstock	1-octene (100 % mol basis)	Feed stock purity selected was 100 % purity for academic purpose and the fact that the literature used excluded effects of feed purities.
Nature of Process	Continuous	The production rate was over batch maximum (Douglas, 1988, McKenna and Malone, 1990)

It will therefore most likely be an annexed plant built alongside the extractive distillation section of the Chemicals Plant, sharing common systems such as utilities, effluent treatment, and personnel. Therefore, facilities to produce utilities at the required capacity, a laboratory, and

waste disposal areas are not included in the designs. The approach to developing a conceptual process of upgrading 1-octene from a Fischer-Tropsch product stream to 2-hexyl-nonanal at Secunda South Africa was adopted from the Douglas' (1988) methodology.

4.2 The Dougas methodology

The hierarchical decomposition based approach of Douglas (1988) was used in this study and this section is a short summary of the methodology. Appendix B gives further details to the Douglas methodology. The Douglas' (1988) methodology for single-product, continuous vapour-liquid processes is a hierarchical design approach, which was adopted in this study due to the inherent hierarchy nature of the conceptual design (Yang and Shi, 2000). Each level includes new decisions and additional flowsheet structures. Heuristics are used to help the designer to make those decisions and the opposite decisions are accumulated in a list of process alternatives to be considered after a base-case design has been generated. The essence of a hierarchical decomposition based approach is a sequential design procedure and each decision level terminates with an economic analysis (McKenna and Malone, 1990). At each hierarchy level, the dominant design variables and parameters are identified, both capital and operating costs are evaluated as a function of these variables.

According to the Douglas methodology, before the hierarchical approach is applied to conceptual process development, the designer has to make a decision on whether to operate a "continuous" or "batch" process. In this investigation, the plant capacity of 10 000 tonnes per annum was used. According to Douglas (1988), a continuous process is used if production rate is more than 500 tonnes per annum. McKenna and Malone (1990) recommends that for petrochemicals with production rate of more than 1 000 tonnes per year (8 000 hrs) a continuous process must be selected. Hence, from the specified design specification in this study, it is clear the process is continuous due to the high production rate. Figure 4.1 is an illustration of the Douglas methodology for developing a continuous process.

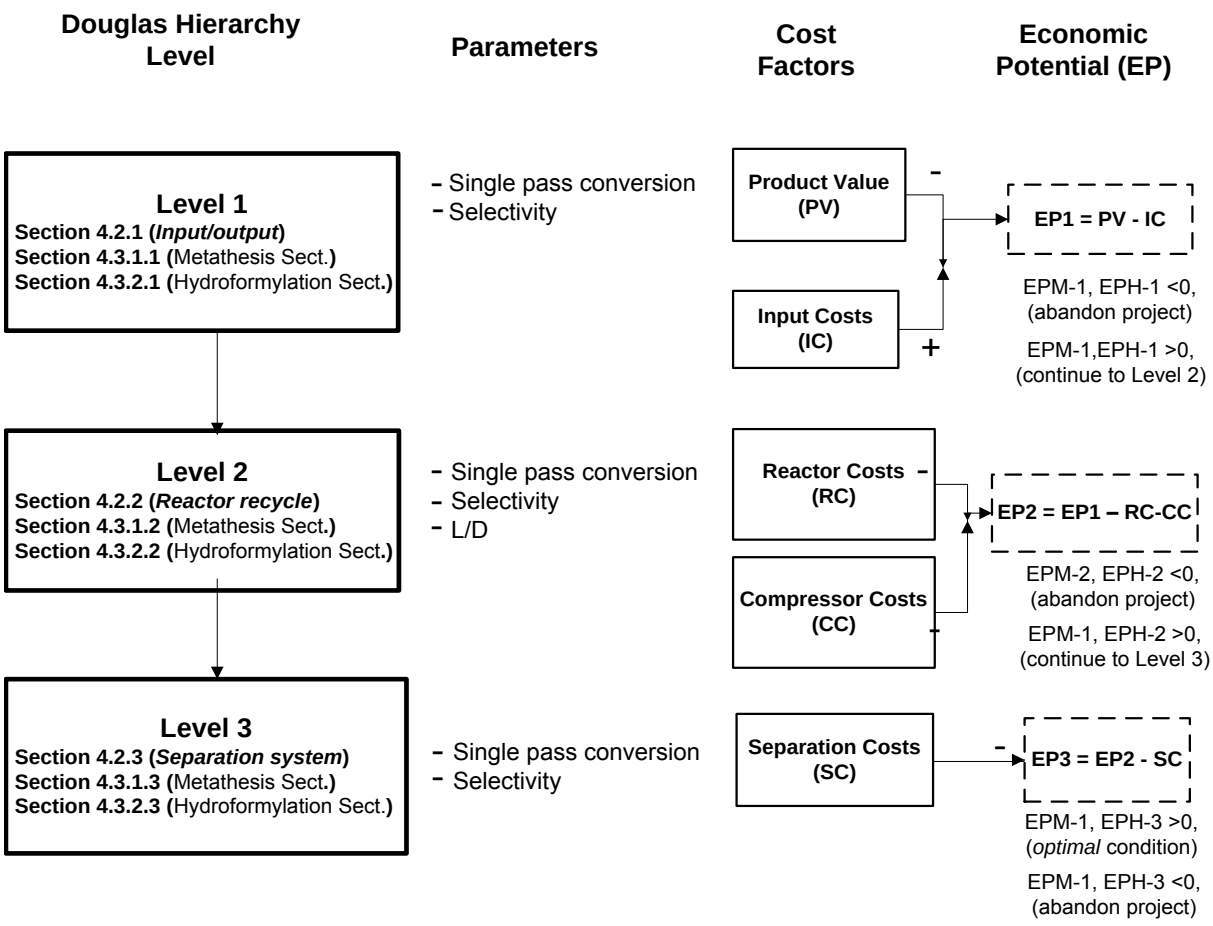

Figure 4.1.: An illustration of the Douglas methodology for continuous process development

4.2.1 Input-output information (Level 1)

According to Douglas (1988), in order to understand the decisions required to fix the input-output structure of a flowsheet, the designer merely draws a box around the total process as shown in Figure 4.2.

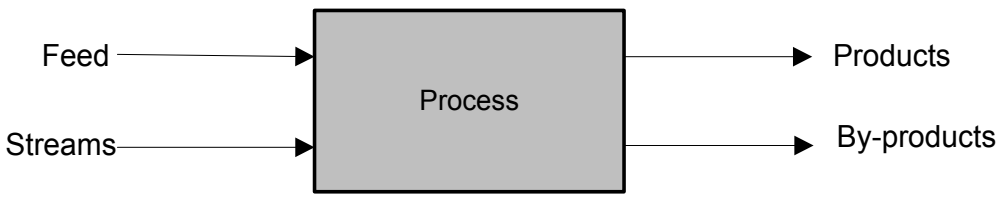

Figure 4.2.: Input-output structure of flowsheet (Douglas, 1988)

Thus, attention is focused on what raw materials are fed to the process and what products and by-products are removed. Figure 4.2 indicates that no reactants leave the system. Since the raw materials costs normally fall in the range from 33 to 85 % of the total processing costs, it is required to calculate these costs before addition of any other detail to the design (Douglas, 1988). Design variables considered at Level 1 are single pass conversion and selectivity or yield to the required product. The “best" values of the design variables depend on the process economics, hence, at Level 1, it is required to calculate the stream costs, i.e., the cost of all raw materials and product streams in terms of the design variables. The economic potential at Level 1 (EP-1) is defined as the difference between the product value and raw material costs. The formula for EP-1 is:

$$EP\text{-}1 = Value\ (Products) - Cost\ (Raw\ materials), \frac{\$}{yr} \tag{4.1}$$

The EP-1 for the metathesis process (EPM-1) is the difference between the revenue from 7-tetradecene and raw material costs, which include 1-octene and catalyst. It is the annual profit obtained without paying anything for capital costs or utilities costs. Thus, formula for EPM-1 is:

$$EPM\text{-}1 = Value\ (7 - tetradecene) - Cost\ (1\text{-}octene, catalysts), \frac{\$}{yr} \tag{4.2}$$

The EP-1 for hydroformylation process section (EPH-1) is the difference between the revenue from the 2-hexyl-nonanal product and the costs of raw materials (1-octene, catalysts) and cost incurred in developing the metathesis process section. The formula for determining EPH-1 is:

$$EPH\text{-}1 = Value\ (2 - HN\ ) - Cost\ (1\text{-}octene, catalysts) - Cost\ (MS), \frac{\$}{yr} \tag{4.3}$$

Where,

2-HN = 2-hexyl-nonanal product

MS = Metathesis Section

Hence, if the EPM-1 or EPH-1 is negative (EP-1<0), i.e., the raw materials are worth more than the products, the decision is either to terminate the design project, look for a less

expensive source of raw materials, or look for another chemistry route that uses less expensive raw materials.

4.2.2 Reactor and recycle structure (Level 2)

At Level 2, the annualised reactor costs, annualized compressor costs and operating costs of the gas-recycle compressors are considered. The catalyst type, temperature, pressure, single pass conversion and L/D ratio of the reactor are parameters investigated at Level 2. A kinetic model is used to estimate the variation of reactor cost and recycle rate with a change in the single pass conversion of 1-octene for the metathesis process and 7-tetradecene for the hydroformylation process. The detailed description of equations for reactor costs and compressor costs is given in Appendix B.2.2. Appendix B.2.2 details the heuristics used to determine the number of reactors, the number of recycle streams and heat effects at Level 2 of process development. At Level 2, the separation system is treated as a perfect-separation unit (black-box) and Figure 4.3 shows the flowsheet structure.

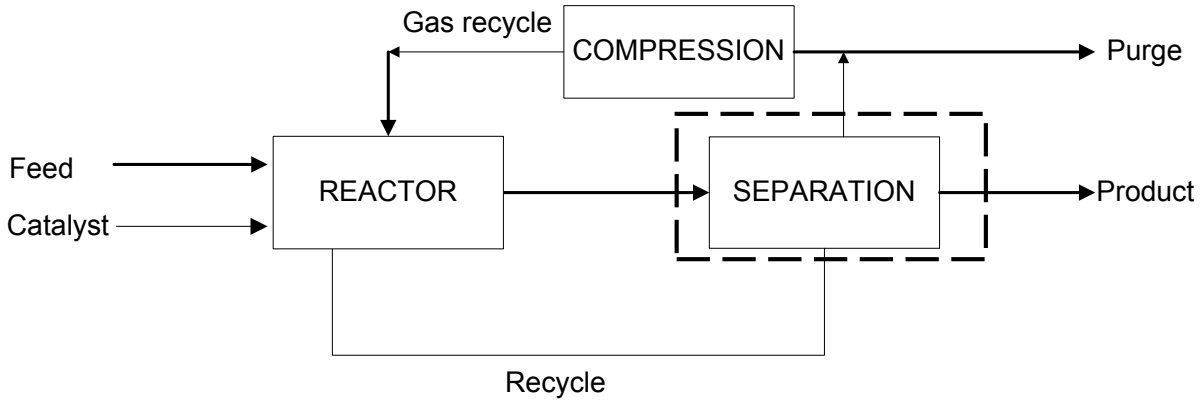

Figure 4.3.: Reactor and recycle structure (Douglas, 1988)

The recycle of unconverted reactants (1-octene, syngas and 7-tetradecene) is considered. EP-2 is defined as profit obtained after subtracting the annualized reactor cost and the compressor costs (annualized capital and power) from the EP-1. The formula for EP-2 is:

$$EP\text{-}2 = EP\text{-}1 - Reactor\ Cost - Compressor\ Costs, \frac{\$}{yr} \tag{4.4}$$

Thus, EPM-2 for the metathesis process section is the annual profit that could be realised after considering the annualised metathesis reactor costs.

$$EPM\text{-}2 = EPM\text{-}1 - Reactor\ Cost, \frac{\$}{yr} \tag{4.5}$$

The EPH-2 for the hydroformylation process section is the annual profit that could be obtained if annualised reactor cost and syngas-recycle compressor costs are considered.

$$EPH\text{-}2 = EPH\text{-}1 - Reactor\ Cost - Syngas - Recycle\ Compressor\ Costs, \frac{\$}{yr} \tag{4.6}$$

Hence, if EPM-2 or EPH-2 is negative, i.e., raw materials, reactor and syngas-recycle compressor are worth more than the products. The designer may want to terminate the design project, look for a less expensive source of raw materials, or look for another chemistry route that uses less expensive raw materials and cheaper equipment.

4.2.3 Separation system design (Level 3)

At Level 3, the analysis considers only the synthesis of a separation system to recover gaseous and liquid components as shown in Figure 4.4. The selectivity, single pass conversion of 1-octene in metathesis process and 7-tetradecene in hydroformylation process are parameters used to develop the separation system at Level 3.

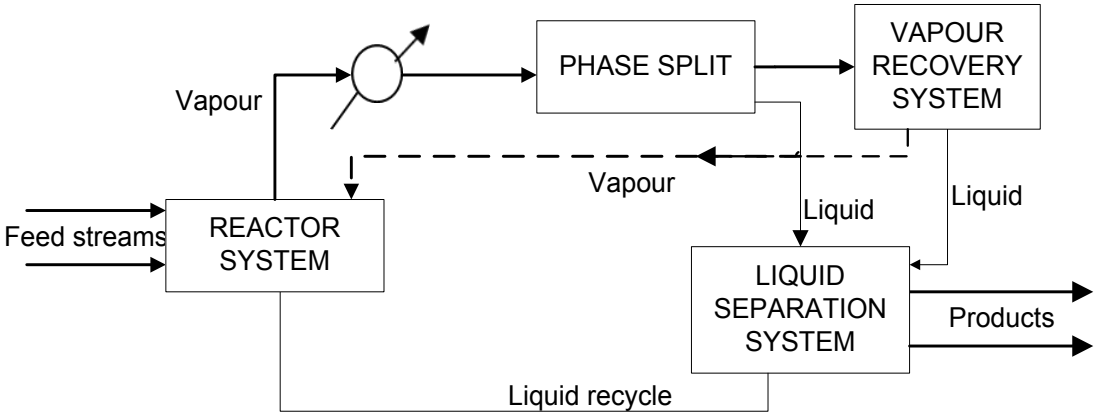

Figure 4.4.: Flowsheet structure for liquid-vapour effluent (Douglas, 1988)

The analysis is broken down into vapor recovery system and liquid separation system as shown in Figure 4.4. The rules and heuristics used to develop the separation system at Level 3 of are given in detail in Appendix B.2.3. The model for the total annual cost of separation included a flash drum, membrane, column shell and trays costs, condenser and reboiler costs, cooling water and steam costs. The equations used to determine separation costs are given in Appendix B.2.3. The economic potential at Level (EP-3) is defined as the profit obtained after considering raw material costs, annualised reactor costs, compressor costs and separation costs. EP-3 is obtained by subtracting the total separation costs from EP-2. The formula for EP-3 is:

$$EP\text{-}3 = EP\text{-}2 - Separation\ Costs, \frac{\$}{yr} \tag{4.7}$$

EPM-3 at Level 3 of metathesis process section is obtained by subtracting the separation cost for the removal of ethylene, recovery of unreacted 1-octene and the catalyst from EPM-2. The formula for EPM-3 is:

$$EPM\text{-}3 = EPM\text{-}2 - Separation\ Costs, \frac{\$}{yr} \tag{4.8}$$

EPH-3 for the hydroformylation process section is obtained by subtracting the separation cost for recovering unreacted 7-tetradecene, unreacted syngas, catalyst and purification of 2-hexyl-nonanal product from EPH-2. The formula for EPH-3 is:

$$EPH\text{-}3 = EPH\text{-}2 - Separation\ Costs, \frac{\$}{yr} \tag{4.9}$$

If the economic potential at Level 3 is negative, then the designer may decide to terminate the project, look for a less expensive source of raw materials, or look for another chemistry route that uses less expensive raw materials and cheaper separation equipment.

The results of analysis at Level 3 of process development for the metathesis and hydroformylation process sections generates base case process flow diagrams (PFDs) in Section 4.4. The base case PFDs, ‘best’ catalyst type, temperature and single pass conversion of 1-octene for metathesis and single pass conversion of 7-tetradecene for the

hydroformylation process section are used in detailed design engineering evaluation in simulation (Chapter 5).

4.3 Overall process development

The overall process was first subdivided into two process units namely metathesis and hydroformylation process sections as shown in Figure 4.5.

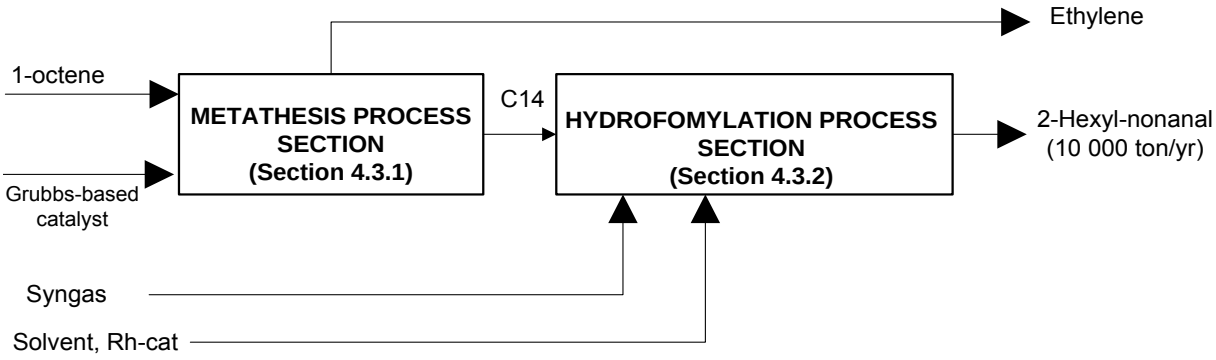

Figure 4.5.: Simplified block flow diagram of the overall process

These two process sections were synthesised separately using the idea of the hierarchical design methodology developed by Douglas (1988) as shown in Section 4.3.1 and Section 4.3.2.

4.3.1 Metathesis process section

4.3.1.1 Input-output information (Level 1)

This section focused on the development of a process to produce 7-tetradecene which will be used as a feedstock in the hydroformylation process to manufacture 2-hexyl-nononal. Table 4.2 gives the relevant input information obtained from literature as was used in this study.

Table 4.2.: Input-output information for Level 1 metathesis section process

Variables	Description	References
1-octene conversion (%)	100	Lehmann et al. (2003); Van der Gryp et al. (2012)
[a]Selectivity to C14 (%)	100	Van der Gryp (2009)
C14 conversion (%)	100	Haumann et al. (2002b)
[b]Selectivity 2-hexyl-nonanal (%)	70	Haumann et al. (2002a, 2002b)
1-octene/**HGr-2** molar ratio	10 0000	Van der Gryp et al. (2012)
C14/**Rh-TPPTS** molar ratio	2 500	Haumann et al. (2002b)
1-octene	$ 1.30/kg	Sasol chemicals (2016)
7-tetradecene	$ 35.50/kg	Alibaba (2016)
HGr-2 catalyst	$ 28 746.00/kg	Alibaba (2016)
HGr-1 catalyst	$ 46 533.00/kg	Alibaba (2016)
Gr-1 catalyst	$ 6 720.00/kg	Alibaba (2016)
Gr-2 catalyst	$ 19 600.00/kg	Alibaba (2016)
Schrock	$ 42 667.00/kg	Alibaba (2016)

[a]Selectivity to 7-tetradecene (%) = $\frac{No.of\ moles\ of\ 7-tetradecene}{Total\ No.of\ moles\ product\ produced}$ %

[b]Selectivity to hexyl-nonanal (%) = $\frac{No.of\ moles\ of\ 7-tetradecene}{Total\ No.of\ moles\ product\ produced}$ %

The design parameters used in this study were the 1-octene to catalyst molar ratio of 10 000 in order to increase conversion rate (TON), selectivity (ratio of moles of primary product to total moles of all products formed) and decrease size of reactor volume at the same time minimising catalyst usage and cost. At Level 1 of metathesis process development, an overall mass balance and a test for the presence of a vapour recycle and purge stream was conducted. The assumptions considered for mass balance calculations at Level 1 are listed in Table 4.2. According to the mass balance calculations, for the production rate of 10 000 tonnes per annum of 2-hexyl-nonanal at 99 wt. % purity, it was found that the feed rate of 1-octene

required is 14 160 tonnes per annum in order to produce 12 390 tonnes per annum of C14 as intermediate. Figure 4.6 illustrates the input-output structure of the flowsheet at Level 1 of metathesis process design.

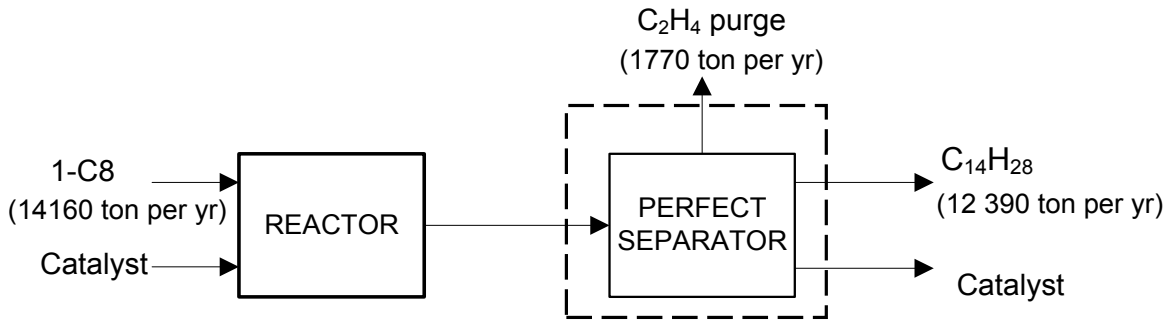

Figure 4.6.: Input-output structure at Level 1 of metathesis process development

The components enter the process in two streams: the first containing 1-octene and the second stream contains precatalyst dissolved in 1-octene. The raw material and product prices were based on supplier bulky costs as summarized in Table 4.2. Equation 4.2 gives EPM-1 for Level 1 of metathesis process design. Moreover, EPM-1 was also determined as a function of catalyst cost. If the value of the purified 7-tetradecene leaving the process was set at US $ 35.50 per kg, then the EPM-1 for different commercial catalysts was determined as summarized in Figure 4.7.

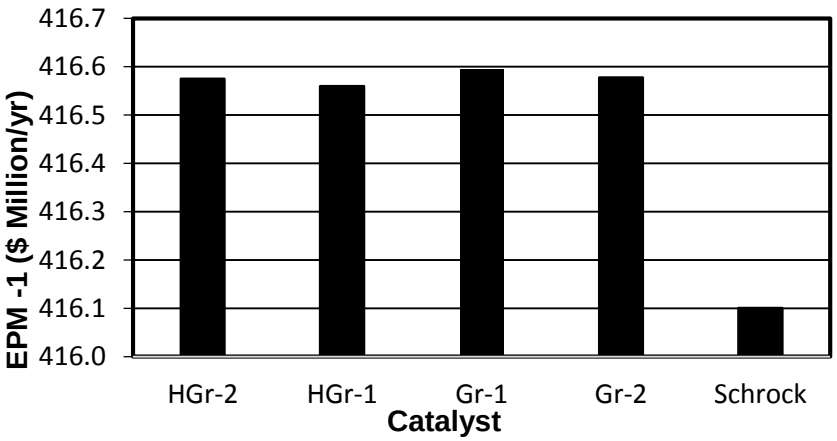

Figure 4.7.: EPM-1 for different commercial metathesis catalysts

The EPM-1 for all commercial catalysts considered gave preferable indicators per year hence; the project was sufficiently promising for further development. It can be seen that Grubbs-based precatalysts gave higher EPM-1 compared to Schrock catalyst. Furthermore, Schrock catalyst has a shorter catalyst lifetime of only seconds compared to Grubbs-based catalysts. Moreover, at Level 1 of metathesis process development, it would be premature to select the best catalyst based on EPM-1 values only, hence, results of EPM-1 together with other design parameters considered in Level 2 will be used to select the best catalyst.

4.3.1.2 Reactor and recycle structure (Level 2)

The main aim of Level 2 was to find operating conditions (single pass 1-octene conversion, catalyst type and optimum temperature) that would maximize EPM-2 by minimizing reactor cost. The parameters investigated at Level 2 includes catalyst type, temperature, single pass 1-octene conversion and the L/D ratio of the reactor. Figure 4.8 shows the reactor and recycle structure at Level 2 of metathesis process design.

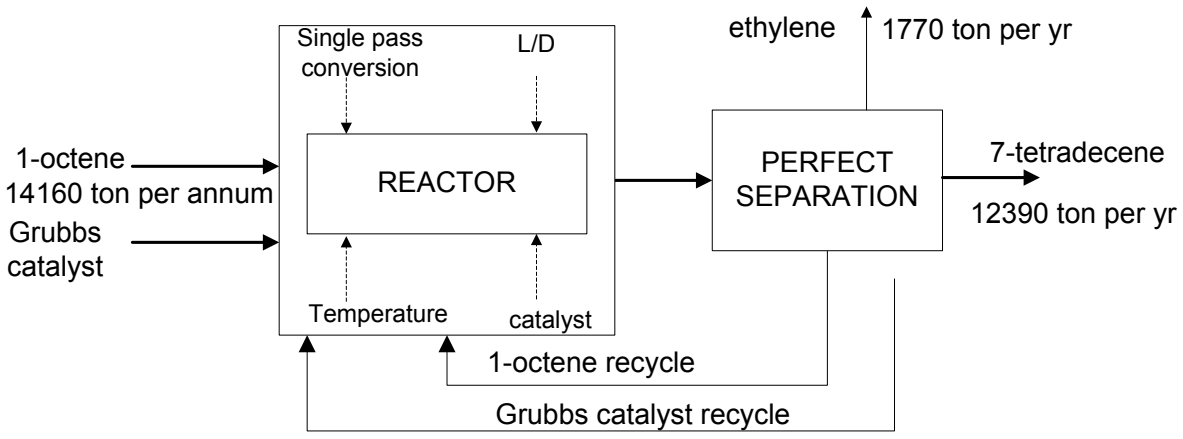

Figure 4.8.: Reactor and recycle structure at Level 2 of metathesis process development

According to Lehmann et al. (2003), simultaneous metathesis and isomerization could easily describe the formation of a product mixture of PMPs, IPs and SMPs during the metathesis reaction of 1-alkenes. The current conceivable pathway to 1-octene metathesis is illustrated in Figure 4.9.

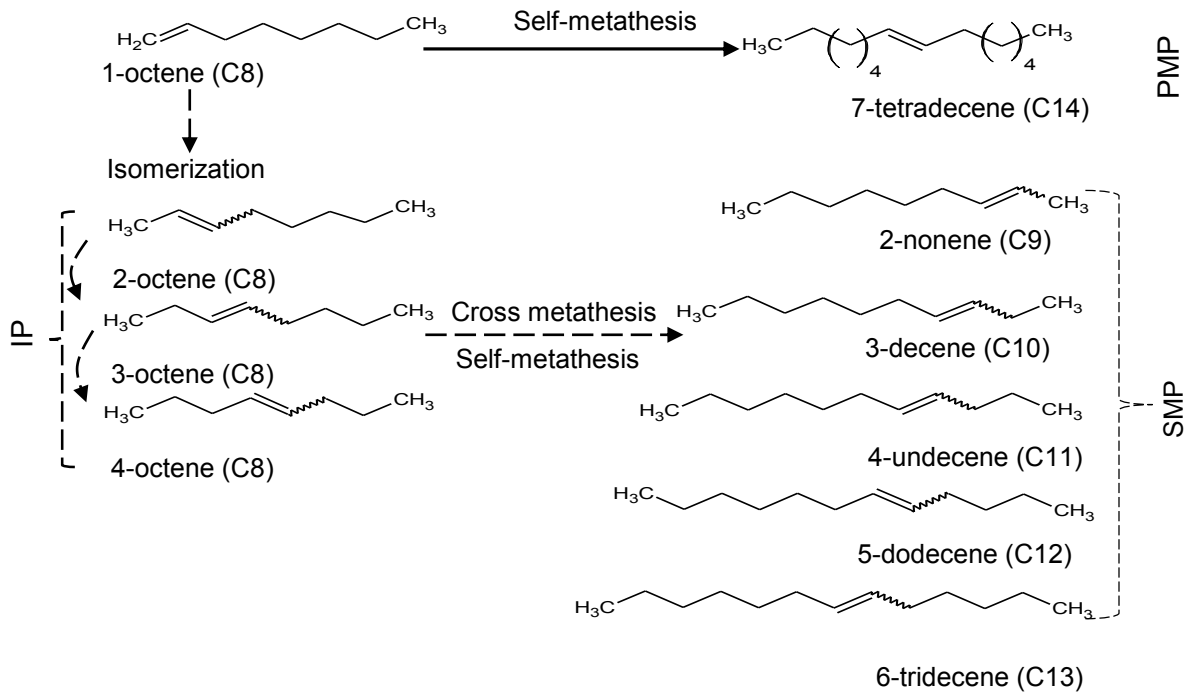

Figure 4.9.: Typical reactions and pathways for 1-octene metathesis (adapted, Lehman et al., 2003, Van der Gryp, 2009)

In this study, only one reactor was required since the objective was to maximise production of 7-tetradecene (PMP). Literature data (Motoboli, 2012; Van der Gryp et al., 2012; Jordaan et al., 2009) for the metathesis of 1-octene using different commercially available metathesis precatalysts including **Gr-1**, **Gr-2**, **HGr-1**, **HGr-2** and Schrock catalyst was used. In this study, independent operating conditions which includes temperature, 1-octene/catalyst molar ratio and reaction time were compared together with output variables such as single pass conversion, TON and selectivity to select the best catalyst. Table 4.3 shows a summary of literature data for comparison of the investigated catalysts based on the reported optimal conditions for each catalyst.

Table 4.3.: Comparison of different commercial catalysts

Catalyst	Operating parameters				Product distribution				Activity	References
	T	1-octene/Cat	Rxn Time	X_{C8}	PMP	IP	SMP	S	TON	
	(ºC)	(molar ratio)	(mins)	(%)	(%)	(%)	(%)	(%)	(-)	
HGr-1	50	10 000	420	39.53	36.87	2.29	0.37	93.28	3 687	Van der Gryp (2009)
HGr-2	***50***	***10 000***	***420***	***64.5***	***64.48***	***0.25***	***0.87***	***98.28***	***6 448***	***Van der Gryp et al. (2012)***
Gr-1	60	9 000	60	32	30.49	0.6	0.53	98	2 756	Motoboli (2012)
Gr-2	60	9 000	60	44	42.71	0.62	0.6	98	1 429	Motoboli (2012)
Schrock	85	100	210	67	63.6	2.5	0.9	-	-	Xaba (2011)
Gr-1	35	9 000	420	-	40.8	0.4	0.3	98.31	-	Max (2014)
Gr-2	35	9 000	420	-	60.8	0	1.3	97.1	-	Max (2014)
Gr-1	25	1 000	300	67	62	5		94	-	Jordaan et al. (2009)
Gr-2	60	9 000	995	-	93	0.1	5.1	94.8	6 373	Huijsmans (2009)
Gr-2	60	9 000	420	-	80.6	0	3.7	96.3	5 250	du Toit et al. (2014)

X_{C8} = 1-octene conversion

S = Selectivity ($S = \frac{\text{PMP}}{\text{PMP+IP+SMP}} \times 100\%$)

TON = Total number of moles product / mole catalyst.

In this study, **HGr-2** precatalyst was the best catalyst as it gave high selectivity to 7-tetradecene (PMP), economic catalyst to substrate molar ratio, a high TON and a comparatively longer catalyst life. **HGr-2** was the most efficient catalyst as it gave the highest catalyst life, selectivity and single pass conversion at low temperatures. It could be concluded that **HGr-2** precatalyst offers the advantage of a reduction in volume as it gave high activities (TON) compared to the other commercial catalysts reported in literature. Figure 4.10 shows the effect of temperature on the selectivity to 7-tetradecene for the metathesis of 1-octene in **HGr-2** catalyst.

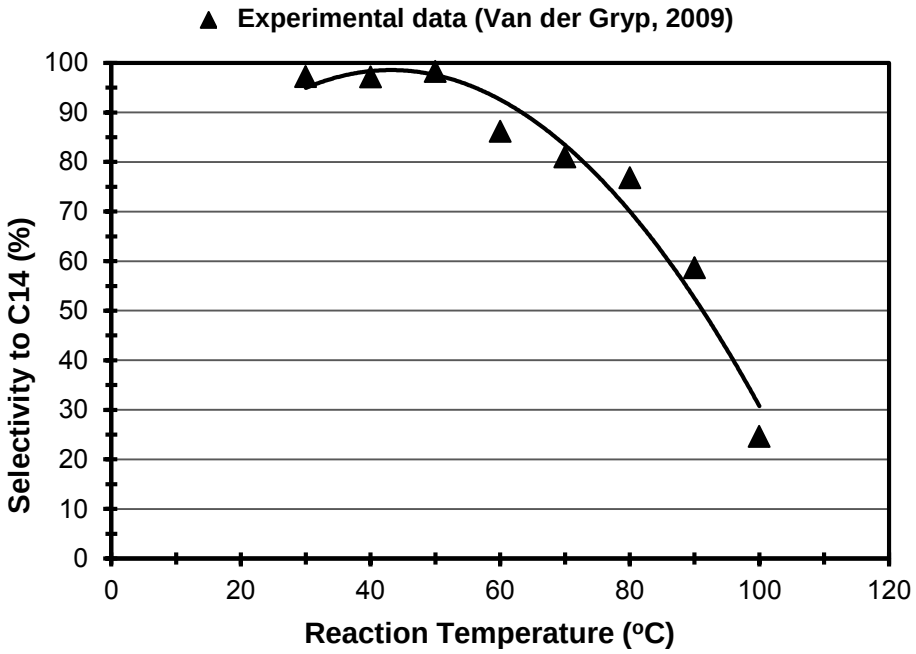

Figure 4.10.: Effect of reaction temperature on selectivity to C14 for the metathesis reaction of 1-octene in HGr-2 catalyst (experimental data from: Van der Gryp, 2009)

It can be seen from Figure 4.10 that operating the reactor at temperatures less than 60 °C resulted in high selectivities (approximately 100 %). However, the design must also consider the effect of conversion (catalytic activity) on the size of the reactor. The effect of single pass 1-octene conversion on the reactor cost and subsequently EPM-2 was determined in order to

find a range of operating single pass 1-octene conversion for a profitable metathesis process. The experimental data by Van der Gryp (2009) was used to determine the size of the metathesis reactor at different single pass 1-octene conversions. Figure 4.11 shows the effect of single pass 1-octene conversion on cost and EPM-2 at Level 2 of metathesis process development.

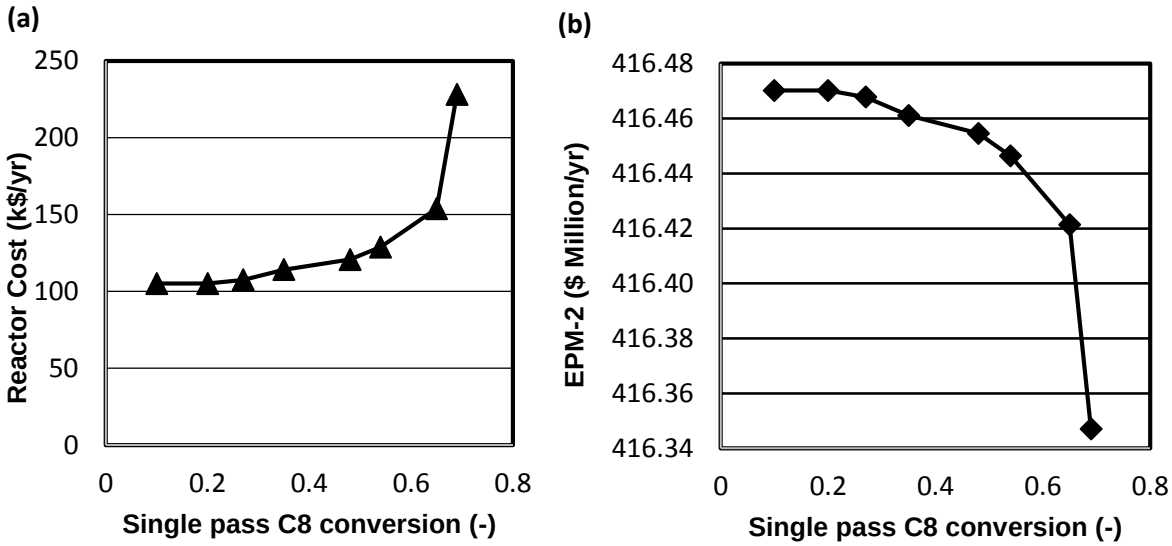

Figure 4.11.: Effect of single pass C8 conversion on (a) Reactor cost and (b) EPM-2 at Level 2 for operating the reactor at 50 ^{o}C and 2 bar using HGr-2.

It can be seen from Figure 4.11 that the cost of the reactor increased with single pass 1-octene conversion. It can be seen from Figure 4.11 that for single pass 1-octene conversion above 60 % the reactor cost increase exponentially as a result of larger reactor sizes required. The metathesis reactor in this case could however be operated at single pass 1-octene conversions below 60 % as operating outside this range resulted in an increase in the cost of reactor and hence, a decrease in EPM-2.

The effect of length to diameter ratio (L/D) on the reactor cost and subsequently EPM-2 was also evaluated in this study. The L/D ratio has an effect on degree of mixing in a CSTR. Engineering design heuristics has identified L/D ratios between 1.0 and 1.5 as near optimum

(Douglas, 1988). Figure 4.12 shows the effect of L/D ratio on the reactor cost and EPM-2 at single pass 1-octene conversion of 10 %.

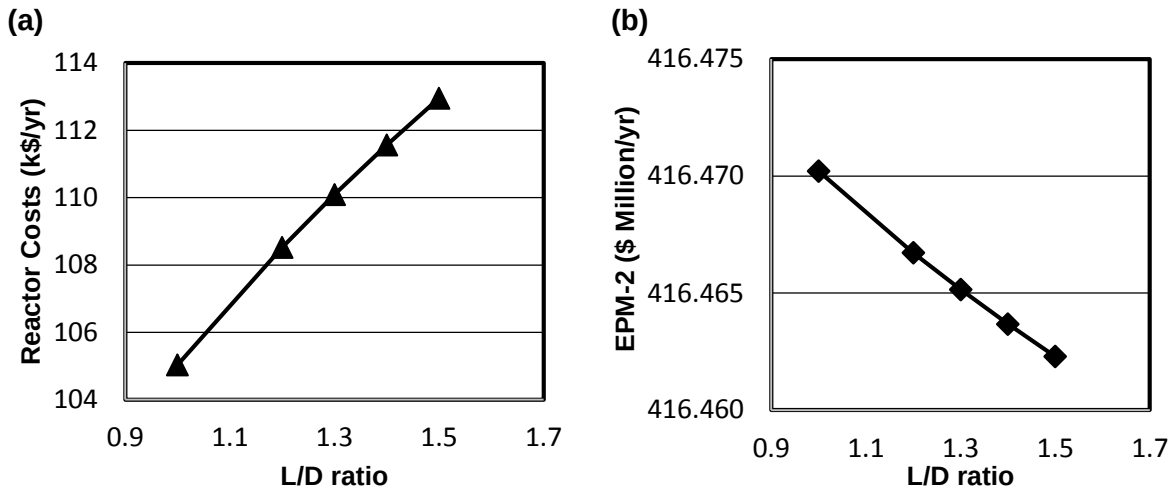

Figure 4.12.: Effect of L/D ratio on (a) Reactor cost and (b) EPM-2 at 50 ºC and 2 bar and C8 single pass conversion of 10 %.

Continuous stirred tank reactors (CSTR) offer the best control over metathesis product quality since concentration and temperature in the tank are uniform and easy to control (McKenna and Malone, 1990). It can be seen from Figure 4.12 that the higher the L/D ratio the higher the cost of the reactor and subsequently the lower the EPM-2. The design of a longer shaft can be more difficult. The cost of a mixer for a tall tank is likely to be greater than an equivalent mixer for a tank with an L/D = 1. Hence, in order to minimise the reactor cost and ensure perfect mixing in the CSTR reactor, the minimum L/D ratio of 1 was used in the design of the metathesis reactor.

The reactor would be operated adiabatically with direct heating since the reaction is endothermic with enthalpy of reaction of 108.45 kJ/mol (Mol, 2003). The reactor heat requirement for 14 160 tonnes per annum (15.75 kmol/hr) 1-octene fresh feed was found to be 1.71 MJ/hr. The reactor is operated at 50 ºC in order to maximise selectivity towards the 7-tetradecene (PMPs). The reactor temperature limit for activity when using **HGr-2** precatalyst

is 30 °C to 80 °C since the catalyst complex undergoes irrevesible decomposition above 80 °C (du Toit et al., 2014). The ethylene product stream could be used as fuel to heat the metathesis reactor.

Maynard and Grubbs (1999), Sharma and Jasra (2015) have emphasized requirements for recovery and recycle of **HGr-2** catalyst from the reaction product. According to Westhus et al. (2004), removal of the metal-containing by-products upon completion of the metathesis reaction is a serious drawback, which affects subsequent synthetic reactions. Hence, there was a need to seriously consider separation of the **HGr-2** catalyst species.

4.3.1.3 Separation and recycle system design (Level 3)

The optimal single pass 1-octene conversion lies below 100 %. The requirement to recover unreacted 1-octene, **HGr-2** catalyst and ethylene gas from the 7-tetradecene product makes it necessary to design a separation system. The streams emerging from the metathesis reactor (or reactor effluent) comprises of 7-tetradecene as main product, ethylene by-products, **HGr-2** catalyst and unreacted 1-octene. A consideration was placed on the equipment required to isolate, recover and recycle **HGr-2** catalyst and unreacted 1-octene and more importantly removal of ethylene from the system. Ethylene accumulation promotes formation of hydride species responsible for olefin isomerisation (Loock, 2009). Olefin isomerisation leads to the cross metathesis and hence, loss of reactants. Due to high selectivities for **HGr-2** catalyst at the reaction conditions, only the primary metathesis product was considered for the recycle system design. Table 4.4 was used to make decisions for the number of recycle streams.

Table 4.4.: Identification of number of recycle streams and destination of recycle streams

Component	Destination	Normal Boiling Point (°C)	Mr (g/mol)
C_8H_{16}	Recycle (Reactor)	121 °C	112.2
C_2H_4	Purge/fuel	-107 °C	28.03
$C_{14}H_{28}$	Primary product	255 °C	196.37
HGr-2 catalyst	Recycle (reactor)	220 °C	626.62

It can be seen that the base case process will have 1 product stream, 2 recycle streams and 1 purge stream. In the development of 1-octene metathesis process, the following decisions were made (1) not to purify ethylene from the process but to use it as a fuel instead (2) to recover and recycle **HGr-2** catalyst and (3) to recycle 1-octene. However, other alternatives for the 1-octene metathesis process could be:

1. To purify ethylene product stream
2. To remove **HGr-2** catalyst from the process
3. To purify 1-octene recycle stream

An attempt to simultaneously develop designs that corresponds to each process alternative could be considered. However, less than 1 % of ideas for new designs become commercialised hence the goal is to eliminate with little effort projects that are unprofitable (Douglas, 1988). Heuristics given in Appendix B.2.3 were used to help make these decisions. More importantly, the sequence of physical separation design to be employed had to consider catalyst stability. The **HGr-2** catalyst complex and unreacted 1-octene should be recovered and recycled to the reactor. This was in line with the economic requirements and the fact that the presence of **HGr-2** catalyst can be very sensitive to subsequent reactions such as hydroformylation. Even though unreacted 1-octene and **HGr-2** catalyst were going to be mixed at the reactor inlet, different separation methods were considered for each of the components (Douglas, 1988). The first consideration was to remove ethylene from reactor effluent. The cost of an additional flash drum was considered in order to make a decision on the single pass 1-octene conversion. The decision to use phase separation was based on the heuristic that phase separation is the cheapest method of separation (Douglas, 1988).

The next stage of separation at Level 3 considered the liquid phase product stream which contains unreacted 1-octene, **HGr-2** catalyst complex and 7-tetradecene product. The design of the metathesis process liquid product separation system aims to:

- recover > 99 wt. % of unreacted 1-octene.

- retain > 99.99 wt. % of **HGr-2** catalyst for reuse as an active catalyst to the metathesis reactor and also to avoid product contamination.

It was considered first to separate and recover **HGr-2** catalyst in its active form from the liquid effluent. The catalyst separation requirements are characterised by the following specifications as reported by Van der Gryp (2009) and Schmidt et al. (2014):

- Highly dilute systems (concentrating catalysts in mixtures 200 ppm).
- High recovery of 99.9 wt. %.
- **HGr-2** catalyst is component of highest molecular weight (MW).
- Catalyst is often component with lowest vapour pressure.
- At atmospheric pressures and moderate temperatures, the catalyst is solid.

The key challenge to the recovery of active catalyst in this process was catalyst instability at high temperatures (Vougioukalakis et al., 2013). The higher boiling points of 7-tetradecene product requires higher temperatures for their volatilization, which causes separation problems due to the narrowing differences in product and catalyst solution volatilities (Schmidt et al., 2014). The biggest problem for the sensitive catalyst system was the irreversible destruction of the catalyst during thermal separation from the reaction products (Wiese et al., 2006). It was considered to manipulated physical properties namely, the difference in boiling points and molecular sizes of the species.

(a) Separation alternative using distillation

It was considered to manipulate the difference in boiling points between **HGr-2** catalyst and the alkenes to effect separation from the product stream. Figure 4.13 shows the proposed separation structure for the catalyst system in this work.

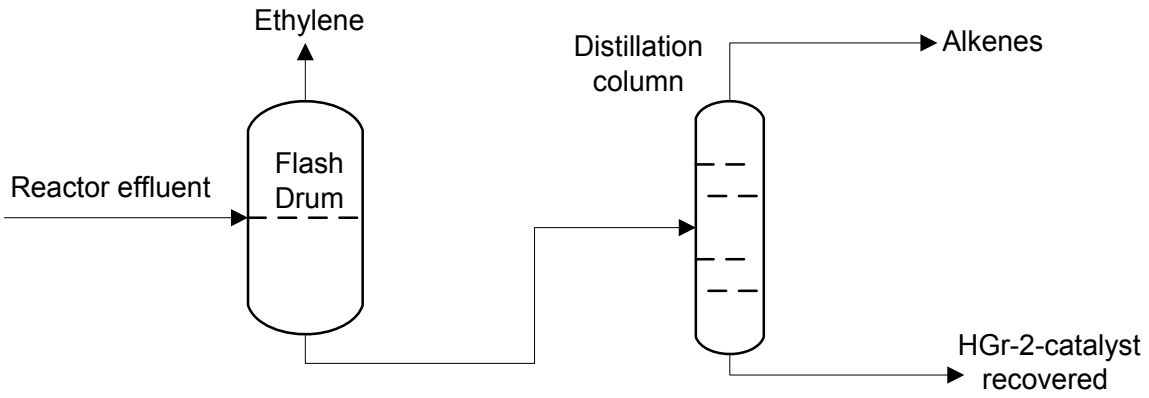

Figure 4.13.: Distillation configuration to recover the HGr-2 catalyst

Distillation technique cannot be used in this study to recover **HGr-2** catalyst due the requirement to recover the catalyst in its active form. High distillation temperatures as a result of high boiling points of alkenes in product stream are not practicable, as the catalyst will decompose irreversibly (Vougioukalakis et al., 2013).

(b) **Separation alternative using OSN membrane**

In this study, it was also considered to employ organic solvent nanofiltration (OSN) membrane process for organic systems because of the need to recover the **HGr-2** catalyst in its active form. Figure 4.14 shows the proposed separation structure for the catalyst recovery system.

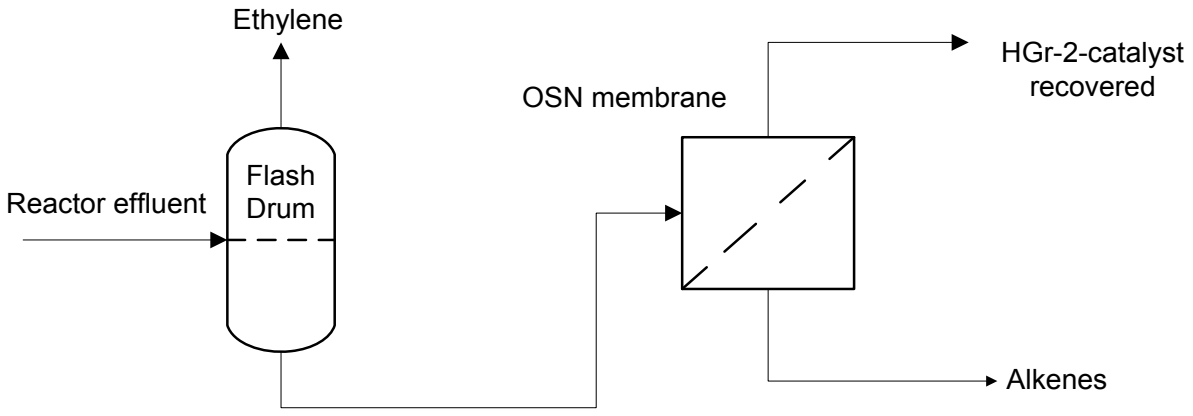

Figure 4.14.: OSN membrane set-up for recovery of HGr-2 catalyst

Organic solvent nanofiltration (OSN) membrane process to recover the **HGr-2** catalyst from the product solution can be carried at or below the reaction temperature. In comparison to conventional unit operations like distillation, OSN is less energy consuming (Dreimann et al., 2015; Schmidt et al., 2013; Seifert et al., 2014) due to low separation temperatures. Permeability data by Van der Gryp (2009) and Bhanushali et al. (2001) was used to predict recovery of **HGr-2** catalyst from the product stream. The cost of the membrane stage was determined as a function of mass flux using Equations B.11 to Equations B.14 as detailed in Appendix B.2.3. The retained **HGr-2** catalyst was recycled back to the reactor as retentate while the liquid permeate was purified in subsequent steps to recover 7-tetradecene.

Finally, liquid recovery system considered the recovery of 1-octene and recycling to metathesis reactor. The separation of 1-octene from 7-tetradecene can be accomplished by traditional distillation methods and there is a large body of literature (Turton et al., 2012; Peters and Timmerhaus, 2001; Kister, 1992) concerning the synthesis of such processes. Thus, if the annualized flash drum costs, annualised membrane costs and 1-octene column costs are added together then the total separation cost at Level 3 of the metathesis process could be determined. Figure 4.15 shows the effect of single pass 1-octene conversion on separation costs and EPM-3 (determined using Equation 4.6).

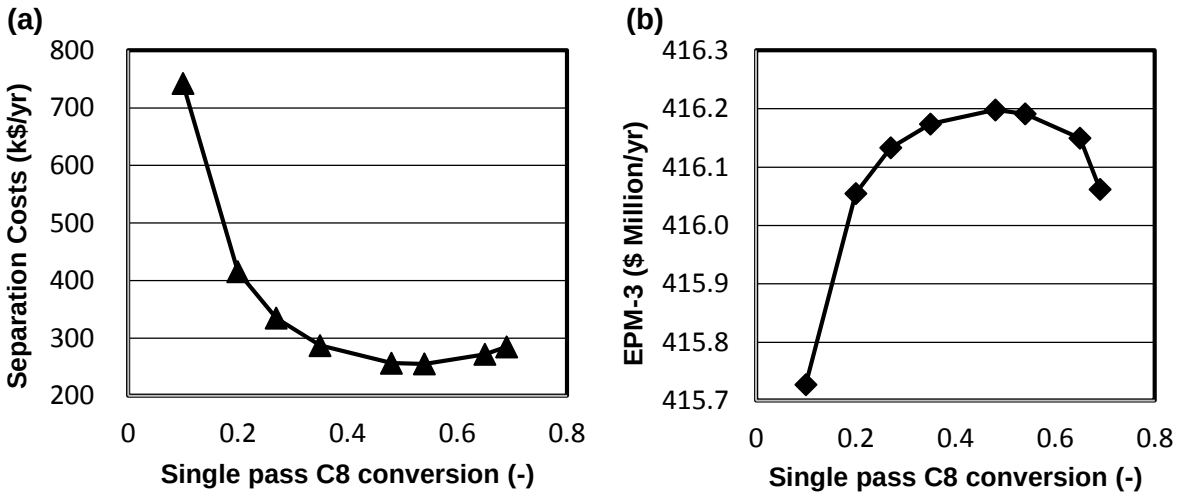

Figure 4.15.: Effect of single pass C8 conversion on (a) Separation costs and (b) EPM-3

At Level 3 of metathesis process development, it can be seen that operating the reactor at lower than 20 % single pass 1-octene conversion resulted in an exponential increase in the separation cost. The increase in the separation costs at lower single pass 1-octene conversion is a result of an increase in membrane area requirement and larger column diameters due to larger recycle volumes. Higher single pass 1-octene conversions above 60 % resulted in an increase in separation costs due to an increase in the size of the flash drum required to contain a large volume of ethylene gas produced. However, it was expected that the true economic potential to be higher than the calculated value at Level 3 by considering the cost savings brought by recovering the **HGr-2** catalyst.

Overall, the EPM-3 obtained for all single pass 1-octene conversions were favourable for advanced design. It can be seen from Figure 4.15 that at Level 3 of metathesis process development, the optimum single pass conversion of 1-octene must be set at 50 % since it gave the highest EPM-3. Figure 4.16 shows the flowsheet structure generated for the metathesis process section.

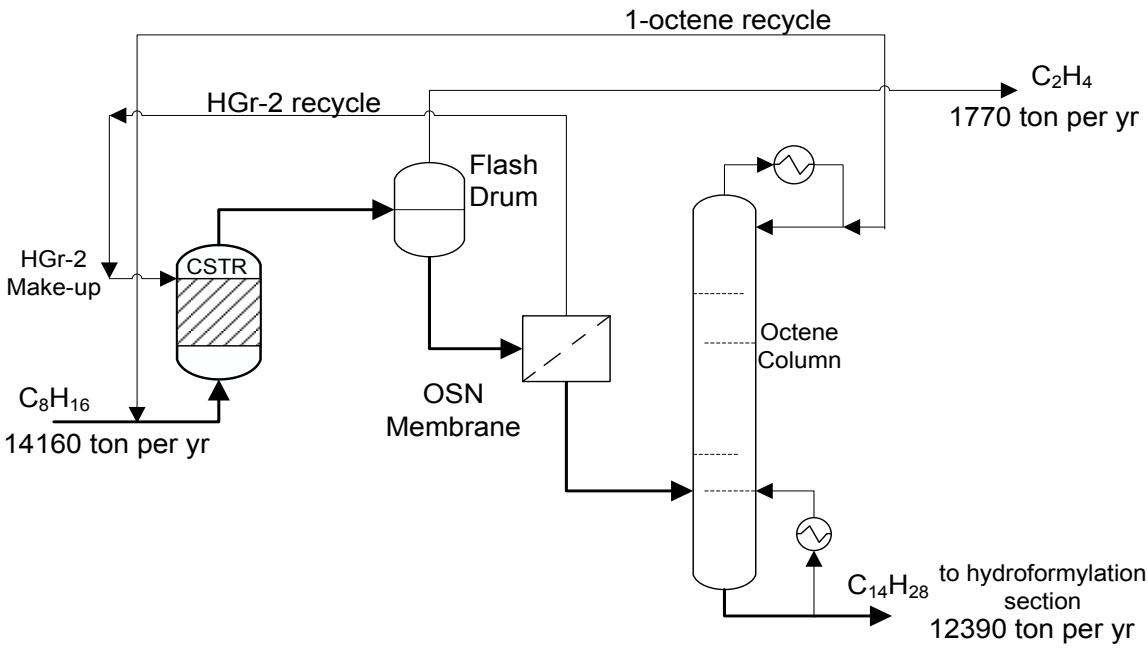

Figure 4.16.: Final flowsheet structure for metathesis process section

The primary product (7-tetradecene) from the metathesis process section will be directed to the hydroformylation process section where it will be further functionalised to a Guebert-type aldehyde, 2-hexyl-nonanal (2-HN) in the presence of a homogeneous Rh-based catalyst. A summary of optimal parameters corresponding to the highest final economic potential for the metathesis process section is listed in Table 4.5.

Table 4.5.: Optimal design parameters for metathesis process section

Parameter	Optimal value
Temperature	50 ^{o}C
Conversion (C_8)	50 %
L/D ratio (Reactor)	1.0
H/D ratio (Column)	10
R/R_m	1.2

4.3.2 Hydroformylation process section

4.3.2.1 Input-output information (Level 1)

Level 1 of hydroformylation process development gives the input-output information obtained from literature for the development of a process to produce 10 000 tons per annum of 2-hexyl-nonanal at a purity of 99 wt. % at Sasol Secunda. The catalyst type, temperature and single pass 7-tetradecene conversion are the parameters used to develop the hydroformylation process section at Level 1. The assumptions for mass balance evaluation at Level 1 of hydroformylation (Table 4.2) were taken at optimum reactor conditions as reported in literature. The 7-tetradecene produced from the metathesis process section is reacted with purified syngas (CO/H_2) purchased from the Sasol/Lurgi Gasification Plant at Secunda. The hydroformylation process was considered continuous according to heuristics by Douglas (1988). The required product purity for 2-hexyl-nonanal was 99 wt. %. According to Hentschel

et al. (2014) and Steimel et al. (2014), downstream processing requires purities above 98 wt. %. Figure 4.17 shows the input-output flowsheet structure at Level 1 of hydroformylation process development.

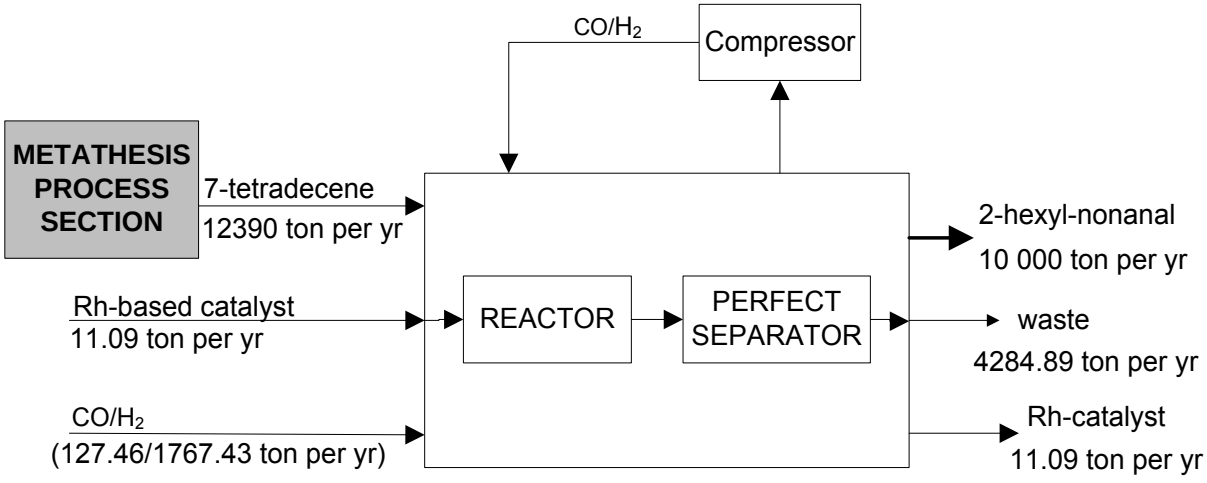

Figure 4.17.: Input-output flowsheet structure at Level 1 of hydroformylation process development

Table 4.6 shows a summary of the input-output information for the hydroformylation section.

Table 4.6.: Input-output (Level 1) information as given in leiterature for hydroformylation process

Variables	Operating parameters	References
Temperature (°C)	60-180	Rost et al. (2013), Muller et al. (2013, 2015)
Pressure (bar)	10-100	Haumann et al. (2002a, 2002b), Muller et al. (2013, 2015)
Maximum Selectivity (%)	70	Markert et al. (2013), Haumann et al. (2002b)
Conversion (%)	100	Haumann et al. (2002b)
Catalyst concentration overall	200 ppm	Haumann et al. (2002b)
7-tetradecene/**Rh-TPPTS** catalyst molar ratio	2 500	Haumann et al. (2002b)
CO/H_2 molar ratio	1:1	Hentschel et al. (2014), Haumann et al. (2002b)
alkene: water mass ratio (**α**)	0.5	Muller et al. (2013, 2015), Haumann et al. (2002a, 2002b)
surfactant concentration mass (**γ**)	0.08	Muller et al. (2013, 2015), Haumann et al. (2002a, 2002b)
2-hexyl-nonanal	$ 150,00/kg (bulk price)	Alibaba (2016)
7-tetradecene	$ 35.50/kg (bulk price	Sasol chemicals (2016)
Rh catalyst	$ 120 000.00/kg (bulk price)	kitco.com (2016)
Bulk syngas from gasifier	$ 0.03/kg (bulk price)	Piet et al. (2014)
Marlipal O13/80	$ 29.00/kg (bulk price)	Sasol chemicals (2016)

The following design specifications for water and marlipal were used. An alkene to water ratio in the mixture (**α**) = 50 %, a surfactant concentration (**γ**) = 8 % and $CO:H_2$ =1:1. These conditions have been recommended in previous work by Haumann et al. (2002a, 2002b), Muller et al. (2013), Muller et al. (2014), Muller et al. (2015), Rost et al. (2013), Schwarze et al. (2009) and Harmela et al. (2012). The resulting multiphase system offers an improved conversion and the possibility to separate the valuable rhodium catalyst from the organic product (Muller et al., 2013).

The EPH-1 for the input-output structure at Level 1 of hydroformylation process development was the difference between revenue from products and raw material costs (1-octene and syngas cost) and catalysts cost (**HGr-2**+**Rh-TPPTS**) and the cost of metathesis process section (Section 4.3.1). EPH-1 also considered single pass 1-octene conversion in the metathesis process section. The graph of the EPH-1 at varying 1-octene single pass conversion is shown in Figure 4.18.

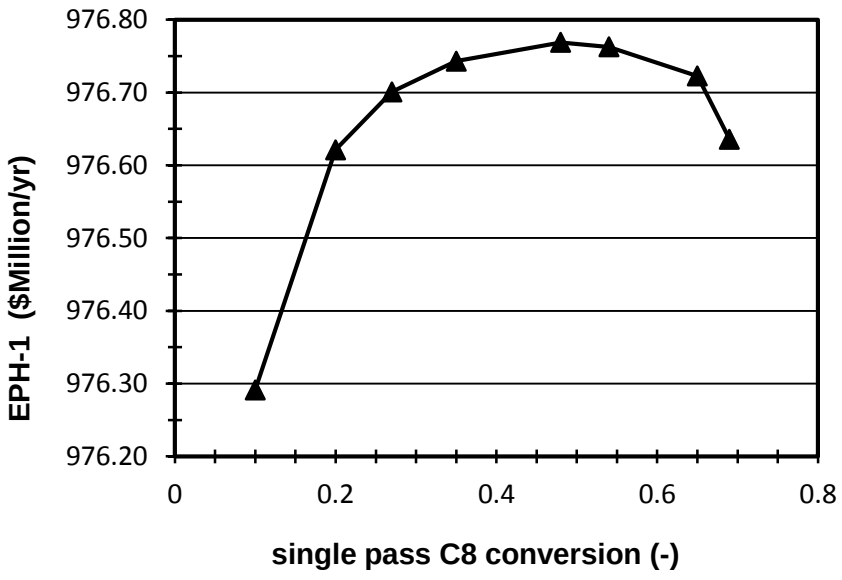

Figure 4.18.: Effect of single pass C8 conversion on EPH-1 at Level 1 of hydroformylation process development

EPH-1 for the hydroformylation process section was sufficiently promising for all single pass conversions of 1-octene in the metathesis process section. It could be concluded again that an optimum single pass 1-octene conversion of 50 % in the metathesis process section gave the highest EPH-1 at Level 1 of hydroformylation process design. Hence, using 50 % conversion of 1-octene in the metathesis process section the hydroformylation process section was further developed as shown in Section 4.3.2.2 and Section 4.3.2.3.

4.3.2.2 Reactor and recycle structure for hydroformylation process (Level 2)

The parameters investigated at Level 2 of hydroformylation process design are single pass 7-tetradecene conversion, Rh-based catalyst type, temperature, pressure and the L/D ratio of the reactor on both the annualised cost of the reactor and syngas-recycle compressor costs. Figure 4.19 shows the reactor and recycle structure for the hydroformylation process at Level 2 of process development.

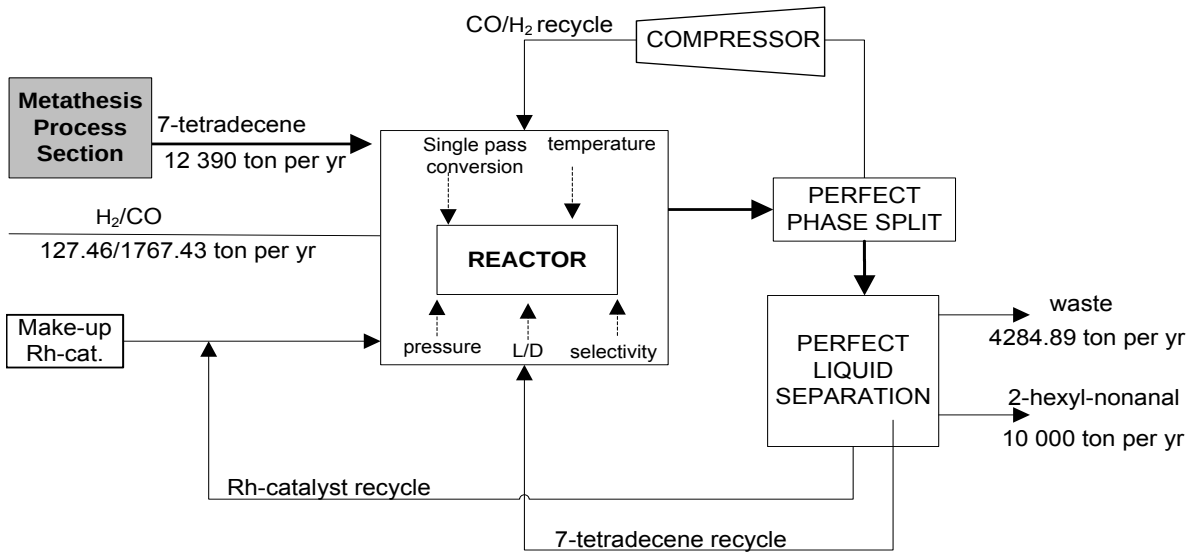

Figure 4.19.: Reactor and recycle structure at Level 2 of hydroformylation process development

In this investigation, the experimental results of hydroformylation of 7-tetradecene in **Rh-TPPTS** catalyst was used due to the limited kinetic information on hydroformylation of 7-tetradecene. In order to analyse the product distribution, simplify the complex reaction network and identify most relevant reactions, Markert et al. (2013) reaction scheme was used. Leeuwen et al. (2000) and Koeken et al. (2011) identified isomerization and hydroformylation reactions as only dominant reactions during hydroformylation of long chain alkenes (Cn > C9). Markert et al. (2013) and Haumann et al. (2002a) also confirmed that consecutive hydrogenation of aldehydes leading to corresponding alcohols was not observed during Rh-catalysed hydroformylation of long chain alkenes (Cn > C9). Markert et al. (2013) proposed a reduced and simplified reaction scheme for the hydroformylation of long chain alkenes. The most relevant reactions of long chain alkenes are reduced to six main reactions as shown in Figure 4.20.

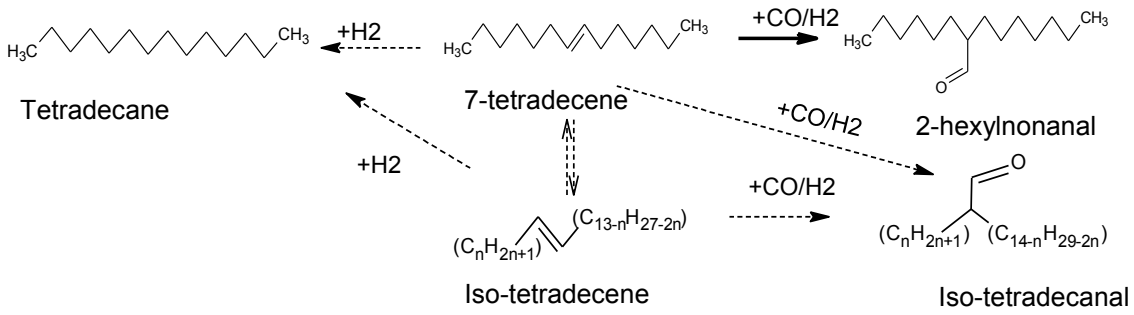

Figure 4.20.: Postulated reduced reaction network of the hydroformylation of 7-tetradecene

Hentschel et al. (2014) used pseudo-components such as “iso-alkene” and “iso-aldehyde” to represent a class of compounds with identical physical properties. These pseudo-components will be represented for example by 6-tetradecene for isomeric alkenes and 2-pentyl-decanal for isomeric aldehydes.

A number of decisions were made at Level 2 for the vapour-liquid process including the set of possible reactors, requirement of catalyst and reactants recycle, the number of recycle

streams, requirements for gas recycle compressor and heat effects in the reactor. Heuristics given in Appendix B.2.3 were used to make these decisions. In commercial plants, continuous stirred tank reactors (CSTR) have been used extensively. The highly sophisticated RCH/RP process, which together with Union Carbide's Mark IV process represents the state-of-the-art in today's hydroformylation technology in terms of the variable and fixed costs per ton of product (Kohlpaintner et al., 2001). In this study, only one reactor was choosen in order to produce 2-hexyl-nonanal product from 7-tetradecene and the reactor was modelled as a CSTR with kinetic parameters developed by Haumann et al. (2002b). Table 4.7 summarises kinetic data for the hydroformylation process as obtained from literature.

Table 4.7.: Kinetic data for the hydroformylation of 7-tetradecene (Haumann et al., 2002b)

Parameter	Equations	Units	Values
K	$k_o . \exp(\frac{-E_{areaction}}{RT})$	$mol/(m^3 s)$	-
P	Reaction pressure	bar	30-100
T	Reaction temperature	°C	60-130
$-E_{a,reaction}$	Activation Energy	kJ/mol	70.05
k_o	Pre- exponential factor	(mol/m^{3}s)	2.201×10^6
(-) ΔH	Heat of reaction	kJ/mol	215.14

Figure 4.21 shows the effect of reaction temperature on reactor cost at with varying single pass 7-tetradecene conversion using experimental data by Haumann et al. (2002b). Guthrie's correlation (Equation B.1 in Appendix B.2.2) was used to calculate the annualised cost for the hydroformylation reactor. The variation of reactor cost with single pass 7-tetradecene conversion was used to select the best temperature for the hydroformylation reactor.

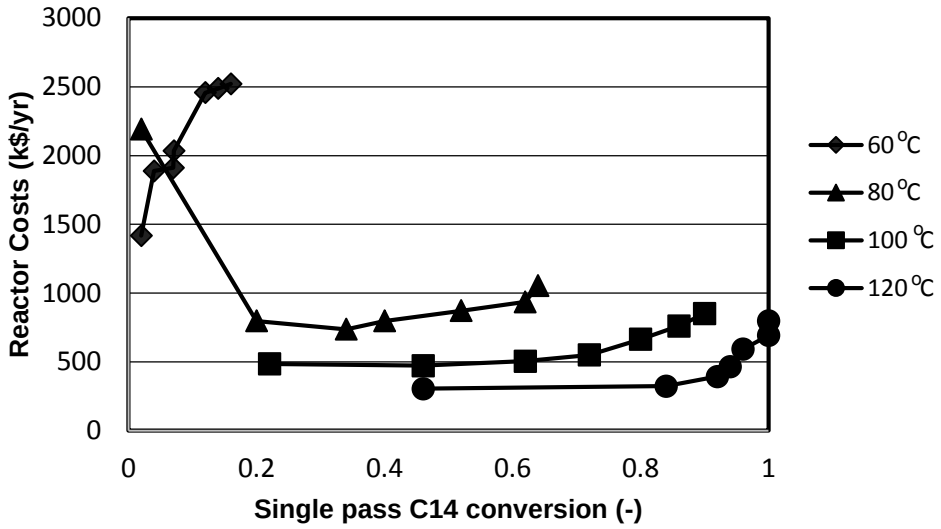

Figure 4.21.: Reactor cost versus single pass C14 conversion at varying temperatures (100 bar)

According to Figure 4.21, operating the hydroformylation reactor at high temperatures above 80 °C resulted in a significant reduction in reactor cost. It is evident that for single pass 7-tetradecene conversion above 80 %, all reaction temperatures will result in an increase in reactor cost. In this case, in order to promote the reaction, minimise the reactor volume and cost, the reactor must be operated at higher temperatures between 100 and 180 °C.

In engineering reactor design, minimizing reactor volume and attaining mild operating conditions are basic “rules of thumb” for an optimal design. According to Haumann et al. (2002b), operating the reactor at high temperatures resulted in significant reduction in size of reactor. It is comparatively safe to conduct a hydroformylation reaction using a small reactor volume due to the high operating pressure involved although consideration need to be made on the extend of recycle volumes. Figure 4.22 shows the effect of pressure on conversion at two reaction temperatures 80 °C and 100 °C.

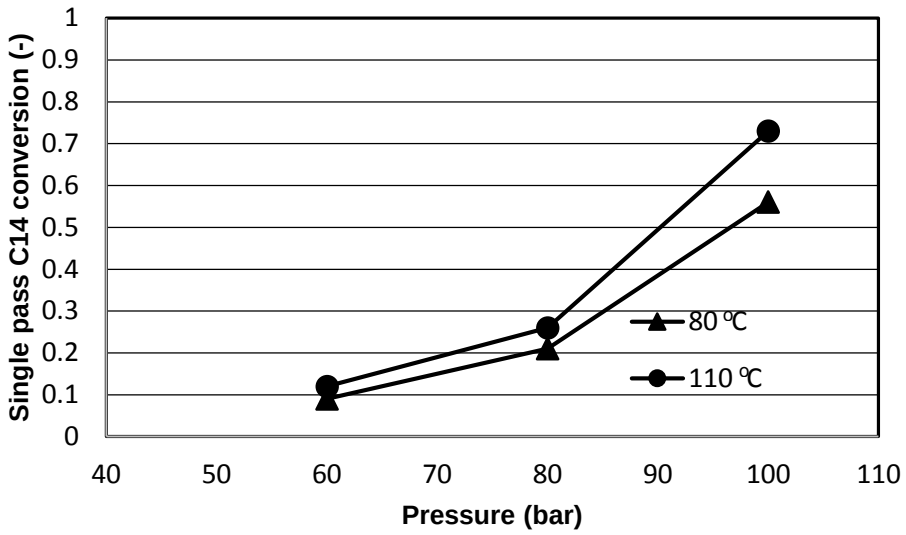

Figure 4.22.: Effect of pressure on single pass C14 conversion at 80 ºC and 100ºC

According to Khan et al. (1989), Koelliker et al. (1993) and Srivatsan et al. (1995), the solubility of syngas in an aqueous catalyst solution increases with increasing temperature hence conversion. Hence, for such systems as the hydroformylation reaction carried out at high pressure, it is important to choose the operating conditions that promotes conversion at the same time not compromising on safety. In light of this, conditions for the reactor were chosen to have the lowest pressure practically possible and the highest economic temperature.

Since, a stream of syngas has to be recycled back to the hydroformylation reactor, operating the reactor at low single pass 7-tetradecene conversion has a significant effect on total cost considering syngas-recycle compression requirements. Hence, the effect on total cost of reactor and syngas-recycle compressor with single pass 7-tetradecene conversion was investigated. If annualised reactor cost and syngas-recycle compressor costs (determined using Equation B.1 and Equation B.2 in Appendix B.2) are subtracted from the EPH-1, then an EPH-2 (determine from Equation 4.6) can be found. Figure 4.23 shows the effect of single pass 7-tetradecene conversion on the reactor plus syngas-recycle compressor costs and EPH-2 at Level 2 of design.

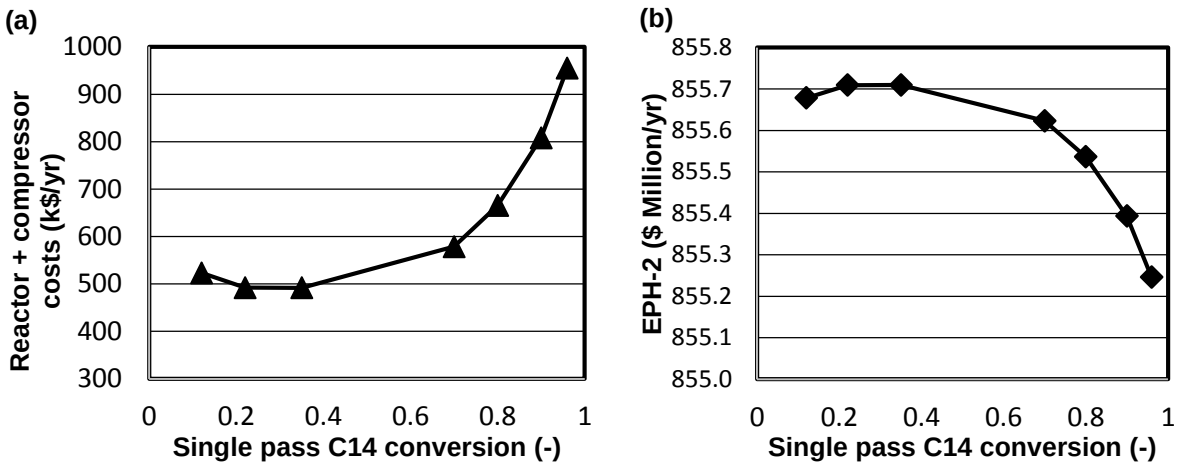

Figure 4.23.: Effect of single pass C14 conversion on (a) Reactor plus syngas-recycle compressor costs and (b) EPH-2 of hydroformylation process at 120 ^{o}C and 100 bar

It can be seen from Figure 4.23 that single pass 7-tetradecene conversion has a significant effect on the total cost (reactor plus syngas-recycle compressor). It can be seen that the optimum single pass 7-tetradecene conversion obtained after including a reactor plus syngas-recycle compressor lies between 20 % and 50 %. It can be concluded that lower single pass 7-tetradecene conversion below 20 % and high single pass 7-tetradecene conversions above 50 % resulted in an increase in costs due to high syngas-recycle compressions and larger reactor volumes required respectively.

The heat released for a 12 390 tonnes per annum (7.9 kmol/hr) 7-tetradecene fresh feed was found to be 1.7 MJ/hr. The reactor base temperature was set at 120 ^{o}C and the adiabatic temperature rise was found to be 368.44 ^{o}C. The reactor temperature limit in long chain aldehyde processing was 180 ^{o}C to avoid aldehyde product decomposition (Hentschel et al., 2014; Steimel et al., 2014). The heat of reaction can be utilised in either the reboiler of product purification column. A similar arrangement is found in the RCH/RP process a very energy efficient process where the reaction heat from the exothermic hydroformylation reactor is recovered and used in the reboiler of the distillation column (Cole-Hamilton and Tooze, 2006). Because of the importance of recovery and need for reuse of highly expensive **Rh-TPPTS**

catalyst, a consideration was put on the choice and design of separation equipment to be employed.

4.3.2.3 Separation and recycle system for hydroformylation process design (Level 3)

For the reactor used in the hydroformylation process development, the 7-tatradecene single pass conversions considered optimum in Level 2 was between 20 % and 50 %, hence, less than 100 % of reactants (7-tetradecene and syngas) were converted. This makes it necessary to have a system that separates products and un-reacted reactants. In removing the hydroformylation product from the reactor, the **Rh-TPPTS** catalyst complex and unreacted 7-tetradecene should be recovered and recycled to the reactor for economic reasons.

The presence of **Rh-TPPTS** catalyst in 2-hexyl-nonanal product was sensitive to subsequent use in either pharmaceutical products or speciality chemicals (Vougioukalakis, 2012). The physical separation method to be employed had to consider catalyst stability. Hence, it was important to determine the separation structure of an efficient recycle system. Moreover, different separation methods must be considered even though recycle streams containing 7-tetradecene and **Rh-TPPTS** catalyst species going to be re-mixed at the reactor inlet (Douglas, 1988). Table 4.8 was used to make decisions on the number of recycle streams and destinations.

Table 4.8.: Identification of number of recycle streams and destination of recycle streams

Component	Destination	Normal Boiling Point	Molecular weight
CO	Recycle (Reactor)	-191 °C	28.01(g/mol)
H_2	Recycle (Reactor)	-252 °C	2.02(g/mol)
Water	Recycle (Reactor)	100 °C	18.02(g/mol)
$7-C_{14}H_{28}$	Recycle (Reactor)	250 °C	196.37(g/mol)
Rh-TPPTS catalyst	Recycle (reactor)	400 °C	626.2 (g/mol)
$2-C_{15}H_{30}O$	Primary product	269 °C	223.01(g/mol)
Iso-Aldehydes	Waste	275 °C	223.01 (g/mol)
Marlipal (24/70)	Waste	250-270 °C	200 (g/mol)

The base case process will have 1 product stream, 4 recycle streams and 1 waste stream. The reactor effluent needed to be treated in subsequent steps to recover unreacted syngas, 7-tetradecene and highly expensive **Rh-TPPTS** catalyst. The phase separators can be defined either by heuristics (e.g., is it possible to separate syngas with an evaporator) or by short-cut models (e.g., using relative volatilities) (Steimel et al., 2014). According to Vougioukalakis (2013), pharmaceutical processes and medical regulation requires metal complexes in post reaction products to be less than 9 ppm. Haumann et al. (2002a) has predicted Rh losses as low as 1 ppm for a 100 000 ton per year potentially leading to US $ 40 million loss as far too high for an economical process based on microemulsion technology. The objectives of the separation system design were to:

- purify 2-hexyl-nonanal product to 99 wt. % purity as required by market specifications (Hentschel et al., 2014; Steimel et al., 2014).
- recover > 99.99 wt. % active Rh-catalyst for reuse in hydroformylation reactor.
- recover and recycle excess syngas (CO/H_2).
- recover and recycle > 99 wt. % unreacted 7-tetradecene.
- recycle solvent for reuse in the hydroformylation reactor.

The treatment of the liquid stream to recover **Rh-TPPTS** catalyst was considered first. According to Dreimann et al. (2016), the catalyst separation requirements are characterised by the following specifications:

- Highly dilute systems (concentrating catalysts in mixtures << 1 wt. %).
- High recovery of 99.9 wt. %.
- Catalyst is often component of highest molecular weight (MW).
- Catalyst is often component with lowest vapour pressure.
- Fragile coordination of ligand to the metal centre.
- At atmospheric pressures and moderate temperatures, the catalyst is solid.

The biggest problem for the sensitive **Rh-TPPTS** catalyst system is the irreversible destruction of the catalyst complex during thermal separation (Wiese et al., 2006). The **Rh-TPPTS**

catalyst-ligand complex cannot be recycled by distillation processes as it tends to cluster at higher temperatures and lower CO partial pressures (Schmidt et al., 2014). Moreover, the applied metal, Rhodium is very valuable (Priske et al., 2010) and must be recovered for recycle. Hence, in line with these objectives it was necessary to consider other different techniques of catalyst recovery.

(a) Separation alternative using liquid multiphase system (LMS)

Since LMS has previously been chosen as a reaction medium in this study one alternative was to manipulate the concept of LMS to effect catalyst recovery. Previous studies have confirmed that it is possible to reduce **Rh-TPPTS** catalyst loss in hydroformylation of long chain olefins by using the principle of LMS (Muller et al., 2013; Muller et al., 2015; Rost et al., 2013). The **Rh-TPPTS** catalyst removal takes place in the 3-phase separation unit (flash drum) in which most of the rhodium is drawn into the aqueous phase. However, preliminary investigations have shown that this step is quite challenging (Muller et al., 2014). The split factor for the catalyst carrying aqueous phase is usually uncertain and depends on conversion, surfactant concentration and operating conditions of temperature and pressure (Muller et al., 2013; Muller et al., 2014; Behr et al., 2006). After recovering **Rh-TPPTS** catalyst and unreacted syngas, unreacted 7-tetradecene was also recovered in a separate distillation column. The final separation column was used to purify 2-hexyl-nonanal from isomeric aldehydes. The total separation cost at Level 3 of hydroformylation process development included the flash drum cost, the 7-tetradecene column cost and the 2-hexyl-nonanal purification costs.

If the total separation costs at Level 3 is subtracted from EPH-2 (Equation 4.7), then EPH-3 versus single pass 7-tetradecene conversion at Level 3 can be found. Figure 4.24 shows the relationship between total separation cost and EPH-3 with single pass 7-tetradecene conversion at Level 3 of hydroformylation process development.

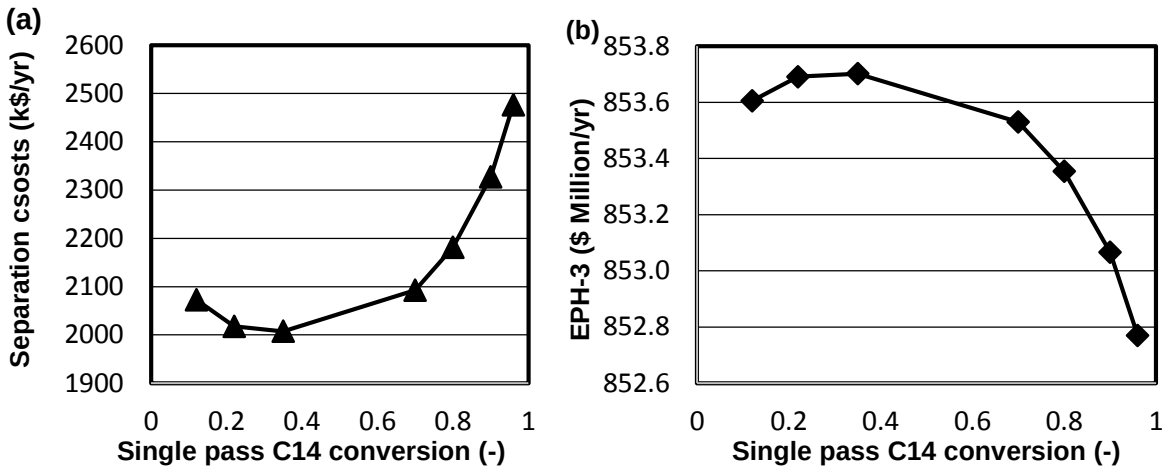

Figure 4.24.: Effect of single pass C14 conversion on (a) Separation costs and (b) EPH-3 (Liquid multiphase system)

It can be seen from Figure 4.24 that for single pass 7-tetradecene conversion below 20 % there is an increase in separation costs mainly due to large volume of flash drum and an increase in diameter of C14 column and product column as a result of large recycle volumes. Figure 4.24 also shows that higher single pass 7-tetradecene conversions above 50 % will result in increase in sepation costs particulary the C14 column. The increase in conversion led to reduction in mass fraction of 7-tetradecene in feed to C14 column (X_{FC14}) which leads to an increase in reflux ratio and number of separation stages in C14 column. Figure B.2 in Appendix B.2 shows the effect of single pass 7-tetradecene conversion on the reflux ratio and number of stages in C14 column.

It could be deduced from Figure 4.24 of EPH-3 versus single pass 7-tetradecene conversion that the optimum conversion for this process scenario was 35 %. Table 4.9 shows the optimal parameters for an economic hydroformylation process development utilising liquid multiphase system (LMS) for **Rh-TPPTS** catalyst recovery.

Table 4.9.: Parameters for the hydroformylation process

Parameter	Value
Temperature	100-180 °C
Pressure	< 100 bar
Conversion (7-tetradecene)	35 %
L/D ratio (reactor)	1
L/D ratio (column)	10
R/Rm	1.2

R/Rm = ratio of reflux to minimum reflux (-)

L/D = length to diameter ratio (-)

Figures 4.25 shows the flowsheet structure for the proposed base case scenario.

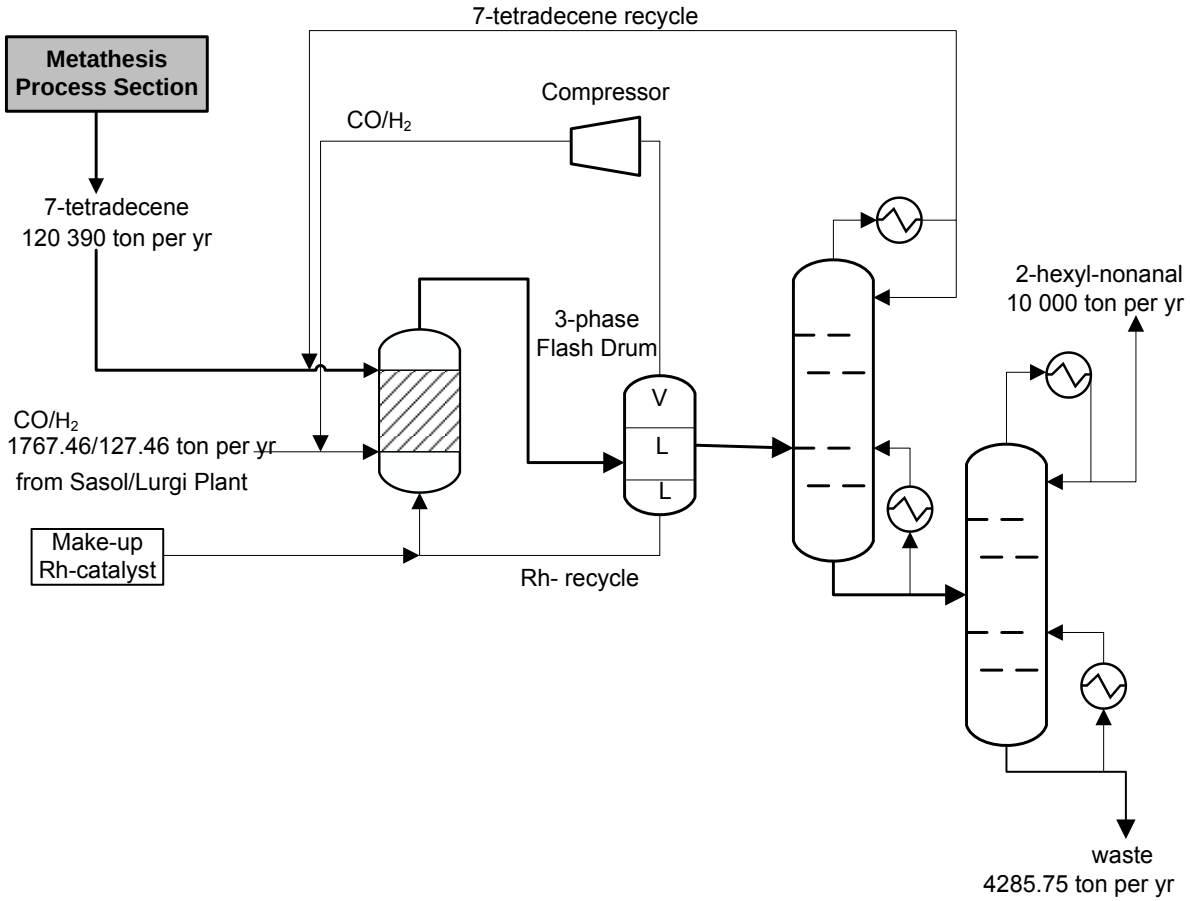

Figure 4.25.: Flowsheet at Level 3 using liquid multiphase system for Rh-TPPTS catalyst recovery

(b) Separation alternative OSN membrane

The other alternative was the OSN membrane process applied directly in the organic phase in which preselection was based on a minimum catalyst rejection of 99.9 wt. % (Schmidt et al., 2014). The decision was influenced by the exploitable difference in molecular weight of the **Rh-TPPTS** complex (626.2 g/mol) which is larger than the molecular weight of 2-hexyl-nonanal (262.3 g/mol). Janssen et al. (2010) have demonstrated that organic solvent nanofiltration membrane can effectively retain 99.96 wt. % of the **Rh-TPPTS** catalyst, thus tremendously simplifying the work-up as the **Rh-TPPTS** catalyst concentration in the product is extremely low. However, incorporating the cost of OSN membrane process (detailed in Equations B11 to Equation B14 in Appendix B) for the recovery of **Rh-TPPTS** catalyst species will influence the total cost at Level 3 of design.

In order to investigate the effect of including an OSN membrane separation stage for the recovery **Rh-TPPTS** catalyst, the membrane area and hence cost, was evaluated for every single pass 7-tetradecene conversion. After recovering **Rh-TPPTS** catalyst, the next stage was to investigate the effect of total separation cost on the inclusion of 7-tetradecene separation column. The final stage considered the purification of 2-hexyl-nonanal product from a mixture of isomeric products or waste. In order to investigate the effect of single pass 7-tetradecene conversion on the total separation cost, the total separation costs versus single pass 7-tetradecene conversion was plotted as shown in Figure 4.26. Equation 4.7 was used to determine the EPH-3 at Level 3 of hydroformylation process design with varying 7-tetradecene single pass conversion.

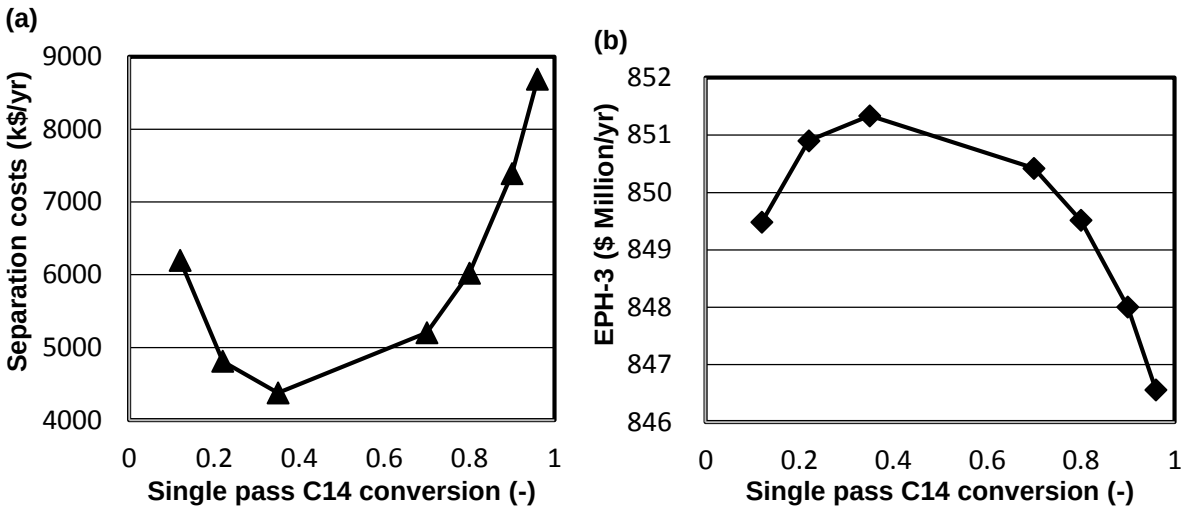

Figure 4.26.: Effect of single pass C14 conversion on (a) Separation costs and (b) EPH-3 at Level 3 hydoformylation process (OSN membrane process)

It can be seen from Figure 4.26 that single pass 7-tetradecene conversion below 20 % leads to an increase in separation costs mainly due to large recycle volumes that results in large membrane area, volume flash drum, C14 column and 2-hexyl-nonanal column. Figure 4.26 also shows that an increase in single pass 7-tetradecene above 60 % will leads to an increase in separation costs; this is particulary dominated by membrane costs. Figure B.4 in Appendix B.2 shows that an increase in single pass 7-tetradecene conversion leads to a decrease in mass fraction of 7-tetradecene in feed to the membrane. This in turn led to a reduction in mass flux ($^{kg}/_{m^2 s}$) across the membrane resulting in an increase in membrane area requirement. The increase in membrane area led to an increase in membrane separation costs.

However, at Level 3 of hydroformylation process development, the EPH-3 obtained for all single pass 7-tetradecene conversions proved it was possible to operate the hydroformylation process at a profit. It can be seen from Figure 4.26 that the highest EPH-3 at Level 3 of hydroformylation process developmnent could be achieved at a conversion of 35 % as it gave the highest EPH-3. Table 4.10 shows the optimal parameters for an economic hydroformylation process.

Table 4.10.: Parameters for the hydroformylation process

	Value
Temperature	120-180 °C
Pressure	< 100 bar
Conversion (7-tetradecene)	35 %
L/D ratio (reactor)	1
L/D ratio (column)	10
R/Rm	1.2

R/Rm = ratio of reflux to minimum reflux (-)

L/D = length to diameter ratio (-)

Figure 4.27 shows the overall process flowsheet at this level of design.

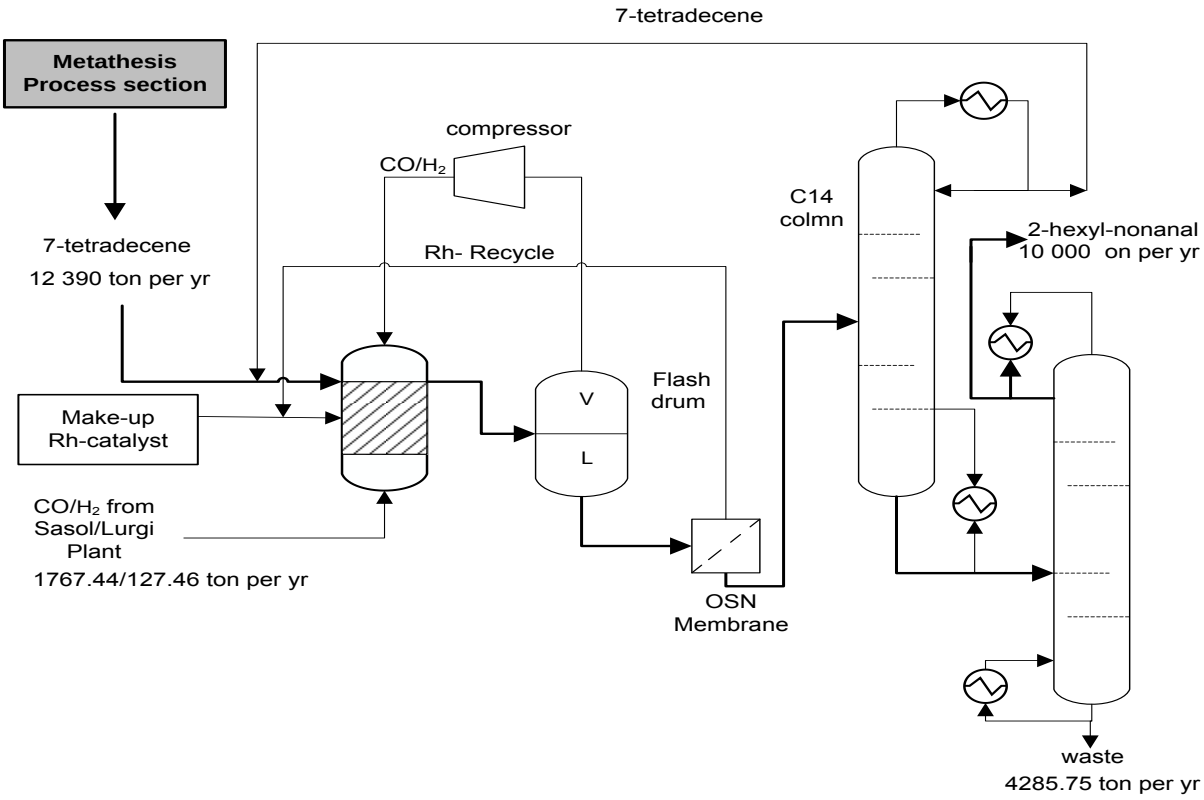

Figure 4.27.: Flowsheet at Level 3 of hydroformylation process development

(c) Separation alternative using distillation (Level 3)

Distillation is usually a dominant alternative because it provides pure components and is economically more attractive for many large-scale petrochemical processes. Malone et al. (1995) have however argued that common heuristics used for selecting distillation columns can be misleading in some cases. Figure 4.28 shows the distillation separation structure for the separation of **Rh-TPPTS** catalyst complex from long chain aldehyde product stream.

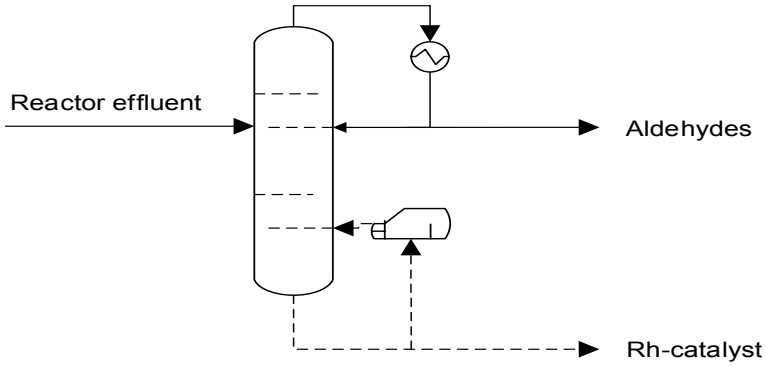

Figure 4.28.: Distillation procedure for catalyst recovery

Evaporation and distillation have been used to recover **Rh-TPPTS** catalysts in short chain aldehydes streams such as Ruhrchemie/Rhone-Poulenc, BASF, UCC and Mitsubishi process. However, the high boiling point of long chain 2-hexyl-nonanal poses great difficulties (Garton et al., 2003; Razak, 2013). At higher distillation temperatures synonymous with long chain aldehydes, the catalyst will decompose and hence this technique will not be used in this study.

4.4 Final process flow diagram

Finally, the process alternatives in metathesis and hydroformylation were combined to form two base case scenarios. In the metathesis process section, the solution to **HGr-2** catalyst recovery was limited to the application of organic solvent nanofiltration (OSN) membrane because of catalyst stability and irreversible degradation thereof. In the hydroformylation process section two **Rh-TPPTS** catalyst recovery techniques namely, liquid multiphase

system (LMS) and organic solvent nanofiltration (OSN) membrane were considered for further detailed engineering investigation.

4.4.1 Process Scenario A: Liquid multiphase system (LMS)

This process scenario integrates metathesis process section and the hydroformylation process section which utilises the alternative of liquid multiphase system (LMS) to recover **Rh-TPPTS** catalyst from the post hydroformylation reaction products. The base case process flow diagram which will be investigated further in Aspen Plus™ is shown in Figure 4.29.

4.4.2 Process Scenario B: OSN membrane separation

This process scenario integrates metathesis process section and hydroformylation process section which utilises the alternative of organic solvent nanofiltration (OSN) membrane to recover **Rh-TPPTS** catalyst from post hydroformylation reaction products. The base case process flow diagram is shown in Figure 4.30 which will be further investigated in Aspen Plus™ simulation.

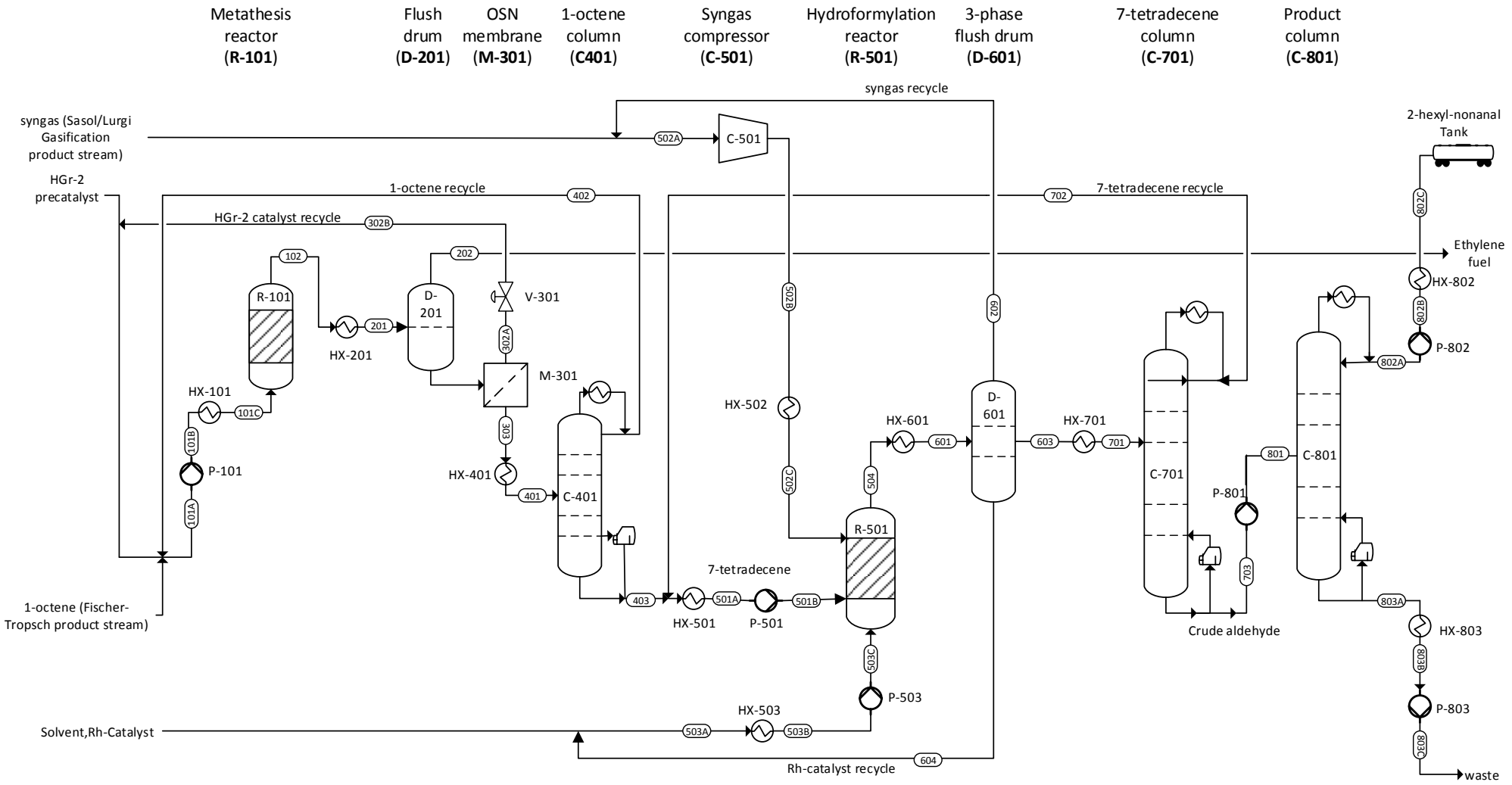

Figure 4.29.: Process flow diagram for Process Scenario A

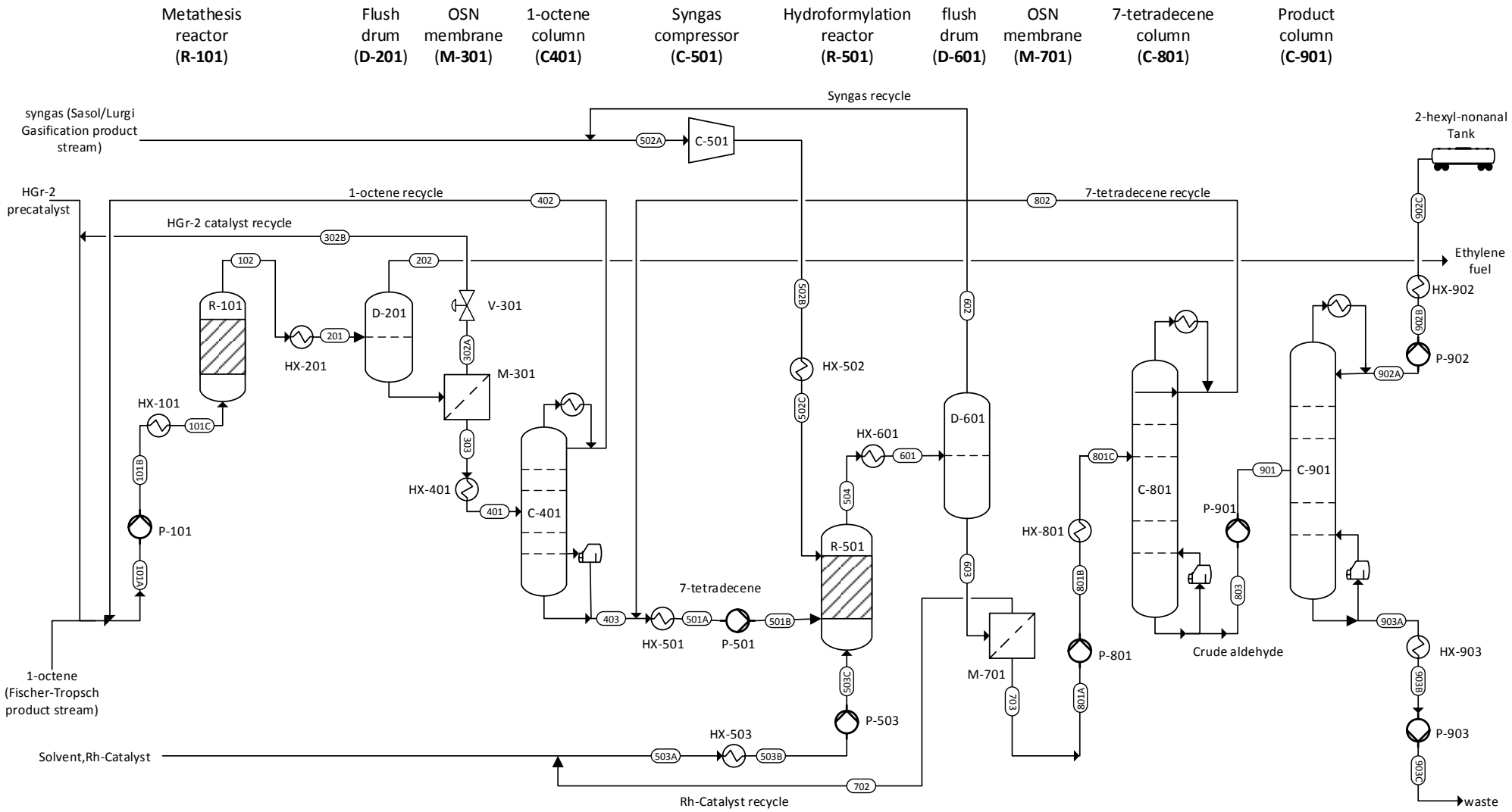

Figure 4.30.: Process flow diagram Process Scenario B

4.5 Summary

Chapter 4 covers preparatory aspects of simulation, such as the defining of process units used in process development, simulation conditions for the simulation study of the process of upgrading low value 1-octene a Fischer-Tropsch product stream to 2-hexyl-nonanal. In the selection of simulation conditions, some of the conditions were extracted entirely from literature and other conditions were determined from results of economic potential. Key outputs from this chapter were two conceptual process flow diagrams, Figure 4.29 for Scenario A and Figure 4.30 for process Scenario B. The two process flow diagrams will be used to develop complete Aspen Plus™ flowsheets which were used to determine optimal conditions for the process of upgrading low value 1-octene from Fischer-Tropsch into 2-hexyl-nonanal. The results obtained from the simulation study are discussed in Chapter 5 of this dissertation.

4.6 References

Arnoldy, P., Process aspects of rhodium-catalysed hydroformylation. In Rhodium catalyzed hydroformylation, van Leeuwen, P. W. N. M.; Claver, C., Eds. Kluwer Academic Publishers: Dordrecht, the Netherlands, **22** (2000)

Baerns, M., Behr, A., Brehm, A., Gmehling, J., Hofmann, H., Onken, U., Renken, A. Technische Chemie. Wiley-VCH, Weinheim (2006)

Douglas, J. M., Conceptual design f chemical process. International Edition (1988) McGraw-Hill Chemical Engineering Series ISBN 0-07-017762-7

du Toit, C.G.C.E. van Sittert, H.C.M. Vosloo, Metal carbenes in homogeneous alkene metathesis: Computational investigations, Journal of Organometallic Chemistry **738** (2013) 76-91

du Toit, M. Jordaan, C. A. A. Huijsmans, J. H. L. Jordaan, C G. C. E. van Sittert and H. C. M. Vosloo Improved Metathesis Lifetime: Chelating Pyridinyl-Alcoholato Ligands in the Second Generation Grubbs Precatalyst, Molecules **19** (2014) 5522-5537; doi:10.3390/molecules19055522

Fang, J., Towards a Benign and Viable Rhodium Catalyzed Hydroformylation of Higher Olefins: Economic and Environmental Impact Analyses, Solvent Effects and Membrane-based Catalyst Separation (2009).

Frohling, C. D.; Kohlpaintner, C. W. In Applied Homogeneous Catalysis with Organometallic Compounds; Cornils, B., Herrmann, W. A., Ed.; VCH: Weinheim, **1** (1996); 27-104

Grubbs, R.H., Tina M. Trnka T.M., Sanford M.S., Transition Metal-Carbene Complexes in Olefin Metathesis and Related Reactions, Current Methods in Inorganic Chemistry, **3** Editors: H. Kurosawa and A. Yamamoto (2003) Elsevier Science B.V

Gual, S., Godard C., Castillón S., Claver C., Highlights of the Rh-catalysed asymmetric hydroformylation of alkenes using phosphorus donor ligands; Tetrahedron: Asymmetry **21** (2010) 1135–1146

Haumann, M., Koch, H., Hugo, P., Schomacker, R., Hydroformylation of 1-dodecene using Rh-TPPTS in a microemulsion, Applied Catalysis A: General **225** (2002a) 239–249

Haumann M., Koch K., Hugo P., Schomacker R., Hydroformylation of 7-dodecene using Rh-TPPTS in a micro emulsion. Applied Catalysis A: General **225** (2002b) 239–249

Hentschel, B., Kiedorf, G, Gerlach, M, Hamel, C., Seidel-Morgenstern, A, Freund, A, Sundmacher, K. Model-Based Identification and Experimental Validation of the Optimal Reaction Route for the Hydroformylation of 1‑Dodecene. Industrial Engineering Chemistry Research **54** (2015), 1755−1765 DOI: 10.1021/ie504388t

Hentschel, B., Peschel, A., Xie M., Vogelpohl, C., Sadowski, G., Freund, H., Sundmacher, K., Model-based prediction of optimal conditions for 1-octene hydroformylation. Chemical Engineering Science **115** (2014) 58–68

Huijsmans, C. A. A, Modelling and synthesis of Grubbs type complexes with hemilabile ligands, North-West University (Potchefstroom campus), (MSc Dissertation), (2009)

Ivin, K.J., Mol, J.C., Olefin Metathesis and Metathesis Polymerization, Academic Press, London, (3rd Edition) (1997)

Iribarren, O. A., Malone M.F, A systematic procedure for batch process design. Paper presented at American Institute of Chemical Engineers Annual Meering, Chicago (1985)

Janssen, M., Muller C., Vogt D., Recent advances in the recycling of homogenous catalyst using membrane separation, Green Chemistry **13** (2011) 2247–2257

Jordaan, M., van Helden P., van Sittert C.G.C.E., Vosloo, H.C.M. Experimental and DFT investigation of the 1-octene metathesis reaction mechanism with the Grubbs 1 precatalyst, Journal of Molecular Catalysis A: Chemical **254** (2006) 145–154

Jorke, A., Seidel-Morgenstern A., Hamel C., Isomerization of 1-decene: Estimation of thermodynamic properties, equilibrium composition calculation and experimental validation using a Rh-BIPHEPHOS catalyst, Chemical Engineering Journal **260** (2015) 513–523

Kegl, T., Computational aspects of hydroformylation, (Review). The Royal Society of Chemistry **5,** (2015), 4304–4327

Kiedorf, G., Hoang D.M, Muller A., Jorke A., Markert J. Arellano-Garcia A., Seidel-Morgenstern A., Hamel C. Kinetics of 1-dodecene hydroformylation in a thermomorphic solvent system using a rhodium-biphephos catalyst. Chemical Engineering Science **115** (2014) 31–48

Kister, H, Z., Chemical Engineering distillation design, 1st ed. Mcgraw-Hill, (1992)

Koeken, A.C.J., van den Broeke, L.J.P., Benes, N.E., Keurentjes, J.T.F., Triphenylphosphine modified rhodium catalyst for hydroformylation in supercritical carbon dioxide. Journal of Molecular Catalysis A: Chemistry **346,** (2011) 94–101

Kohlpaintner, C.W., Richard W. Fischer a, Boy Cornils, Aqueous biphasic catalysis: Ruhrchemie/Rhone-Poulenc oxo process Applied Catalysis A: General **221** (2001) 219–225

Khan, M.M. T., Halligudi, S.B., Shukla S., Solubility of carbon-monoxide in water, n-butylamine, ethanol, cyclohexene and water – dimethylformamide mixtures, Journal of Chemical & Engineering Data **34** (1989) 353–355.

Koelliker, R., Thies H., Solubility of carbon-monoxide in n-hexane between 293K and 473K and CO pressures up to 200 bar, Journal of Chemical & Engineering Data **38** (1993) 437–440.

Lehman, J. Jr., J. E. Schwendeman, P. M. O'Donnell, K. B. Wagener; Olefin isomerization promoted by olefin metathesis catalysts, Inorganica Chimica Acta **345** (2003) 190-198

Malone, F., M McKenna,. TF and Polymer process design. Continuous production of chain growth homopolymers Computers and Chemical Engineering **14**, No. 10, (1990) pp. 1127-1149,

Muller, D., Minh D.H., Merchan V.A, Arellano-Garcia H., Kasaka Y., Muller M., Schomacker R., Wozny G., Towards a novel process concept for the hydroformylation of higher

alkenes: Mini-plant operation strategies via model development and optimal experimental design, Chemical Engineering Science **115** (2014) 127–138

Neelis, M, Worrell E., and Eric Masanet, Energy Efficiency Improvement and Cost Saving Opportunities for the Petrochemical Industry An ENERGY STAR® Guide for Energy and Plant Managers Energy Analysis Department Environmental Energy Technologies Division, Ernest Orlando Lawrence Berkeley National Laboratory (2008)

Peschel, A., Hentschel B., Freund H., Sundmacher K., Design of optimal multiphase reactors exemplified on the hydroformylation of long chain alkenes. Chemical Engineering Journal **188** (2012) 126– 141

Priske, M, Wiese K.W., Drews A., Kraume M., Baumgarten G., Reaction integrated separation of homogenous catalysts in the hydroformylation of higher olefins by means of organophilic nanofiltration, Journal of Membrane Science **360** (2010) 77–83

Pogrzeba, D., Muller, Illner M., Schmidt M., Kasaka Y., Weber A., Wozny G., Schomäcker R., Schwarze M., Superior catalyst recycling in surfactant based multiphase systems -Quo vadis catalyst complex? Chemical Engineering and Processing **99** (2016) 155–166

Rabiller-Baudry, M., Nasser G., Renouard T., Delaunay D., Camus M., Comparison of two nanofiltration membrane reactors for a model reaction of olefin metathesis achieved in toluene. Separation and Purification Technology **116** (2013) 46–60

Rost, A., Müller M., Hamerla T., Kasaka Y., Wozny G., Schomacker R., Development of a continuous process for the hydroformylation of long-chain olefins in aqueous multiphase systems, Chemical Engineering and Processing **67** (2013) 130– 135

Schafer, A., Brunsch Y., Sadowski G., Behr A., Hydroformylation of 1‑Dodecene in the Thermomorphic Solvent System Dimethylformamide/Decane. Phase Behaviour−Reaction Performance−Catalyst Recycling, Industrial Engineering Chemistry Research **51**, (2012), 10296−10306 dx.doi.org/10.1021/ie300484q

Shahane, S., Toupet, L., Fischmeister, C, Bruneau, C., Synthesis and charactorization of Sterrically Enlarged Hoveyda-Type Olefin Metathesis Catalysts, European Journal of Inorganic Chemistry **24** (2013) 54-60

Steimel, J., Harrmann M., Schembecker G., Engell S., A framework for the modelling and optimization of process superstructures under uncertainty, Chemical Engineering Science **115** (2014) 225–237

Steimel, J., Harrmann M., Schembecker G., Engell S. A framework for the modelling and optimization of process superstructures under uncertainty. Chemical Engineering Science **115** (2014) 225–237

Srivatsan, X., Yi H., Robinson R.L., Gasem K.A.M., Solubilities of carbonmonoxide in heavy normal-paraffins at temperatures from 311-K to 423-K and pressures to 10.2-MPa, Journal of Chemical & Engineering Data **40** (1995) 237–240

Tomasek, J. and Schatz J., Olefin metathesis in aqueous media, The Royal Society of Chemistry (Review) Green Chemistry, **15,** (2013), 2317–2338

Vandezande, P., Lieven E., Gevers M. and. Vankelecom I. F.J, Solvent resistant nanofiltration: separating on a molecular level, Chemical Society Reviews, **37**, (2008), 365–405

Van der Gryp P, Barnard A, Cronje J.P., de Vlieger D., Marx S, Vosloo HCM., Separation of different metathesis Grubbs-type catalysts using organic solvent nanofiltration, Journal of Membrane Science **353** (2010) 70–77

Van der Gryp, P, Separation of Grubbs-based catalysts with Nanofiltration, (PhD Thesis), North-West University, 2009.

Van der Gryp, P., Marx S., Vosloo H. C. M., Experimental, DFT and kinetic study of 1-octene metathesis with Hoveyda–Grubbs second generation precatalyst, Journal of Molecular Catalysis A: Chemical **355** (2012) 85– 95

Van Leeuwen, P.W.N.M. Claver C., Rhodium Catalysed Hydroformylation, Kluwer Academic Publishers, Dordrecht (2000).

Vougioukalakis, G. C., Removing Ruthenium Residues from Olefin Metathesis Reaction Products, Chemistry a European Journal. **18**, (2012), 8868 – 8880

Webb, M., Sellin M.F., Kunene TE., Williamson S, Alexandra MS., Slawin Z., and David Cole-Hamilton D.J., Continuous Flow Hydroformylation of Alkenes in Supercritical Fluid-Ionic Liquid Biphasic Systems Journal of American Chemical Society. **125**, (2003), 15577-15588

Wiese, K D., and Obst D, Hydrofomylation, Top Organometallic Chemistry **18** (2006), 1-33.

Wiebus, E., Cornils, B., Organic Solvent Nanofiltration (OSN), Chemie Ingenieur Technik **66,** (1994), 916–923.

White, L. S., Development of large-scale applications in organic solvent nanofiltration and pervaporation for chemical and refining processes, Journal of Membrane Science **286** (2006) 26–35.

White, L. S., Nitsch A.R., Solvent recovery from lube oil filtrates with a polyimide membrane, Journal of Membrane Science **179** (2000) 267–274

Xaba, M. S., Synthesis and modelling of Tungsten catalysts for alkene metathesis; North-West University (Potchefstroom campus), (MSc Dissertation), (2010)

Yang, Y., Shi L., Integrating environmental impact minimization into conceptual chemical process design a process systems engineering review Computers and Chemical Engineering **24** (2000) 1409-1419

Zagajewski, M., Behr A., Sasse. P., Wittmann J., Continuously operated miniplant for the rhodium catalyzed hydroformylation of 1-dodecene in a thermomorphic multicomponent solvent system (TMS), Chemical EngineeringScience **115** (2014) 88-94

CHAPTER 5: Aspen Plus™ SIMULATION

"Simulation is no longer a referential being or a substance. It is the generation by models of a real without origin or reality: a hyper reality"

Jean Baudrillard

Overview

Chapter 5 provides a detailed description of the simulation of the two process alternatives developed in Chapter 4 for upgrading low value 1-octene from a Fischer-Tropsch product stream to 2-hexyl-nonanal a Guebert-type surfactant feedstock. The chapter is subdivided into five main sections which are, section 5.1 which gives a brief background into the selection of simulation software. Section 5.2 details the final Aspen Plus™ process scenarios. Section 5.3 and Section 5.4 detailed description of models for the two process scenarios A and B. Section 5.5 presents the design approach to heat integration.

5.1 Simulation software selection

The next stage after the application of Douglas' (1988) qualitative process synthesis technique to identify potential solutions to a design problem is usually a quantitative approach to determine optimal process conditions (Halim and Srinivasm, 2011) by process simulation. The need to evaluate many, often complex, process alternatives leaves the process engineer with no choice but to use computer models if he is to find the 'best' solution within the resources at his disposal. In recent years there have been a dramatic increase in the use of, and the reliance on, process simulation programs, for modelling of steady-state mass and energy flow in the chemical and petroleum industries (Brannock et al., 1979). The main advantages of the process simulator are that various process modifications can be evaluated easily using standard software packages (such as CHEMCAD, Aspen Plus™, Hysys, PRO/II and gPROMS) in a short time without the need for extensive experimentation or pilot plant testing (Halim and Srinivasm, 2011). It is generally agreed that a comprehensive simulator represents 2-60 man-years of development and more than one million dollars in investment (Aspen Technology, 2009).

The usefulness of simulation results depend on how accurately the simulated process is modeled and how well the simulation software can handle complex block interactions which result from recycle streams and complex equipment such as distillation columns. In order to handle complex systems, simulation software must have flexible input submission interface with input error control, a robust calculation execution capacity and capacity for easy retrieval of results without unreasonable demands on computing hardware (Franks, 1972).

The modern day simulation software is no longer just expected to provide results but more expectations are in line with how the process model is developed and inbuilt properties such as property databases and result analysis tools (Sundaran, 2005). A detailed comparison of some of the popular advanced process simulators available is tabulated in Table 5.1.

Table 5.1.: Selection of simulation package (Adapted: WinSim Inc. 2015)

	Category	DESIGN for Windows™	Hysys®	Pro/II	ProMax®	Aspen Plus®	Chem CAD
General	1-Click Data Export to MS Excel	☺	☺	☺	☺	☺	☺
	Component library	☺	☺	☺	☺	☺	☺
	Thermodynamic options	☺	☺	☺	☺	☺	☺
	Recycle convergence	☺	☺	☺	☺	☺	☺
	Gas processing	☺	☺	☺	☺	☺	☺
	Batch simulation		+	+		+	+
	Dynamic simulation	☺	+	+		+	+
	Heat exchanger rating	☺	+	+	☺	+	+
	Claus process	☺	+	+	☺	+	+
Unit Modules	Rigorous distillation columns	☺	☺	☺	☺	☺	☺
	Batch distillation column	☺	☺	☺		☺	☺
	Pipeline		☺	☺	☺	☺	☺
	Heat exchangers	☺	☺	☺	☺	☺	☺
	Flash	☺	☺	☺	☺	☺	☺
	Reactors	☺	☺		☺	☺	☺
	Pumps & compressors	☺	☺	☺	☺	☺	☺
	Storage tanks	☺	☺	+		☺	+
Interface	Windows based GUI	☺	☺	☺	☺	☺	☺
	Text based UI	☺					
Training	Onsite	☺	☺	☺	☺	☺	☺
	Offsite	☺	☺	☺	☺	☺	☺
	Seminar	☺	☺	☺	☺	☺	☺
Support and Upgrades	Usage support	☺	☺	☺	☺	☺	☺
	Expert process support	☺	☺	☺	☺	☺	☺
	Support by phone	☺	☺	☺	☺	☺	☺
	Support by e-mail	☺	☺	☺	☺	☺	☺

In Table 5.1, the (+) shows optional features and (☺) shows standard features. Results from Table 5.1 shows that there are many possible commercial simulators on the market and using functional comparisons alone, it is difficult to objectively select a software that can be said to be the best. For the current work additional considerations were made on top of the functional considerations in Table 5.1. The additional considerations used in the selection of simulation software include; software availability, licensing requirements and cost, user friendliness of interface, depth and accuracy of unit operation calculation models, vailability of component data and technical support functionally available within reasonable communication cost

After factoring in additional factors Aspen Plus™ was selected by this author. Key motivation for the selection were the availability of a current license for the software and the relatively short time required to learn the software. Aspen Plus™ has been developed for the simulation of a wide variety of processes, such as chemical and petrochemical, petroleum refining, polymer, coal based processes (Jana, 2012). Aspen Technology Inc. has also included many inbuilt unit operation models which are sufficient to cover the diverse processes of its users, yet leaving room for customized models called user models (Aspen Technology, 2009). Close interaction with users has also ensured that the inbuilt models in Aspen Plus™ software has a closer representation of unit operations modelled in chemical process industries. The most important advantage of Aspen Plus™ package compared to other simulation packages is the availability of an experimental data bank for thermodynamic and physical parameters. Therefore, limited input data is required for solving even a process plant having a large number of units, thus avoiding human errors (Jana, 2012). Having inbuilt properties helps provide some level of consistence in simulation as automated manipulation and retrieval of properties tend to reduce the errors of entry.

Aspen Plus™ offers two simulation approaches which allow the user to manipulate a simulation differently depending on the desired objectives. Typical user objectives in choosing a particular approach may include speeding up the simulation convergence or increasing the level of simulation sequence customization. The simulation approaches are the sequential

modular approach and equation oriented approach (Aspen Technology, 2009). Sequential modular flowsheets solve the blocks individually according to a particular sequence. Equation oriented simulations solve block equations simultaneously, thus a good starting point is necessary for use of equation oriented simulation. Sequential modular modelling is used especially when simulating a large number of blocks, and equation oriented simulation is more useful where precise solutions are required (Aspen Technology, 2009). A combination of the two approaches can be used in simulation. When combining the approaches, sequential modular simulation is used to obtain an initial solution and then equation oriented approach is used to optimize the solution.

Aspen Plus™ has many analytical capabilities which enable the user to analyse the model. Some of these analysis tools include sensitivity analysis, optimization and constraint analysis and regression tools. The sensitivity analysis tool allows the user to carry out parametric studies of the model to understand the influence of particular variables on the cycle (Aspen Technology, 2009). An example of sensitivity analysis could be the study of the flow rate of a particular stream on the conversion of either the whole process or just one reactor. Optimization and constraint analysis tools allow one to maximize or minimize certain functions representing aspects of the simulated process while taking into consideration bottlenecks in the cycle (Aspen Technology, 2009). The regression tool allows analysis of results to see trends in the data and fit relationships, etc. (Aspen Technology, 2009). Having such a set of tools inbuilt in the software ensures that a process being simulated can be better understood and made to operate at the best conditions. Hence, Aspen Plus™ tools also make it possible to minimize the capital and operational costs associated with the development and testing of processes.

5.1.1 Selection of thermodynamic model

It is important to select a thermodynamic properties model which enable the accurate description of the system which is being modelled. Selection of inappropriate property methods results in wrong properties which will result in wrong specifications of plant equipment

and operating conditions (Aspen Technology, 2009). Physical property methods used in Aspen Plus™ for simulation calculations are either based on a property model or on a grouping of these property models (Aspen Technology, 2009). Simple methods, for instance, use the ideal models and more advanced methods can be a combination of equation of state (EOS) and activity coefficient models. In a combined property method, the vapour phase calculations can be done using an equation of state model, and the liquid phase done using an activity coefficient method.

Several detailed ways of choosing a property method, including consideration of process type there are available. The Aspen Tech property method selection algorithm (Aspen Technology, 2009), Bob Seader method (Seider et al., 2004) and the Eric Carlson (1996) method were used in this study as illustrated in Appendix C. It was also important to define different sections of the process into low pressure (<10 bar), the high pressure (>10 bar), polar and nonpolar mixtures according to Aspen Tech property method selection algorithm. The Eric Carlson (1996) method uses criteria of nature of mixture and operating range (<10 bar or >10 bar) for the selection of appropriate property model. The Bob Seader method groups different mixtures into polar and non-polar hydrocarbons. According to the Bob Seader method, for non-polar hydrocarbons the difference in boiling points can be used as a guide to the selection of property method while for polar hydrocarbons the choice of property method depends on the availability of binary interaction parameters.

The Aspen Plus™ method recommends the use of Peng-Robinson (PR) EOS, Redlich- Kwong-Soave (RKS) EOS and Lee-Kesler-Plocker (LKP) EOS for nonpolar mixtures at low pressures (<10 bar) of the metathesis section and Soave-Redlich-Kwong (SRK) EOS, Redlich-Kwong-Soave (RKS) EOS for the polar mixtures at high pressures (>10 bar) especially the hydroformylation process section. The Bob Seader method recommends Soave- Redlich-Kwong (SRK) EOS, Peng-Robinson (PR) EOS for hydrocarbons with narrow and wide boiling points especially treated in the metathesis section. In consideration of the hydroformylation section where both polar compounds and hydrocarbon mixtures are being

treated and binary interaction parameters are not available Bob Seader recommends the use of UNIFAC property method. Either Peng-Robinson (PR) EOS, Redlich-Kwong-Soave (RKS) EOS, Lee-Kesler-Plocker (LKP) EOS, Peng-Robinson-BM (PRBM) EOS and Redlich-Kwong-Soave-BM (RKSBM) EOS can be used for the metathesis process (<10 bar) section according to Carlson (1996). In consideration of higher pressures (>10 bar) and polar components and in cases where interaction parameters are not available such as in the hydroformylation section Carlson (1996) recommends the use of, Peng-Robinson (PR) EOS, Soave-Redlich-Kwong (SRK) EOS, Soave-Redlich-Kwong (SRK) EOS, Wilson, NRTL, and UNIQUAC property methods.

In previous simulation study on the hydroformylation of long chain alkenes, Hentschel et al. (2014) and Schafer et al. (2012) considered PC-SAFT property method for the hydroformylation system and the UNIFAC-Dortmund to model the three phase decanter system. However, PC-SAFT property method is still under developed and binary interaction parameters for many compounds are difficult to find in literature. Vogelpohl et al. (2013) has recomendend Peng-Robinson (PR) EOS and Soave-Redlich-Kwong (SRK) EOS for systems of CO and H_2 in hydrocarbons over a wide temperature and pressure range.

Using the three methods of thermodynamic property method selection and a consideration of process type, conditions and other modelling constrains, the Soave-Redlich-Kwong (SRK) EOS method was selected in this study for both metathesis section and hydroformylation section. The phase separation units in hydroformylation were treated with UNIFAC method. Appendix A.5 shows how the thermodynamic method was selected in this study. A summary is given in Table 5.2.

Table 5.2.: Summary of property methods

Property method	Metathesis section	Hydrofomylation section
	(Non-polar hydrocarbons, <10 bar)	*(Polar hydrocarbons >10 bar)*
Aspen Tech (2009)	Lee-Kesler-Plocker (LKP) EOS, Peng-Robinson (PR) EOS, Redlich-Kwong-Soave (RKS) EOS	Soave-Redlich-Kwong (SRK) EOS, Redlich-Kwong (RK) EOS
Seider et al. (2004)	Peng-Robinson (PR) EOS, Redlich-Kwong-Soave (RKS) EOS	UNIFAC
Carlson (1996)	Pen-Robinson (PR) EOS, Redlich-Kwong-Soave (RKS) EOS, LK-Plock (LKP) EOS, Peng-Robinson-BM (PRBM) EOS, Rendlich-Kwong-Soave-BM (RKBM) EOS	Peng-Robinson (PR) EOS, Soave-Redlich-Kwong (SRK) EOS, Wilson, NRTL, and UNIQUAC
Hentschel et al. (2014)	-	PC-SAFT, UNIFAC-Dortmund
Schafer et al. (2012)	-	PC-SAFT
Vogelpohl et al. (2013	-	Peng-Robinson (PR) EOS and Soave-Redlich-Kwong (SRK) EOS
Current study	***Soave-Redlich–Kwong (SRK) EOS***	***Soave-Redlich-Kwong (SRK) EOS, UNIFAC***

5.2 Final Aspen Plus™ process scenarios

Section 5.3 and 5.4 discusses the final Aspen Plus™ simulation for the two process scenarios developed for upgrading 1-octene from a Fischer-Tropsch product stream to 2-hexyl-nonanal an important feedstock for the Guerbet-type surfactants. The process being analysed in this project can be described as an integrated metathesis of 1-octene from a Fischer-Tropsch Synthol product stream to an internal alkene, 7-tetradecene and subsequent hydroformylation

of 7-tetradecene to 2-hexyl-nonanal, separation and recovery of catalysts, purification and separation of products. The Aspen Plus™ flowsheets were developed from base case process flow diagrams developed in Section 4.4 as discussed in Chapter 4. The two process simulations for Scenario A (liquid multiphase system) and Scenario B (OSN membrane system), arose from two different design approaches to recovery of **Rh-TPPTS** catalyst from post reaction mixtures developed in Chapter 4. Scenario A proposes the use of liquid multiphase system (LMS) while Scenario B proposes the use organic solvent nanofiltration (OSN) membrane as a solution to the recovery of Rh-catalyst from post hydroformylation reaction mixture. The data used in these designs have been demonstrated in either a laboratory, pilot plant, or previously operated full-scale plant. To avoid redundancy in the description of separate model sub-sections, process design Scenario A (liquid multiphase system) is used as basis for the two process designs discussed hereafter. Only changes between this basis and subsequent designs are discussed in the subsections of the altered process design itself. Important assumptions made for all the process designs include:

- A 10 000 tonnes per annum 2-hexylnonanal product of 99 % purity will be produced and that the resulting size of the process designs are optimal for industry.
- A 1-octene/**HGr-2** catalyst initial feed ratio of 10 000 according to Van der Gryp et al. (2012) was used.
- A 7-tetradecene**/Rh-TPPTS** catalyst initial feed ratio of 2 500 according to Haumann et al. (2002) was used.
- A water/7-teytradecene feed ratio (**α)** of 0.5 was used in the hydroformylation reactor according to Muller et a. (2013, 2015), Haumman et al. (2002a, 2002b), Rost et al. 2013).
- A marlipal to water mass fraction (**γ**) of 0.08 was used according to Muller et a. (2013, 2015), Haumman et al. (2002a, 2002b), Rost et al. (2013).

5.3 Scenario A: Liquid multiphase system

The simulation model used in this study was divided into Sections (AREAs) that corresponds to each of the main process steps developed in Chapter 4 that make up the overall process as shown in Figure 5.1;

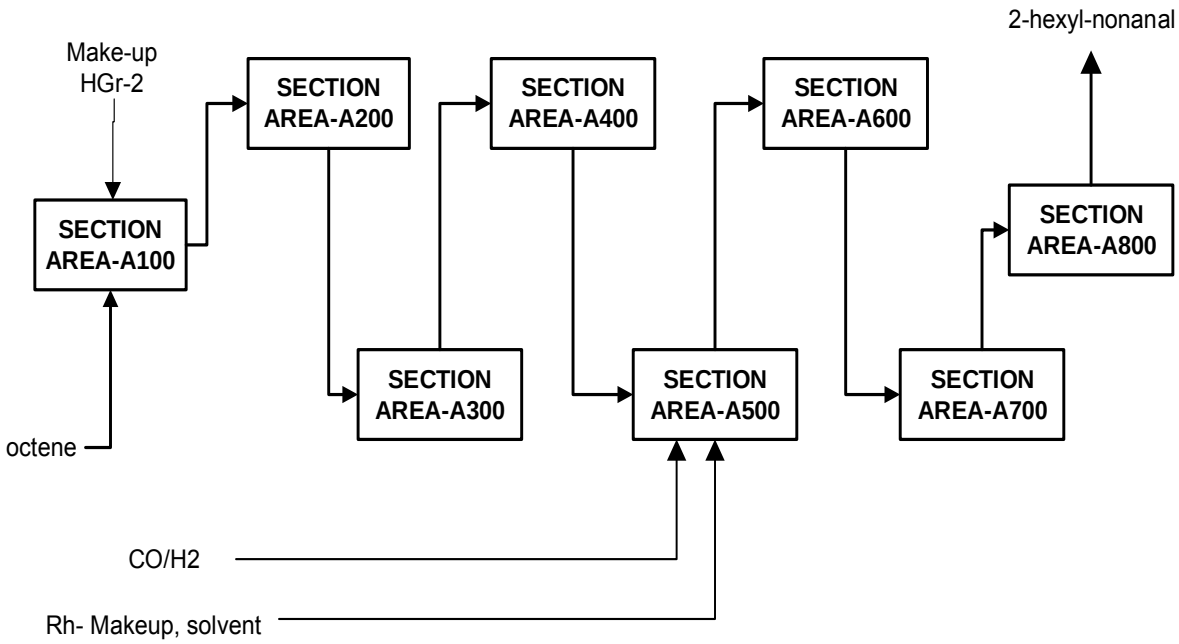

Figure 5.1.: Block flow diagram for process scenario A

A description of the sections of the main process steps is as follows;

- Section AREA-A100 describes the 1-octene metathesis reaction and considered as the metathesis section,
- Section AREA-A200 details the ethylene removal and considered as the Ethylene removal section,
- Section AREA-A300 is where **HGr-2** catalyst is recovered for recycle into the metathesis process and is considered the catalyst recovery section. This is the most important section since the operating cost is influenced by catalyst cost.

- Section AREA-A400 is where unreacted 1-octene is recovered and is termed 1-octene recovery section,
- Section AREA-A500 contains the hydroformylation reactor and is considered the hydroformylation section. This section is however the most understated section in the process due to the limited information on the kinetic data for the hydroformylation of long chain internal alkenes.
- Section AREA-A600 considered the use of a liquid multiphase system to recover homogeneous **Rh-TPPTS** catalyst. This is the most important section as the operating costs are mostly influenced by the **Rh-TPPTS** catalyst loss. This section is however, underrated due to the limited information on recovery of Rh-catalyst in post reaction mixtures of high boiling points long chain aldehydes.
- Section AREA-A700 is where unreacted 7-tetradecene is recovered and recycled back to the hydroformylation reactor.
- Section AREA-A800 is where 99 wt. % 2-hexyl-nonanal is separated from isomeric aldehydes. This section reflects major challenges of separation of long chain isomeric aldehydes especially when selectivities and yields are low.

5.3.1 Section AREA-A100: Metathesis section

This process Section AREA-100 was modelled with four Aspen Plus™ user models as depicted in Figure 5.2 and described in detail in Table 5.3.The process begins when a pure stream of 1-octene from Fischer-Tropsch Synthol product stream at 30 °C and 1 bar is sent to mixer (M-101) where it was mixed with 1-octene recycle (403) from 1-octene column. A steam-jacketed reactor is used to maintain an optimum temperature of 50 °C to achieve high activity since the reaction is endothermic (108.45 kJ/mol) (Ivin and Mol, 1997, Jordaan and Vosloo, 2011). **HGr-2** make-up catalyst was also added to the reactor to satisfy a design specification (DES-HGr-2) of 1-octene/HGr-2 of 10 000 (mol) as given in literature by Van der Gryp (2009).

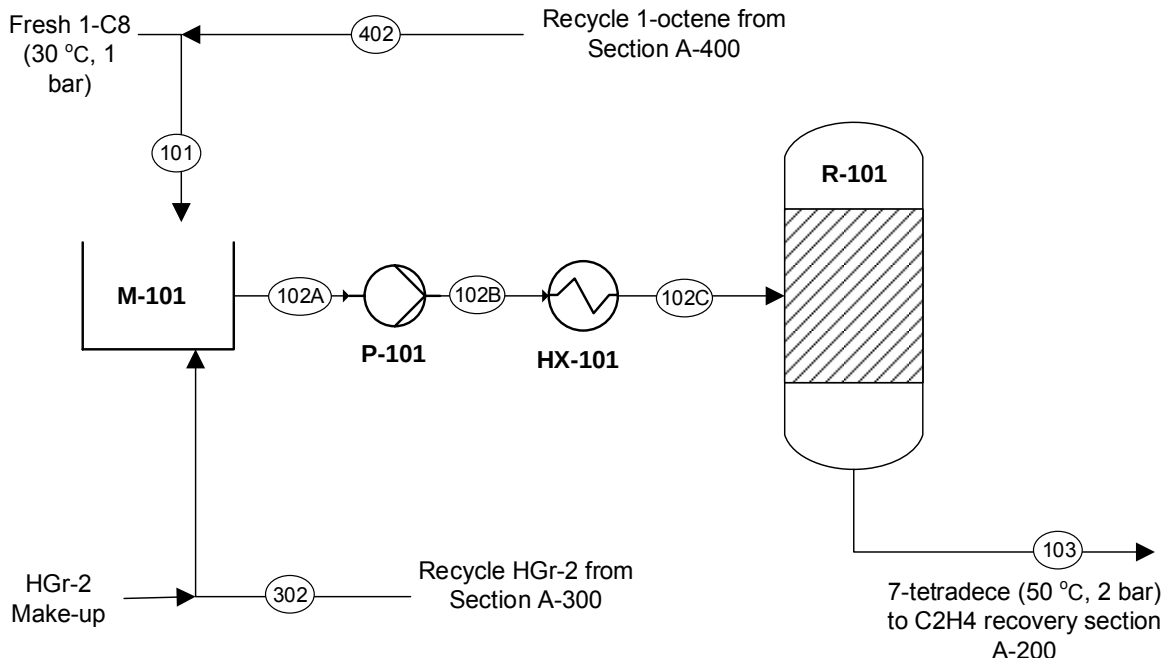

Figure 5.2.: Metathesis flow sheet for the metathesis of 1-octene Section AREA-A100

A description of the modelling purpose is shown in Table 5.3.

Table 5.3.: Metathesis process unit operations

Equipment name	Modelling purpose and description
M - 101	Models a mixing tank for fresh 1-octene stream (101), HGr-2 catalyst recycle streams (303) from Section AREA-300 and 1-octene recycle stream (403) from section AREA-A400
P - 101	Models a pump which is used to raise the feed stream (102A) pressure to 2 bar before it reaches the feed heater
HX - 101	Models a heat exchanger which is used to raise the feed stream (102B) temperature to stream (102C) at 50 °C
R – 101	Models a continuous stirred tank reactor. The reactor is modelled using kinetics by Van Der Gryp (2009).

(i) Validation of metathesis reactor model

A plot of selectivity against temperature for Aspen Plus™ model results compared to literature results (Van der Gryp, 2009) is shown in Figure 5.3. It can be seen from Figure 5.3 that the Aspen Plus™ metathesis reaction model results agree considerably well with literature data throughout the whole temperature range, hence is a reliable prediction of self-metathesis at low temperature (below 60 °C) and isomerisation at high temperatures (above 60 °C). This was also in agreement with literature results by Lehmann et al. (2003), du Toit et al. (2014) and Jordaan et al. (2008).

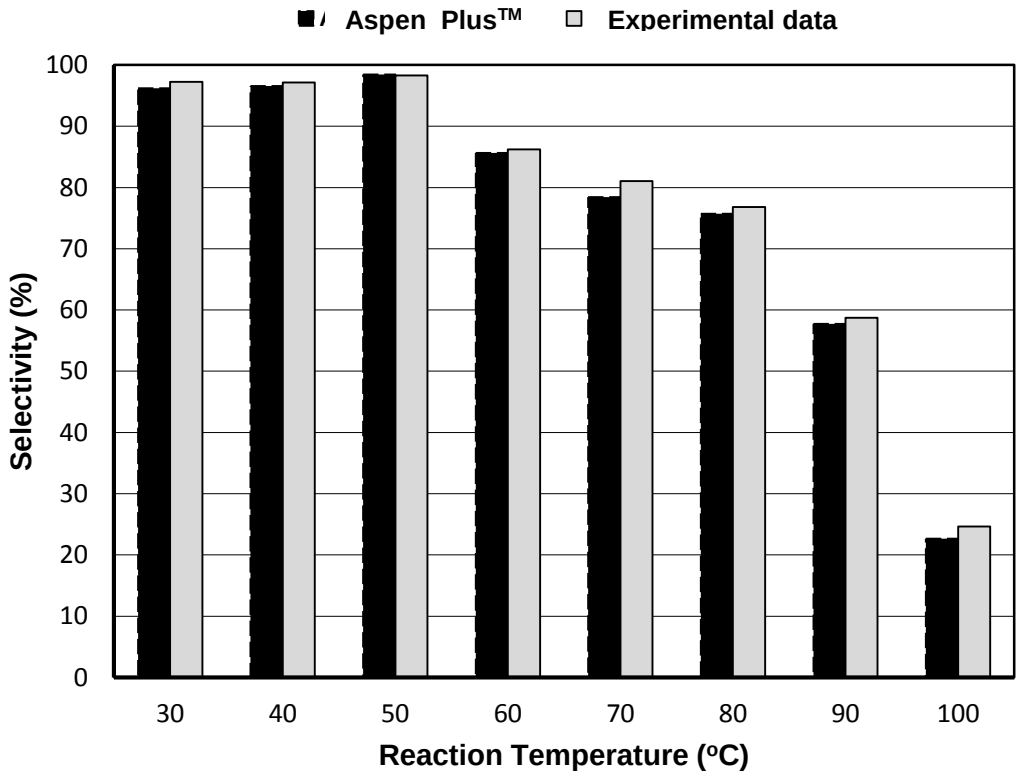

Figure 5.3.: Comparison between model and Van der Gryp (2009) experimental data for 1-octene metathesis with HGr-2 precatalyst (RMSE=0,988)

The EP3 calculated for separation and recycle system in Chapter 4 confirmed that selectivity rather than conversion has a significant effect on the separation equipment cost. The higher

the selectivity the lower the separation costs. From an economic standpoint, maximizing selectivity and TON will maximize profits.

Reaction engineering identifies a small reactor size and maximization of PMP products as the two extremely important requirements in designing a reactor. Literature data of activity against temperature for HGr-2 catalyst (Van der Gryp, 2009) confirms that TON increases with temperature up to 50 ^{o}C but starts to decrease as temperatures increases. Literature results (du Toit et al., 2014; Lehmann et al., 2003; Jordaan et al., 2008) have also confirmed that at temperatures above 60 ^{o}C, the precatalyst starts to decompose, lose activity for metathesis and possibly deactivates and promotes isomerisation reactions. Since high selectivities and TON could be obtained at 50 ^{o}C, the optimal temperature for the metathesis reactor in this simulation was set at 50 ^{o}C.

5.3.2 Section AREA-A200: Ethylene recovery section

After metathesis reaction, the product was passed onto the ethylene recovery section. The purpose of this section was to remove ethylene from the main product 7-tetradecene stream (201A). Ethylene gas stream could be purged directly from the reactor but however, due to solubility in the alkenes an additional separator was required in order to avoid complicating the reactor system. In previous work by Lee et al. (2008), experimental results show that the solubility of ethylene in a 2,2,4-trimethylpentane and 1-octene mixture increases with system pressure but decreases with system temperature. Ethylene accumulation promotes coordination to the catalyst complex, forming hydride species (decomposition catalyst) that increases isomerization and reverse metathesis of 7-tetradecene (Loock et al., 2009). Hence, ethylene must be removed before unreacted 1-octene is recovered and recycled to the metathesis section area. A detailed description of this section is shown in Figure 5.4.

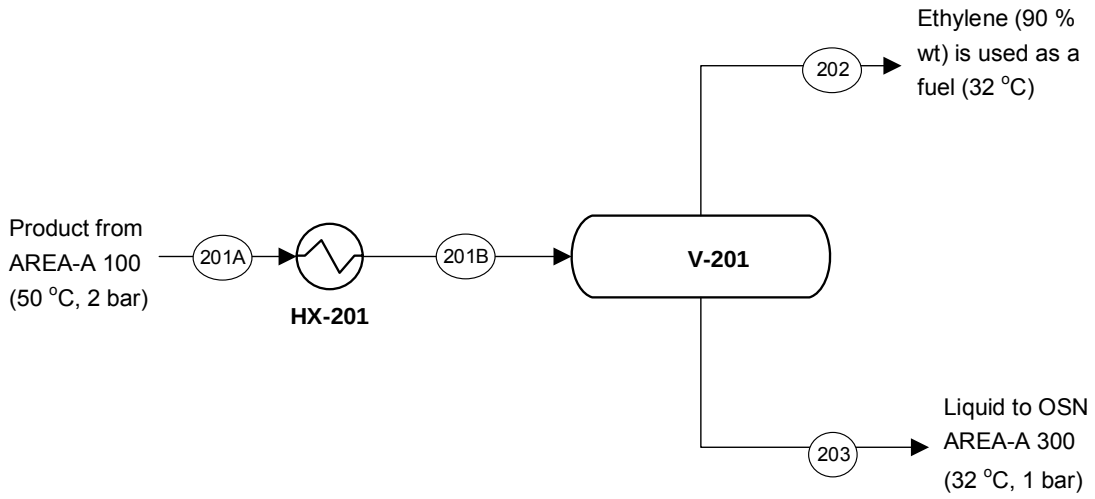

Figure 5.4.: Schematic diagram for the removal of ethylene in product stream

Product stream (201A) from the metathesis Section AREA-100 at 2 bar and 50 °C is precooled to 32 °C before it enters the flash drum (V-201). Results of a temperature sensitivity analysis in Figure 5.5 shows that if the flash drum is operated at 32 °C and 1 bar it is possible to achieve 96 % recovery of ethylene from the product stream. Outlet water temperature from a cooling tower at Sasol Secunda can be obtained at 22 °C (Kloppers and Kroger, 2005).

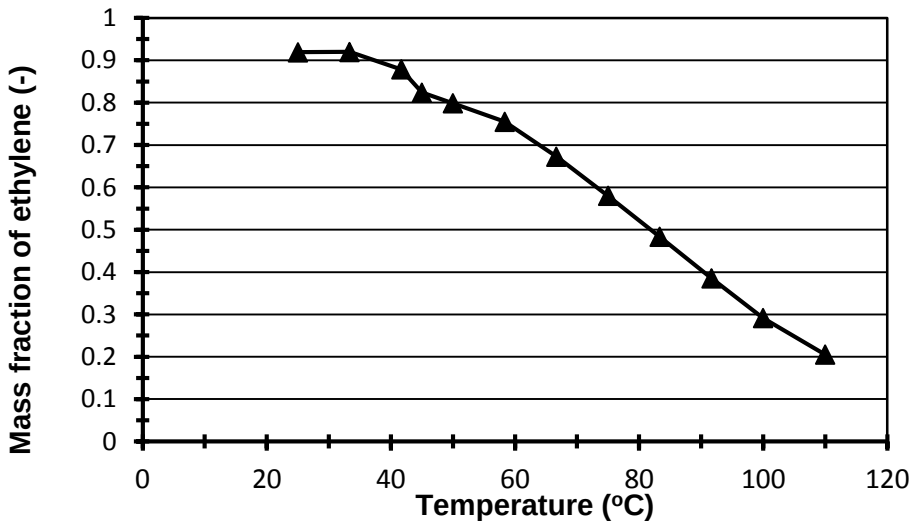

Figure 5.5.: Temperature versus mass fraction of ethylene in flash drum vapour stream

Table 5.4 shows the modelling purpose and description of each unit operation used in developing section A-200 in this work.

Table 5.4.: Description of unit operations

Equipment name	Modelling purpose and description
HX - 201	Models a heat exchanger for cooling product stream (201A) from 50 °C to 32 °C.
V - 201	Models a flash drum which is used to separate product stream (201B) into 98 wt.% ethylene in stream (202) and liquid stream (203) which is predominantly 7-tetradecene. The vessel is operated at 1 bar and 33 °C to achieve high ethylene recovery (96%) also minimising 1-octene loss.

5.3.3 Section AREA-A 300: HGr-2 catalyst recovery section

The liquid product from the ethylene recovery section is directed to the catalyst recovery Section AREA-A300. The main purpose is to achieve >99.99 % recovery of expensive **HGr-2** catalyst from the product stream in its active form so that it can be reused. A point of high interest is that degradation products of these ruthenium catalysts can be highly active and selective double-bond isomerization and hydrogenation catalysts leading to product degradation (Huang et al., 2015). Moreover, for pharmaceutical and fragrances, the separation of the homogeneous catalysts and ligands from the product is critical to meet regulations of less than 9 ppm (Bhanushali et al., 2001).

5.3.3.1 Developing membrane Aspen Plus™ Model

A model of a membrane unit is not (yet) available as a build-in process model in Aspen Plus™ model library. As a result, the objective of section 5.3.3.1 was to develop a generic custom model of a **HGr-2** catalyst separation membrane unit interfaced for use in Aspen Plus™ as like the other unit models available in Aspen Plus™ model library. A FORTRAN block of an Aspen Custom Model of a nanofiltration membrane unit interfaced in Aspen Plus™ was

developed for recovery of species whose permeabilities are given in Table 5.5. A modified Hagen-Poiseuille-2 (HP-2) model was used to predict solvent flux (J) in Starmem™ membrane as a function of both species permeability (p) and mass fractions (x). Algorithms used in Aspen Plus™ are shown Appendix A. Fixed structural parameters such as recycling structure were adopted from Seifert et al. (2013) and Schmidt et al, (2014). In every membrane stage, a parallel setup of membrane modules is simulated. The membrane area in every stage is calculated based on the feed flow demand of industrial OSN membrane modules. As OSN membrane modules, 2.5″x 40″ spiral-wound Starmem™ 228 membrane modules with a membrane area of 2.09 m² (Evonik MET, 2011) were applied.

Table 5.5.: Species permeabilities using Starmem™ 228 membrane

Species	Permeability(m)	Reference
1-octene	6.581×10^{-16}	Van der Gryp (2008)
2-octene	6.581×10^{-16}	Van der Gryp (2008)
6-tridecene	2.834×10^{-18}	Correlated using Bhanushali et al. (2001) model
7-tetradecene	1.311×10^{-18}	Van der Gryp (2009)

(ii) Modelling limitations

In this approach, several critical points or challenges have been identified. Key factors in this approach have been the effects of interactions in a multi-component system. It is not clear at what magnitude the interactions between solute and solvent and the inorganic matrix is on membrane rejections. Finally, the second critical point is identified as the non-availability of pilot-plant data necessary for model validation.

(iii) Model assumptions

The key assumptions made in this model are (Wijmans et al., 1995):

i. Each species diffuses across the membrane in an uncoupled manner due to its own chemical potential gradient, which is the result of the concentration and pressure differences across the membrane.

ii. The driving force is essentially the difference in pressure on the feed side and permeate side.

iii. No concentration polarization.

(iv) Aspen Pus™ custom model validation

The objective of simulation model validation was to determine how accurately the measures extracted from the model corresponds to the measures obtained from the represented system. Hence, two important criteria i.e. non-separation of species and flux versus mass fraction of 1-octene were used to validate the OSN membrane model developed in this work. The non-separation of species in membrane models has been used previously as a characteristic test of the Hagen-Poiseuille-2 model (Bhanushali et al., 2001). This phenomenon has been reported in different studies of Silva et al. (2005), Van der Gryp et al. (2012) and Schmidt et al. (2014). According to Van der Gryp et al. (2012), the non-separation of the solvent species is attributed to the Starmem™-228 membrane's MWCO of 280 $gmol^{-1}$, compared to 7-tetradecene's molecular weight of 196 $g.mol^{-1}$ and 1-octene's of 112 $g.mol^{-1}$. Figure 5.6 shows results of mass fraction of 1-octene in retentate vs mass fraction of 1-octene in the permeate stream plotted against literature data of Van der Gryp et al. (2012).

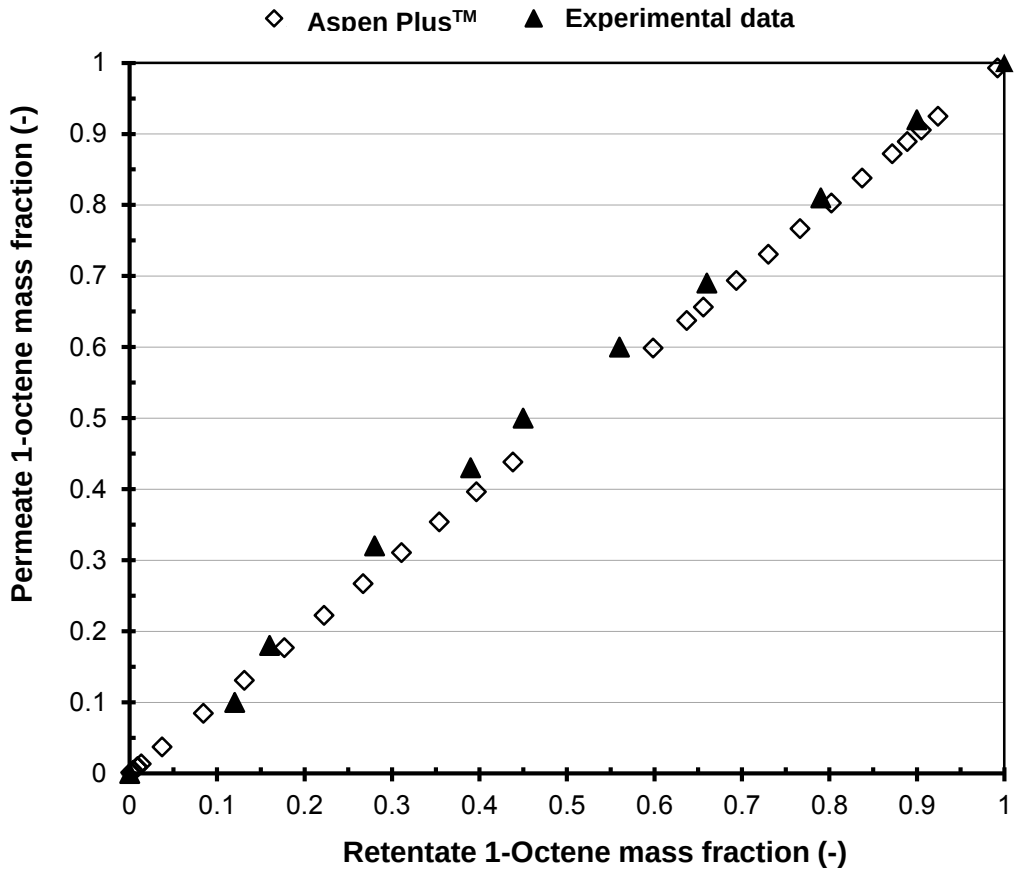

Figure 5.6.: Results for 1-octene mass fraction in retentate vs. 1-octene mass fraction in permeate obtained with Aspen Plus and experimental data by Van Der Gryp et al. (2012).

It can be concluded from fit of model data to literature results that the Aspen Plus™ custom model of **HGr-2** catalyst separation membrane unit developed in this work sufficiently describes the membrane process as regards separation of species into retentate and permeate.

The results of flux versus mass fraction of 1-octene for the model was also compared with the literature results. In this investigation, the mass fraction of 1-octene in feed stream to membrane was varied by changing the residence time of the RCSTR metathesis reactor unit. Results of total flux at varied mass fraction of 1-octene for model compared to literature results is shown in Figure 5.8.

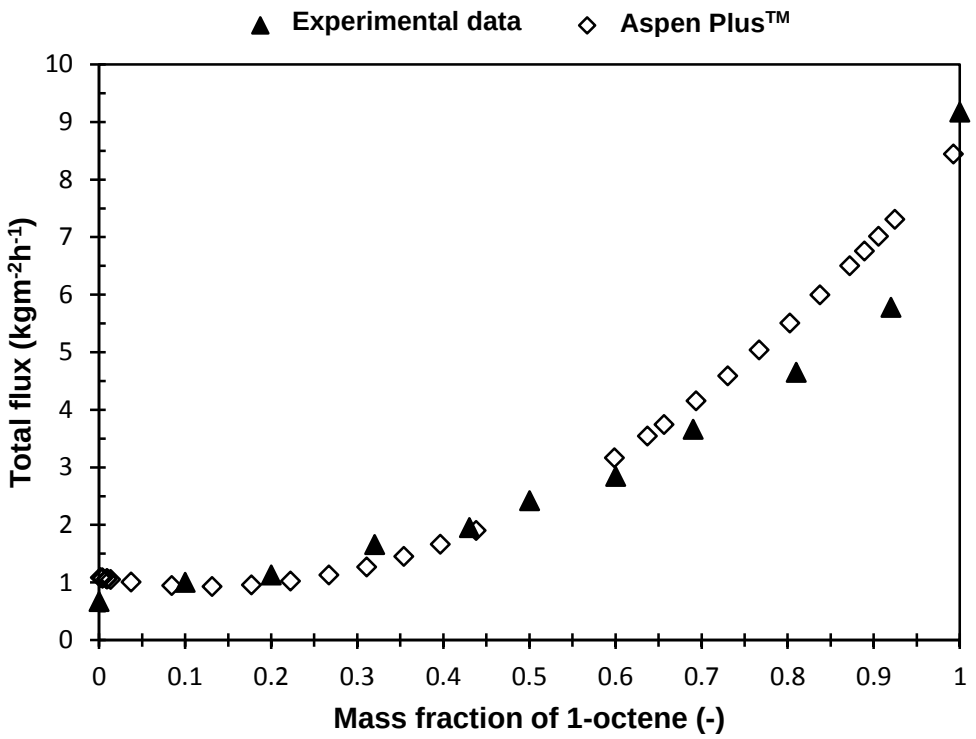

Figure 5.7.: Comparison of literature vs. model solvent fluxes at 30 bar

Figure 5.7 shows a graph of the comparison of Aspen Custom Model results of OSN membrane module against literature, for the total flux as a function of 1-octene mass fraction in feed. It can be shown that simulated results fits quite well between literature results and an ideal scenario where flux is proportional to mass fraction of 1-octene. Moreover, the model developed in this work was based on Hagen-Poiseuille-2 model with the assumption that pole-flow model provides the best fit between experimental data which has been previously recommended by Van der Gryp (2009) and Bhanushali et al., (2001). Hence, it can be concluded that solvent properties such as viscosity, solvent-membrane interaction together with solvent-solvent structural properties were sufficiently incorporated in the model (Silva et al., 2005). Hence, from model complexity viewpoint the model developed in this work is valid and adequately describes the transport across Starmem™ 228 membrane.

(v) Optimisation results

In this section, the optimisation results for recycling of homogeneous Rh-catalyst based on the results of the validated model of Starmem™ 228 membrane is presented. The objective was to minimize the membrane costs per kg of 2-hexyl-nonanal product. The optimisations were performed individually for different membrane setups, i.e. fixed structural parameters such as stage rejections and recycling structure were assumed. Then, operational parameters in the membrane part were optimised and finally given the optimised membrane cascade. For operating costs of the OSN membranes, a membrane price/stability factor of 250 \$ m^2/yr (Schmidt et al., 2014) was assumed. As can be seen from Figure 5.9, the overall membrane costs per kg 2-hexyl-nonanal is a function of the number of OSN membrane stages, with higher costs for processes with more stages and less costs for processes with fewer stages. These results are a direct consequence of the low individual stage rejections, resulting in 86.16 % overall HGr-2 catalyst rejection for the one-stage process up to 99.96 % rejection in case of the five-stage process.

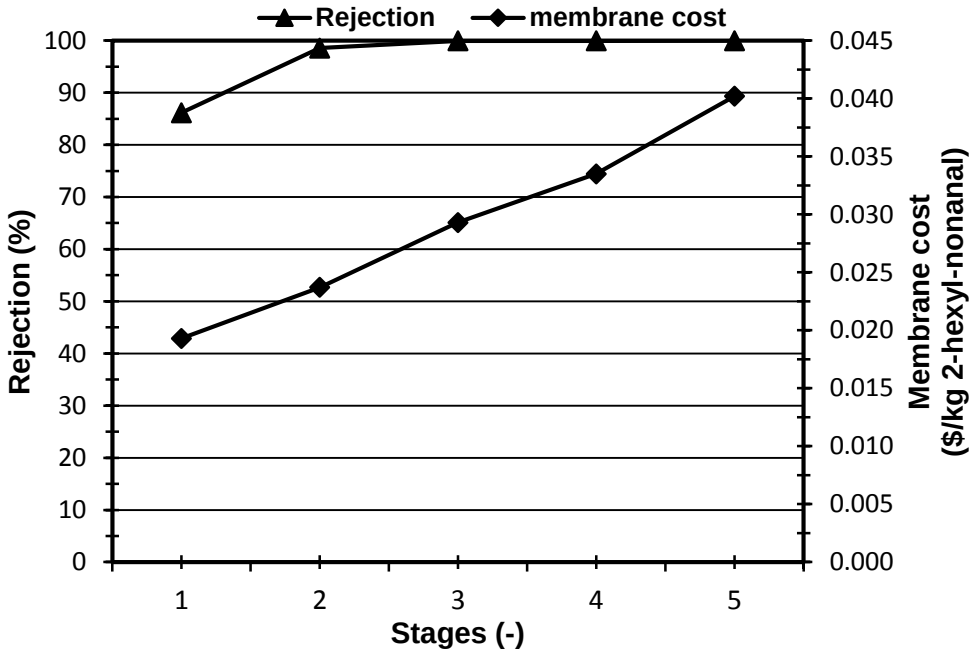

Figure 5.8.: Membrane cost versus reaction and number of stages

The overall rejection in this study was almost constant for 3, 4 and 5 stages configuration while cost of membrane per kg of 2-hexyl-nonanal increased linearly. The cost for a three-stage process lies within a reasonable range (0.0293 $/kg) whereas the five-stage process has a two times higher production cost of 0.04 ($/kg). This promotes the application of OSN, as mostly, in industrial settings, the number of stages can be a key operating criterion for an investment decision within early phases of process development. In this study a 3-stage membrane set-up was selected based on a low operating cost per kg of 2-hexyl-nonanal and also maximising catalyst rejection. Figure 5.9 shows an optimised three-stage cascade model arrangement used to develop the catalyst recovery unit. The arrangement of retentate and permeate streams is similar to one proposed by Seifert et al. (2013).

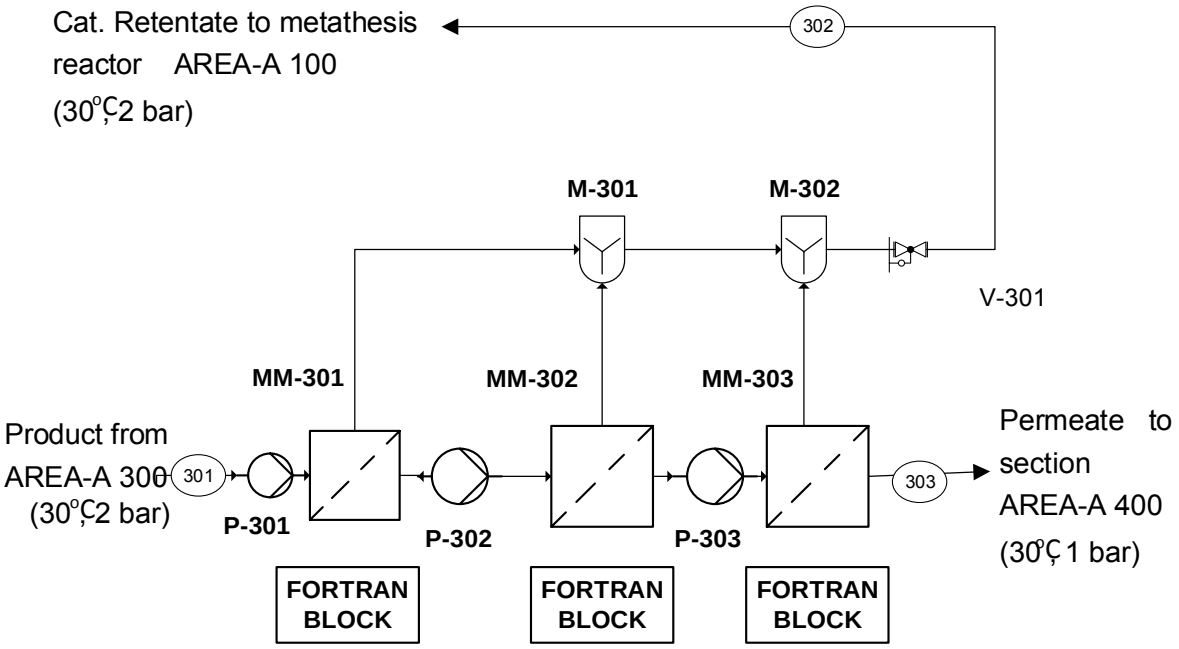

Figure 5.9.: Schematic diagram for the 3-Stage process of recovery of HGr-2 precatalyst

Details of OSN membrane and a description of modelling purpose is shown in Table 5.6.

Table 5.6.: Membrane process unit operations and description

Equipment name	Modelling purpose and description
MEMB Stage 1, MEMB Stage 2, MEMB Stage 3,	Models a membrane separator used to recover the catalyst species from the product stream (301) into catalyst retentate stream (302) and product permeate stream (303). A custom build membrane was developed using FORTRAN blocks which predicts species flux by a modified Hagen-Poiseuille-2 model with 3 stages in order to achieve >99.99 % overall recovery of **HGr-2** catalyst.
P – 201, 202, 203	Models OSN pumps required to provide the transmembrane pressure of 40 bar as driving force for the species flux through the membrane

5.3.4 Section AREA-A 400: 1-octene recovery section

The purpose of this section is to recover unreacted 1-octene from the product stream so that it can be recycled back to the metathesis reactor (section AREA-100). Distillation provides a convenient way to make the separation and there will be a large break between the boiling point of the 1-octene (120 ^{o}C) and 7-tetradecene (250 ^{o}C). For the simulation boiling points are good initial estimates for the separation system design, however, detailed design of the physical system would require calculation of the bubble points and dew points. According to US patent US 4,386,229, the separation of the alpha olefins from the internal olefins utilizing olefins with 8 to 10 carbon atoms can be carried out by distillation in which the end point for alpha olefins at atmospheric pressure is not above about 175° C and the initial boiling point of the internal olefin is not below about 213° C. Figure 5.10 below shows the set-up of the 1-octene recovery section and the units used in Aspen Plus™ to develop the section.

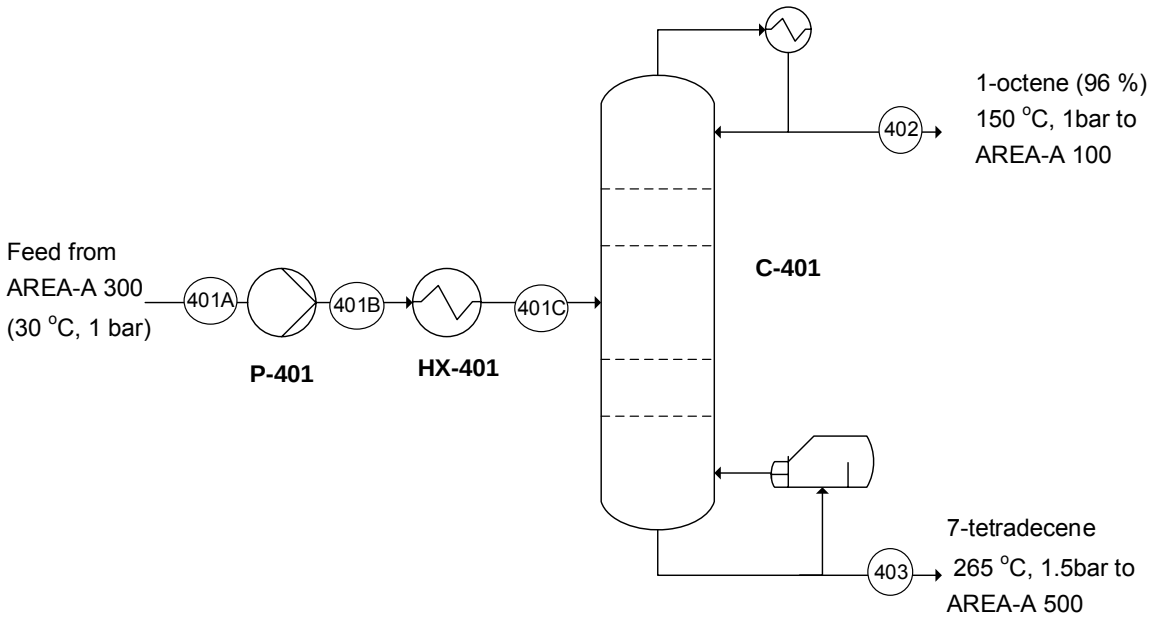

Figure 5.10.: Schematic diagram for the 1-octene recovery section A300

This column operates at 1 bar, has 21 equilibrium stages assuming a column efficiency of 70 % and a minimum reflux to actual reflux of 1.2 stages with the feed on stage 10 a reflux ratio of 0.163667, and operates as total condenser. A sensitivity analysis of the recovery of 1-octene versus the number of stages (Figure 5.12) shows that 99.99 wt. % of 1-octene can be recovered with a minimum equilibrium stages of 21.

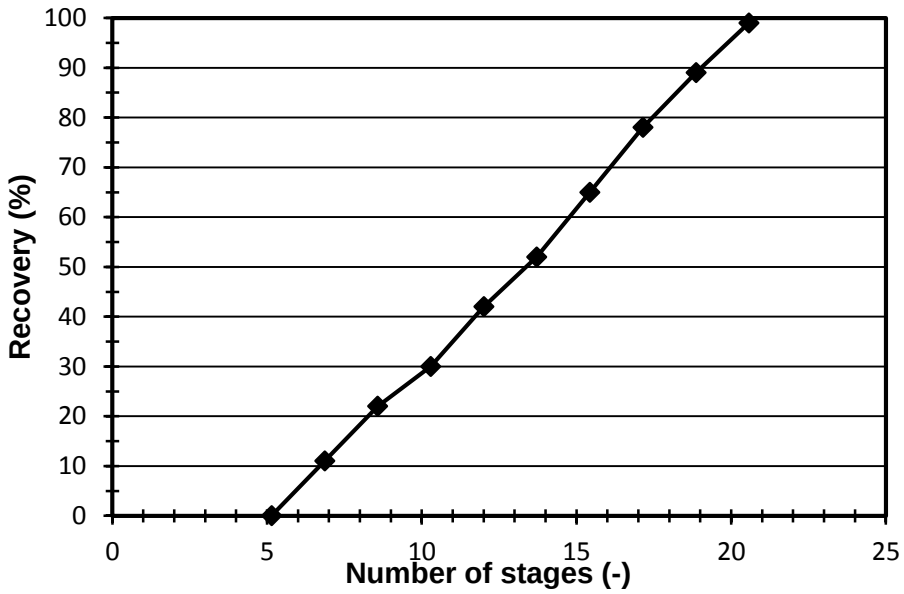

Figure 5.11.: Recovery and number of stages relationship for 1-octene column

A sensitivity analysis on the effect of the reflux ratio on condenser and reboiler duty was also carried out which also shows that both the reboiler and condenser duties increased with increase in reflux ratios however an optimal reflux ratio of 0.25305 was selected so as to achieve a 99.9 % recovery of 1-octene. Since 1-octene is very reactive compared to 7-tetradecene the objective of designing the 1-octene column must be to maximise its recovery so as to prevent its presence in the hydroformylation reactor to prevent formation of short chain aldehydes and alcohols. Table 5.7 describes the purpose of the model and description of each unit.

Table 5.7.: Description of each unit and modelling purpose

Equipment name	Modelling purpose and description
C - 401	Models a distillation column used to separate the product stream into 99 % 1-octene distillate stream (402) and bottoms product steam (403) which is predominantly 7-tetradecene and the column operates at 0.01 bar. The feed enters the column at 150 °C and 1 bar.
HX - 401	Models a heat exchanger which is used to heat the feed stream (401A) coming in at 30 °C to feed stream (401B) at 120 °C.
P - 401	Models the pump used to raise the pressure in order to overcome pressure losses during liquid transport. The pump is used to supply the feed to the column at 2 bar.

5.3.5 Section AREA-A500: 7-tetradecene hydroformylation section

The base conditions for the simulation of hydroformylation reactor was set at 100 bar and 120 °C (Haumann et al., 2002b). A design specification (RHO-CAT) was used to set the **Rh-TPPTS** catalyst to 7-tetradecene feed to 200 ppm (Haumann et al., 2002b). The folowing graph (Figure 5.12) shows results of invetsigation eof temperature on conversion for the Aspen Plus™ model. Figure 5.12 shows that conversion increase as temperature is increases, hence, inorder to ensure a small reactor volume and improve safety of the hyfroformylation reactor, it was decided to opearte the reactor at a higher temperature.

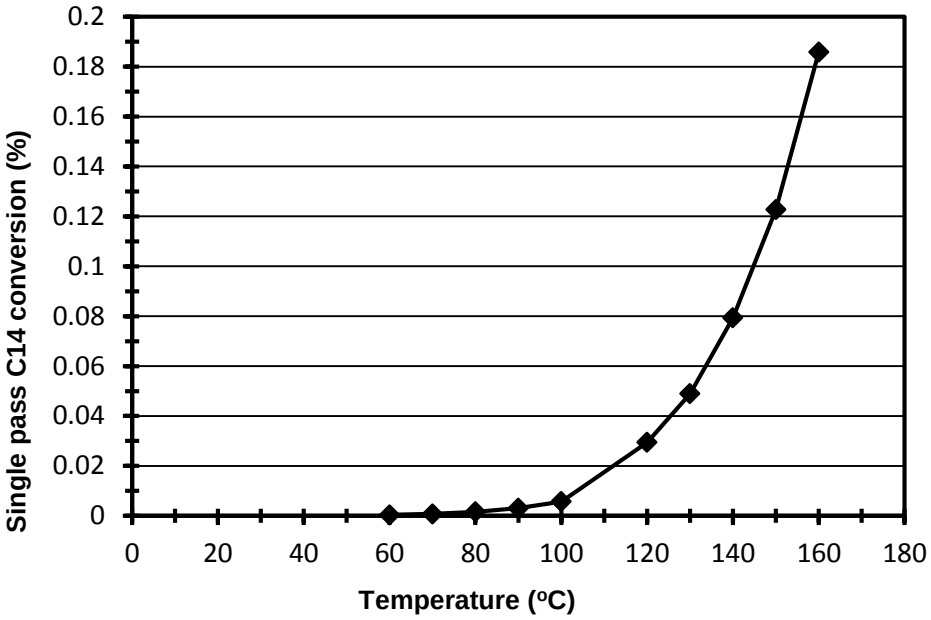

Figure 5.12.: Effect of temperature on conversion at 100 bar

However, aldehydes have been known to be temperature sensitive and degrade above180 °C (Hentschel et al., 2014, Steimel et al., 2014), an optimal temperature for this work was chosen to be 160 °C. In order to determine the optimal reaction pressure the effect of pressure on both conversion and cost of reactor was investigated as shown in Figure 5.13.

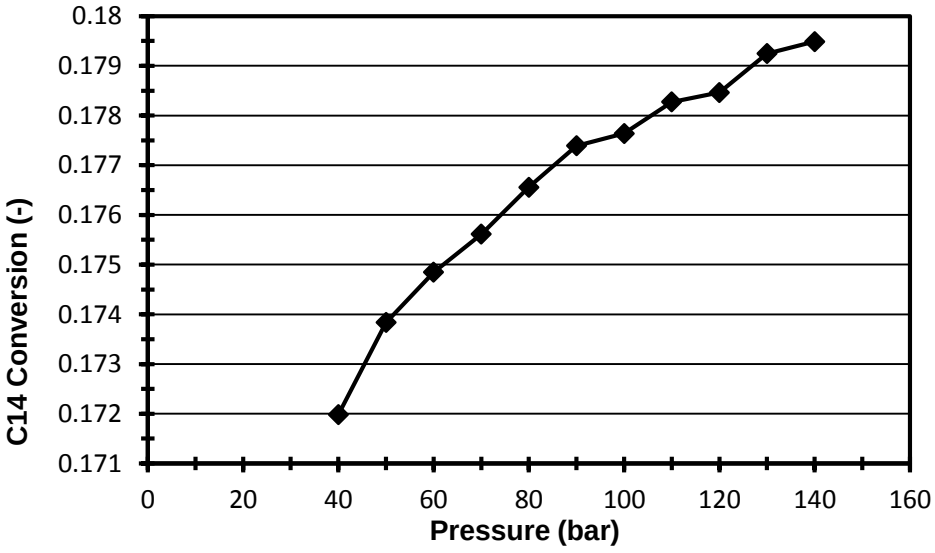

Figure 5.13.: Effect of pressure on conversion

A balance between conversion, operational cost and capital cost of the reactor, were critical considerations in the initial selection of the operating pressure. Since the recycle of 7-tetradecene mainly depends on the conversion in the reactor, conversion has an influence on the total production costs and hence needs to be investigated (Hentschel et al., 2014). The increase in production costs at lower conversions results from the higher costs for the unreacted 7-tetradecene recycle, whereas the cost increase for higher conversions results from decreasing selectivity and n/iso ratio hence, higher costs for the product separation and higher energy demands. It can be seen from Figure 5.13 that an increase in pressure had a minor effect on the conversion of 7-tetradecene as an increase in pressure from 40 to 140 bar caused a minor change in conversion of 0.0078. Figure 5.15 shows the effect of the operating pressure on the cost of the hydroformylation reactor due to material of construction and safety demands. It can be seen below that pressure has a significant effect on the cost of the reactor due to a high demand in material of construction. An increase in pressure of 1 bar resulted in an increase in the cost of the reactor by approximately US $0.575 million.

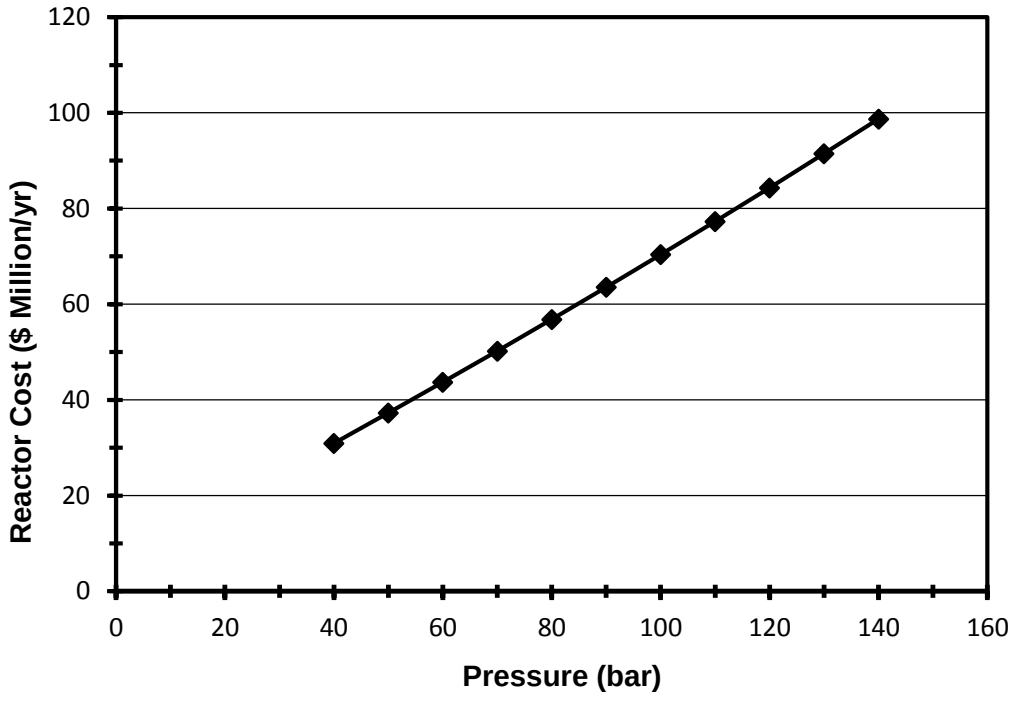

Figure 5.14.: Effect of pressure on Cost of reactor

It can be seen above that an increase in pressure causes an increase in conversion, the rapid rise in the cost of the reactor from $ 30 million to $ 99 million at the expense of an only 0.0078 increase in conversion meant that it was profitable to operate the reactor at 40 bar in order to minimise reactor cost and operating costs. In light of this, conditions for the reactor were chosen to have the lowest pressure practically possible and the highest economic temperature.

Figure 5.15 shows the set-up of the 7-tetradecene hydroformylation section and the units used in Aspen Plus™ to develop the section.

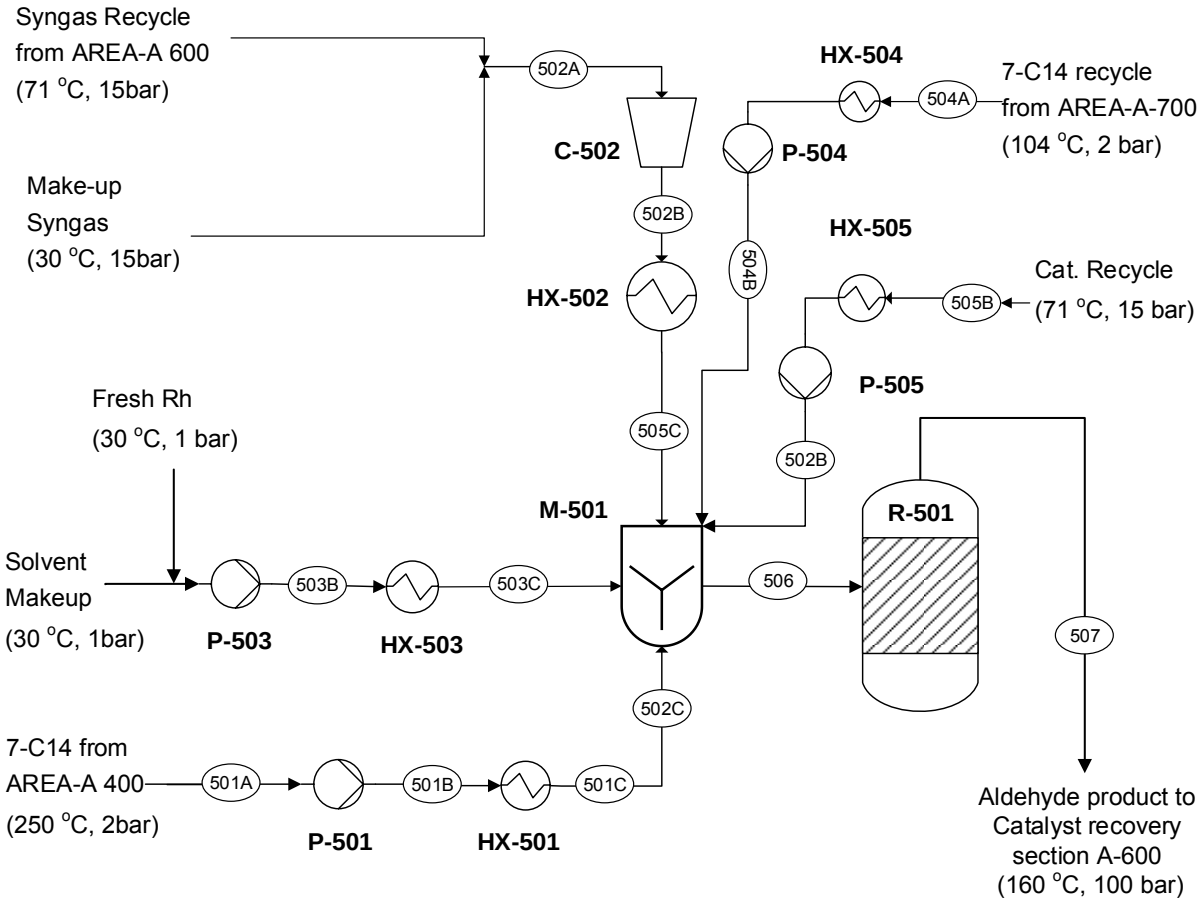

Figure 5.15.: Schematic diagram for the hydroformylation area A400 in Aspen Plus™

Table 5.8 describes the description of each unit and purpose in the model.

Table 5.8.: Description of unit operations and modelling objective

Equipment name	Modelling purpose and description
R - 501	Models a continuously stirred tank reactor for the hydroformylation of 7-tetradecene. The optimum operating temperature of the reactor was 160 °C and was maintained by means of a water-cooled jacket. Pressure is kept at 40 bar by means of syngas injection. The reactor was modelled using kinetics by Haumann et al. (2002b).
C - 501	Models a compressor that was used to raise the make-up syngas feed stream (503) pressure from 15 bar to stream (503A) at 40 bar.
C - 502	Models a compressor that was used to raise the recycle syngas feed stream (504) pressure from 2 bar to stream (504A) at 40 bar.
P - 501	Models a positive displacement pump used raise feed stream (501) pressure from 1 bar to stream (501A) at pressure 40 bar.
P - 502	Models a positive displacement pump used raise solvent stream (502) pressure from 1 bar to stream (502A) at pressure 40 bar.
P - 503	Models a positive displacement pump used raise catalyst recycle stream (504) pressure from 1 bar to stream (504A) at pressure 40 bar.
P - 504	Models a positive displacement pump used raise recycle 7-tetradecene stream (506) pressure from 1bar to stream (506A) at pressure 40 bar.

Table 5.9.: Description of unit operations and modelling objective

Equipment name	Modelling purpose and description
HX - 501	Models a heat exchanger to preheat feed stream (501A) at 30 °C to stream (501B), 160 °C before it enters the CSTR reactor (R-501). High pressure steam at 200 °C is used to preheat the feed.
HX - 502	Models a heat exchanger to preheat solvent stream (502A) from 30 °C to stream (502B) at 160 °C before it enters CSTR (R-501). High pressure steam at 200 °C is used to preheat the feed.
HX - 503	Models a heat exchanger to preheat catalyst recycle stream (504A) from 70 °C to stream (504B) at 160 °C before it enters CSTR (R-501). High pressure steam at 200 °C is used to preheat the feed.
HX - 504	Models a heat exchanger to heat 7-tetradecene recycle stream (505A) from 150 °C to stream (L-512) at 160 °C before it enters the CSTR (R-501).
HX - 505	Models a heat exchanger to preheat syngas make-up stream (503A) from 30 °C to stream (503B) at 160 °C before it enters the CSTR (R-501). High pressure steam at 200 °C is used to preheat the feed.
HX - 506	Models a heat exchanger to preheat syngas recycle stream (505A) from 30 °C to stream (505B) at 160 °C before it enters the CSTR (R-501). High pressure steam at 200 °C is used to preheat the feed.

5.3.6 Section AREA-A 600: Rh-TPPTS catalyst recovery section

The purpose of this section is to recover the catalyst in its active form so that it can be recycled back into the hydroformylation reactor (R-501) hence reducing the cost of catalyst. The objective of simulation for this section was to determine optimal conditions for catalyst recovery. Figure 5.16 shows the graph of sensitivity analysis for the mass fraction of catalyst leached in organic product stream versus pressure at a temperature of 72 °C (upper limit of heterogeneity, Muller et al. (2013)). It can be seen that catalyst leaching as low as 1 ppm can be achieved by operating the flash drum at 15 bar. Pilot plant results have also confirmed

rhodium concentrations lower than 1 ppm in the organic product phase (Muller et al., 2013, Rost et al., 2012, Harmela et al., 2012).

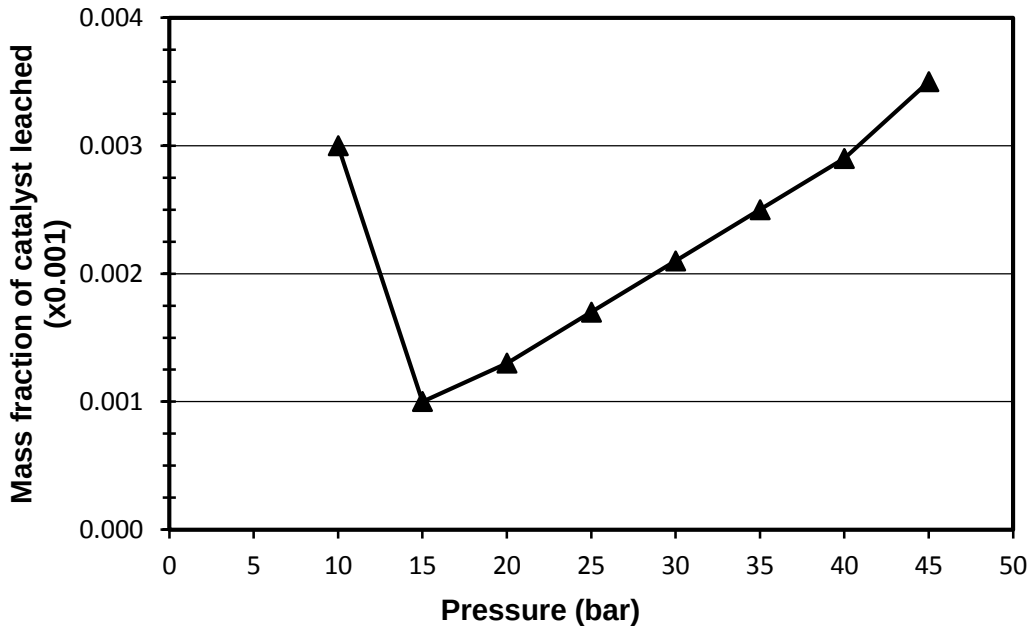

Figure 5.16.: Mass fraction and operating pressure in flash drum at 71 ºC

The separation progress of the flash drum at different temperatures can be seen in Figure 5.17 below. As can be seen the separation of this mixture into the individual phases is affected by temperature thus the formation of a homogeneous mixture at temperatures above 80 ºC resulted in an increase in catalyst leached with the organic product.

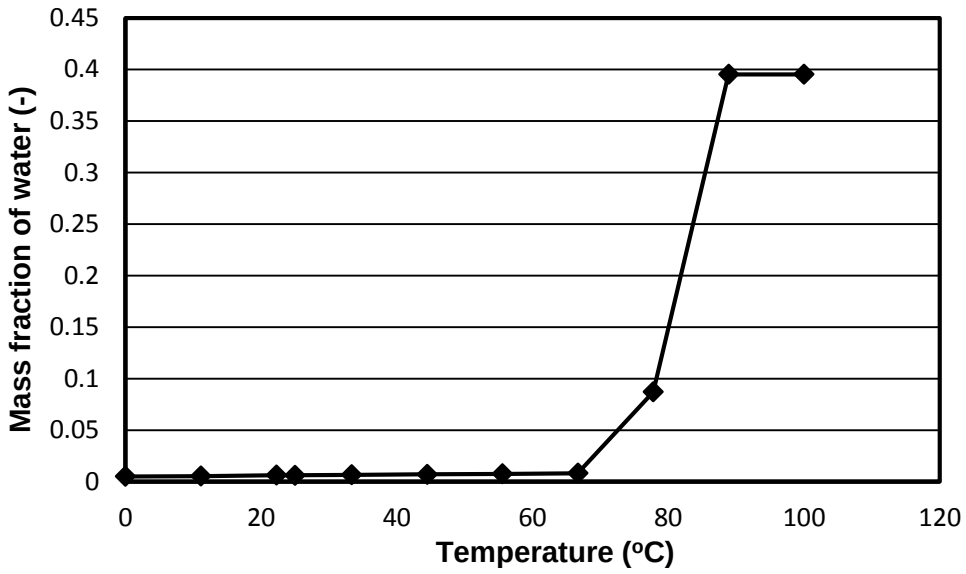

Figure 5.17.: Effect of temperature on the catalyst separation in flash drum

Rost et al. (2013) previously confirmed that the separation of the product mixture into three phases occurs faster at 72 °C hence a need to determine the sharpness of separation. In this investigation the mass fraction of water was used to determine the effectiveness of separation since the catalyst was dissolved in the aqueous media.

The set of optimal conditions for the operation of the flash drum to ensure that less than 9 ppm of the catalyst is leached with the organic product and hence ensure an economic process in this work was chosen to be 15 bar and 72 °C. Figure 5.18 shows the set-up of the liquid multiphase system for **Rh-TPPTS** catalyst recovery section and the units used in Aspen Plus™ to develop the section.

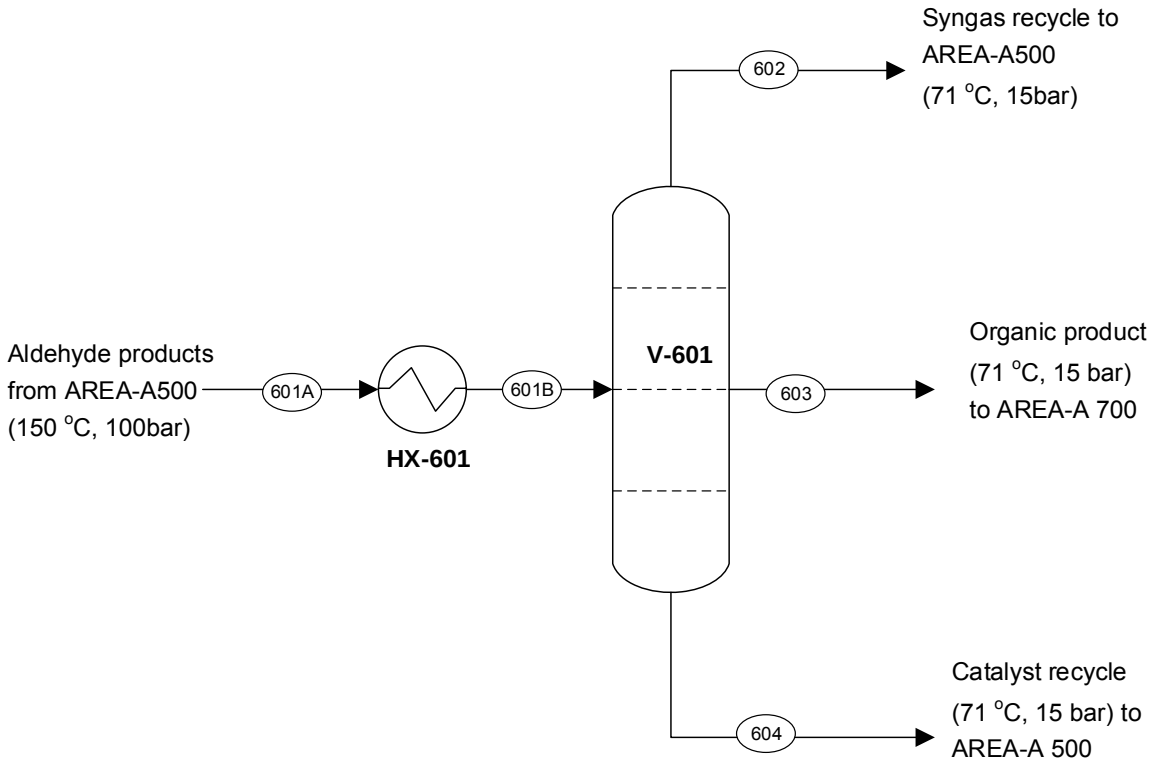

Figure 5.18.: Schematic diagram of the phase separator for recovery and recycle catalyst

Table 5.9 shows the description of each unit and model purpose.

Table 5.9.: Description of unit operations and modelling purpose

Equipment name	Modelling purpose and description
D - 601	Models a 3-phase Vapour-Liquid-Liquid flash to separate the product stream (601A) into polar catalyst stream (604) and nonpolar organic product stream (603). The flash drum operates at 71 °C and 15 bar base conditions according to Muller et al., 2013.
HX - 601	Models a feed cooler to reduce the temperature of product stream (601A) at 160 °C to stream (601B) at 71 °C before it enters the flash drum while the pressure is kept at 100 bar.

5.3.7 Section AREA-A 700: 7-Tetradecene recovery section

The purpose of this section is to recover > 99 % of unreacted 7-tetradecene in organic product and then recycle it back to the hydroformylation reactor section. In order to avoid product degradation at temperatures above 180 °C the column is operated under vacuum conditions and it is also assumed that a pressure loss of 50 % can be maintained between reboiler and condenser (Hentschel et al., 2014). It can be seen (Figure 5.19) from results of sensitivity analysis that as the number of stages increases the recovery also increases until 29 equilibrium stages are attained assuming 70 % column efficiency and $^{R_m}/_{R}$ of 1.2. An investigation was also carried out on the reflux ratio versus condenser and reboiler duty and it was found that both reflux ratio and condenser and reboiler duties remained approximately constant between 83 and 99 % recoveries of 7-tetradecene.

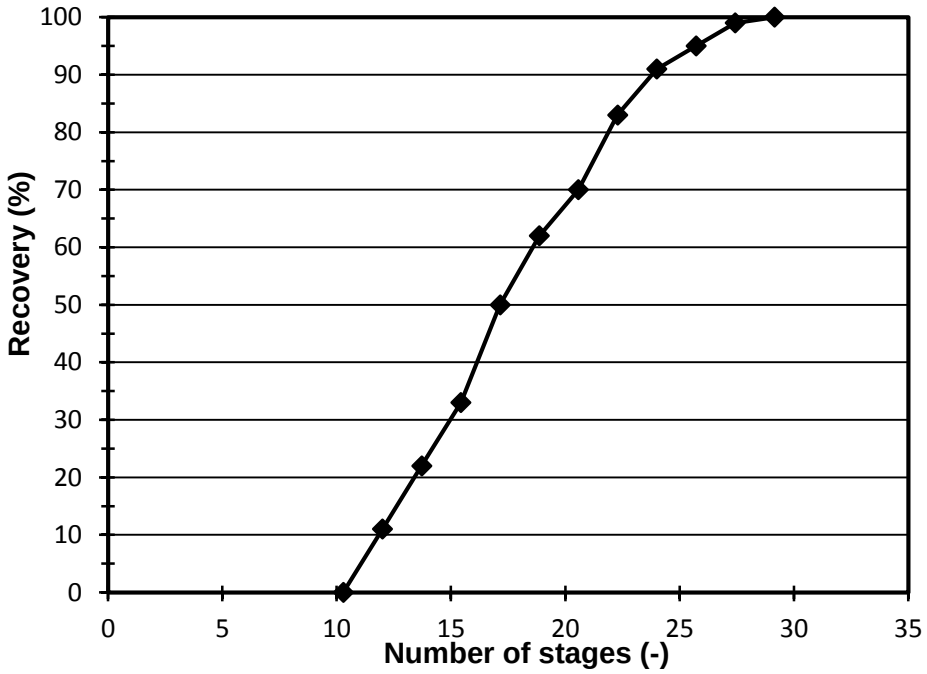

Figure 5.19.: Recovery versus number of stages in 7-tetradecene recovery column

The section comprises of the feed heater (HX-701) and the 7-tetradecene separation column (C-702) as shown in Figure 5.20.

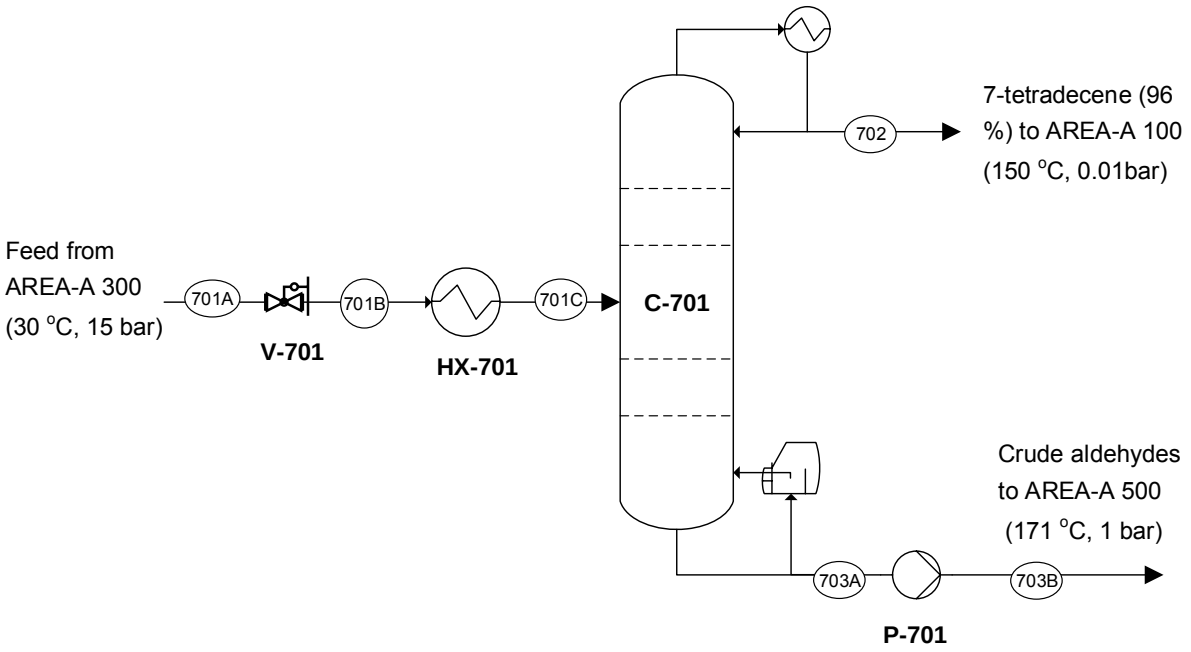

Figure 5.20.: Schematic diagram of 7-tetradecene recovery section

Table 5.10 shows the description of each unit operation and modelling purpose.

Table 5.10.: Description of each unit operation and modelling purpose.

Equipment name	Modelling purpose and description
C - 601	Models a distillation column used to recover unreacted 7-tetradecene from the product stream (701A) operated at 1 bar and the optimum number of stages required to achieve 99 % recovery is 29.
HX-701	Models a feed preheater used to raise the temperature of feed stream (701A) from 30 °C to 150 °C stream (701B)
V-701	Models a pressure reduction valve used to reduce stream pressure from 15 bars to 0.01 bar.
P-701	Models a pump used to raise the pressure of bottoms product to atmospheric pressure

5.3.8 Section AREA-A 800: Product Purification Section

According to Hentschel et al. (2014) and Steimel et al. (2014) downstream processing require minimum aldehyde purities of 98 %. The purpose of this section is to separate 2-hexyl-nonanal into a distillate stream of 99 % wt. purity which can be used as a feedstock to Geubert-type surfactants. Since the products will degrade at temperatures above 180 °C the pressure of columns is at vacuum conditions (Hentschel et al., 2014). The actual number of of stages were determined assuming a column efficiency of 70 % and ratio of minimum to actual reflux of 1.2. The pressure levels of the columns have been estimated assuming a pressure loss of 50%. Figure 5.21 below is a graph of the number of stages against 2-hexyl-nonanal purity.

It can be seen that the separation of 2-hexyl-nonanal from its isomers is a challenging step hence a larger number of steps are required. Hentschel et al. (2014) also observed that production costs during hydroformylation of 1-dodecene to *n*-tridecanal are dominated by the product separation column. The costs of the n/iso column arise from the comparably difficult separation of the two very similar aldehydes, hence a high number of stages is required (Hentschel et al., 2014). Micovic et al. (2012) also confirmed that the distillation separation of long-chain isomers tends to be more costly or even technically infeasible due to the decreasing difference in boiling points with increasing chain length.

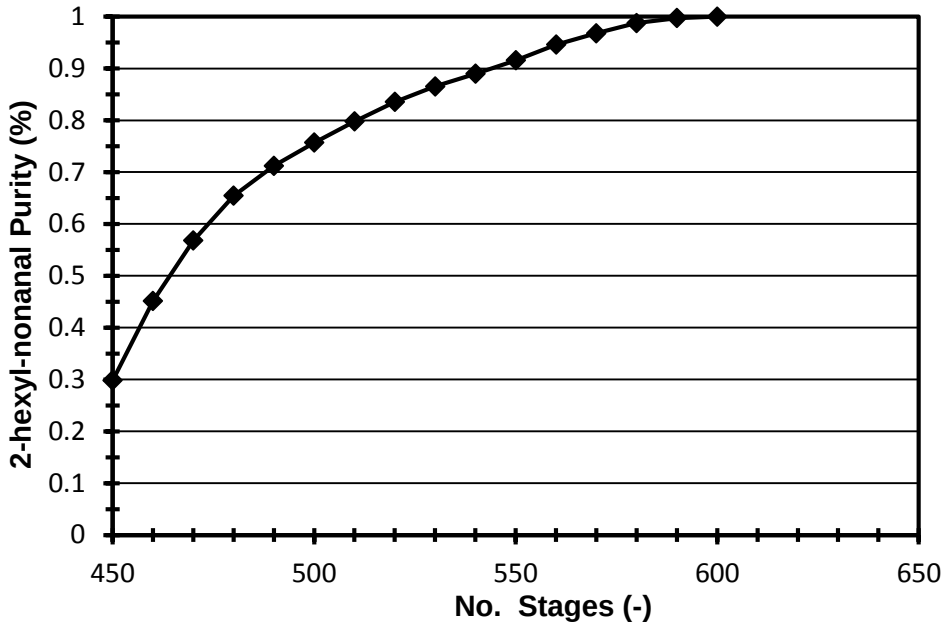

Figure 5.21.: Number of stages versus 2-hexyl-nonanal purity

Figure 5.22 shows arrangement of equipment models used in Aspen Plus™ to achieve this purpose.

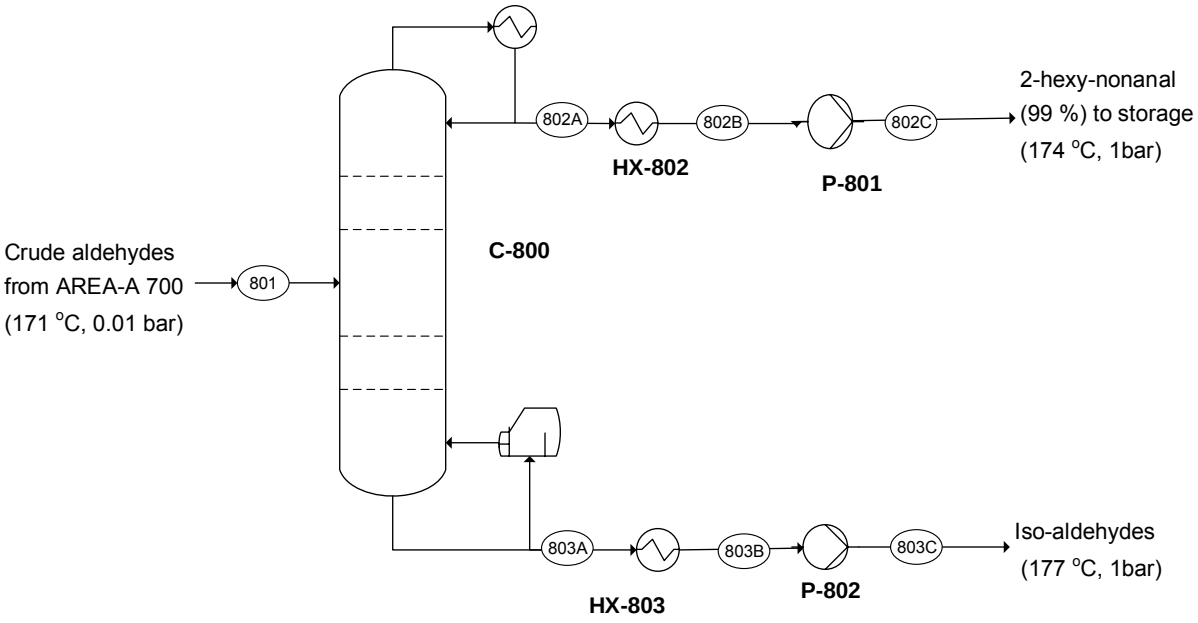

Figure 5.22.: Schematic diagram of product purification section

Table 5.11shows the description of each unit operation and modelling purpose.

Table 5.11.: Description of each unit operation and modelling purpose

Equipment name	Modelling purpose and description
C - 801	Models a distillation column used to separate 2-hexyl-nonanal from isomeric aldehydes identified by 2-pentyl-decanal. The column is operated at vacuum conditions.
HX-802 & HX-803	Models feed coolers used to reduce the temperature of product streams to storage temperatures (30 ^{o}C)
P-801&P-802	Models centrifugal pumps used to pump distillate and bottoms product streams to storage conditions

5.4 Aspen Plus™ simulation scenario B (OSN membrane separation)

Process scenario B is similar to scenario A except that liquid multiphase system was replaced by a two phase flash drum to separate unreacted syngas and OSN membrane process which was investigated as an alternative solution to reduce **Rh-TPPTS** catalyst loss during the hydroformylation process. According to Muller et al. (2013) and Wiese and Obst (2000) there is a need to guarantee at least 99,99 % recovery of **Rh-TPPTS** catalyst to ensure economic feasibility. Organic solvent membrane (OSN) is a plausible method to ensure recovery of active **Rh-TPPTS** catalyst considering high boiling points of aldehyde products (Schwarze et al., 2008). Together with models described in process scenario A in Section 5.3, OSN membrane model developed for **Rh-TPPTS** catalyst recovery was investigated in this scenario. Figure 5.23 shows the block flow diagram for process scenario B.

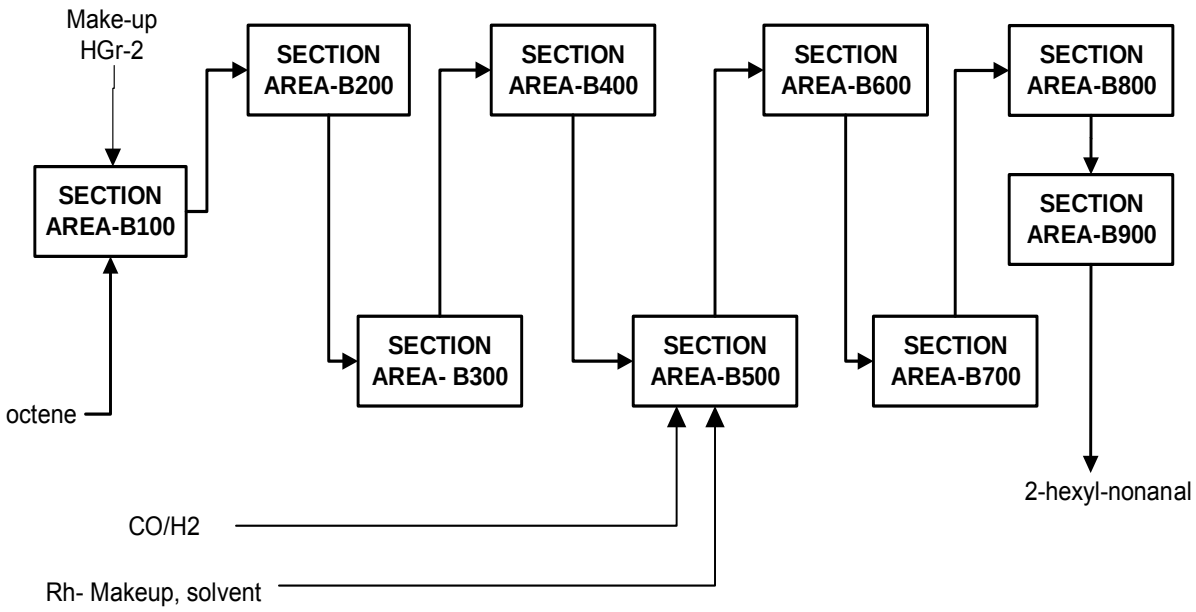

Figure 5.23.: Block Flow diagram for process scenario B: membrane process

5.4.1Section AREA- B100 –1-octene metathesis section

Refer to section AREA-A100 of Process Scenario A (pg. 94-98) as its process description is similar to that of this design.

5.4.2 Section AREA-B200 – Ethylene recovery section

Refer to Area A200 of Process Scenario A (pg.98-100), as its process area description is identical to this design.

5.4.3 Section AREA-B300 –Catalyst recovery section

Refer to Area A200 of Process Scenario A (pg.101-105), as its process area description is identical to this design.

5.4.4 Section AREA-B400-1-octene recovery column

Refer to Area A200 of Process Scenario A (pg. 106-108), as its process area description is identical to this design.

5.4.5 Section AREA-B500 Hydroformylation Section

Refer to Area A200 of Process Scenario A (pg. 108-115), as its process area description is identical to this design.

5.4.6 Section AREA-B600 Phase separator

After the hydroformylation reaction, the product is passed onto syngas recovery section. The purpose of this section is to recover unreacted syngas from the aldehydes product stream (201A). According to Vogelpohl et al. (2013) syngas is soluble in aldehyde and alkenes at high pressures hence can be separated from the product stream by using a flash drum. Figures 5.24 and Figure 5.25 shows the effect of temperature and pressure on the recovery of syngas from the flash drum. It can be seen that cooling the product stream to 45 °C resulted in an increase in the syngas recovered, however, due to high conversions attained in the reactor the change in syngas composition in the product stream was not significant hence an optimal temperature of 45 °C was chosen so as to limit recovery of the product.

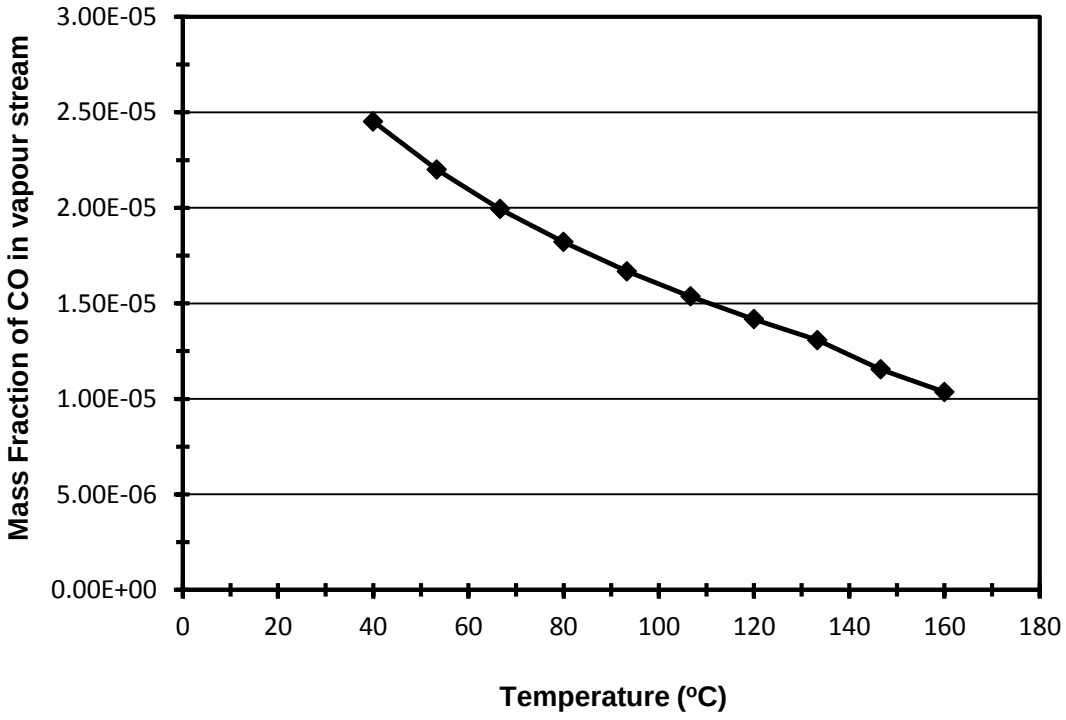

Figure 5. 24.: Effect of Temperature on the recovery of CO in V-L flash drum

The effect of operating pressure on the recovery of syngas is shown in Figure 5.25. It can be seen that operating the flash drum at pressures lower than 15 bar resulted in high recovery of syngas from the product stream. The result agrees well with Vogelpohl et al. (2013) who observed an increase in solubility of syngas in aldehyde product. The optimal pressure for the flash drum in this case was chosen to be 15 bar in order to maximise recovery of syngas.

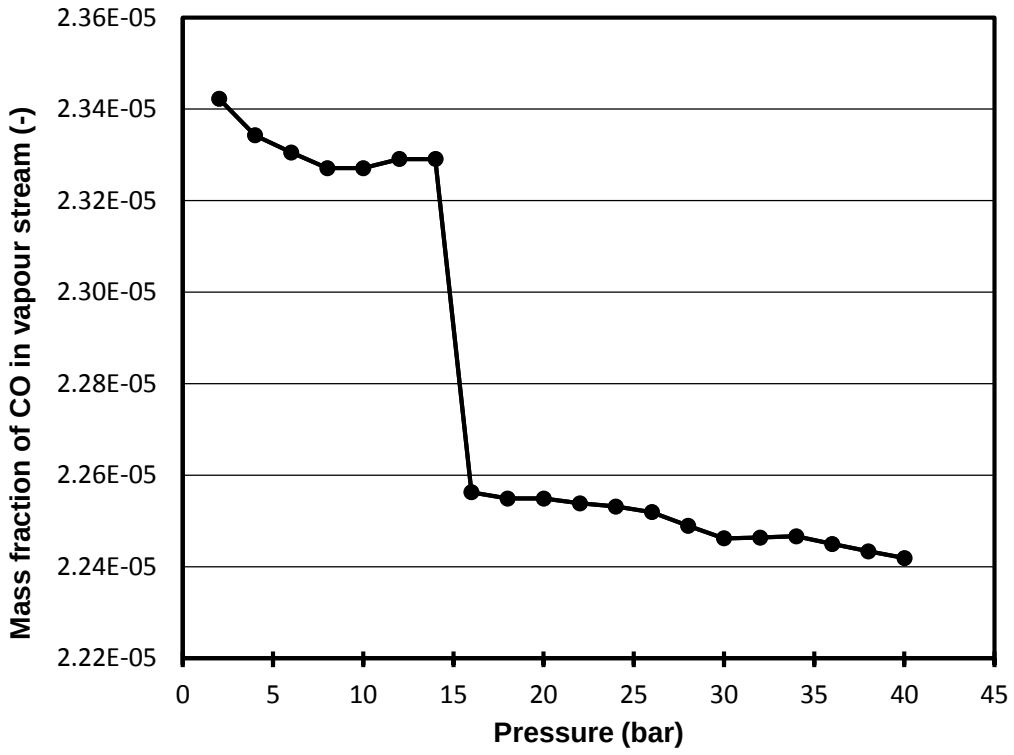

Figure 5.25.: Effect of pressure on Co recovery in V-L flash drum

A detailed description of the section is shown in Figure 5.26.

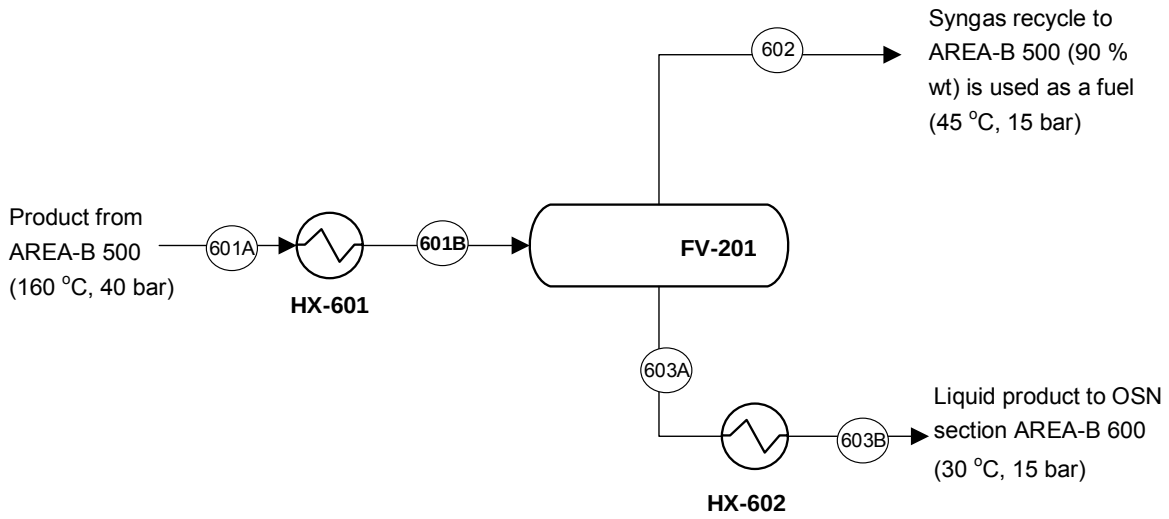

Figure 5.26.: Schematic diagram for the recovery of syngas in product stream

Product stream (601A) from the hydroformylation reactor, section AREA-B-500 at 2 bar and 160 °C is precooled to 45 °C before it enters the flash drum (V-201). Results of a temperature and pressure sensitivity analysis shows that if the flash drum is operated at 40 °C and 15 bar it is possible to achieve a 98 % recovery of syngas from the product stream. Outlet water temperature from a cooling tower at Sasol Secunda can be obtained at 22 °C (Kloppers and Kroger, 2005). Table 5.12 below shows the description of units and modelling purposes

Table 5.12.: Description of unit operations

Equipment name	Modelling purpose and description
HX - 601	Models a heat exchanger for cooling product stream (601A) from 160 °C to 45 °C.
HX - 602	Models a heat exchanger for cooling product stream (601A) from 45 °C to 30 °C.
V - 601	Models a flash drum which is used to separate product stream (601B) into 98 % syngas in stream (602) and liquid stream (603). The vessel is operated at 15 bar and 45 °C in order to achieve high syngas recovery (98%).

5.4.7 Section AREA-B700 Rh-TPPTS catalyst recovery process

This objective of this section is to demonstrate the recovery of **Rh-TPPTS** catalyst using OSN membrane process. Due to high costs of **Rh-TPPTS** catalysts and high catalyst loadings during hydroformylation of long chain internal alkenes, an efficient catalyst separation step especially an ultra-filtration step is needed to reduce the losses to a minimum (lower than 1 ppm) and attain recoveries > 99.9 % and to ensure economic feasibility of the overall process (Rost et al., 2013; Muller et al., 2015). In order to develop an Aspen Custom Model of **Rh-TPPTS** catalyst-OSN recovery unit in this work permeability of species which could not be obtained from literature were correlated and compared to experimental values for hydrophobic membranes with physical properties obtained from Aspen Plus physical properties data bank.

(i) Determining permeabilities using the Bhanushali et al. (2001) Correlation

The Bhanushali et al. (2001) model uses two factors that govern transport (P) through a membrane to determine permeability of unknown species using permebilities of known species using the following relationship:

- Viscosity (η)
- Molar volume (V_m)

$$P \propto \frac{V_m}{\eta} \qquad \textbf{Eqn. 5.1}$$

According to Bhanushali et al. (2001) the permeability of a reference species can be chosen as the basis to normalize the different solvent permeabilities through different hydrophobic membranes. A similar approach was also employed previously by Machado et al. (1999) where permeability of acetone was used to normalize other solvents permeabilities. According to Bhanushali et al. (2001) and Machado et al. (1999) it could be shown that a reasonable prediction (R^2 = 0.89) could be obtained using the correlation:

$$\frac{\text{Species (i) permeability}}{\text{Permeability of known specie}} = \mathrm{k}\left(\frac{\mathrm{V_m}}{\eta}\right) \qquad \textbf{Eqn. 5.2}$$

In this work nonanal permeability at 30 °C is chosen as the basis to normalize the species permeabilities through hydrophobic Starmem™ 240 membrane. Permeabilities of species were correlated and compared to experimental values and a correlation coefficient of $R^2 = 0.91$ was obtained. Figure 5.27 shows a correlation of solvent permeabilities (using nonanal permeability) of polar and non-polar solvents with ration of molar volume and viscosity for hydrophobic Starmem™ 240 membrane.

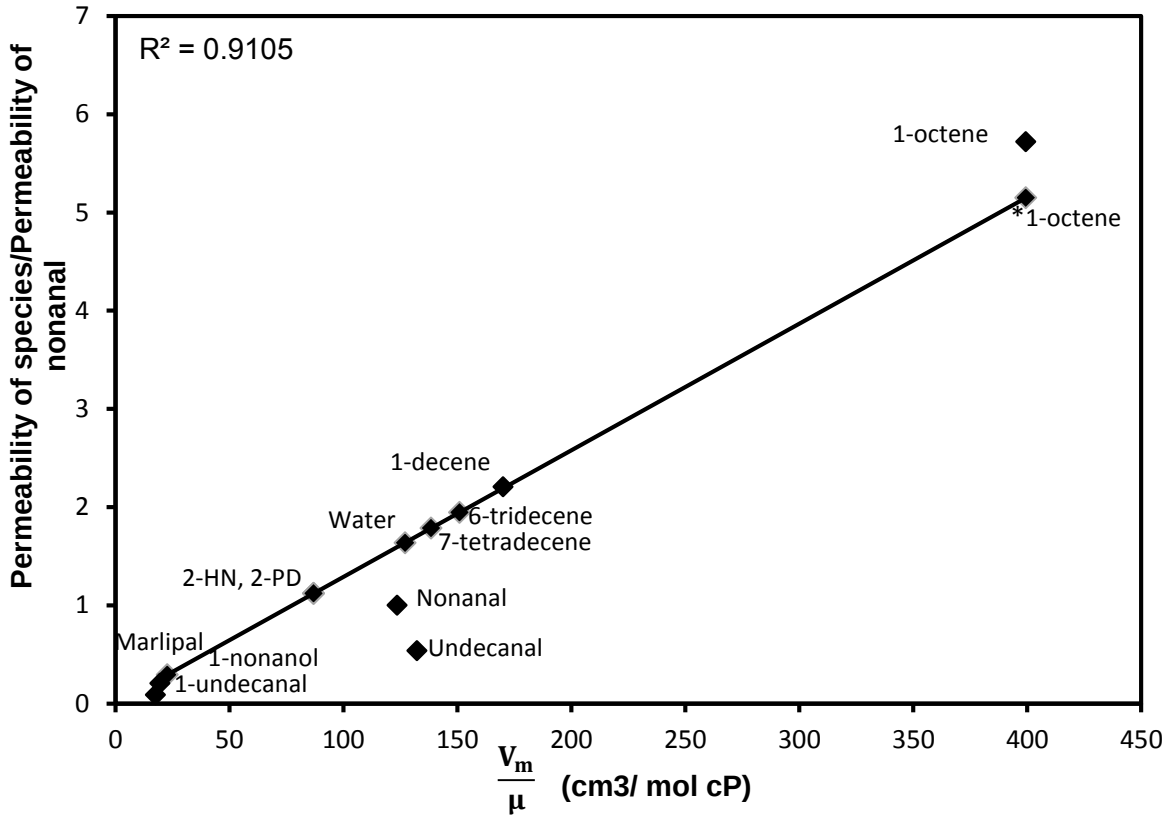

Figure 5.27.: Correlation of solvent permeabilities (using nonanal permeability) for hydrophobic Starmem™-240 membrane.

Thus, these permeabilities (Table 5.13) were used to develop an Aspen Plus™ Customized membrane for **Rh-TPPTS** catalyst separation and recovery system.

Table 5.13.: Normalised permeabilities of species used in modified Hagen-Poiseuille model

Species	Pi(cm^3/cm^2bar)	Pi(m)
1-octene	9,11159E-05	1,26833E-14
7-tetadecene	3,60047E-05	5,01185E-15
6-tridecene	3,92416E-05	5,46244E-15
2HN	2,26074E-05	3,14695E-15
2PD	2,26074E-05	3,14695E-15
Water	6,46337E-05	8,99701E-15
Marlipal 24/70	2,63547E-05	1,66857E-16

5.4.7.1 Development of Aspen Plus™ custom model of membrane unit

A model of a membrane unit is not (yet) available as a build-in process model in Aspen Plus™ model library. The purpose of simulation in this section is to determine the optimal parameters required for an annual production of 10 000 tonnes of 2-hexyl-nonanal using commercial OSN membrane modules, 2.5″x 40″ spiral-wound Starmem™ 240 by Evonik. A FORTRAN block of an Aspen Custom Model of a nanofiltration membrane unit interfaced in Aspen Plus™ was developed to demonstrate recovery of **Rh-TPPTS** catalyst. Algorithms used in Aspen Plus are shown Appendix A. Fixed structural parameters such as number of stages and recycling structure was adopted from Seifert et al. (2013) and Schmidt et al. (2014) with objective of achieving > 99.99 % Rh-catalyst. recovery.

(i) Modelling Limitations

This model uses flexible parameters from Aspen Plus™ physical properties data bank like viscosity and molar volume of the solvent to obtain a reasonable prediction of pure solvent flux (polar and non-polar) for hydrophobic membranes. By extending model developed by Bhanushali et al. (2001) to different types of membranes (polar and non-polar) using membrane properties measured from independent experiments permeabilities of species were correlated and compared to experimental values and a correlation coefficient of R^2= 0.91.

The result agreed well to previous results reported by Bhanushali et al. (2001) and Machado et al. (1999).

(ii) Model assumptions

The key assumptions made in this model are:

1. The factor that controls the transport through a given membrane is the viscosity of the solvent (Bhanushali et al., 2001, Machado et al., 1999).
2. Both solute and solvent dissolve in the non-porous and homogeneous surface layers of the membrane (Wijmans et al., 1995)
3. The flow is convective in nature and can be predicted by the Hagen–Poisuelle-2 equation for convective flow (Bhanushali et al., 2001),
4. Each species diffuses across the membrane in an uncoupled manner due to its own chemical potential gradient, which is the result of the concentration and pressure differences across the membrane.
5. The pressure within a membrane is uniform and that the chemical potential gradient across the membrane is essentially due to a concentration gradient.
6. No concentration polarization.

(iii) Optimisation results

In this section, the optimisation results for recycling of homogeneous **Rh-TPPTS** catalyst based on the results of the validation experiments are shown for Starmem™ 240, focusing on the effect of total production costs per kg of 2-hexyl-nonanal product. The optimisations were performed individually for different membrane setups, i.e. fixed structural parameters such as stage rejections and recycling structure were assumed. Then, operational parameters in the membrane part were optimised and finally given the optimised membrane cascade. For operating costs of the OSN membranes, a membrane price/stability factor of 250 ($ m^2 yr^1) was assumed. As can be observed, the overall membrane production costs of 2-hexyl-nonanal is a function of the number of OSN membrane stages, with more costs for processes with more stages and less costs for processes with fewer stages. These results are a direct

consequence of the low individual stage rejections, resulting in 86.16 % overall **Rh-TPPTS** catalyst rejection, overall for the one-stage process up to 99.98 % rejection in case of the five-stage process. Comparing the overall membrane cost per kg of 2-hexyl-nonanal with overall rejection, it can be observed that the optimal configuration was a 3-stage OSN membrane setup.

Moreover, the production costs for a 3-stage process lies within a reasonable range (0.0941 $/kg) whereas the five-stage process has a two times higher production cost of 0.1277 ($/kg). This promotes the application of OSN, as mostly, in industrial settings, the number of stages can be a key operating criterion for an investment decision within early phases of process development. Figure 5.28 is the diagram of membrane optimization with number of stages.

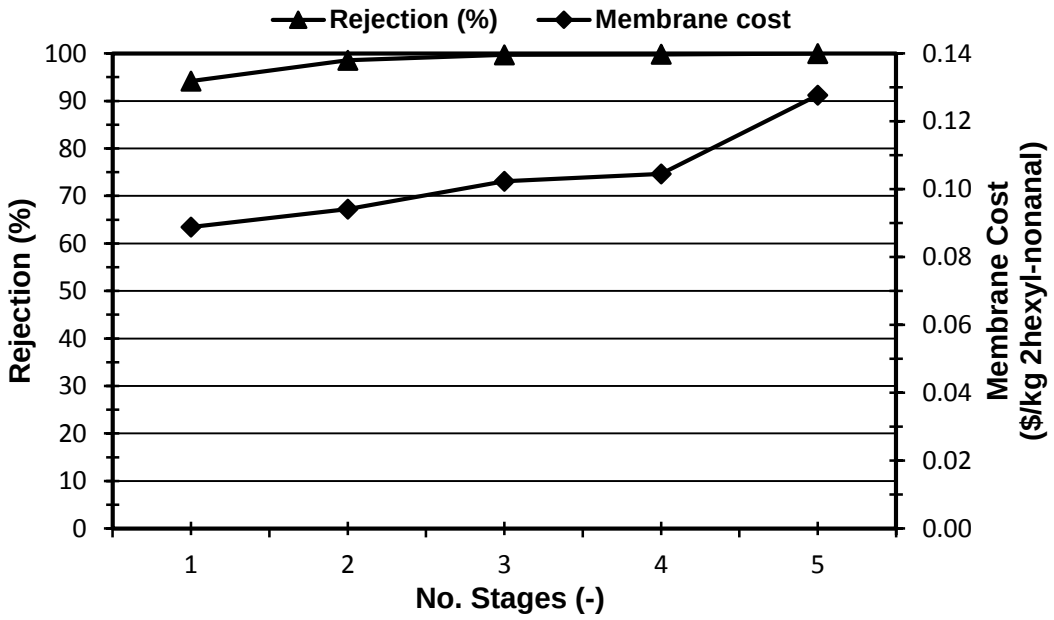

Figure 5.28.: Membrane rejection and cost versus number of stages

Figure 5.29 shows an optimised three-stage cascade model arrangement used to develop the catalyst recovery unit. The arrangement of retentate and permeate streams is similar to one proposed by Seifert et al. (2014).

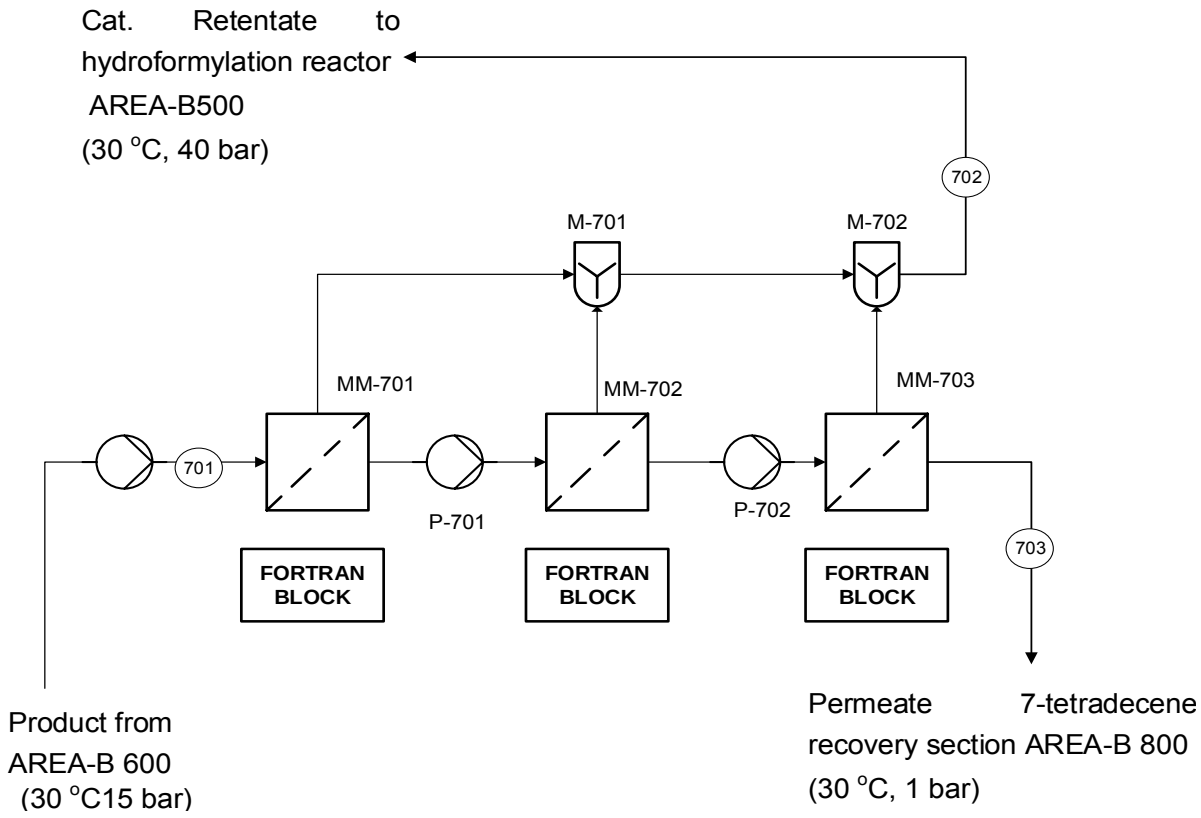

Figure 5.29.: Single-stage membrane process for Rh-TPPTS catalyst recovery process

Table 5.14 shows the description of each unit operation and modelling purpose.

Table 5.14.: Description of each unit operation and modelling purpose.

Equipment name	Modelling purpose and description
Membranes MEMB Stage 1, MEMB Stage 2, MEMB Stage 3,	Models a membrane separator used to recover the catalyst species from the product stream (701) into catalyst retentate stream (702) and product permeate stream (703). A custom build membrane was developed using FORTRAN blocks which predicts species flux by modified Hagen-Poiseuille-2 model.
P – 701,P-702, P-703	Models OSN pumps required to provide the transmembrane pressure as driving force for the species flux through the membrane.

5.4.8 Section AREA-B800 7-Tetradecene Recovery Section

Refer to Area A800 of Process Design 1.1 (pg.119-121), as its process area description is identical to this design.

5.4.9 Section AREA-B900 Product Purification Section

Refer to Area A800 of Process Design 1.1 (pg.121-123), as its process area description is identical to this design.

5.5 Process heat recovery system design

Heat integration was considered in order to recover energy from process streams and to use it to reduce external utility demands. Heat transfer limitations in unit operations were also treated as part of equipment design. A properly designed heat recovery network can reduce the amount of energy required by a process when heat rejected by one unit is recovered and reused in another that requires heat. For an effective heat recovery system, the heat recovery system design has to be systematic. Hence, “pinch analysis” is one such recommended method in use in heat exchanger network design (Sinnot, 2005). Pinch analysis builds the heat exchanger network design around a thermodynamic constraint known as the process pinch (Smith, 2005). Using the heating and cooling targets established in the design of reactors and the separation system, design of the heat exchanger network is done to avoid transfer of heat across the thermodynamic constraint (Smith, 2005).

In 2001, ASPEN Tech’s Nick Hallale highlighted that, “pinch analysis” has an enormous amount of applications, with thousands of projects having been commissioned all over the world with companies such as Shell, Exxon, BP-Amaco, Neste-Oy, and Mitsubishi reporting fuel savings of up to 25 % and similar emissions reductions, worth millions of dollars per year” (Friedler, 2010). The largest energy-consuming site ever analysed by pinch techniques is the fuels and petrochemicals at the coal complex of Sasol Synthetic Fuels in South Africa (Neelis et al., 2008).

According to ASPEN Tech's Nick Hallale (Friedler, 2010), "pinch analysis" has an enormous amount of applications, with thousands of projects having been carried out all over the world, companies such as Shell, Exxon, BP-Amaco, neste Oy and mitsusbish have reported fuel savings of up to 25 % and similar emissions reductions, worth millions of dollars.

The application of pinch analysis to the simulated process of upgrading low value 1-octene to 2-hexylnonanal was done in this design. Data from the simulation of process Scenario A was used to demonstrate the application of pinch analysis. The process starts with the extraction of process Stream data. The data required is summarized in Table 5.15

Table 5.15.: Scenario A process stream summary

Stream Name	Supply Temp.	Target Temp.	Heat Duty	Heat Flow	Stream Type	Supply Shift	Target Shift
	°C	°C	kW	kW		°C	°C
L103	30	50	161.706	161.706	COLD	35.0	55.0
L201	50	30	370.780	370.78	HOT	45.0	25.0
L401	45	30	274.643	274.643	HOT	40.0	25.0
L401B	39	121	710.751	710.751	COLD	44.0	126.0
L402	121	30	1647.010	1647.01	HOT	116.0	25.0
L502	265	160	129.082	129.082	HOT	260.0	155.0
L504	34	160	0.003	0.0035	COLD	39.0	165.0
L506A	103	160	1.829	1.8293	COLD	108.0	165.0
L507B	68	160	385.766	385.766	COLD	73.0	165.0
L601A	160	72	680.835	680.835	HOT	155.0	67.0
L701	67	150	170.433	170.433	COLD	72.0	155.0
L802	159	30	106.626	106.626	HOT	154.0	25.0
L803	170	30	49.957	49.9569	HOT	165.0	25.0

After collecting the process stream information in the next stage of pinch analysis was to find the pinch conditions through application of the problem table method. The problem table method is a numerical method which, when used, can indicate the position of the thermodynamic constraint on system of process streams (Sinnot, 2005). It is an iterative process where heat loads are cascaded to identify the thermodynamic constraint. Table 5.16 summarizes the results of application of the problem table method to the process scenario A.

Table 5.16.: Problem Table Algorithm results summary for process Scenario A

Actual Temp.	MCP $_{Hot}$	MCP $_{Cold}$	ΔH Cold	ΔH Hot	ΔH Cascade
	kW/K	kW/K	kW	kW	kW
265	1,2294	0,0	0,0	0,0	**0,0**
170	1,5862	0,0	0,0	116,7885	116,7885
160	8,0936	4,2252	4,2252	15,8619	132,6504
159	8,9202	4,2252	38,0271	8,0936	136,5187
150	8,9202	6,2786	182,0805	80,2814	178,7730
121	27,0192	14,9463	269,034	258,6845	255,3770
103	27,0192	14,9142	462,3415	486,345	472,6880
72	19,2824	14,9142	59,657	837,5941	847,9406
68	19,2824	10,7211	10,7211	77,1296	865,4133
67	19,2824	8,6677	147,3513	19,2824	873,9745
50	37,8214	16,753	83,7651	327,8009	1054,4241
45	56,1309	16,753	100,5181	189,107	1159,7660
39	56,1309	8,0853	40,4266	336,7856	1396,0335
34	56,1309	8,0853	32,3412	280,6547	1636,2616
30	0,0	0,0	0,0	224,5237	**1828,4441**

The problem table results above shows the temperature interval in which the heat recovery constraint is located and the utility demands. In Table 5.16 the values of Δ H are all positive indicating that all the process streams are above pinch. The overall Δ H cascade (in bold) represents the cold utility requirement. The interval with the zero Δ H cascade in this scenario is the pinch interval (in bold case). The procedure was repeated for the second scenario and results are summarized in Table 5.17.

Table 5.17.: Summary of pinch results for the two process scenarios

	Scenario A	Scenario B
Hot Utility (kJ/kmol 2-HN)	0	0
Cold Utility (kJ/kmol 2-HN)	182,844	151.175
Pinch temperature (°C)	265	265
Net Heat	182.844	151.175

The heat exchanger network was designed with the aid of an Aspen Plus Energy Analyser™ see Appendix C for more detail.

5.6 References

Bhanushali, D.S., Solvent-resistant nanofiltration membranes: separation studies and modelling, A dissertation submitted in partial fulfilment of the requirements for the degree of Doctor of Philosophy in the College of Engineering at the University of Kentucky (2002)

Brannock, VN Verneuilan V. S., Wang D Y. L. Processs simulation program a comprehensive flowsheeting tool for chemical engineers, Computers & Chemical Engineering, **3,** (2012), (329.-352,1979

Cross. R.A., Optimum process designs for ultrafiltration and crossflow microfiltration systems Desalination **145** (2002) 159-163

du Toit, J. I., Jordaan, M., Carlijn, A., Huijsmans, A., Jordaan, J.H.L., van Sittert, C.G.C.E., Vosloo, H.C.M. Improved Metathesis Lifetime: Chelating Pyridinyl-Alcoholato Ligands in the Second Generation Grubbs Precatalyst. Molecules **19** (2014), 5522-5537; doi: 10.3390/molecules19055522

Evonik Membrane Extraction Technology Limited (US PATENT 8598376) http://www.google.com/patents/US8598376

Florusse, L.J., Peters, C.J., Pamies, J.C., Vega, L.F., Meijer, H. Solubility of hydrogen in heavy n-alkanes: experiments and SAFT modeling, American Institute of Chemical Engineers Journal **49** (2003) 3260–3269.

Ghosh, A., Chapman, W.G., French, R.N. Gas solubility in hydrocarbons – a SAFT based approach, Fluid Phase Equilibria **209** (2003) 229–243

Halima, I., Srinivasan, R. A knowledge-based simulation-optimization framework and system for sustainable process operations, Computers and Chemical Engineering **35** (2011) 92–105

Hanspal. N.S., Waghodeb A. N., Nassehic V., Wakemanc R.J., Development of a predictive mathematical model for coupled stokes/darcy flows in cross-flow membrane filtration, Chem. Eng. J. (2008), doi:10.1016/j.cej.2008.10.012

Haumann, M., Koch, K., Hugo, P., Schomacker, R. Hydroformylation of 1-dodecene using Rh-TPPTS in a micro emulsion. Applied Catalysis A: General **225** (2002a) 239–249

Hentschel, B., Kiedorf, G., Gerlach, M., Hamel, C., Seidel-Morgenstern, A., Freund, A, Sundmacher, K. Model-Based Identification and Experimental Validation of the Optimal Reaction Route for the Hydroformylation of 1‑Dodecene. Industrial Engineering Chemistry Research **54**, (2015), 1755−1765 DOI: 10.1021/ie504388t

Hoffman, J, Gijsbertsen, A.M.H .,Cornelissen E., Nanofiltration retention models for organic contaminants Awaarf and Kiwa Water Research **146** (2007) 281-298

Jana, A.K Process simulation and control using ASPEN , PHI Learning Pvt. Ltd Technology and Engineering (2012) ISBN 8120345861

Jonsson, G., Boundary layer phenomenon during ultrafiltration of dextran and whey proteins solution, *Desalination.* 51 (1984), 66-77

Jordaan, M., van Helden, P., van Sittert, C.G.C.E., Vosloo, H.C.M., Experimental and DFT investigation of the 1-octene metathesis reaction mechanism with the Grubbs 1 precatalyst. Journal of Molecular Catalysis A: Chemistry **254**, (2006), 145–154.

Kiedorf, G., Hoang, D.M., Muller, A., Jorke, A., Markert, J., Arellano-Garcia, A., Seidel-Morgenstern, A., Hamel, C. Kinetics of 1-dodecene hydroformylation in a thermomorphic solvent system using a rhodium-biphephos catalyst. Chemical Engineering Science **115** (2014) 31–48

Koeken, A.C.J., van dar Broeke, L.J.P., Benes, N.E., Keurentjes, J.T.F. Triphenylphosphine modified rhodium catalyst for hydroformylation in supercritical carbon dioxide. Journal of Molecular Catalysis A: Chemistry **346**, (2011) 94–101

Lehman, S., John, E. Schwendeman, Patrick, M. O'Donnell, K., Wagener, B. Olefin isomerization promoted by olefin metathesis catalysts, Inorganica Chimica Acta **345** (2003) 190-198

Lonsdale, H.K. U. Merten and R. L Riley, Transport properties of cellulose acetone osmotic membranes, Journal of Applied Polymer Science **252** (2005) 195-203

Meerkerk, M.A., Hoffman, J.A.M.H., Huiting. H., Removal of pesticides by nanofiltration and reverse osmosis, Kiwa report SWO 97.101, Niewegein (1998)

Mohammad, A. W Simple mass transfer experiment using nanofiltration membranes ChE laboratory ASEE (2000)

Nghiem, L.D A. I Schafer, T. D Waite Adsorptive interactions between membranes and trace organics, Desalination **147** (2002), 269-274

Park J, Robinson R.L., Gasem K.A.M., Solubilities of hydrogen in heavy normal paraffins at temperatures from 323.2-K to 423.2-K and pressures to 17.4-Mpa, Journal of Chemical & Engineering Data **40** (1995) 241–244.

Peschel, A., Hentschel, B., Freund, H., Sundmacher, K. Design of optimal multiphase reactors exemplified on the hydroformylation of long chain alkenes. Chemical Engineering Journal **188** (2012) 126-141

Queiroz, J., Vitor, M., Rodrigues, S., Henrique, A., Matos, F., Martins, G. Modelling of existing cooling towers in ASPEN PLUS using an equilibrium stage method. Energy Conversion and Management **64** (2012) 473–481

Rajendran, H.R., Kankanala, M., Lundin, M., Taherzadeh, J., Process simulation model for anaerobic digestion, Proceedings of the International Conference on Solid Waste Innovation in Technology and Management, Hong Kong SAR, P.R. China, 5 – 9 May (2013)

Seider, W. D., Seader, J. D., Lewin, D. R. Product and process design principles : synthesis, analysis, and evaluation. New York: Wiley and Sons (2004)

Sethi, S., Transient permeate flux analysis, cost estimation, and design optimization in crossflow membrane filtration (PhD Thesis) (1997)

Schmidt P., Bednarz E.L., Lutze P., Górak A., Characterisation of organic solvent nanofiltration membranes in multi-component mixtures: process design work flow for utilising targeted solvent modifications Chemical Engineering Science**115** (2014)115–126

Schock, G., Miquel, A. Mass transfer and pressure loss in spiral wound modules, Desalination **64** (1987) 339-52

Silva, P., Ludmila G. Peeva, Andrew G. Livingston, Organic solvent nanofiltration (OSN) with spiral-wound membrane elements—highly rejected solute system, Journal of Membrane Science **349** (2010) 167–174

Sousa, S. I., Martins, F.G., Alvim-Ferraz, M.C.M., Pereira, M.C., Multiple linear regression and artificial neural networks based on principal components to predict ozone concentrations Environmental Modelling & Software **22** (2007) 97-103

Srivatsan, S., X.H. Yi, R.L. Robinson, K.A.M. Gasem, Solubilities of carbonmonoxide in heavy normal-paraffins at temperatures from 311-K to 423-K and pressures to 10.2-MPa, Journal of Chemical & Engineering Data **40** (1995) 237–240.

Steele, W.V., and R.D., Chirico Thermodynamic properties of Alkenes (Mono-Olefins Larger than C4), IIT research Institute for Petrochemical and Energy Research 1992

Steimel J., Harrmann M., Schembecker G., Engell S. A framework for the modelling and optimization of process superstructures under uncertainty. Chemical Engineering Science **115** (2014) 225-237

Van der Bruggen B., Manttari M., Nystrom, DRAWBACKS OF APPLYING NANOFILTRATION AND HOW TO AVOID THEM: A REVIEW, Separation and Purification Technology **63** (2008) 251–263

Van der Gryp, P., Barnard, A., Cronje, J.-P., de Vlieger, D., Marx, S., Vosloo, H.C.M. Separation of different metathesis Grubbs-type catalysts using organic solvent nanofiltration. Journal of Membrane Science **353**, (2010), 70–77.

Van Leeuwen P.W.N.M. Claver C., Rhodium Catalysed Hydroformylation, Kluwer Academic Publishers, Dordrecht, (2000)

Yan, Y. Z., Zhang, D. K., Modelling of a Low Temperature Pyrolysis Process Using ASPEN PLUS, Developments in Chemical Engineering & Mineral Processing, **7**, (1999) 577-591

Wijmans, J G., Nakao, S., Van dar Berg, J.W.A., Troelstra, F.R., Smolders, CA., Hydrodynamic resistance of 'concentration polarization boundary layers in ultrafiltration, Journal of Membrane Science, **22** (1985) 117-135

CHAPTER 6: ECONOMIC EVALUATION

"There are three rules to a successful business. Rule # 1, if it doesn't make money the other rules don't matter"

T Boone Pickens

Overview

Chapter 6 presents results of economic evaluation of the two process scenarios of upgrading low value 1-octene from Fischer-Tropsch product stream to 2-hexyl-nonanal. Section 6.1 is introduction to economic evaluation. Section 6.2 discusses the methodology and assumptions of TEA. Section 6.3 details the capital cost estimation. Section 6.4 provides details of operating costs. Section 6.4 is subdivided into Section 6.4.1 and Section 6.4.2 detailing fixed operating costs and variable operating costs respectively. Section 6.5 considers the revenue. A profitability assessment is detailed in Section 6.6. Finally, Section 6.6 summarises the results of economic analysis. More details to this chapter is also given in Appendix D.

6.1 Introduction

Techno-economic analysis (TEA) is defined as a systematic analysis used to evaluate the economic feasibility (Simba et al., 2012). In conceptual design of a new plant, techno-economic analysis, (TEA), is used to compare alternative plant configurations. In testing alternatives, designers require both an absolute measure and a normalized measure in order to make a definitive evaluation (Mellichamp, 2013). In recent years, NPV (Net Present Value) has often been chosen as the absolute metric and IRR % (Internal Rate of Return) as the normalized one. In this study several standard engineering profitability criteria according Turton et al. (2009) were used, namely;

(i) Net Present Value (NPV), gives the profit of the plant for a certain period by considering the time value of money. NPV gives the present value of all payments and provides a basis of comparison for projects with different payment schedules but similar lifetimes (Biegler et al., 1997). In making comparisons between projects, the larger the NPV, the more favourable the investment (Peters and Timmerhaus, 2003). The NPV always provides a reliable indication of project profitability and it can handle both positive and negative cash flows throughout the project (Turton et al., 2009).

(ii) Internal Rate of Return (IRR %), is a measure that provides the rate of interest or discount factor which when applied to a series of projected cash flows will yield a zero NPV (Poherecki et al., 2010). It is the maximum rate at which a loan could be raised to finance an investment such that the investment would just pay off the capital and interest by the end of the investment period (Turton et al., 2009). To evaluate if the project is worth considering, the IRR is compared to the cost of capital (hurdle rate), i, if the IRR equals or exceeds the cost of capital then the project is acceptable (Poherecki et al., 2010). According to Miremadi et al. (2013), the average IRR % for specialty chemical products lie within 13 and 17 %.

(iii) Pay Back Period (PBP), is the calculation of the time it takes to recover the initial capital outlay from the project's cash flows. It is the length of time taken for a project to pay for itself (Turton et al., 2009). It is shown on the cumulative cash flow diagram as a point where the cumulative cash flow becomes positive. Project with a shorter PBP are normally attractive (Poherecki et al., 2010).

6.2 Methodology and assumptions

In the past two to three decades, the methodology for TEA at the conceptual design stage has converged to use of just a few main approaches and metrics. The discounted cash flow (DCF) method is a well-known economic assessment method estimating the attractiveness of an investment opportunity and several economic indexes can be chosen as NPV, IRR % and PBP (Cucchiella et a., 2015, Bortoluzzi et al., 2014). The DCF method has been defined in recent years by Douglas (1988); Peters and Timmerhaus (2003) and Turton, et al. (2012). The methodology framework adopted for a TEA in this study is shown in Figure 6.1 and important stages shown which will serve as a route map for the remainder of this chapter.

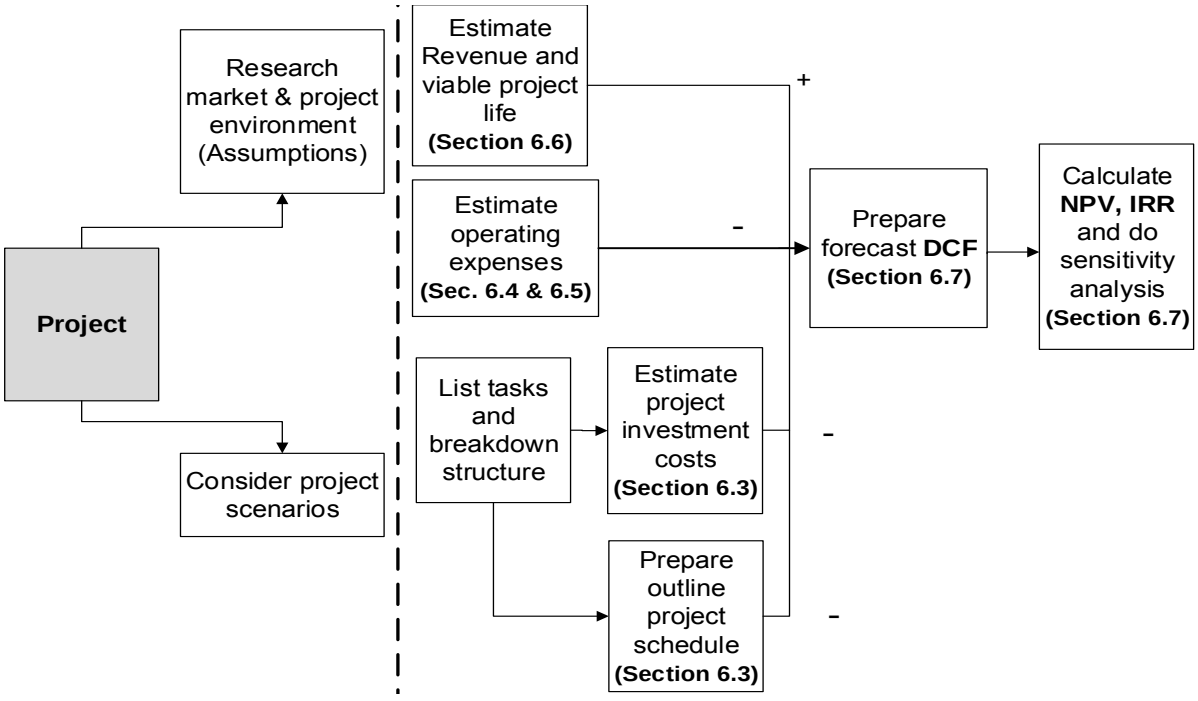

Figure 6.1.: A framework for DCF method for TEA in this study

The DCF definition and their use in design practice have been aided via spreadsheet calculations (Mellichamp, 2013). The preliminary economic analysis was based on a set of assumptions outlined below.

6.2.1 Assumptions

Table 6.1 is a list of basic assumptions used to simplify the preliminary economic analysis.

Table 6.1.: List of assumptions

Definition	Value	References
Construction schedule	2 years	Seifert et al. (2014)
Depreciation	5 years	South African Taxation and Investment (2015)
Project life	15 years	Sinnot (2005)
Taxation rate	28 %	South African Revenue Services (2016)
Discount rate	15 %	Miremadi et al. (2013)

6.3 Estimation of capital cost

The capital investment is funds required to design and purchase equipment, structures, and buildings as well as to bring the facility into operation (Green and Perry 2008). Figure 6.3. shows the standard capital investment estimation methodology adopted in this study.

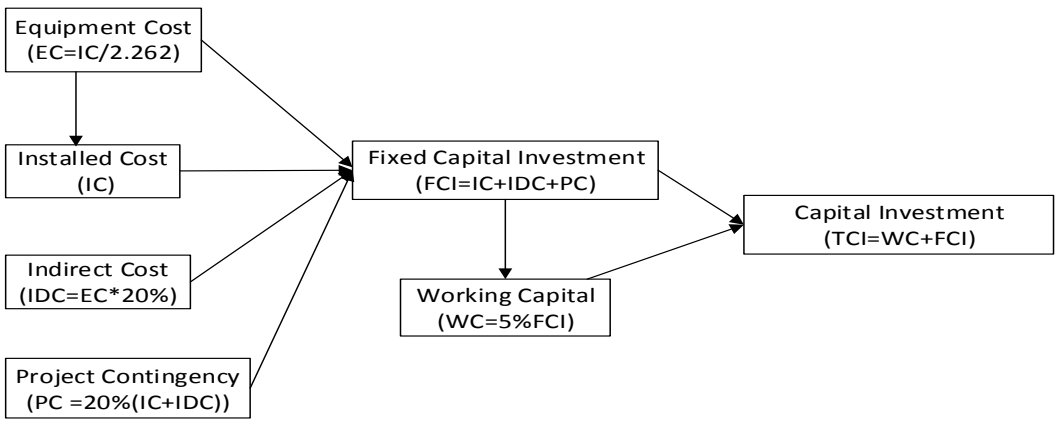

Figure 6.2.: Capital investment estimation methodology (adapted from Shemfe et al., 2015)

Indirect cost (IDC), which includes design and engineering costs and contractor's fees, is taken as 20 % of purchased equipment cost (PEC). Project contingency (PC) is taken as 20 % of the sum of Installed Cost (IC) and indirect costs (IDC). Fixed Capital Investment (FCI) is estimated from the sum of IC, IDC and PEC. The capital investment (CI) is estimated from the summation of working capital (5% of FCI) and FCI.

6.3.1 Installed equipment costs

Equipment cost estimation and sizing was carried out in Aspen Process Economic Analyser V8.2 (APEA) based on Q1. 2016 cost data. APEA maps unit operations from Aspen Plus flow sheet to equipment cost models, which in turn size them based on relevant design codes and estimate the Purchased Equipment Costs (PEC) and Total Direct Costs (TDC) based on vendor quotes. The installed capital cost of specialized unit process such as the metathesis and hydroformylation isothermal reactors was obtained from Aspen Plus™ and Cost Tables given by Turton et al. (2012). The costs of the OSN membrane equipment that cannot be estimated from APEA are estimated from supplier costs reported by Evonik Industries (2015) as basis for estimation. The exponential scaling expression is used to determine the new cost based on the new size or other valid size related characteristics as shown in Appendix D.

In the estimation of equipment cost a variety of sources were used, hence, the equipment costs were derived based upon different cost years. In this case cost indices can be used for estimating the escalation of costs over the years. Several indices are available to the process engineer. The Nelson–Farrar Refinery Cost Index (NFRCI) published in the Oil and Gas Journal is widely used in the oil and gas industry. The Marshall and Swift equipment cost index (M&S) is intended for the wider process and allied industries (chemicals, minerals, glass, power etc.). The Chemical Engineering Plant Cost Index (CEPCI) was used in this work.

The best known process plant cost index worldwide is the CEPCI, which has appeared every month in the publication Chemical Engineering since 1963 (Mignard, 2014). According to The Institution of Chemical Engineers (2000), the relative lack of local and specialised cost indices for the process industries amongst the countries in the world might explain its widespread

adoption. The dominance of the United States dollar (US $) as an international currency has also favoured the use of an index based in the US (Mignard, 2014). Therefore, all capital costs were adjusted with the CEPCI to a common basis period April 2016 (Chemical Engineering, 2016). Table 6.2 is a list of the basic equipment cost for the investigation of capital investment for process scenarios A and B.

Table 6.2.: Basic equipment list

Scenario A		Scenario B		Est. Method
Equipment Unit	Instal. Cost ($ M)	Equipment Unit	Instal. Cost ($ M)	
Hydroform. Rctr.	60.71	Hydroform. Rctr	61.32	Guthrie, (1974)
Metathesis Rctr	2.60	Metathesis Rctr.	2.60	Guthrie, (1974)
Ethylene flash	0.13	Ethylene flash	0.13	Aspen Plus™
C8 column	0.20	C8 column	0.20	Aspen Plus™
OSN (**HGr-2**) Stage 1 Stage 2 Stage 3	 2.793 2.155 1.803	OSN (**HGr-2**) Stage 1 Stage 2 Stage 3	 2.793 2.155 1.803	Evonik Industry & (6/10)'s Rule details in Appendix A
3-phase flash drum	0.161	2-phase flash drum	0.161	Aspen Plus™
	-	OSN (**Rh-TPPTS**) Stage 1 Stage 2 Stage 3	 2.612 2.013 1.753	Evonik Industry & (6/10)'s Rule details in Appendix A
Syngas Compr	2.37	Syngas Compr	2.37	Aspen Plus™
C14 column	0.24	C14 column	0.20	Aspen Plus™
Product column	14.76	Product column	14.76	Guthrie, (1974)

Figure 6.3 shows a comparison of the installed equipment costs for the two process scenarios.

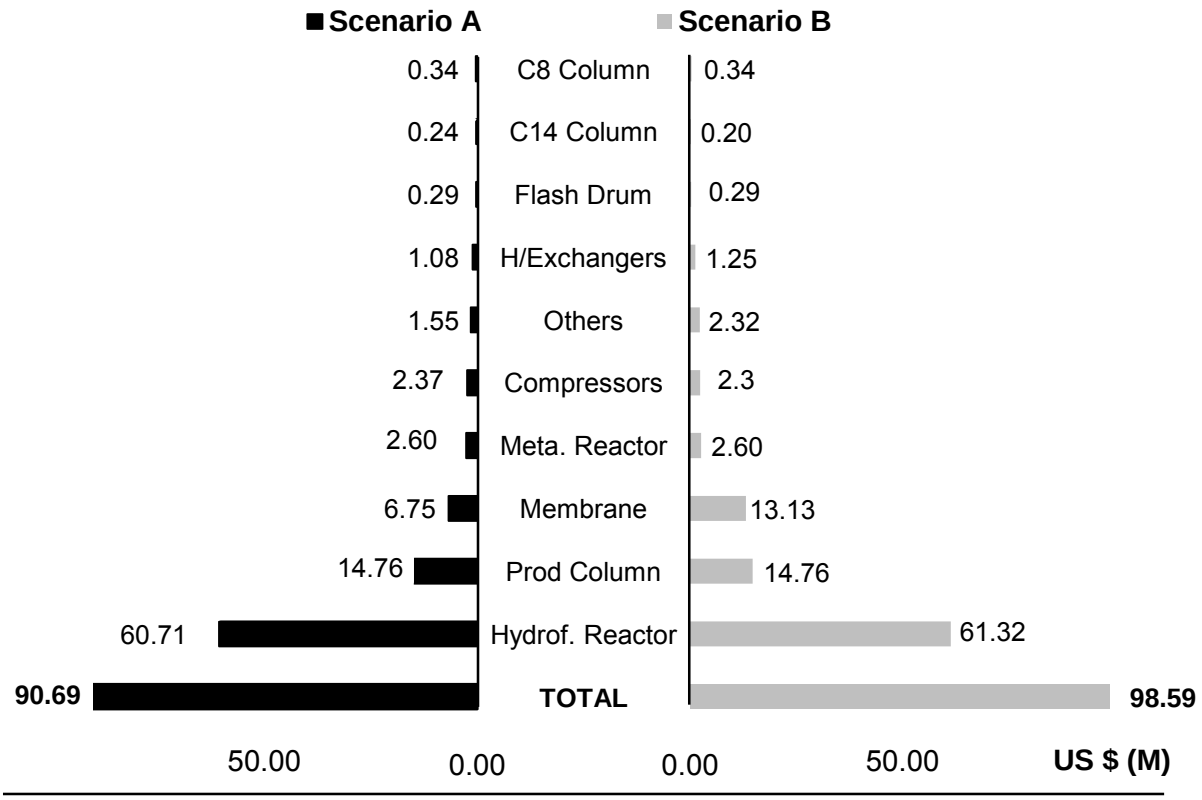

Figure 6.3.: Equipment cost structure for process scenario A and B

It could be shown from Figure 6.3 that the hydroformylation reactor had the highest installed cost followed by the product column, the membrane stage and metathesis reactor. The high cost of hydroformylation reactor could be attributed to the material of construction requirement as a result of high operating pressures and the bigger volumes as a result of liquid-gas phase reaction. The total capital investment for scenario A was estimated as $ 182 M, which was the lowest, compared to scenario B with $ 186 M.

6.4 Operating costs (OC)

Operating expenses occur annually and are characterized as either fixed or variable. Fixed operating expenses are constant expenses and independent of production levels. Variable

expenses are not constant and are proportional to the levels of production. Each type of expense is explained in the following section.

6.4.1 Fixed operating costs (FOC)

Fixed operating costs recur every year regardless of the amount of finished product. These expenses include insurance, taxes, and maintenance and plant staff salaries. For a new product or process, most costs components of product cost are not accurately known and experience based order of magnitude estimates are commonly used (Turton et al., 2012). Fixed operating expenses were estimated from capital expenses based on heuristics in the literature and personal experts familiar with process. A 10 % of OC was included on top of these estimates in a manner similar to the general expenses to account for overhead costs. Figure 6.4 shows the methodology used to summarise the fixed operating expenses.

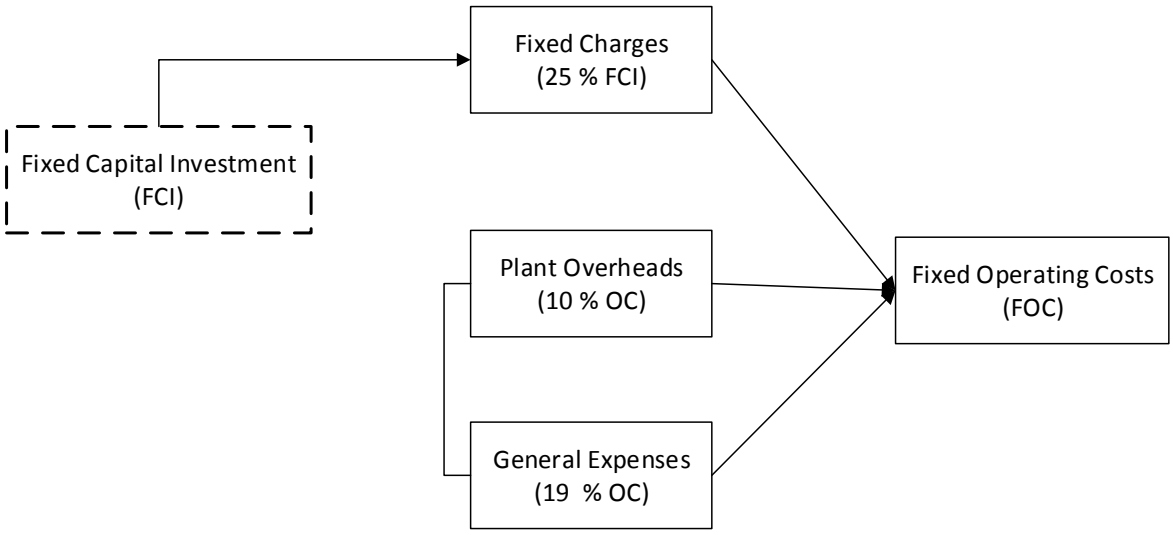

Figure 6.4.: Methodology for determination of fixed operating cost (FOC)

6.4.2 Variable operating expenses (VOC)

Variable operating expenses depend on the amount of production at the facility. For example, if the facility cuts its production rate in half, then the variable operating expenses would be exactly one half as expensive because producing less products requires less material and

energy. The expenses include utility costs, such as electricity, boiler feed water, solvents and raw materials such as 1-octene and syngas.

(i) Catalysts costs

Catalysts have a finite lifetime and need to be replaced or regenerated periodically. Initial catalysts expenses were calculated from (Van der Gryp et al., 2012 and Haumann et al., 2002b) for the standard metathesis and hydroformylation reactors. The operating costs were analysed based on costs for not-retained (make-up) quantities. Table 6.3 shows the raw material and product prizes.

Table 6.3.: Raw material costs

Variables	Description	References
2-hexyl-nonanal	$ 150,00 /kg (bulk)	Alibaba (2016)
1-octene	$ 1.30/kg	Sasol chemicals (2016)
7-tetradecene	$ 35.50/kg	Alibaba (2016)
HGr-2 catalyst	$ 28 746.00/kg	Alibaba (2016)
HGr-1 catalyst	$ 46 533.00/kg	Alibaba (2016)
Gr-1 catalyst	$ 6 720.00/kg	Alibaba (2016)
Gr-2 catalyst	$ 19 600.00/kg	Alibaba (2016)
2-hexyl-nonanal	$ 150,00 /kg (bulk)	Alibaba (2016)
7-tetradecene	$ 35.50 Bulk Price/kg	Sasol chemicals(2016)
Rh catalyst	$ 120 000.00 Bulk Price/kg	kitco.com (2016)
Bulk syngas from gasifier	$ 0.03 Bulk Price/kg	Piet et al. (2014)
MarlipalO13/80	$ 29.00 Bulk Price/kg	Sasol chemicals (2016)

(ii) OSN membrane operating cost

Concerning membrane module cost parameters, a medium membrane price/stability factor of \$ 500/m^{2}yr (Schmidt et al., 2014). This represented a unit cost of \$ 1000/m^2 with a stability of two years due to uncertainties in both OSN membrane lifetime and large-scale fabrication costs (Schmidt et al., 2014).

The total variable costs for the two process scenarios were \$ 130.22 per kg of 2-hexyl-nonanal and \$ 129.80 per kg 2-hexyl-nonanal for Scenario A and Scenario B respectively. Although the variable costs increased with additional OSN membrane unit in scenario B, (as a result of costs membrane replacement), the additional benefit of recovery of expensive **Rh-TPPTS** catalyst led to an overall lower total variable costs. Moreover, it can be seen from Table D.10 in Appendix D that the total variable costs were influenced mostly by raw materials costs. In order to compare individual cost parameters which contributes towards raw material costs, the raw material costs were further broken down as shown in Figure 6.5. Figure 6.5 shows a comparison of variable operating costs for the two process scenarios A and B.

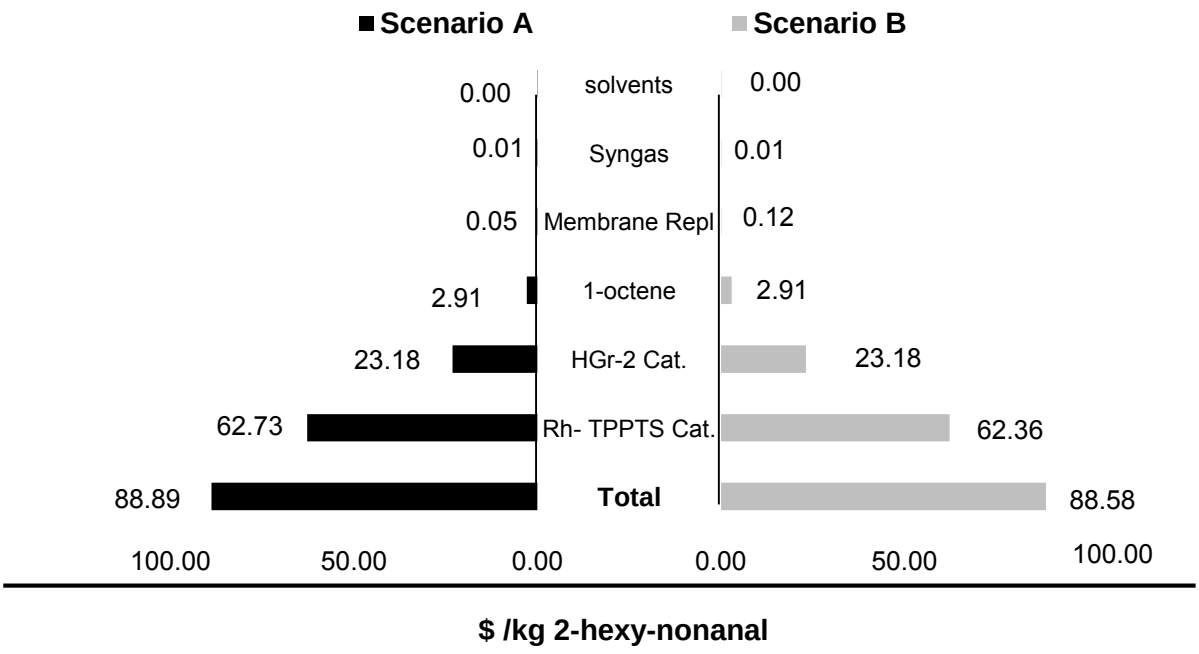

Figure 6.5.: Comparison of raw material costs of process Scenarios A and B

It could be shown from Figure 6.5 that the **Rh-TPPTS** catalyst followed by **HGr-2** catalyst followed by 1-octene feedstocks had the most significant contribution towards raw material costs. The high catalyst loading required for hydroformylation of internal alkenes has a major influence towards **Rh-TPPTS** catalyst cost. This could also be attributed to the high cost of Rh-metal on the global market. Hence, in order to reduce operating costs in such scenarios, catalyst recovery techniques especially OSN membrane process must be seriously considered.

It could be shown from Figure 6.5 that the benefits of OSN membrane (Scenario B) outweighs liquid multiphase system (scenario A). Although the use of OSN membrane process brings with it additional costs such as membrane replacement (membrane stability), it could be shown that the overall operating costs were less than that obtained for liquid multiphase system. The results of **Rh-TPPTS** catalyst loss for scenario A using liquid multiphase system were also compared to literature results. Sharma (2009) investigated the rhodium loss in the microemulsion by simple phase separation and observed rhodium loss in the range of 0.6-6 ppm. Fang (2009) reported **Rh-TPPTS** recovery rate equivalent to 560 ppb in crude product stream when Rh concentration in the reactor is 280 ppm, in which the yearly loss of Rh for a 200 kton production plant was about 118 kg. According to Fang (2009), the 118 kg loss of **Rh-TPPTS** accounted for 3.5 million dollars at an assumed Rh price of $30,000/kg. Sharma and Jasra (2015) further highlighted that the leaching of 1 ppm rhodium per kg of product from a 400 000 ton per annum plant may result into the financial loss of several million dollars. Weise and Obst (2006) also observed that for a liquid multiphase system, a loss of only 1 ppm (1 mg/kg of product), would led to a loss of $ 32 million per year on the year 2006 Rh price basis ($ 80 000/kg) for a world scale 400 000 ton per year plant. Haumann et al. (2002) also confirmed that with **Rh-TPPTS** losses after phase separation as low as 1 ppm, for a 100 000 tonnes per year production plant will result in $ 40 million losses per year.

6.4.3 Effect of production capacity on profitability

The challenge of liquid multiphase system could be the increase in **Rh-TPPTS** loss as a result of an increase in production tonnage. Literature results also indicates that total **Rh-TPPTS** losses are a function of production rate. A promising separation technique in **Rh-TPPTS** could be the use of OSN membrane process. Table 6.4 is a summary of the comparison of literature results of **Rh-TPPTS** catalysts losses in liquid multiphase systems.

Table 6.4.: Comparison of literature results on Rh-TPPTS catalyst loss in microemulsion

Source	Product	Ton per yr.	Rh loss (ppm)	Cost of Rh $ (M)
Haumann et al. (2002)	n-tridecanal	100 000	1,00	40
Fang (2009)	n-nonanal	200 000	0,56	3,5
Sharma and Jasra (2014)	Butyl-aldyhyde	400 000	1,00	40
Wiese and Obst (2006)	n-nonanal	400 000	1,00	16
Current Study	2-hexylnonanal	10 000	1,02	3,73

According to the current study, 1.02 ppm **Rh-TPPTS** catalyst was leached with the crude product when 1:2 500 ratio of 7-tetradecene to **Rh-TPPTS** is available in the reactor. The yearly loss of **Rh-TPPTS** for a 10 000 ton per annum production plant was 31 kg accounting for $ 3.7 million at an assumed **Rh-TPPTS** price of $ 120 000/kg. Hence, the make-up Rh catalyst cost per kg of 2-hexyl-nonanal was calculated as;

$$= \frac{1\ kg\ crude\ product\ x\ 1{,}02\ ppm\ x10^{-6} x \$120\ 000/(kg\ Rh)}{1\ kg\ crude\ product\ x\ 0.7\ kg\ 2-hexyl-nonanal/kg crude\ product}$$

$$= \$0.17/kg\ 2-hexyl-nonanal$$

Hence, compared to OSN membrane process of scenario B the cost of make-up **Rh-TPPTS** catalyst per kg of 2-hexyl-nonanal product resulted in an additional increase in operating costs.

6.5 Revenue

In this study only the sales of 2-hexyl-nonanal product were considered. The ethylene product stream was not considered since initial design considered ethylene as a purge stream and did not consider vapour recovery system. The ethylene purge stream will be used as fuel instead. The isomeric product stream was treated as waste.

6.6 Profitability analysis

The knowledge of the economic viability/feasibility of a project is a prerequisite tool investors look out for before investing money into any project (Turton et al., 2012). Economic viability of the two scenarios A and B modeled in this study were therefore evaluated through a DCF method. A DCF analysis was used to compare the two process scenarios based on the different profitability criteria of NPV, IRR % and PBP.

6.6.1 Discounted cash flow (DCF)

A DCF determines the cash flow obtained in nth year but it also includes the net present value (NPV) of those cash flows over the entire economic life of the project. The construction period is estimated to be two years (24 months), which includes engineering, procurement and construction phases. Construction costs were distributed between first and second years with 60 % and 40 % of the TCI for each year, respectively. The plant operates for 8 000 hours per year, which is equivalent to a 90 % on-stream capacity. The net present value was calculated in the last year of the construction period (year n).

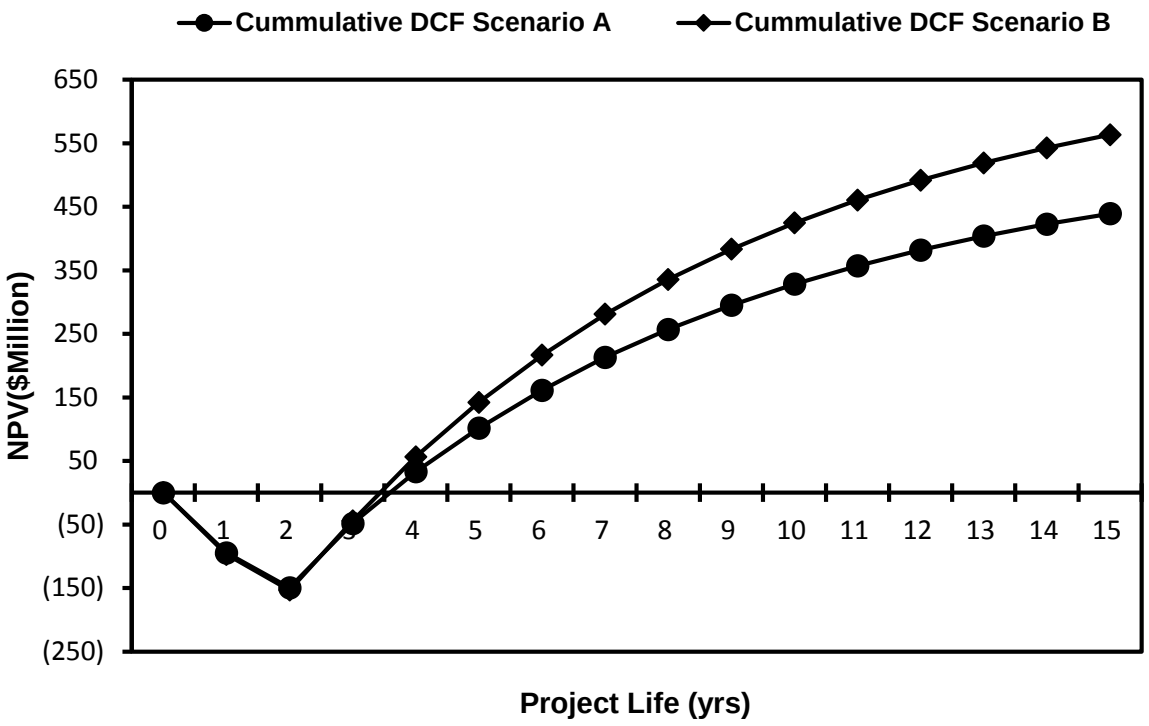

Figure 6.6.: DCF diagram of Scenarios A and B if total capacity is installed at production start-up.

The graph of CDCF diagram of Scenarios A and B if total capacity is installed at production start-up is shown in Figure 6.6. Figure 6.6 clearly shows the benefit of the OSN membrane process for catalyst recovery. The NPV for scenario A and scenario B were $ 439 M and $ 563 M after 15 years respectively. The OSN membrane process design lead to an NPV improvement of $ 124 M compared to liquid multiphase process. It can be seen from Figure 6.6 that the two process scenarios had almost similar PBP of 3 years. The IRR was 58.7 % for scenario A and 81.3 % for scenario B. The high IRR % for scenario B was a direct result of the reduction in raw material, especially **Rh-TPPTS** catalyst, consumption. As investment costs are slightly different for the two process alternatives present value index (PVI) has to be used to allow for a meaningful statement. PVI is the quotient of the present value of the cumulative cash flows and the present value of the investment. The result represents the profitability of an investment. The PVI for process scenario B is 0.67 while for scenario A is 0.57. As the difference in investment cost is small it is obvious that scenario B (OSN membrane) is more economic compared to process scenario A (liquid multiphase system).

6.6.2 Sensitivity analysis

To evaluate the relative importance of input parameters over the project's economic results, a sensitivity analysis was performed. Sensitivity analysis measured the impact on project out-comes when input values about which there was some uncertainty were changed. In this case, the sensitivity analysis was performed over the main economic parameters of the model: the commercialization price of 2-hexyl-nonanal, the cost of **Rh-TPPTS**, the cost of **HGr-2**, the cost 1-octene and the income tax. A change in the parameters of ± 25 % in relation to the typical market values was considered: Taxation rate-28 %, input **HGr-2**- $ 26 762/kg, **Rh-TPPTS**- $ 120 000/kg, 2-hexyl-nonanal $ 150/kg and 1-octene-$ 1.92/kg. The analysis was performed for scenario A (liquid multiphase system) and scenario B (OSN membrane process). The results are presented in Figure 6.7.-6.11.

6.6.2.1 Sensitivity of NPV

The horizontal axis in Figure 6.7 and Figure 6.8 shows the percentage change of the parameter in relation to the base value. The vertical axis shows the NPV result. It can be observed that all curves intersect at the same place, which is the standard behaviour, when all variables are replaced with their base values.

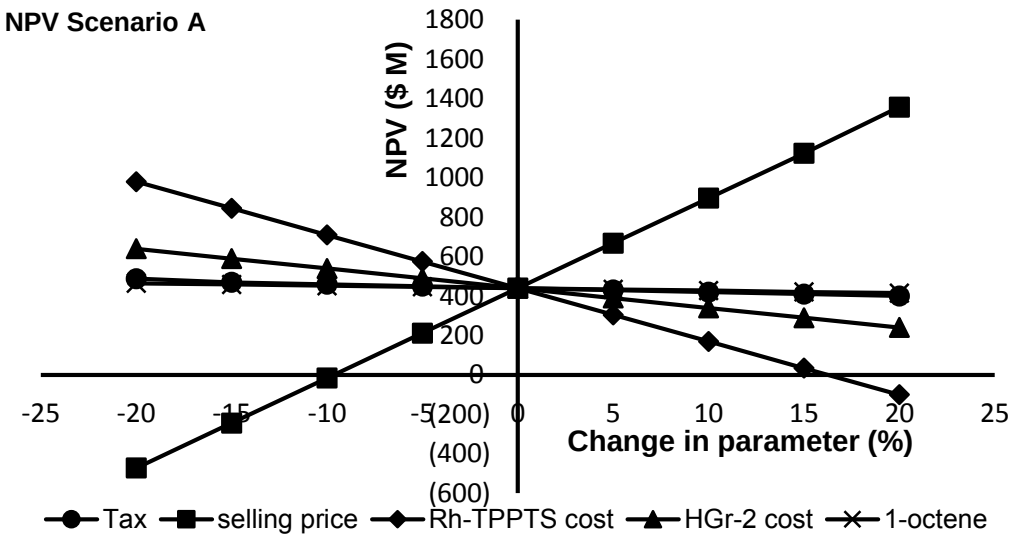

Figure 6.7.: Sensitivity of NPV to process scenario A variables

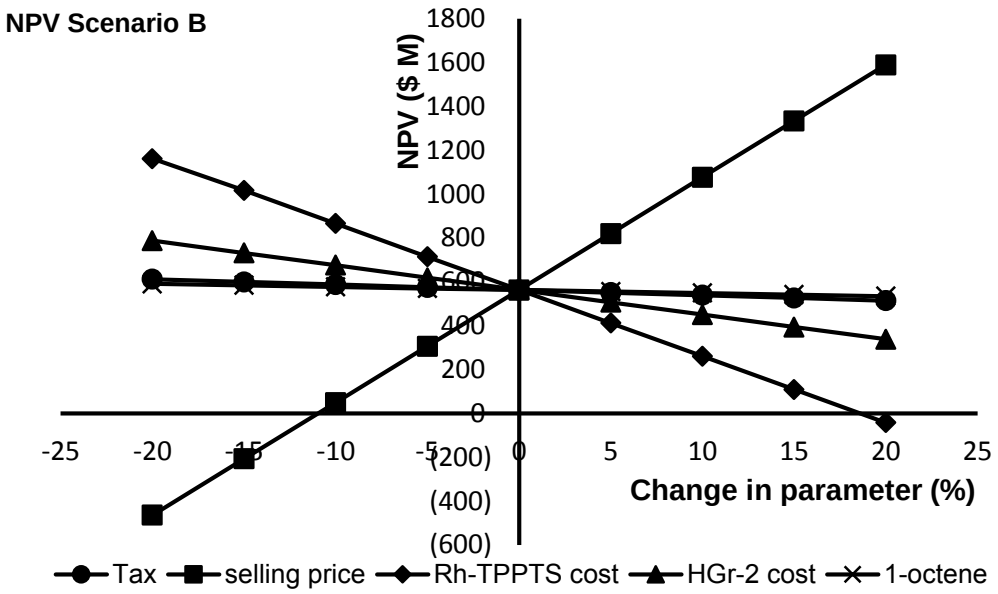

Figure 6.8.: Sensitivity of NPV to process variables

The main aspect to take into consideration in Figure 6.7 and Figure 6.8 is how the curves behave regarding the variations in the horizontal axis. The curves that have higher gradient, either positive or negative, deserve special attention, because a small change in the expected value will be reflected as large changes of the NPV. For both scenarios A and B it was observed that the curves with greater gradient were 2-hexyl-nonanal selling price, **Rh-TPPTS** and **HGr-2** catalysts, which obviously meant that these parameters have great influence on the project viability, because their variation had a great influence over the investment return.

6.6.2.2 Sensitivity of IRR %

In the same way, the horizontal axis in Figure 6.9 and Figure 6.10 shows the percentage change of the parameter in relation to the base value. The vertical axis shows the IRR % result. It can be observed that all curves intersect at the same place, which is the standard behaviour, when all variables are replaced with their base values.

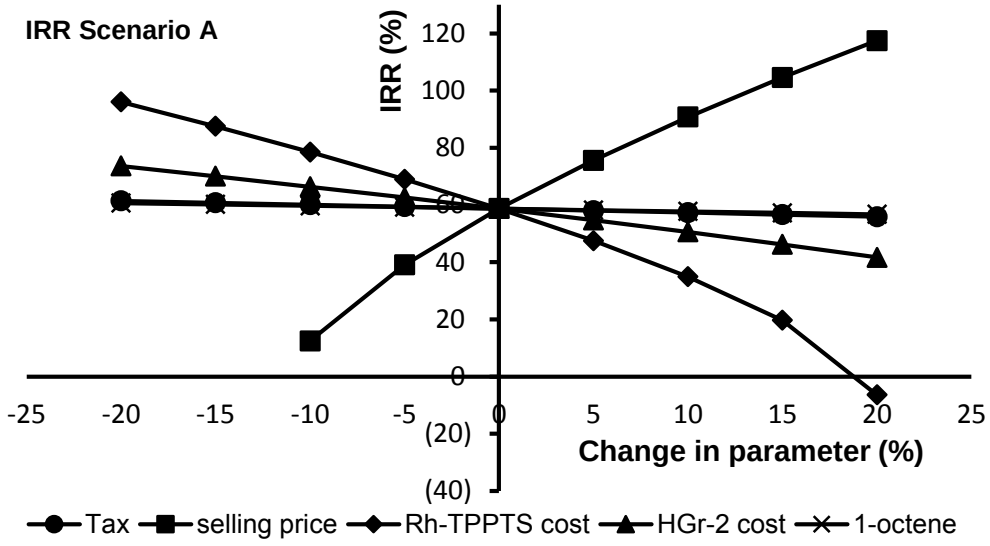

Figure 6.9.: Sensitivity of IRR to process variables (scenario A)

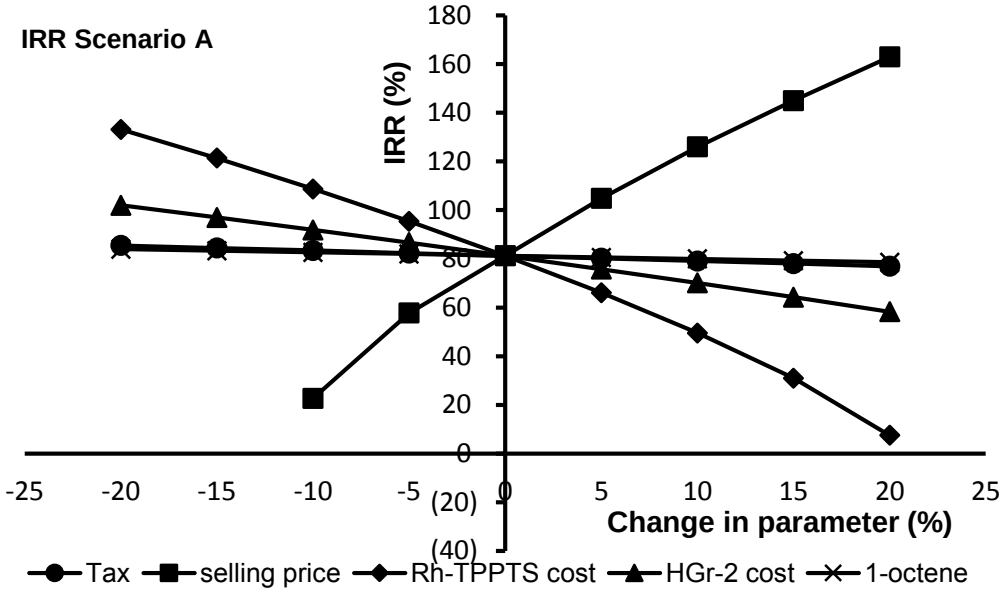

Figure 6.10.: Sensitivity of IRR to process variables (scenario B)

As shown in Figure 6.10, the product selling price, **Rh-TPPTS** cost and **HGr-2** cost have the greatest impact on IRR in both scenarios A and B. To achieve an IRR % greater than 15 % in scenario A, the product selling price should not be 5 % lower than that of the baseline ($ 150/kg), or at least one of the **Rh-TPPTS** cost, **HGr-2** cost and 1-octene cost must not increase

above $ 138 000/kg, $ 30 776.3/kg and $ 2.22/kg (15 %), from the base line costs respectively. In a similar manner, to achieve an IRR % greater than 15 % in scenario B, the product selling price should not be 10 % lower than that of the baseline ($ 150 /kg), or at least one of the **Rh-TPPTS** cost, HGr 2 cost and 1-octene cost must not increase above $ 138 000/kg, $ 30 776.3/kg and $ 2.22/kg (15 %), from the base line costs respectively. A ± 20% range in Rh-TPPTS cost results in an IRR % range of 96- -6.3 % for scenario A and 133-7.5 % in scenario B. A ± 20% range in 1-octene cost results in an IRR % range of 60.68-56.75 % for scenario A and 83.98-78.75 % in scenario B. A ± 20% range in taxation rate results in an IRR % range of 61.45-55.92 % for scenario A and 85.52-76.96 % in scenario B.

The high sensitivity to cost of **Rh-TPPTS** catalyst is expected because of the high cost of Rh-metal and **Rh-TPPTS** catalyst loading required during the hydroformylation of internal alkenes (Haumann et al., 2002b). The low sensitivity to 1-octene was expected as the process recycles the unreacted 1-octene. The change in cost price of 1-octene feed has little effect on the profitability of this process.

6.7 Economic analysis summary

Table 6.6 summarizes the key economic results, which are the capital requirements, 2-hexyl-nonanal price and the respective project internal rate of returns. The present values indices (PVI) were included to allow comparison of the economic viability of the different plant configurations.

Table 6.6.: Summary economic analysis results ($/kg) [a] Cost per kg of 2-hexyl-nonanal

Scenario	TCI ($ millions)	Min. S/Price ($/kg)[a]	NPV ($ millions)	IRR % %	PBP (Years)
Scenario A	181.6	142.12	439	58.75	3
Scenario B	186.2	140.12	563	81.3	3

In this work, economic benefit of OSN membrane technology was demonstrated. The improvement in catalyst rejection and recycling of **Rh-TPPTS** catalyst lead to a reduction in **Rh-TPPTS** catalyst consumption of nearly $ 4 million per annum with nearly the same investment costs compared to conventional process for **Rh-TPPTS** catalyst recovery (Scenario A). The two scenarios proved to be economic at the set production rate. The membrane process led to an NPV improvement of $ 124 M dollars at the end of 15-year project life. Catalyst loss in scenario A utilising conventional **Rh-TPPTS** catalyst recovery method is a factor of production rate hence, process becomes riskier with high production tonnages demanding further recovery of **Rh-TPPTS** catalyst.

The Aspen In-Plant Cost Estimator has been used for over 30 years in commercial plants and engineering designs, and provides more accurate estimation (Seider et al., 2004). Aspen In-Plant Cost Estimator provides specifications for detailed design, estimation and economic data, allowing quick modifications of the process equipment and sensitivity analysis. In this work, a three step targeted model validation step, process modelling and optimisation design work flow for OSN processes was developed and implemented accounting for the currently limited database and understanding in OSN technology. The optimisation results were compared to literatiure results by Scmidt et al. (2014), who also used a cascade approach recommended by Seifert et al. (2014). Hence, the results of this study are very important for the understanding of homogeneous catalyst system especially utilising OSN membrane process.

6.3 References

Biegler L, Grossmann I, Westerberg A, Systematic Methods of Chemical Process Design, Prentice-Hall: Upper Saddle River, 1997.

Bortoluzzi G, Gattia M, Sognia A, Consonnia S. Biomethane production from agricultural resources in the Italian scenario: techno-economic analysis of water wash. Journal of Chemical Engineering (2014) **37**

Chemical Engineering Plant Cost Index (CEPCI). tekim.undip.ac.id/download/pci_20122016.pdf [accessed 22.04.2016.].

Colin A. Houston & Associates, Inc. announces a new multiclient study ALPHA-OLEFINS - WORLD MARKETS, 2005-2015

Cucchiella F, D'Adamo I, Gastaldi M. Profitability analysis for biomethane: a strategic role in the italian transport sector. International Journal of Energy Economic Policy (2015) **5** 440–9.

Deloitte Texation and investment in South Africa (2015) http://www.deloitte.com/tax

Douglas, J. M. Conceptual design f chemical process. International Edition (1988) McGraw-Hill Chemical Engineering Series. Pp 15-89 ISBN 0-07-017762-7

Evonik, 2014; http://www.design-meets-polymers.com/sites/dc/Downloadcenter/Evonik/Product/DuraMem-PuraMem/brochures/duramem-and-puramem---general-brochure.pdf

Fang, J. Towards a Benign and Viable Rhodium Catalyzed Hydroformylation of Higher Olefins: Economic and Environmental Impact Analyses, Solvent Effects and Membrane-based Catalyst Separation (2009) (Masters of Engineering Thesis).

First National Bank. 2016. Rates view [Online]. Pretoria. Available: https://www.fnb.co.za/rates/cRatesView.html?productGroup=Indicators&productNames=SA_Indicators [Accessed 16 March 2016].

Gary, G., Handwerk, J., Petroleum refining technology and economics, CrC press, Boca raton, 5 edition, (2007) Don W.

Green, D, W; Robert H. Perry: Perry's Chemical Engineers' Handbook, Eighth Edition. CAPITAL COST ESTIMATION, McGraw-Hill Professional, (2008)

Haumann, M, Herbert, Koch H., Hugo, P., Schomacker, R. Hydroformylation of 7-dodecene using Rh-TPPTS in a microemulsionApplied Catalysis A: General **225** (2002b) 239-249

Jana, A.K. Process simulation and control using ASPEN , PHI Learning Pvt. Ltd Technology and Engineering (2012) ISBN 8120345861

Lee, L.S, Liu, H.Y, Horng, S.S. Solubility of ethylene in 2,2,4-trimethylpentane and 1-octene mixture. Journal of the Chinese Institute of Chemical Engineers **39** (2008) 49–57

Marsh, P. The Choice Between Equity and Debt: An Empirical Study. The Journal of Finance, **37** (1982)121-144.

Mignard, G. Correlating the chemical engineering plant cost index with macro-economic indicators, chemical engineering research and design Journal of Chemical Engineering **9 2** (2 0 1 4) 285–294 http://dx.doi.org/10.1016/j.cherd.2013.07.022

Miremadi, M. Musso, H., Oxgaard., J, Chemical innovation: An investment for the ages, McKinsey on Chemicals May 2013

Neelis, M., Patel, M., Blok, K., Haije, W., Bach, P. Approximation of theoretical energy-saving potentials for the petrochemical industry using energy balances for 68 key processes. Energy **32** (2007) pp. 1104-1123doi:10.1016/j.energy.2006.08.005

Peters., M, Timmerhaus., K, Plant Design and Economics for Chemical Engineers, 5th Ed., McGraw-Hill: New York, 2003

Pohorecki, R, Bridgwater., J., M. Molzahn., M, Gani., Gallegos., C, Chemical Engineering and Chemical Process Technology - Volume (IV), Process Development, Modeling, Optimization, Control and Process Management EOLSS Publications, 30 Nov 2010

Schmidt P., E.L. Bednarz, P. Lutze, A. Górak, Characterisation of organic solvent nanofiltration membranes in multi-component mixtures: process design workflow for utilising

targeted solvent modifications, Journal of Chemical Engineering Science **115** (2014) 115–126.

Sharma S.K, Jasra., R.V, Aqueous phase catalytic hydroformylation reactions of alkenes Catalysis Today **247** (2015) 70–81

Shemfe, M.B., Gu, S., Ranganathan, P., Techno-economic performance analysis of biofuel production and miniature electric power generation from biomass fast pyrolysis and bio-oil upgrading. Fuel **143** (2015), 361–372.

Sinnot, R. K. Coulson and Richardson's chemical engineering: Chemical Engineering (2005) .Design. New York: Elsevier Butterworth-Heinemann.

Smith, R. Chemical process design and Integration. (2005) London: John Wiley and Sonsp.

South Africa Taxation and Investment. Wear and Tear or Depreciation Allowance. Interpretation Notes [Online]. Available: http://www.sars.co.za/home.asp?pid=5993# [Accessed 15 March 2016].

Steele, W.V., Chirico, R.D. Thermodynamic properyies of Alkenes (Mono-Olefins Larger than C4), IIT research Institute for Petrochemical and Enrgry Research 1992. http://encyclopedia.airliquide.com/Encyclopedia.asp?GasID=29

The Institution of Chemical Engineers, 2000. In: Gerrard, A.M. (Ed.), Guide to Capital Cost Estimating. Institution of Chemical Engineers, Rugby, UK.

Turton, R., Richard, C.,Wallace, B., Joseph, W., Debangsu, A., Bhattachar, B. Analysis, Synthesis, and Design of Chemical Processes Fourth Edition Copyright (2012) Pearson Education, Inc.

Turton, R., Bailie, R., Whiting, W., Shaeiwiz, J. (2009). Analysis, synthesis and design of chemical processes (3rd ed.). Printice Hall

Wiese, K.D, Obst., D, Catalytic carbonylation reactions, in: M. Beller (Ed.),Topics in Organometallic Chemistry, 18, Springer, Heidelberg, Germany, 2006, pp. 1–33.

CHAPTER 7: CONCLUSIONS & DIRECTIONS FOR FUTURE RESEARCH

"*Once the toothpaste is out of the tube, it's hard to get it back in*"

Harrold Robbins Haldeman

Overview

This chapter summarizes the work that has been presented in this thesis. Section 7.1 details the main findings of an optimal process of upgrading low value unique olefinic feedstocks from Fischer-Tropsch Synthol product stream to functionalised hydrocarbons for the manufacture of Geubert-type surfactants. Section 7.2 describes the main contributions of this work and finally Section 7.3 discusses recommendations for future research.

7.1 Main process findings

The metathesis reaction of low value unique olefinic feedstocks (C5-C9) from the Fischer-Tropsch process can be used an important tool to increase access to speciality chemicals. The detergent range linear internal alkenes (C10-C19) produced during metathesis of low value olefins can be functionalised during hydroformylation to produce intermediate feedstocks for manufacturing specialty surfactants, especially of the Geubert-type. The complete separation of highly expensive homogeneous catalysts employed during metathesis and hydroformylation reactions, from their post reaction mixtures has been identified as a major challenge to the commercialisation these technologies. This is particularly true when high catalyst loadings are necessary, as increased catalyst loadings will result in increased residual metal impurities in the final product. Besides relatively low acceptable metal content in pharmaceutical chemistry applications, residual metal species may cause isomerization, decomposition, or other undesirable side reactions in subsequent synthetic steps. Advances in development of very active and selective homogeneous based, yet stable catalysts now allow for the possible recovery and reuse by employing novel techniques such as organic solvent nanofiltration (OSN) membrane process.

Although Rh-based catalysts have been used commercially for the hydroformylation of short chain alkenes (C2-C5), it is seemingly impossible to use for higher alkenes (Cn > C5). The Rh-catalyst complex is often the component with lowest vapour pressure hence, decomposes at temperatures below the boiling point of the aldehyde product making catalyst separation and reuse difficult. Commercially, this separation problem is overcome by the use of water-soluble catalysts in aqueous-organic biphase systems. The aqueous biphasic approach is only applied to the hydroformylation of short chain olefins (C2-C5) because of the limited solubility of higher olefins in water resulting in rates that are simply too slow for the process to be commercially viable. The development of Rh catalysed processes, for the hydroformylation of long chain alkenes (C8-C20), therefore remains one of the biggest challenges in this area. The Rhodium catalysts system have not been commercialised for this reaction despite their

attractive features of milder operating conditions and higher selectivity to the desired linear aldehyde. Moreover, in Rh-catalysed hydroformylation processes, the exorbitant cost of Rh, has made it a requirement to achieve nearly total catalyst recovery and recycle.

This dissertation focused on the development of a process of metathesis of 1-octene from a Fischer-Tropsch Synthol product stream using Grubbs based precatalsysts. The 7-tetradecene produced was further functionalised to 2-hexyl-nonanal in a reaction with syngas in a microemulsion using **Rh-TPPTS** catalyst. Using the Douglas (1988), methodology to develop the metathesis and hydroformylation processes optimum conditions were evaluated using economic potentials calculated at each decision level. In the metathesis process, **HGr-2** precatalyst was selected as the best catalyst and the optimum conversion for 1-octene and **HGr-2**/1-octene molar ratios were found to be 0.5 and 10 000 respectively. These conditions were then used to develop an Aspen Plus™ model in which optimum conditions of pressure and temperature were obtained on the basis of selectivity or product distribution. The highest selectivity to 7-tetradecene was found to be 98.28 % at 50 ^{o}C and 2 bars. In developing the hydroformylation process and using the condition of highest economic potential the optimum 7-tetradecene conversion was found to be 0.35 at 120 ^{o}C and 60 bars. Two process scenarios utilizing liquid multiphase system and organic solvent nanofiltration membrane (OSN) to recover **Rh-TPPTS** catalysts were developed and investigated in Aspen Plus™. Using Aspen Plus™ to develop the hydroformylation reactor, optimum conditions of pressure and temperature were found to be 160 ^{o}C and 40 bars. The application OSN membrane technique to recover **HGr-2** and **Rh-TPPTS** catalysts was demonstrated and 99.96 % recovery of catalysts achieved. The **Rh-TPPTS** catalyst leached in product was reduced to 1 ppm using liquid multiphase system.

A techno-economic study of the two process scenarios was conducted and key economic indicators such as NPV and IRR % were used to select the most profitable process. The process scenario B which utilises organic solvent nanofiltration (OSN) membrane process to recover **Rh-TPPTS** was the most profitable configuration compared to the liquid multiphase

system. The most sensitive parameters were 2-hexyl-nonanal selling price, **Rh-TPPTS** catalyst cost, **HGr-2** catalyst cost and 1-octene costs. However, challenges to the process are separation and purification of aldehyde product from isomeric mixtures. There is a potential for reducing separation costs by developing highly selective Rh-based catalyst systems.

7.2 Main contributions

(a) Conceptual process for upgrading low value olefins from Fischer-Tropsch process

In this dissertation the Douglas's (1988) methodology of process synthesis which generates EP values at each of the five decision levels of process development was applied to develop a conceptual process of upgrading low value 1-octene to 2-hexyl-nonanal. Key design parameters such as effect of conversion, reactor and column configuration were evaluated in order to develop the most economic process of upgrading 1-octene to 2-hexyl-nonanal. The impact on cost of OSN membrane stage at different conversions were evaluated for both metathesis and hydroformylation processes. The EP values for product purification confirmed that in order to reduce separation equipment costs for product purification it is important to develop a catalyst with high selectivity. Two conceptual process scenarios for the upgrading of low value 1-octene feedstock from Fischer-Tropsch Synthol product stream to high value functionalised aldehydes were presented. The generic conceptual process developed in this study could be extended to other low value C5, C6, C7, and C9 olefinic feedstocks from the Fische-Tropsch process.

(b) Detailed Aspen Plus™ simulation

The optimum process conditions for a process upgrading low value 1-octene olefinic feedstocks from a Fischer-Tropsch to 2-hexyl-nonanal were determinined with the aid of Aspen Plus™ simulator. The limited kinetic data from literature for the hydrofomylation of 7-tetradecene could be cited as a major challenge in comparing different kinetic models for the hydroformylation of 7-tetradecene. Aspen Plus™ models for the two candidate process scenarios A (liquid multiphase system) and scenario B (OSN membrane process) were developed to allow a quantitative comparison between the two process scenarios.

(c) Development of Aspen Plus™ OSN custom models of HGr-2 and Rh-TPPTS

The successful recovery of **HGr-2** and **Rh-TPPTS** catalysts using OSN membrane process was demonstrated using the developed custom models in Aspen Plus™. The results obtained were comparable to literature data confirming that OSN membrane process for recovery of species can be successfully up scaled and commercialised for highly sensitive homogeneous **HGr-2** and **Rh-TPPTS** catalysts. The use of OSN in recovering **Rh-TPPTS** catalyst resulted in a catalyst cost saving of nearly $ 4 million per annum. Overally, OSN membrane process has a potential of improving the profitability of the process by reducing catalyst loss. Despite having a slightly higher capital cost, the membrane process (scenario B) offers the best solution to recovery and reuse of homogeneous catalysts.

(d) Techno-economic analysis

The key economic indicators, net present value (NPV), internal rate of return (IRR) and payback period (PBP) were evaluated for the two process scenarios. A sensitivity analysis was performed for the main economic model parameters: the selling price of 2-hexyl-nonanal, **Rh-TPPTS** cost, **HGr-2** cost, 1-octene cost and tax rate, results of such evaluation show that, selling price of 2-hexyl-nonanal, **Rh-TPPTS** cost, **HGr-2** cost have great influence, because their variations have a decisive influence on the NPV and IRR %. Further work can also include the effect of plant capacity on profitability especially using liquid multiphase process, according to literature Rh-TPPTS cost contribution to the total operating costs is directly proportional to the plant capacity. It was proposed that process scenario B (OSN membrane process) has an economic benefit for all the two cases in the plant sizes for the 10 000 t/yr. considered in this study.

7.3 Directions for future research

The limitations of the research presented in this thesis and the related directions for future work are now discussed.

7.3.1 Extending this research

The development of a data bank of kinetic models for the metathesis of different olefinic feedstocks and hydroformylation of long chain internal alkenes considering different commercially available catalysts cannot be over emphasised. Due to challenges of separation of isomeric aldehydes, the development of highly selective catalysts has been emphasised especially during hydroformylation of internal alkenes (Muller et al., 2015). In general, isomer separation is difficult to achieve. The question should of course be asked if the effort to separate is truly worth it. Moreover, membrane selection has been on a single criterion; ‘to have high retention of the catalysts’. It should be probably better adapted to look for a compromise between high retention of the catalyst and the high transmission of product species in order to limit the number of filtration steps.

APPENDIX

The appendix is divided into several chapters (A, B, C and D). This is done to ease the search for tables or figures from the respective chapters. In Appendix A.: Chapter 3 the literature results concerning metathesis, hydroformylation catalyst recovery processes are given. In Appendix B: Chapter 4 results and information concerning the Douglas (1988) methodology for process development is presented. In Appendix C: Chapter 5 the Aspen Plus™ process simulation flow sheets for the different sections of process models are presented. Secondly, a summary of Aspen Plus™ codes used in developing models are also given. In Appendix D: Chapter 6 the economic model parameters, initial conditions, solver parameters, and additional results are given.

Appendix A: Chapter 3: Literature review

Table A.1: Summary of 1-octene metathesis and high efficiency commercial catalysts, product distribution at optimal conditions ([a], C8/Ru mol ratio)

Author, Year	Description of Investigation	Pre-catalyst	C8[a] (mol/mol)	T (°C)	$X_{1\text{-}C8}$ (%)	PMP (%)	IP (%)	SMP (%)	S (%)
2003									
Lehman et al.	Olefin isomerization promoted by olefin metathesis catalysts	**Grubbs 2nd**	1000	60	86	54.1	9.4	2.7	81.7
		Schrock	1000	45	-	99.9	0.01	-	99
		Grubbs 1st	1000	50					
2006									
Jordaan et al.	Experimental and DFT investigation of the 1-octene metathesis reaction mechanism with the Grubbs 1 precatalyst	**Grubbs 1st**	1000	25	67	62	-	5	94.0
2009									
Van der Gryp	Separation of Grubbs-based catalysts with Nanofiltration (coupled reaction and separation)	**Hoveyda-Grubbs 1st**	5000	30	57.96	75.03	0.41	0.51	98.41
		Hoveyda-Grubbs 2nd	7000	50	65.86	64.48	0.25	0.87	98.28
		PUK-Grubbs 2nd	7000	50	25.21	24.79	0.29	0.47	97.01
Huijmans	Modelling and synthesis of Grubbs type catalyts with hamilable catalysts	**Hoveyda-Grubbs 2nd**	9000	60	-	93	0.1	5.1	94.8
		PUK-Grubbs	9000	60					
Boeda et al.	Phosphabicyclononane-Containing Ru Complexes: Efficient Pre-Catalysts for Olefin Metathesis Reactions	**Grubbs 1st**	9000	50	65	-	-	-	-
2010									
Motoboloi	Synthesis and modelling of imine derivatives as ligands for Grubbs type pre-catalysts	**Grubbs 1st**	9000	60	68	30.49	1.22	0.53	98
		Grubbs 2nd	9000	60	56	42	1.4	0.6	98
2011									
Xaba	Synthesis and modelling of Tungsten catalysts for alkene metathesis	**Schrock**	100	85	77	63.6	2.5	0.9	94.9
2012									
Van der Gryp et al.	Experimental, DFT and kinetic study of 1-octene metathesis with Hoveyda–Grubbs second generation precatalyst	**Hoveyda-Grubbs 2nd**	7000	60	64.48	68.60	0.24	1.01	98.00
2014	Improved Metathesis Lifetime: Chelating Pyridinyl-Alcoholato Ligands								
du Toit et al.		**Grubbs 2nd**	9000	35	-	80.6	0	3.7	96.1

Table A.2: Table Summary of Literature on Biphasic Hydroformylation of Long Chain alkenes (Temp[a] = upper critical temperature)

Year & Author	Description of Reaction system	Solvent system	Catalysts	Ligands	Temp[a]
1997 Bhanage et al.	Kinetics of Hydroformylation of 1-dodecene using homogeneous HRh(CO) (PPh,) 3 catalyst	Water/toluene	HRh(CO)(PPh3)3	TPPS	50
2002 Haumann et al.	Hydroformylation of 1-dodecene using Rh-TPPTS in a microemulsion	Water/ MarlipalO13/E*i*)	HRh(CO)2(TPP)2	TPPTS)	80
2003 Li et al.	Studies on 1-dodecene Hydroformylation in biphasic catalytic system containing mixed micelle	Water/ Triton X-100	RhCl(CO)(TPPTS)2	TPPTS	90
2005 Behr et al.	Selection process of new solvents in temperature-dependent multi-component solvent systems and its application in isomerising Hydroformylation (4-C8)	Ethylene carbonate/n-Dodecane/N-octyl-2-pyrrolidone propylene carbonate/n-Dodecane/N-octyl-2-pyrrolidone butylene carbonate/n-Dodecane/N-octyl-2-pyrrolidone	Rh(acac)(CO)2	Biphephos	125
2008 Behr et al.	Advances in thermomorphic liquid/liquid recycling of homogeneous transition metal catalysts (4-C8)	*N*,*N*-Dimethylformamide/*N*,*N*-dimethyl propylene urea/ *n*-decane *N*,*N*-Dimethylformamide, *N*/methylpyrrolidone/*n*-decane Methanol/*N*,*N*-dimethyl propylene urea/*n*-decane	Rh(acac)(CO)2	Biphephos	-

Table A.2 (cont'd): Summary of Literature on Biphasic Hydroformylation systems for Long Chain alkenes

Year & Author	Description of reaction system	Solvent System	Precatalyst	Ligand	Temp[a]
2012					
Schafer et al.,	Hydroformylation of 1‑Dodecene in the Thermomorphic Solvent System Dimethylformamide/Decane. Phase Behaviour−Reaction Performance−Catalyst Recycling	N,N-Dimethylformamide (DMF)/decane	Rh(acac)(CO)2	Biphephos	100
2013					
Markert et al.,	Analysis of the reaction network for the Rh-catalysed hydroformylation of 1-dodecene in thermomophic multicomponent solvent system	N,N-Dimethylformamide (DMF)/decane	Rh(acac)(CO)2	TPPS, Xantphos, Biphephos	90
Rost et al.,	Development of a continuous process for the hydroformylation of long-chain olefins in aqueous multiphase systems	Water/ Marlophen NP9 Water/ MarlipalO13/200	Rh(acac)(CO)2	SulfoXantPhos	80
Steimel et al.,	Model-based conceptual design and optimization tool support for the early stage development of chemical process under uncertanity	Dimethylformamide (DMF)/decane	Rh(acac)(CO)2	-	-
Behr & Brunsch	Temperature-Controlled Catalyst Recycling in Homogeneous	Propylene carbonate/decane Acetonitrile/decane Dimethylformamide/decane	Rh(acac)(CO)2	BIPHEPHOS	100

Table A.2 (cont'd): Summary of Literature on Biphasic Hydroformylation systems for Long Chain alkenes

Year & Author	Description of reaction system	Solvent system	Precatalyst	Ligand	Temp[a]
2014					
Zagajewski et al.,	Continuously operated miniplant for the hydroformylation of 1-C12 in a thermomophic multicomponent solvent system (TMS)	N,N-Dimethylformamide (DMF)/decane	Rh(acac)(CO)2	BIPHEPHOS	-
Steimel et al.,	A framework for the modelling and optimization of process superstructure under uncertainty	Dimethylformamide/decane/methanol	Rh(acac)(CO)2	BIPHEPHOS	-
Hentschel et al.,	Simultaneous design of the optimal reaction and process concept for multiphase systems	Dimethylformamide (DMF)/decane	Rh(acac)(CO)2	BIPHEPHOS	-
Muller et al.,	Towards a novel process concept for the hydroformylation of higher alkenes: Mini-plant operation strategies via model development and optimal experimental design	Water/Marlipal O13/200 Water/Marlophen NP 9 Water/Marlophen NP 6	Rh(acac)(CO)2	BIPHEPHOS	110
Kiedorf et al.,	Kinetics of 1C12 hydroformylation in a thermomophic solvent system using rhodium-biphephos catalysts	N,N-Dimethylformamide (DMF)/decane	Rh(acac)(CO)2	BIPHEPHOS	85
Schafer et al.,	Calculation of complex phase equilibria of DMF/alkanes(C5-C10) system using the PCP-SAFT equation of state	N<N-Dimethylformamide(DMF)/decane	-	-	-
2015					
Jorke et al.,	Isomerization of 1-decene: Estimation of thermodynamic properties equilibrium condition calculation and experimental validation using Rh-BIPHEPHOS catalyst	N<N-Dimethylformamide/(DMF)/toluene	Rh(acac)(CO)2	BIPHEPHOS	105

Appendix B: Chapter 4: Process Development

B.1: Definition of terms and assumptions

B.1.1 Economic potential

The first step in the analysis of any design problem is to evaluate the economic significance of the project. Initially, the fraction of the product to be recovered is unknown, however, rather than spending time on this decision, the base calculation assumes complete recovery. Thus, an economic potential at Level n (EP-n) is determined whose definition when used in the Douglas methodology depends on the level of decision-making.

B.1.2 Operating time

It is conventional practice to report operating costs or stream costs on an annual basis. Different design companies use somewhat different values for the number of operating hours per year, and they may even use different values for different types of projects. Normally, in process engineering design, 8000 hr/yr is used for continuous processes and 7000 hr/yr for batch (thus operating time includes scheduled shutdowns for maintenance, unplanned downtime due to mechanical failures, and/or production losses caused capacity limitations or lack of feed).

B.1.3 Assumption of maximum selectivity

Information concerning how the product distribution changes with conversion and or reactor temperature, molar ratio of reactants, etc., is often difficult to obtain. A chemist's focus is on scouting different catalyst attempting to define a mechanism and looking for ways to write a broad patent claim. During these scouting expeditions, the chemist normally attempts to find reaction conditions that maximize the yield. Thus, experience indicates that the existing data base will have most of the points grouped in a small range of conversions close to the maximum yield. Normally, raw material costs and selectivity losses are the dominant factors in the design of a petrochemical process. Raw materials costs are usually in the range from 35 to 85% of the total production costs. The optimum economic conversion is nornally fixed

by an economic trade-off between large selectivity losses and large reactor costs at high conversions balanced against large recycle costs at low conversions.

B.1.4 Raw material purity

A chemist normally uses very pure chemical reagents in laboratory studies, whereas natural or purchased raw materials always contam some impurities. Hence, there is a need to gather some information from the marketing group about raw-material price versus purity in order to decide whether to include a purification facility as part of the design project or not. Moreover, designers must work with the chemist to see whether the impurities in the raw materials are inert or will affect the reactions. The effect of impurities on the separation system must also be investigated. In particular, trace amounts of impurities can build up to large values in recycle loops unless the impurities are removed from the process.

B.1.5 Effect on economics of purify the feed

A decision to purify the feeds before they enter the process is equivalent to a decision to design a preprocess purification system, which is different from a decision to feed the process through a separation system that is required in any event. At this stage of process synthesis and analysis procedure it is not know what kind of separation system will be required for the process with no feed impurities, hence, it is difficult to make a definite decision. According to Douglas (1988), some guidelines may be used to make a decision, “consider a separation unit if the feed impurity is not inert, if the feed impurity is a gas, if the feed impurity is present in large quantities or if a feed impurity is a catalyst poison”. The decision of purifying the feed streams before they are processed involves an economic trade-off between building a preprocess separation system and increasing the cost of the process because we are handling the increased flow rates of inert materials. Therefore, according to Douglas (1988), there is no simple design criterion that always indicates the correct decision.

B.2.1 Douglas methodology

The "Douglas Method" is based on hierarchical decision-making using economic feasibility as a main criterion for process evaluation. A complex problem is gradually solved through completion of a number of arbitrary "stages" or levels of analysis. The Douglas' (1988) hierarchical approach is a simple but powerful methodology for the synthesis of process flowsheets. It consists of a top-down analysis organised as a clearly defined sequence of tasks grouped in levels. In applying the methodology, the designer has to identify dominant design variables and take design decisions. Each level includes new decisions and additional flowsheet structures. Heuristics are used to help the designer to make those decisions, and the opposite decisions are accumulated in a list of process alternatives to be considered after a base-case design has been generated.

B.2.1 Level 1 of process development (Input-output)

Level 1 consideres raw materials input and product output from a process. There is a "rule of thumb" in process design that it is desirable to recover more than 99 % of all valuable materials. For initial design calculations, the order-of-magnitude argument which says that this rule of thumb is equivalent to requiring that we completely recover and then recycle all valuable reactants is applied (Douglas, 1988).

B.2.2 Level 2 of process development (Recycle and recycle structure)

Level 2 of Douglas methodology considers the reactor and compressor costs on the economic potential of the project. The economic analysis for the input-output structure considered only the stream costs, i.e., products minus raw-material costs. However, when recycle of unconverted reactants (1-octene, syngas and 7-tetradecene) is considered, an infinite recycle is required, hence high costs of reactor and compression when the conversion is close to zero. Thus, the annualized reactor cost and the annualized compressor costs (both capital and power) is subtracted from the EP-1 (EPM-1, EPH-1), then it is expect to find both an optimum conversion. These values for the optimum at Level 2 are not the *true optimum* values because

they have not included any separations of the 1-octene, 7-tetradecene, syngas and catalysts or purification of the 2-hexyl-nonanal product or heating and cooling costs.

B.2.2.1 Annualised reactor cost

Guthrie's correlation (Equation B.1) can be used to calculate the installed cost for various types of reactors. A capital charge factor of 1/3 per year is used to annualize the installed equipment cost in terms of the design variables. For first designs, a volume fill efficiency of 75 % is assumed to account for fluid for the volume fraction of reactor that is not filled by the liquid.

$$Installed\ Cost = \left(\frac{M\&S}{282}\right)\frac{(101.9)D^{1.066}L^{0.82}\left(2.18+F_m+F_p\right)}{3}\text{, \$/yr} \quad \text{(B.1)}$$

Where;

M&S = Marshal and Swift Index published each month in Chemical Engineering.

F_m =material factor

F_p = pressure factor

L = length of reactor, ft

D = diameter, ft

For stirred tank reactos (CSTR) the optimum L/D is consider optimum between 1 and 1.5 (Peters and Timmerhaus, 2004).

B.2.2.2 Annualised compressor cost

Equation B.2 in gives the design equation for the costs of the syngas-recycle compressor.

$$Installed\ Cost = \left(\frac{M\&S}{280}\right)(517.5)(bhp)^{0.82}(2.11 + F_c) \quad \text{(B.2)}$$

Where,

M&S = Marshal and Swift Index published each month in Chemical Engineering.

bhp = brake horse power ($^{hp}/_{0.9}$)

F_c = material factor for centrifugal compressor

A fixed temperature and a constant pressure difference was assumed for the isentropic compression of the gas stream in a cascade of N_{CPS} = 4 isentropic compressors with intermediate cooling in a similar effort by Hentschel et al. (2014).

For first designs, a compressor efficiency of 90 % is assumed to account for fluid friction in suction and discharge valves, ports, friction of moving metal surfaces, fluid turbulence, etc. A driver efficiency of 90 % is assumed to account for the conversion of the input energy to shaft work.

$$h_p = \left(\frac{3.03x10^{-5}}{\gamma}\right) P_{in} Q_{in} \left[\left(\frac{P_{out}}{P_{in}}\right)^{\gamma} - 1\right] \quad \text{(B.3)}$$

The exit temperature form the compressor is given by:

$$\frac{T_{out}}{T_{in}} = \left(\frac{P_{out}}{P_{in}}\right)^{\gamma} \quad \text{(B.4)}$$

Where;

P_{in} = 1bf/ft^2

Q_{in} = ft^3/min

γ = compression factor

T = Temperature (K)

P = Pressure (are absolute values, barg).

B.2.2.3 Decision on the number of reactors

According to the Douglas methodology, if the reactions take place at different temperatures or pressures, or if they require different catalysts, then different reactor systems are considered for these reaction sets. Hence, if only one reactor is required or if the all the reactions place at the same temperature and pressure without a catalyst, only one reactor is required.

B.2.2.4 Decision on the number of recycle streams

The components leaving the reactor are listed according to the order of their normal boiling points, and the reactor number is used as the destination code for each recycle stream. The recycle components having neighbouring boiling points can then be grouped together if they

have the same reactor destination. The number of recycle streams is merely the number of groups.This simple procedure is based on this common sense heuristic that “do not separate two components and then remix them at a reactor inlet”. The gas and liquid recycle streams are also distinguished, because gas recycle streams require compressors, which are always expensive. A stream is considered a gas-recycle stream if it boils at a lower temperature than propylene (i.e. propylene can be condensed with cooling water at high pressure, whereas lower-boiling materials require refrigerated condensers, which require a compressor). Liquid-recycle streams require only pumps. In overall design calculations, the costs of the pumps are not included because they are usually small compared to reactors, compressors, furnaces, distillation columns, etc.

B.2.2.5 Decision on reactor heat effects

To make the decision concerning the reactor heat effects, the reactor head load and the adiabatic temperature change are estimated. These calculations provide some guidance as to the difficult of dealing with the reactor heat effects. Similarly, any temperature constrains imposed on the design problem is considered. For single reactions, all the fresh feed of the limiting reactant usually gets converted in the process (the per-pass conversion might be small so that there is a large recycle flow, but all the fresh feed is converted except for small losses in product and by-product streams or losses in a purge stream). Thus, for single reactions:

$$\text{Reactor heat load} = \text{Heat of reaction} \times \text{Fresh feed rate} \qquad \text{(B.4)}$$

Where, the heat of reaction is calculated at the reactor operating conditions.

B.2.2.6 Decision on compressor cost and design

According to Douglas (1988), a gas-recycle compressor is required whenever a gas-recycle stream is present. Equation B.3 gives the design equation for the theoretical horsepower (hp) for a centrifugal gas compressor. The Guthrie's correlation (Equation B.2) or some equivalent correlation can be used to calculate the installed cost for various types of compressors. The operating cost, the utility cost is obtained by dividing the brake horsepower by the driver efficiency, and then multiply the utility factor by 8 000 hrs per annum.

B.2.3 Level 3 of process development (Separation system design)

When separation costs and recycle are considered, high separation costs and an infinite recycle is required when the conversion is close to zero. According to Douglas (1988), the phase of the reactor effluent stream determines the general structure of the separation system for vapour-liquid processes.

B.2.3.1 Separation system design decisions

In design of separation system general structure, there are only three possibilities:

(a) Reactor effluent is liquid

If the reactor effluent is a liquid, it is assumed that only a liquid separation system is required. This system might include distillation columns, extraction units, azeotropic distillation, etc., but normally there will not be any gas absorber, gas adsorption units. etc.

(b) Reactor effluent is a two phase mixture

If the reactor effluent is a two-phase mixture, the reactor can be used as a phase splitter (or put a flash drum after the reactor). The liquids are send to a liquid separation system. If the reactor is operating above cooling-water temperature, the reactor vapor stream is cooled to 30 ^{o}C and the stream is phase-split. If the low-temperature flash liquid obtained containts mostly reactants (and no product components that are formed as intermediates in a consecutive reaction scheme), then reactants are recycled to the reactor. However, if the low-temperature flash liquid contains mostly products, the stream is send to the liquid recovery system. The low-temperature flash vapor is usually sent to a vapor recovery system. However, if the reactor effluent stream contains only a small amount of vapor, the reactor effluent is often send directly to a liquid separation system (i.e, distillation train).

(c) Reactor effluent is all vapour

If the reactor effluent is all vapour, the stream is cooled to 30 ^{o}C (cooling-water temperature) and attempt to achieve a phase split or to completely condense this stream. The condensed liquid is sent to a liquid recovery system, and the vapor is sent to a vapor recovery system.

B.2.3.2 Decision on vapour recovery system

In an attempt to synthesise the vapour recovery system two decision are made on the best location vapour recovery system and the choice of a cheapest vapour system recovery system (Douglas, 1988). The decisions are based on the heurisctic;

1) Place the recovery system on the purge stream if significant amounts of valuable matenals are being lost in the purge. The reason for this heuristic is that the purge stream normally has the smallest flow rate.
2) Place the vapour recovery system on the gas-recycle stream if materials that are deleterious to the reactor operation (catalyst poisoning, etc.) are present in this stream or if recycling of some components degrades the product distribution. The gas recycle stream normally has the second smallest flow rate.
3) Place the vapor recovery system on the flash vapor stream if both items (1) and (2) are valid. i.e., the flow rate is higher but two objectives are accomplished.
4) Do not use a vapor recovery system if neither item (1) nor item (2) are important.

B.2.3.3 Decision on adjusting material balance

However, it is required to realise that unless item (3) in Section B.2.3.2 is chosen, our simple material balance equations will not be valid; i.e., some materials that was assumed to be recovered as liquids will be lost in the purge stream or recycled with the gas stream (which will change the compressor size). However, in many cases, the errors introduced are small, so, that previous approximations still provide good estimates (Douglas, 1988). It is also expected to develop a rigorous material balances if development proceed to a final design, and therefore, engineering judgment is used to see whether corrections need to be made at this point. Moreover, rather than attempting to evaluate the various alternatives at this time, designers merely make some decisions and continue to develop a base case. The other alternatives are listed as items that need to be considered after estimating the profitability of the process and have a better understanding of the allocation of the costs. The design of vapour recovery system is considered first before considering the liquid separation system

because each of the vapour recovery processes usually generates a liquid stream that must be further purified.

B.2.3.4 Decision on compining vapour and liquid recovery

If a partial condenser and a flash drum is used to phase-split the reactor effluent some of the lightest liquid components will leave with the flash vapour (i.e., a flash drum never yields perfect spilt) and therefore will not be recovered in the liquid recovery system. However, if there is only a small amount of vapor in the stream leaving the partial condenser and if the first split in the liquid separation system is chosen to be distillation, the phase splitter can be eliminated and reactor effluent stream is fed directly into the distillation column. The diameter of a distillation column with the two-phase feed will need to be larger (to handle the increased vapour traffic) than a column that follows a flash drum. However, this increased cost may be less than the cost associated with using a vapor recovery system to remove the liquid components from the flash vapour stream. According to Douglas (1988), there does not seem to be a heuristic available for making this decision and so there is need to add another process alternative to our list.

B.2.3.5 Decision on the liquid recovery system

The decisions that need to be considered in the synthes of the liquid separation system include:

1) How should light ends be removed if they might contaminate the product?
2) What should be the destinations of the light ends?
3) Do components that form azeotropes with the reactants need to be eliminated or split the azeotropes?
4) What separations can be made by distillation?
5) What is the sequence of columns to be used?
6) How should separations be accomplished if distlllation is not feasible?

In general, distillation is the least expensive means of separating mixtures of liquids. However, If the relative volatilities of two components with neighboring boiling points is less than 1.1,

distillation becomes very expensive; i.e., a large reflux ratio is required which corresponds to a large vapor rate, a large column diameter, large condensers and reboilers, and large steam and cooling water costs. Whenever two neighbouring components having a relative volatility of less than 1.1 in a mixture are encountered, the components are grouped together and treated as a single component to the mixture. In other words, the best distillation sequence for the group and the other components is developed and then lumped components are separated by using other procedures.

B.2.3.6 Decision on the sequence of the distillation columns

Some general heuristics can be used to simplify the selection procedure for column sequences. The first heuristic in this list is based on the fact that the material of construction of the column is much more expensive than carbon steel if corrosive components are present. Thus, the more columns that a corrosive component passes through, the more expensive will be the distillation train. Other heuristics used in column sequencing include:

1) Most plentiful first
2) The lighest first
3) The highest recovery first
4) The next separation should be cheapest.

It must also be noted that as a result of change the conversion in a process; it is expected that the unconverted reactant will go from being the most plentiful component at very low conversions to the least plentiful at very high conversions. Hence, the heuristics (1) to (4) imply that the best column sequences will change as we alter the design variables. However, studies used to develop the heuristics were limited to sequences of simple columns having a single feed stream that were isolated from the remainder of the process, so that different results may be obtained when we consider the interactions between a distillation train and the remainder of the plant.

B.2.3.7 Decision on cost of the column and size

Once the tower height and diameter are determined, Guthrie's correlations (Equation B.5 to Equation B.10) can be used to estimate the total cost, i.e., the shell cost is evaluated assuming a pressure vessel and this include the cost of trays. As a quick approximation, it is assumed that the cost of the trays is about 20 % the cost of the column shell (assuming that everything is carbon steel). For dlistillation columns, the design include the condenser and reboiler. In addition, the the coolling-water and steam requirements must also be considered. Usually for short-cut design, it is assumed that an overall heat transfer coefficient for the condenser of Uc is equal to 100 Btu/(hr· ft^2 .^{o}F) gives reasonable results (Douglas, 1988).

$$Column\ Cost = \left(\frac{M\&S}{280}\right)\frac{(3.28)(101.9)D^{1.066}L^{0.82}}{3}\text{, \$/y} \quad \text{(B.6)}$$

Where;

M&S = Marshal and Swift Index published each month in Chemical Engineering.

L = length of reactor (ft)

D = diameter (ft)

$$Condenser\ Cost = \left(\frac{M\&S}{280}\right)\frac{(3.28)(101.3)\left(\frac{\Delta H}{U\Delta T}\right)^{1.066}V^{0.65}}{3}\text{, \$/y} \quad \text{(B.7)}$$

Where;

M&S = Marshal and Swift Index published each month in Chemical Engineering.

ΔH = Enthalpy of vaporization (Btu/klbmol)

$U =$ Heat transfer coefficient, (100 Btu/(hr.ft^2.^{o}F)

V = Volumetric flow (ft^3/hr)

$$Reboiler\ Cost = \left(\frac{M\&S}{280}\right)\frac{(3.28)(101.3)\left(\frac{\Delta H}{11250}\right)^{0.92}V^{0.65}}{3}\text{, \$/y} \quad \text{(B.8)}$$

Where;

M&S = Marshal and Swift Index published each month in Chemical Engineering.

ΔH =enthalpy of vaporization (Btu/klbmol)

$$Steam\ Cost = (C_s)\left(\frac{\Delta H}{933}\right)(8000)V,\ \$/\text{yr} \quad \text{(B.9)}$$

Where;

C_s = Cost of steam ($/gal)

ΔH = Heat value Btu/klbmol

V = Volumetric flow, (ft^3)

$$Cooling\ water\ Cost = (C_{CW})\left(\frac{1}{8.13}\right)\left(\frac{\Delta H}{30}\right)(8000)V,\ \$/\text{yr} \quad \text{(B.10)}$$

Where;

C_{Cw} = Cost of cooling water ($/gal)

ΔH = Enthalpy of vaporization (Btu/klbmol)

V = Volumetric flow rate (ft^3/h)

(Let $^{R}/_{R_m}$ =1.2 to ensure that the column is operated above optimum but in the neighbourhood of the optimum)

For optimum reflux ratio assume;

Uc = 100 Btu/ (hr.ft^2.^{o}F)

$N = {}^{N_{m,}}/_{E_o}$, N_m is the minimum number of stages, E_o is column efficiency

The driving force in the reboiler must be considered to be constrained to be within 0 to 8 ^{o}C to prevent film boiling. It is expected to that the high value of overall heat transfer can be obtained because heat transfer is between the condensing vapour and a boiling liquid.

B.2.3.8 Decision on membrane cost

At any 1-octene or 7-tetradecene conversion, the mass fraction (x) of 1-octene or 7-tetradecene in the feed to the membrane can be found:

$$Mass\ fraction\ (X_{Cx}) = \frac{No.moles\ Cx * Mr\ Cx}{No.moles\ x * Mr\ Cx + No.moles\ Cy * MrCy + No.moles\ Cz * Mr\ Cz} \quad \text{(B.11)}$$

To determine the mass flux across the membrane, a correlation of mass flux versus 1-octene was carried out using experimental data as shown in Figure B.1

$$Flux = 9.422X_{C8} - 2.5102X_{C8} + 1.0856 \quad \text{(B.12)}$$

Where,

X_{C8} = mass fraction of 1-octene

Hence, the membrane area required for this quantity of flux:

$$Membrane\ area\ required\ for\ X_{C8} = \frac{Volumetric\ flow\ rate\left(\frac{m^3}{hr}\right) * Density(\frac{kg}{m^3})}{Flux(\frac{kg}{m^2 h})} \quad \text{(B.13)}$$

Using the membrane area the total cost of membrane required at any conversion becomes:

$$Cost\ of\ membrane = Area\ of\ membrane * Cost\ of\ membrane\ (\frac{\$}{m^2}) \quad \text{(B.14)}$$

(a) Experimental data

Experimental data

1-Octene mass fraction (-)	Total flux (kg.m^{-2}.h^{-1})
0	0.67
0.1	1
0.2	1.13
0.32	1.66
0.43	1.95
0.5	2.42
0.6	2.84
0.69	3.66
0.81	4.65
0.92	5.78
1	9.19

(b) Flux correlation

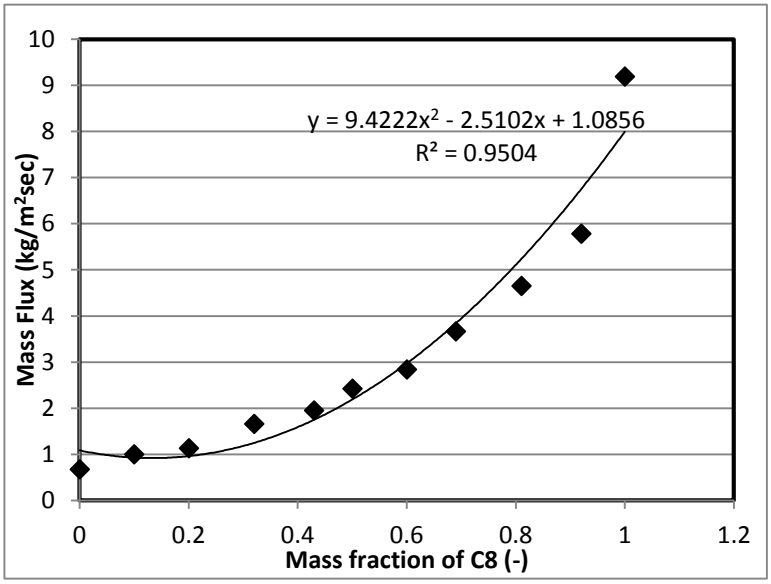

Figure B.1: A correlation between flux and C8 mass fraction

Table B.1: Determination of stream costs and EPM-1 at Level 1 of metathesis process development

Properties of species:				**Cost Aspects**				EPM-1 catalysts		$/kg	$/kmol
C8				**C8**		1.6	$/kg	416.57525	**HGr-2**	28 746	18012818.5
	MW=	112.2	g/mol	C14		35.5	$/kg	416.55957	**HGr-1**	46533.33333	27948385.3
	density=	715	kg/m3					416.59494	**Gr-1**	6720	5530291.2
C14				**EPM-1=**	**416.58**			416.57741	**Gr-2**	19600	16639812
	MW=	196.37	g/mol	M&S (2016)	1595.645965			416.10084	Schrock	421667	318746519
	density=	700	kg/m3								
C2											
	MW=	28.05	g/mol								
	density=	567.65	kg/m3								
HGr-2		626.62	g/mol								
HGr-1		600.61	g/mol		2A -> B + C		A = 1-octene				
Gr-1		822.96	g/mol				B = 7-tetradecene				
Gr-2		848.97	g/mol				C = ethylene				
Sc		755.92	g/mol								

Table B.2: Determination of reactor cost and EPM-2 at Level 2 of metathesis process process development

Reaction 2A -> B + C A = 1-octene, B = 7-tetradecene, C= ethylene | Conversion | Ft to m (0.3048)

'(kmol/hr) | % Filled Volume 75.00%

	min	hr	In	Out			must be 1.0-1.5 Douglas (1988) pg 262				Cost ($M/yr)		
Conv	time	time	A	A	B	C	v0 (m3/hr)	Volume (m3)	D	L	L/D	Reactor Cost ($M/yr)	EPM-2 ($M/yr)
0.1	10	0.17	157.7	142.0	7.9	7.9	24.75272347	5.501	6.28	6.277093	1.00	0.11	416.47
0.2	20	0.33	78.9	63.1	7.9	7.9	12.37636173	5.501	6.28	6.277093	1.00	0.11	416.47
0.27	28	0.47	58.4	42.6	7.9	7.9	9.167675359	5.704	6.35	6.353651	1.00	0.11	416.47
0.35	40	0.67	45.1	29.3	7.9	7.9	7.072206706	6.286	6.56	6.562801	1.00	0.11	416.46
0.48	60	1.00	32.9	17.1	7.9	7.9	5.156817389	6.876	6.76	6.761794	1.00	0.12	416.45
0.54	75	1.25	29.2	13.4	7.9	7.9	4.58383768	7.640	7.00	7.003488	1.00	0.13	416.45
0.65	120	2.00	24.3	8.5	7.9	7.9	3.808111303	10.155	7.70	7.700422	1.00	0.15	416.42
0.69	240	4.00	22.9	7.1	7.9	7.9	3.587351227	19.133	9.51	9.510703	1.00	0.23	416.35

Material Properties		
Fp	1	
Fm	3.67	SS cladding
Fc	3.67	

Table B.3: Detemination of flash drum cost at Level 3 of metathesis process development

								Material of construction		
					Ft conversion (0.3048)			Fp	1	< 50 bar
								Fm	1	Stainless steel
					Flash residence	5	mins	Fc	1	
Separation-part with drum										
1) Assume single drum (size depend on volume of outlet from reactor)								L/D	3	
	outlet flow M3/hr calculated from reactor oulet mol/hr									
Conversion	**A**	**B**	**C**	**flow(m3/hr)**	**Volume drum**	**D**	**L**	**L/D**	**Cost of drum ($M/yr)**	
0.1	22.28	2.2125	*0.3897*	24.88	2.073306354	3.143903097	9.431709	3	0.037870709	
0.2	9.90	2.2125	*0.3897*	12.50	1.041942876	2.499554604	7.498664	3	0.024673937	
0.27	6.69	2.2125	*0.3897*	9.29	0.774552345	2.264287572	6.792863	3	0.020513665	
0.35	4.60	2.2125	*0.3897*	7.20	0.599929957	2.079448528	6.238346	3	0.017496785	
0.48	2.68	2.2125	*0.3897*	5.28	0.44031418	1.875723773	5.627171	3	0.014431469	
0.54	2.11	2.2125	*0.3897*	4.71	0.392565871	1.805311597	5.415935	3	0.013436016	
0.65	1.33	2.2125	*0.3897*	3.94	0.327922007	1.700218926	5.100657	3	0.012011966	
0.69	1.11	2.2125	*0.3897*	3.71	0.309525334	1.667810583	5.003432	3	0.011587804	

Table B.4: Determination of HGr-2 membrane cost at level 3 of metathesis process development

R/P = 0.6 membrane+reactor+drum

Conversion	A	B	wt-frac C8	*Flux*	Area need for 60% pass	Cost of membrane
0.1	141.96	7.9	0.947368	*7.165595568*	34.85429	0.69
0.2	63.10	7.9	0.888889	*6.299753086*	18.77906	0.37
0.27	42.65	7.9	0.843931	*5.677958502*	14.83355	0.29
0.35	29.29	7.9	0.787879	*4.956124885*	12.50341	0.25
0.48	17.09	7.9	0.684211	*3.777229917*	11.02006	0.22
0.54	13.44	7.9	0.630137	*3.242750985*	10.95974	0.22
0.65	8.49	7.9	0.518519	*2.31388203*	11.7987	0.23
0.69	7.09	7.9	0.473282	*2.004345901*	12.45101	0.25

Membrane Cost = 1970.44335 $/m2 membrane cost

609 cm2

120 pound per sheet 1970.44335

0.0609 m2

Table B.5: Determination of 1-octene column cost at Level 3 of metathesis process development

		PvapouC8	17.4	mmHg	Btu/bmol	2.32601	kJ/kmol
ΔH (Btu/lbmol)		PvapourC14	7.25	mmmHg	Gal	3.79	kg
1-octene	107.526	α	2.4				
Tetradecene	376.01	R/Rm	1.2				
Hexyl-nonal	201.778	N/Nm	2				
		% recovery	0.995				
		% purity	0.9997				
		Eo	0.5				

Separation part with 1-octene column

	feed to column									
converion	**A**	**B**	**xf**	**Rm**	**R**	**dC8**	**wC8**	**dC14**	**wC14**	**xw**
0.1	141.96	7.886897	0.947368	0.75396825	0.9047619	141.2543286	0.709820746549894	0.04238902	7.844508169	0.090486
0.2	63.10	7.886897	0.888889	0.80357143	0.96428571	62.77970158	0.315475887355504	0.01883956	7.868057622	0.040096
0.27	42.65	7.886897	0.843931	0.84637965	1.01565558	42.43442792	0.213238331268073	0.01273415	7.874163035	0.027081
0.35	29.29	7.886897	0.787879	0.90659341	1.08791209	29.14771859	0.146470947700770	0.00874694	7.878150244	0.018592
0.48	17.09	7.886897	0.684211	1.04395604	1.25274725	17.00283585	0.085441386158781	0.00510238	7.881794802	0.01084
0.54	13.44	7.886897	0.630137	1.13354037	1.36024845	13.36975126	0.067184679714599	0.00401213	7.882885055	0.008523
0.65	8.49	7.886897	0.518519	1.37755102	1.65306122	8.451113675	0.042467907913240	0.00253609	7.884361089	0.005386
0.69	7.09	7.886897	0.473282	1.50921659	1.81105991	7.051343294	0.035433885898625	0.00211604	7.884781146	0.004494

Table B.6: Determination of 1-octene column cost at Level 3 of metathesis process development

					Ft	0.3048	(in/m) (Stainless steel)
					L/D	10	
							Cost ($Million /yr)
Nm	**N**	**Nactual**	**H**	**D**	**H**	**D**	**Cost of column ($M/yr)**
12.5925	23.8024	47.6048	110.209	11.0209	110.209	11.0209	0.00696789
12.8925	25.7850	51.5700	118.140	11.8140	118.140	11.8140	0.00793365
13.3561	26.7123	53.4246	121.849	12.1849	121.849	12.1849	0.00840528
13.7956	27.5913	55.1827	125.365	12.5365	125.365	12.5365	0.00886402
14.4208	28.8417	57.6834	130.366	13.0366	130.366	13.0366	0.00953602
14.6982	29.3965	58.7930	132.586	13.2586	132.586	13.2586	0.00984150
15.2260	30.4520	60.9041	136.808	13.6808	136.808	13.6808	0.01043500
15.4339	30.8679	61.7358	138.471	13.8471	138.471	13.8471	0.01067325

Table B.7: Comparison of separation cost and EPM-3 at Level 3 of metathes process development

Conversion	Flash drum	membrane	column	Total separation Costs	EPM-3
0.1	0.0378707	0.69	0.018125	742.78	415.73
0.2	0.0246739	0.37	0.020721	415.43	416.05
0.27	0.0205137	0.29	0.021992	334.79	416.13
0.35	0.0174968	0.25	0.023231	287.10	416.17
0.48	0.0144315	0.22	0.025049	256.62	416.20
0.54	0.013436	0.22	0.025877	255.27	416.19
0.65	0.012012	0.23	0.027489	271.99	416.15
0.69	0.0115878	0.25	0.028136	285.06	416.06

Figure B.2 shows the effect of single pass 7-tetradecene conversion on the number of stages of C14 column and reflux ratio

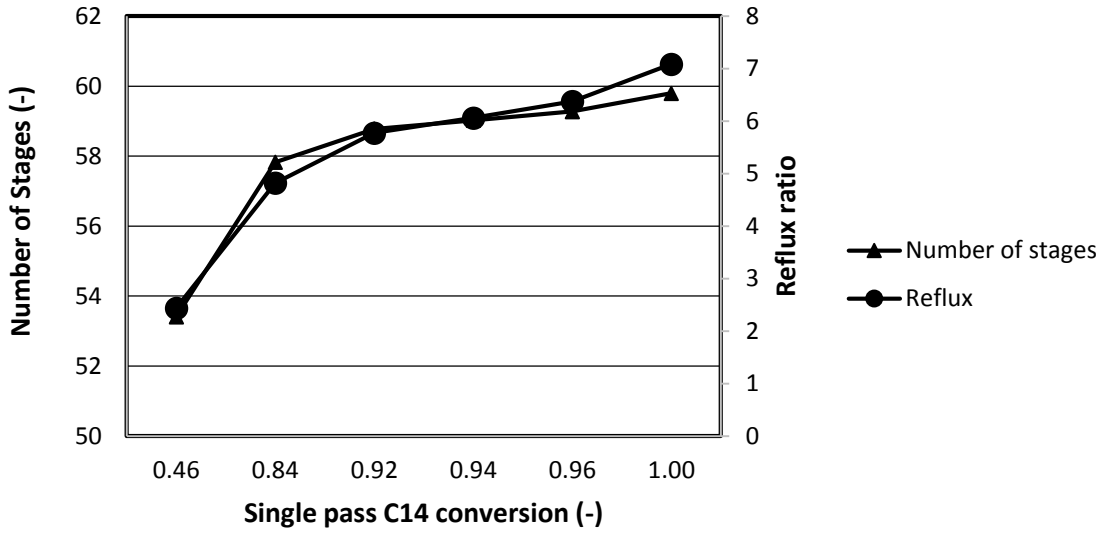

Figure B. 2: Effect of single pass C14 conversion on Reflux ratio and number of stages

Figure B.3 shows the effect of mass fraction of 7-tetradecene in feed to membrane with mass flux across the membrane.

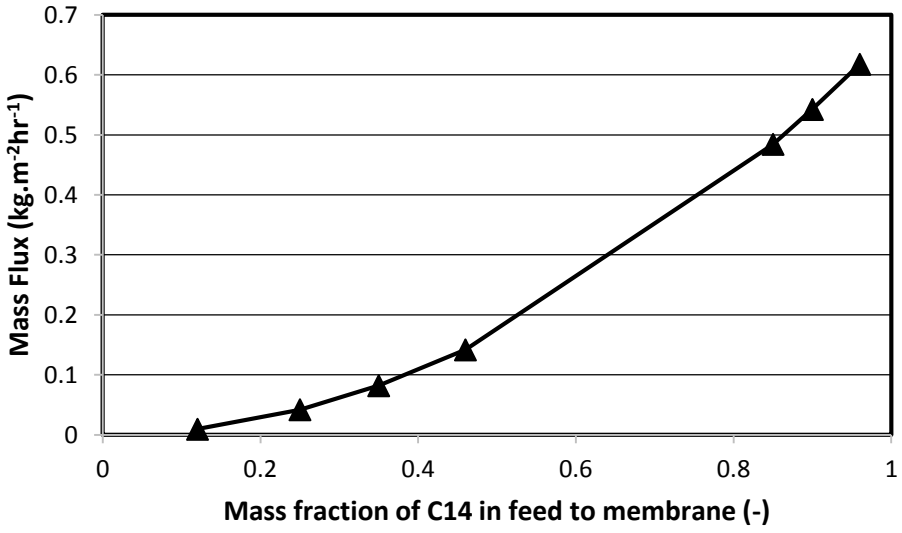

Figure B.3: Effect of C14 mass fraction on membrane flux

Figure B.4 shows the effect of 7-tetradecene conversion on the mass fraction of 7-tetradecene in feed to the membrane. Figure B.4 also shows the effect of single pass 7-tetradecene conversion on the total membrane area required.

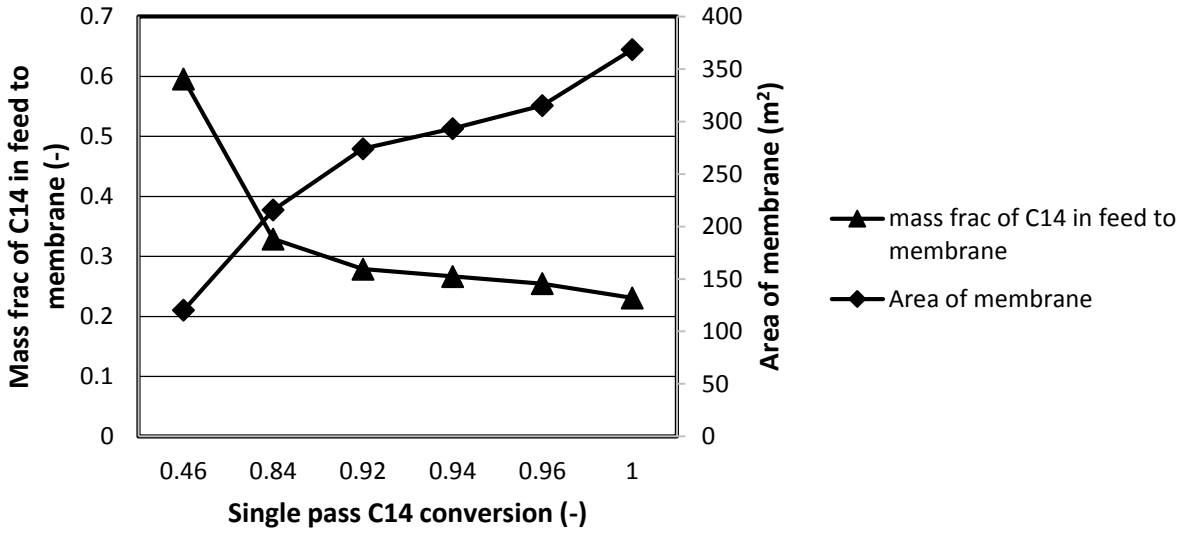

Figure B.4: Effect of single pass C14 conversion on mass fraction of C14 in feed to membrane and membrane area

Table B.8: Determination of stream costs and EPH-1 at Level 1 of hydroformylation process development

Properties of species:								Metathesis Section					
								Conversion	Cost MU	Catalyst (Rh+HGr-2) ($M/yr)	Cost syngas ($M/yr)	Cost C8 ($M/yr)	EPH-1 ($M/yr)
C15				Cost Aspects				0.1	0.83	0.166679947	0.05684698	22.65542	976.29
	MW=	226.89	g/mol	C15	100.0	$/kg		0.2	0.50	0.166679947	0.05684698	22.65542	976.62
	density=	715	kg/m3	CO/H2	0.0	$/kg		0.27	0.42	0.166679947	0.05684698	22.65542	976.70
CO				C14	35.45			0.35	0.38	0.166679947	0.05684698	22.65542	976.74
	MW=	28.01	g/mol	**EP2=**	**976.77**			0.48	0.35	0.166679947	0.05684698	22.65542	976.77
	density=	793.2	kg/m3	M&S (2016)	1595.645965			0.54	0.36	0.166679947	0.05684698	22.65542	976.76
H2								0.65	0.40	0.166679947	0.05684698	22.65542	976.72
	MW=	28.05	g/mol	Mr-Rh-TPPTS	365.2	g/mol		0.69	0.49	0.166679947	0.05684698	22.65542	976.64
	density=	70.85	kg/m3	Cost	120000	$/kg							
C14					43824000	$/kmol							
	MW=	196.37	g/mol										
	density=	700	kg/m3										

REACTION:	A+B+C>D+W

D = C15
W = waste

A=C14
B=CO
C=H2

Table B.9: Determination of Reactor Cost and EPH-2 with single pass C14 conversion at Level 2 of hydroformylation process development

Data at 120 °C, 100 bar, Haumman et al 2002b									
Conversion	**time**	**time**	**In (kmol/hr)**	**A =7-tetradecene**		**Out**	**(kmol/hr)**		
			A(C14)	**B (CO)**	**C (H2)**	**A(C14)**	**B(CO)**	**C(H2)**	**W(waste)**
0.12	40	0.666666667	65.7291689	65.729169	65.7291689	60.20791871	60.2079187	60.20792	2.36625
0.22	80	1.333333333	35.8522739	35.852274	35.85227395	30.33102376	30.3310238	30.33102	2.36625
0.35	140	2.333333333	22.5357151	22.535715	22.53571505	17.01446486	17.0144649	17.01446	2.36625
0.7	400	6.666666667	11.2678575	11.267858	11.26785753	5.746607338	5.74660734	5.746607	2.36625
0.8	580	9.666666667	9.85937534	9.8593753	9.859375335	4.338125147	4.33812515	4.338125	2.36625
0.9	900	15	8.76388919	8.7638892	8.763889187	3.242638999	3.242639	3.242639	2.36625
0.96	1260	21	8.21614611	8.2161461	8.216146113	2.694895925	2.69489592	2.694896	2.36625

Table B.10: Determination of Reactor costs and EPH-2 at Level 2 of hydroformylation process development

						Material Properties			
						Fp	1.05	Design pressure(100 bar)	
						Fm	3.67	Stainless steel Clad	
		Vary	L/D	1		Fc	3.8535		
			% fill	0.75				Ft/m	0.3048
V0A (m3/hr)	**V0B (m3/hr)**	**V0C (m3/hr)**	**v0 (m3/hr)**	**Volume (m3)**	**D**	**L**	**L/D**	**Reactor Cost ($Million/yr)**	**EPH-2 ($ million/yr)**
18.4389099	2.321071635	26.0226279	46.78261	41.5845417	12.31967	12.31967	1	0.399385061	976.37
10.0575872	1.266039074	14.1941607	25.51779	45.3649546	12.68222	12.68222	1	0.421840453	976.35
6.32191195	0.795795989	8.92204386	16.03975	49.90145	13.0916	13.0916	1	0.447889031	976.32
3.16095597	0.397897995	4.46102193	8.019876	71.2877858	14.74439	14.74439	1	0.560469682	976.21
2.76583648	0.348160745	3.90339419	7.017391	90.4463782	15.96193	15.96193	1	0.650940368	976.12
2.45852131	0.309476218	3.46968372	6.237681	124.753625	17.76804	17.76804	1	0.796786643	975.97
2.30486373	0.290133954	3.25282849	5.847826	163.739133	19.45387	19.45387	1	0.945338066	975.82

Table B.11: Determination of compressor costs at Level 2 of hydroformylation process development

		Assume E	70 %		X	2088.544		
					bar	lb/ft2	Material of construction	
				Pin	15	31328.16	**Fp**	1.05
	Recycle Compressor cost			Pout	100	208854.4	**Fm**	3.67
							Fc	3.8535
	Qin (m3/hr)		X	0.588578				

Conversion	**B**	**C**	**Vtotal**	**Q(ft3/min)**	**hp (BTU)**	**bhp (BTU)**	**Cost ($M/yr)**
0.12	2.1261016	23.83673	25.96282879	15.28114	34.49987	38.33319	0.123738
0.22	1.0710691	12.00826	13.07932899	7.698202	17.38004	19.31116	0.070524
0.35	0.600826	6.736143	7.336969083	4.318377	9.749495	10.83277	0.043899
0.7	0.202928	2.275121	2.478049161	1.458525	3.292876	3.658751	0.018026
0.8	0.1531907	1.717493	1.87068417	1.101043	2.485798	2.761998	0.014314
0.9	0.1145062	1.283783	1.398289178	0.823002	1.858071	2.064524	0.011275
0.96	0.0951639	1.066928	1.162091681	0.683981	1.544208	1.715787	0.009688

Table B.12: Determination of flash drum costs at Level 3 (Separation costs) of hydroformylation process development

Separation with flash drum										Residence time 5 mins	
	Inlet flow										
Conv	**A**	**B**	**C**	**W**	**D**	**VA**	**VB**	**VC**	**VW**	**VD**	**V(m3/hr)**
0.12	60.207919	60.20792	60.20791871	2.36625008	5.52125	16.89004	2.126102	23.83673	0.750879	1.752051	45.35580019
0.22	30.331024	30.33102	30.33102376	2.36625008	5.52125	8.508719	1.071069	12.00826	0.750879	1.752051	24.09097774
0.35	17.014465	17.01446	17.01446486	2.36625008	5.52125	4.773044	0.600826	6.736143	0.750879	1.752051	14.61294259
0.7	5.7466073	5.746607	5.746607338	2.36625008	5.52125	1.612088	0.202928	2.275121	0.750879	1.752051	6.593066688
0.8	4.3381251	4.338125	4.338125147	2.36625008	5.52125	1.216968	0.153191	1.717493	0.750879	1.752051	5.590582201
0.9	3.242639	3.242639	3.242638999	2.36625008	5.52125	0.909653	0.114506	1.283783	0.750879	1.752051	4.810872044
0.96	2.6948959	2.694896	2.694895925	2.36625008	5.52125	0.755995	0.095164	1.066928	0.750879	1.752051	4.421016966

Table B.13: Determination of flash drum costs at Level 3 of hydroformylation process development

Material of construction (Stainless steel) Fc =1			L/D = 3
Fp		1	Fm
Vdrum	**D**	**L**	**Cost of flash ($M/yr)**
3.77965	3.840595	11.5217852	0.05504115
2.007581	3.110325	9.33097387	0.03711865
1.217745	2.632895	7.89868372	0.02718947
0.549422	2.019374	6.05812162	0.01656441
0.465882	1.911349	5.73404606	0.01494769
0.400906	1.818007	5.45402051	0.01361305
0.368418	1.767509	5.30252704	0.01291524

Table B.14: Determination of membrane costs at Level 3 hydroformylation process development (OSN membrane scenario)

Separation-part with membrane							
	Feed to membrane					X	0.6
Conversion	**A**	**W**	**D**	**wt-frac C8**	***Flux***	**Area need for 60% pass**	**Cost of membrane ($M/yr)**
0.12	60.20792	2.36625	5.52125	0.88417	0.523777	209.15134	4.12120867
0.22	30.33102	2.36625	5.52125	0.793621	0.421989	141.600353	2.79015474
0.35	17.01446	2.36625	5.52125	0.683258	0.312784	120.081455	2.36613705
0.7	5.746607	2.36625	5.52125	0.421488	0.119027	157.777722	3.10892064
0.8	4.338125	2.36625	5.52125	0.354839	0.08436	194.787626	3.83817982
0.9	3.242639	2.36625	5.52125	0.291339	0.056868	256.84719	5.06102837
0.96	2.694896	2.36625	5.52125	0.254658	0.04345	315.156406	6.20997845
		Membrane cost		**1970.44335**	**$/m2**		

Table B.15: Determination of 7-tetradecene column column costs at Level 3 of hydroformylation process development (OSN membrane)

PvapouC8	7.25	mmHg
PvapourC14	3.7	mmHg
α	1.95945946	
R/Rm	1.2	
N/Nm	2	
% recovery	0.995	
% purity	0.9997	
Eo	0.5	

Convers	A	W	D	xf	Rm	R	dC14	wC14	dC15	wC15	xw
0.12	60.20792	2.36625	5.521250188	0.8841698	1.178793284	1.4145519	59.90688	0.30104	0.017977	7.869523	0.038254
0.22	30.33102	2.36625	5.521250188	0.7936210	1.313288716	1.5759464	30.17937	0.151655	0.009057	7.878444	0.019249
0.35	17.01446	2.36625	5.521250188	0.6832579	1.525417405	1.8305008	16.92939	0.085072	0.00508	7.88242	0.010793
0.7	5.746607	2.36625	5.521250188	0.4214876	2.47279757	2.9673570	5.717874	0.028733	0.001716	7.885784	0.003644
0.8	4.338125	2.36625	5.521250188	0.3548387	2.937259923	3.5247119	4.316435	0.021691	0.001295	7.886205	0.00275
0.9	3.242639	2.36625	5.521250188	0.2913385	3.577464789	4.2929577	3.226426	0.016213	0.000968	7.886532	0.002056
0.96	2.694896	2.36625	5.521250188	0.2546583	4.092751632	4.9113019	2.681421	0.013474	0.000805	7.886696	0.001709

Table B.16: Determination of 7-tetradecene column costs at Level 3 of hydroformylation process development (OSN membrane process)

	PvapouC8	7.25	mmHg
	PvapourC14	3.7	mmHg
	α	1.95945946	
	R/Rm	1.2	
	N/Nm	2	
	% recovery	0.995	
	% purity	0.9997	
	Eo	0.5	
ALTERNATIVE			
Separation with C14 recovery	X	0.5	

Inlet

Conver	**A**	**D**	**xf**	**Rm**	**R**	**dC14**	**wC14**	**dC15**	**wC15**	**xw**	**Nm**	**Nactual**
0.12	30.10395936	5.52125	0.845018	1.23340919	1.48009103	29.95344	0.150519797	0.008989	5.512261	0.027306	11.68438	46.73751
0.22	15.16551188	5.52125	0.733102	1.42170279	1.70604335	15.08968	0.075827559	0.004528	5.516722	0.013745	12.38466	49.53866
0.35	8.507232432	5.52125	0.606426	1.71868296	2.06241955	8.464696	0.042536162	0.00254	5.51871	0.007708	12.96924	51.87694
0.7	2.873303669	5.52125	0.342282	3.04501519	3.65401823	2.858937	0.014366518	0.000858	5.520392	0.002602	14.06013	56.2405
0.8	2.169062574	5.52125	0.282051	3.69526248	4.43431498	2.158217	0.010845313	0.000648	5.520603	0.001965	14.34197	57.36788
0.9	1.6213195	5.52125	0.226994	4.5915493	5.50985915	1.613213	0.008106597	0.000484	5.520766	0.001468	14.63355	58.53421
0.96	1.347447962	5.52125	0.196172	5.31295088	6.37554105	1.340711	0.00673724	0.000402	5.520848	0.00122	14.81884	59.27537

Table B.17: Determination of 7-tetradecene column at level 3 of hydroformylation process development (OSN membrane process) continoued

				Material of construction			
Ft	0.3048			**Fp**	1		
				Fm	1		
L/D	10			**Fc**	1		
H	**D**	**H**	**D**	**Cost of column**	**Total cost ($ M/yr)**	**R+C ($ M/yr)**	**Total cost ($M/yr)**
108.475	10.8475	33.06319	3.30631862	0.10927372	0.687437831	0.01	0.70
114.0773	11.40773	34.77077	3.4770767	0.12005163	0.649534286	0.01	0.66
118.7539	11.87539	36.19618	3.61961836	0.12940823	0.64838605	0.01	0.66
127.481	12.7481	38.85621	3.88562113	0.1477379	0.742798197	0.01	0.75
129.7358	12.97358	39.54346	3.95434618	0.15265651	0.83285901	0.01	0.84
132.0684	13.20684	40.25445	4.02544538	0.15782371	0.979498588	0.01	0.99
133.5507	13.35507	40.70627	4.07062677	0.16114881	1.12909005	0.01	1.14

Table B.18: Determination of 2-hexyl-nonanal column costs at Level 3 of hydroformylation process development (OSN membrane process)

PvapouC8	7.25	mmHg
PvapourC14	3.7	mmHg
α	1.95945946	
R/Rm	1.2	
N/Nm	2	
% recovery	0.995	
% purity	0.9997	
Eo	0.5	

Convers	A	W	D	xf	Rm	R	dC14	wC14	dC15	wC15	xw
0.12	60.20792	2.36625	5.521250188	0.8841698	1.178793284	1.4145519	59.90688	0.30104	0.017977	7.869523	0.038254
0.22	30.33102	2.36625	5.521250188	0.7936210	1.313288716	1.5759464	30.17937	0.151655	0.009057	7.878444	0.019249
0.35	17.01446	2.36625	5.521250188	0.6832579	1.525417405	1.8305008	16.92939	0.085072	0.00508	7.88242	0.010793
0.7	5.746607	2.36625	5.521250188	0.4214876	2.47279757	2.9673570	5.717874	0.028733	0.001716	7.885784	0.003644
0.8	4.338125	2.36625	5.521250188	0.3548387	2.937259923	3.5247119	4.316435	0.021691	0.001295	7.886205	0.00275
0.9	3.242639	2.36625	5.521250188	0.2913385	3.577464789	4.2929577	3.226426	0.016213	0.000968	7.886532	0.002056
0.96	2.694896	2.36625	5.521250188	0.2546583	4.092751632	4.9113019	2.681421	0.013474	0.000805	7.886696	0.001709

Table B.19: Determination of 2-hexyl-nonanal column costs at Level 3 of hydroformylation process development (OSN membrane process) continued

							Material of construction			
			Ft	0.3048 (Ft/m)			**Fp**	1		
							Fm	1		
			L/D	10			**Fc**	1		
Nm	**N**	**Nactual**	**H**	**D**	**H**	**D**	**Column ($M/yr)**	**Total cost ($M/yr)**	**Reboiler ($M/yr)**	**Total cost ($M/yr)**
411.3359	422.67187	453.3437	905.6875	90.56875	905.6875	90.56875	1.32	5.657131	0.01	5.66
412.0422	424.08454	485.1690	911.3381	91.13381	911.3381	91.13381	1.32	4.375265	0.01	4.38
412.6294	425.25893	502.5178	916.0357	91.60357	916.0357	91.60357	1.32	4.025462	0.01	4.03
413.7225	427.44509	542.8901	924.7804	92.47804	924.7804	92.47804	1.32	5.010095	0.01	5.02
414.0046	482.00933	562.0186	927.0373	92.70373	927.0373	92.70373	1.32	5.868972	0.01	5.88
414.2964	488.59291	572.1858	929.3717	92.93717	929.3717	92.93717	1.32	7.280021	0.01	7.29
414.4818	489.96371	572.9274	930.8548	93.08548	930.8548	93.08548	1.32	8.605311	0.01	8.62

Table B.20: Effect of single pass C14 conversion on Separation Cost and EPH3 at Level 3 of hydroformylation process developmet

(OSN scenario)

C14 conversion	flash	membrane	C14 column	C15 column	Total sep cost	Total separation cost (k$/yr)	EPH-2	EPH-3
0.12	0.055041	4.12120867	0.70	1.32	6.19	6 194.06	855.68	849.48
0.22	0.037119	2.79015474	0.66	1.32	4.81	4 808.00	855.71	850.90
0.35	0.027189	2.36613705	0.66	1.32	4.37	4 373.62	855.71	851.34
0.7	0.016564	3.10892064	0.75	1.32	5.20	5 201.59	855.62	850.42
0.8	0.014948	3.83817982	0.84	1.32	6.02	6 019.68	855.54	849.52
0.9	0.013613	5.06102837	0.99	1.32	7.39	7 388.23	855.39	848.01
0.96	0.012915	6.20997845	1.14	1.32	8.69	8 686.33	855.25	846.56

Table B.21: Determination of 7-tetradecene column column costs at Level 3 of hydroformylation process development (Liquid multiphase system)

PvapouC8	7.25	mmHg
PvapourC14	3.7	mmHg
α	1.95945946	
R/Rm	1.2	
N/Nm	2	
% recovery	0.995	
% purity	0.9997	
Eo	0.5	

Convers	A	W	D	xf	Rm	R	dC14	wC14	dC15	wC15	xw
0.12	60.20792	2.36625	5.521250188	0.8841698	1.178793284	1.4145519	59.90688	0.30104	0.017977	7.869523	0.038254
0.22	30.33102	2.36625	5.521250188	0.7936210	1.313288716	1.5759464	30.17937	0.151655	0.009057	7.878444	0.019249
0.35	17.01446	2.36625	5.521250188	0.6832579	1.525417405	1.8305008	16.92939	0.085072	0.00508	7.88242	0.010793
0.7	5.746607	2.36625	5.521250188	0.4214876	2.47279757	2.9673570	5.717874	0.028733	0.001716	7.885784	0.003644
0.8	4.338125	2.36625	5.521250188	0.3548387	2.937259923	3.5247119	4.316435	0.021691	0.001295	7.886205	0.00275
0.9	3.242639	2.36625	5.521250188	0.2913385	3.577464789	4.2929577	3.226426	0.016213	0.000968	7.886532	0.002056
0.96	2.694896	2.36625	5.521250188	0.2546583	4.092751632	4.9113019	2.681421	0.013474	0.000805	7.886696	0.001709

Table B.22: Determination of 7-tetradecene column costs at Level 3 of hydroformylation process development (Liquid multiphase system)

	PvapouC8	7.25	mmHg
	PvapourC14	3.7	mmHg
	α	1.95945946	
	R/Rm	1.2	
	N/Nm	2	
	% recovery	0.995	
	% purity	0.9997	
	Eo	0.5	
ALTERNATIVE			
Separation with C14 recovery	X	0.5	

Inlet

Conver	**A**	**D**	**xf**	**Rm**	**R**	**dC14**	**wC14**	**dC15**	**wC15**	**xw**	**Nm**	**Nactual**
0.12	30.10395936	5.52125	0.845018	1.23340919	1.48009103	29.95344	0.150519797	0.008989	5.512261	0.027306	11.68438	46.73751
0.22	15.16551188	5.52125	0.733102	1.42170279	1.70604335	15.08968	0.075827559	0.004528	5.516722	0.013745	12.38466	49.53866
0.35	8.507232432	5.52125	0.606426	1.71868296	2.06241955	8.464696	0.042536162	0.00254	5.51871	0.007708	12.96924	51.87694
0.7	2.873303669	5.52125	0.342282	3.04501519	3.65401823	2.858937	0.014366518	0.000858	5.520392	0.002602	14.06013	56.2405
0.8	2.169062574	5.52125	0.282051	3.69526248	4.43431498	2.158217	0.010845313	0.000648	5.520603	0.001965	14.34197	57.36788
0.9	1.6213195	5.52125	0.226994	4.5915493	5.50985915	1.613213	0.008106597	0.000484	5.520766	0.001468	14.63355	58.53421
0.96	1.347447962	5.52125	0.196172	5.31295088	6.37554105	1.340711	0.00673724	0.000402	5.520848	0.00122	14.81884	59.27537

Table B.23: Determination of 7-tetradecene column (Hydroformylation Process section) (Liquid multiphase system) continoued

				Material of construction			
Ft	0.3048			**Fp**	1		
				Fm	1		
L/D	10			**Fc**	1		
H	**D**	**H**	**D**	**Cost of column**	**Total cost ($ M/yr)**	**R+C ($ M/yr)**	**Total cost ($M/yr)**
108.475	10.8475	33.06319	3.30631862	0.10927372	0.687437831	0.01	0.70
114.0773	11.40773	34.77077	3.4770767	0.12005163	0.649534286	0.01	0.66
118.7539	11.87539	36.19618	3.61961836	0.12940823	0.64838605	0.01	0.66
127.481	12.7481	38.85621	3.88562113	0.1477379	0.742798197	0.01	0.75
129.7358	12.97358	39.54346	3.95434618	0.15265651	0.83285901	0.01	0.84
132.0684	13.20684	40.25445	4.02544538	0.15782371	0.979498588	0.01	0.99
133.5507	13.35507	40.70627	4.07062677	0.16114881	1.12909005	0.01	1.14

Table B.24: Determination of 2-hexyl-nonanal column costs at Level 3 of hydroformylation process development (Liquid multiphase system) continoued

		Material of construction	
Ft	0.3048	**Fp**	1
		Fm	1
L/D	10	**Fc**	1

H	**D**	**H**	**D**	**Cost of column**	**Total cost ($ M/yr)**	**R+C ($ M/yr)**	**Total cost ($M/yr)**
108.475	10.8475	33.06319	3.30631862	0.10927372	0.687437831	0.01	0.70
114.0773	11.40773	34.77077	3.4770767	0.12005163	0.649534286	0.01	0.66
118.7539	11.87539	36.19618	3.61961836	0.12940823	0.64838605	0.01	0.66
127.481	12.7481	38.85621	3.88562113	0.1477379	0.742798197	0.01	0.75
129.7358	12.97358	39.54346	3.95434618	0.15265651	0.83285901	0.01	0.84
132.0684	13.20684	40.25445	4.02544538	0.15782371	0.979498588	0.01	0.99
133.5507	13.35507	40.70627	4.07062677	0.16114881	1.12909005	0.01	1.14

Table B.25: Determination of 2-hexyl-nonanal column costs at Level 3 of hydroformylation process development (LMS scenario)

PvapouC8	7.25	mmHg	
PvapourC14	3.7	mmHg	
α	1.95945946		
R/Rm	1.2		
N/Nm	2		
% recovery	0.995		
% purity	0.9997		
Eo	0.5		

Convers	A	W	D	xf	Rm	R	dC14	wC14	dC15	wC15	xw
0.12	60.20792	2.36625	5.521250188	0.8841698	1.178793284	1.4145519	59.90688	0.30104	0.017977	7.869523	0.038254
0.22	30.33102	2.36625	5.521250188	0.7936210	1.313288716	1.5759464	30.17937	0.151655	0.009057	7.878444	0.019249
0.35	17.01446	2.36625	5.521250188	0.6832579	1.525417405	1.8305008	16.92939	0.085072	0.00508	7.88242	0.010793
0.7	5.746607	2.36625	5.521250188	0.4214876	2.47279757	2.9673570	5.717874	0.028733	0.001716	7.885784	0.003644
0.8	4.338125	2.36625	5.521250188	0.3548387	2.937259923	3.5247119	4.316435	0.021691	0.001295	7.886205	0.00275
0.9	3.242639	2.36625	5.521250188	0.2913385	3.577464789	4.2929577	3.226426	0.016213	0.000968	7.886532	0.002056
0.96	2.694896	2.36625	5.521250188	0.2546583	4.092751632	4.9113019	2.681421	0.013474	0.000805	7.886696	0.001709

Table B.26: Determination of 2-hexyl-nonanal column costs at Level 3 of hydroformylation process development (LMS scenario)

							Material of construction			
			Ft	0.3048 (Ft/m)			**Fp**	1		
							Fm	1		
			L/D	10			**Fc**	1		
Nm	**N**	**Nactual**	**H**	**D**	**H**	**D**	**Column ($M/yr)**	**Total cost ($M/yr)**	**Reboiler ($M/yr)**	**Total cost ($M/yr)**
411.3359	422.67187	453.3437	905.6875	90.56875	905.6875	90.56875	0.957758	5.657131	0.01	5.66
412.0422	424.08454	485.1690	911.3381	91.13381	911.3381	91.13381	1.055628	4.375265	0.01	4.38
412.6294	425.25893	502.5178	916.0357	91.60357	916.0357	91.60357	1.140347	4.025462	0.01	4.03
413.7225	427.44509	542.8901	924.7804	92.47804	924.7804	92.47804	1.306114	5.010095	0.01	5.02
414.0046	482.00933	562.0186	927.0373	92.70373	927.0373	92.70373	1.35059	5.868972	0.01	5.88
414.2964	488.59291	572.1858	929.3717	92.93717	929.3717	92.93717	1.397318	7.280021	0.01	7.29
414.4818	489.96371	572.9274	930.8548	93.08548	930.8548	93.08548	1.427391	8.605311	0.01	8.62

Table B.27: Determination 2-hexyl-nonanal column costs at Level 3 of hydroformylation process development (LMS scenario) continued

				Material of construction		
Ft	0.3048			**Fp**		1
				Fm		1
L/D	10			**Fc**		1
H	**D**	**H**	**D**	**Total cost ($M/yr)**	**total cost ($M/yr)**	**EPH-3 ($M/yr)**
928.475	90.8475	533.06319	53.30631862	1.32	2.02	974.06
914.0773	91.40773	534.77077	53.4770767	1.32	1.98	974.13
918.7539	91.87539	536.19618	53.61961836	1.32	1.98	974.13
927.481	92.7481	538.85621	53.88562113	1.32	2.08	973.94
929.7358	92.97358	539.54346	53.95434618	1.32	2.17	973.76
932.0684	93.20684	540.25445	54.02544538	1.32	2.31	973.46
933.5507	93.35507	540.70627	54.07062677	1.32	2.46	973.16

Table B.28: Effect of single pass C14 conversion on separation costs and EPH-3 at Level 3 of hydroformylation process development (LMS Scenario)

C14 conversion	flash	C14 column	C15 column	total	EPH-2	Cost (k$/yr)	EPH-3
0.12	0.055041	0.70	1.32	2.07	855.68	2 072.85	853.61
0.22	0.037119	0.66	1.32	2.02	855.71	2 017.84	853.69
0.35	0.027189	0.66	1.32	2.01	855.71	2 007.48	853.70
0.7	0.016564	0.75	1.32	2.09	855.62	2 092.67	853.53
0.8	0.014948	0.84	1.32	2.18	855.54	2 181.50	853.35
0.9	0.013613	0.99	1.32	2.33	855.39	2 327.20	853.07
0.96	0.012915	1.14	1.32	2.48	855.25	2 476.35	852.77

Table B.29: Assumptions and justifications

Unit	Description	Justification
% Filled Volume	75 %	75 % of the vessel is dedicated to fluid (Douglas, 1988)
Material factor	Fm	Determined from Guthrie cost tables (Turton et al., 2012)
Pressure factor	Fp	Determined from Guthrie cost tables (Turton et al., 2012)
Flash residence time	5 mins	Peters and Timmerhaus 2004
L/D (CSTR reactor)	1-1.5	Peters and Timmerhaus 2004
L/D (columns)	At least 10	Peters and Timmerhaus 2004

Appendix C: Chapter 5: Aspen Plus™ Simulation

C.1.1 Determination of physical property method

High temperature or pressure process steps are encountered in these designs. However, two different phases of matter (gas phase, and liquid phase) are processed and the components present (H_2, CO, Marlipal, Water, alkenes, aldehydes and gasses above their critical temperatures) make for a highly complex system. This means that no single physical property method is sufficient for accurate simulation of this system. The following passage details how the thermodynamic property method was selected in this study.

C.1.1.1 Model Selection Algorithm

Before application of any algorithm to the selection of a physical property method it is important to define the system in terms of its components. The nature of the components and the level of their interaction determine whether an equation of state based (EOS) or activity coefficient based method will be used or not. The components and their critical properties in the C8 upgrading to C15 aldehydes are listed in Table C.1

Table C.1: Key components and critical properties

Component	Critical Temperature (T_c/°C)	Critical Pressure (P_c/bar)	References
H_2	-242	20.3	www.airliquide.com
CO	-140.7	34.99	www.airliquide.com
C_2H_4	9.20	50.42	Steele and Chirico 1992
C_7H_{14}	264.15	29.21	Steele and Chirico 1992
C_8H_{16}	294.25	26.75	Steele and Chirico 1992
$C_{14}H_{28}$	418.85	16.20	Steele and Chirico 1992
$C_{10}H_{22}$	244.55	21.10	www.colonicalchemical.com
Marlipal	374.15	44.20	www.colonicalchemical.com
$C_{15}H_{30}O$	454.34	65.34	www.alibaba.com

Several algorithms are documented for selecting physical property methods are listed in literature. For the purpose of this project three of those many algorithms were reviewed and compared for the purpose of developing a physical property model for the whole or sections of the simulation. The Aspen method (Aspen Technology, 2009), Bob Seader method (Seider et al., 2004) and the Eric Carlson (1996) method were reviewed. The Aspen method is in reality composed of a number of alternative algorithms. One set emerges from the use of the built-in property method selection assistant and another algorithm that is presented in the Aspen User Manual (2009). The use of the property method selection assistant will be discussed briefly but not illustrated like the other three methods, shown in Figure C.1-C.3.

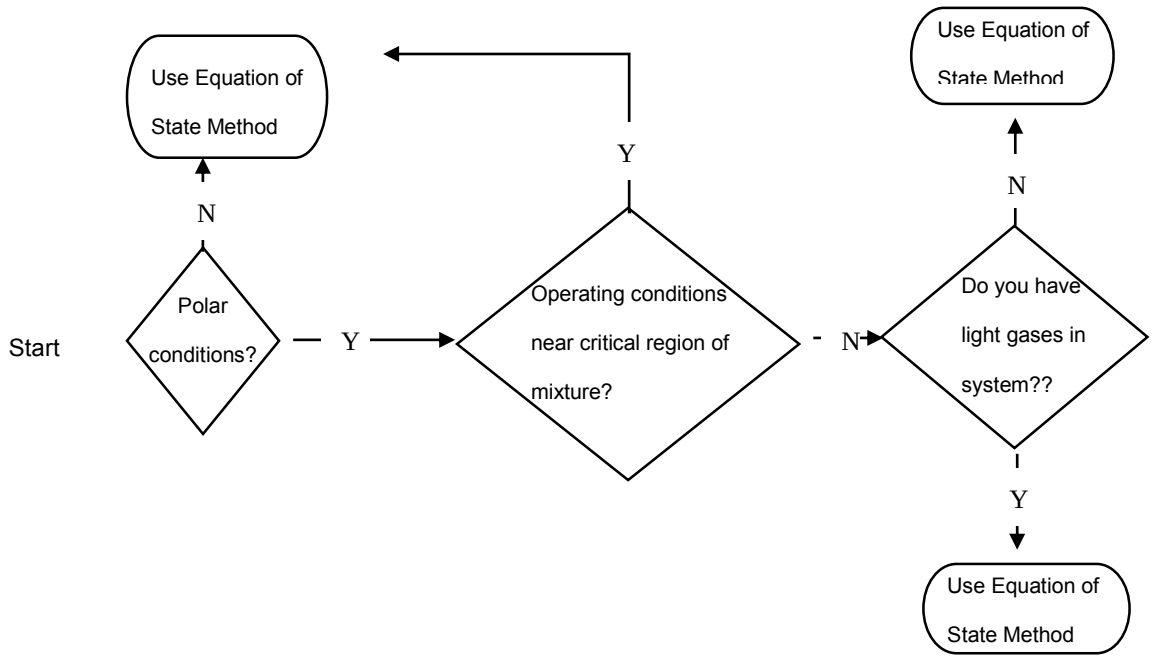

Figure C.1: The Aspen property method selection algorithm (ASPEN TECH 2009)

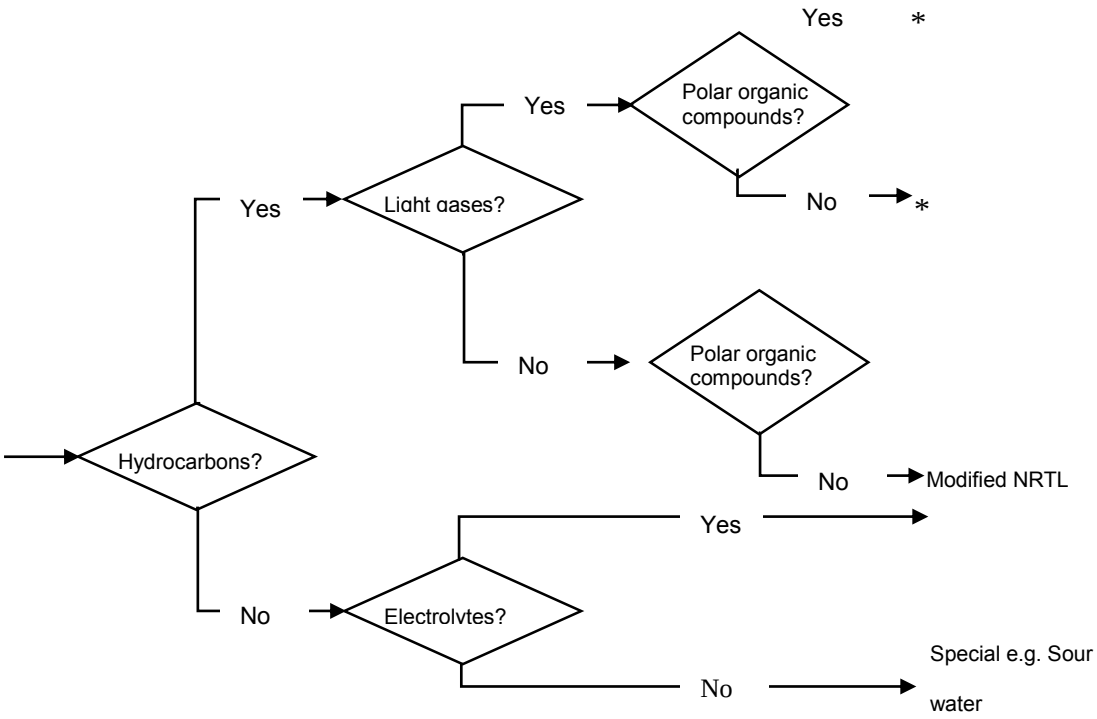

Figure C.2: The Bob Seader property method selection algorithm

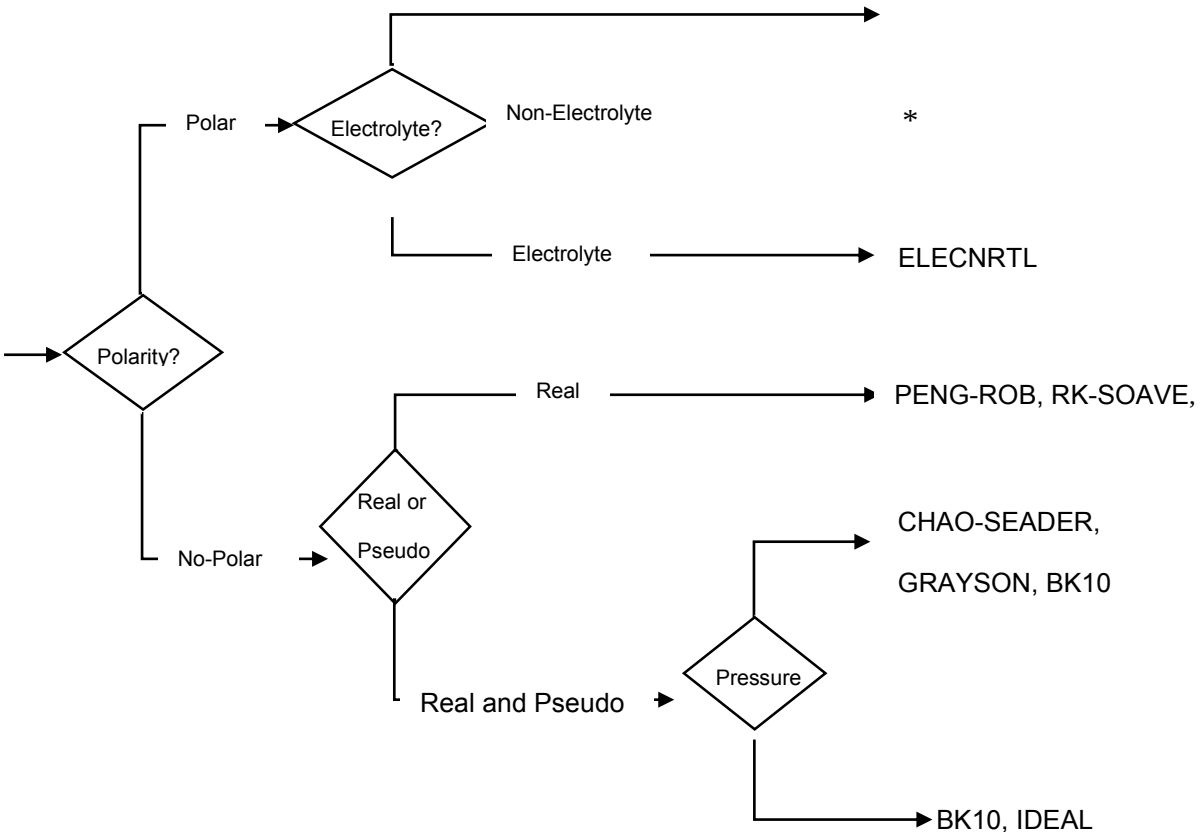

Figure C.3: The Eric Carlson physical property method selection algorithm (Carlson 1996)

The Figures C.1-C.3 above shows an Aspen Technology (2009), Bob Seader and Carlson, (1996) physical property selection algorithms. Rules for the physical property selection as given by the three algorithms were considered in order to come up with physical property method that accurately represent the system under question. The Aspen flowchart in Figure C.1 recommends the use of EOS for the Metathesis section and the activity coefficient based method with Henry's law for the Hydroformylation section. The Bob Seader method recommends a further evaluation of the physical property for nonpolar Metathesis reaction system and a special system e.g. PC-SAFT method for the Hydroformylation section since it contains non-hydrocarbon components. Either PENG-ROB, RK-SOAVE, LK-PLOCK, PR-BM, RKS-BM can be used for the metathesis section according to Carlson 1996 and a further evaluation of polar non-electrolyte hydroformylation system be conducted as was shown in the selected physical property method in Figure C.3. However, in previous simulation study on the Hydroformylation of long chain alkenes, Hentschel et al. (2014), Hentschel et al. (2015) and Schafer et al. (2012), recommends the use of PC-SAFT property method for the more complex Hydroformylation system and the UNIFAC-Dortmund to model the LLE three phase decanter system.

The available activity coefficient based methods in Aspen Plus™ include UNIFAC, UNIQUAC, Non- Random-Two-Liquid (NRTL), and WILSON among others. It is also important to define different sections of the process into low pressure (<10bar), high pressure (>10bar) region and polar and nonpolar sections according to Aspen Tech recommendations. As already mentioned, the composition of the mixture is highly complex. Components, such as Marlipal, and water, have strong dipoles and many of the polar compounds are associative and form complexes. Therefore, it is suggested that equation-of-state models like CPA or SAFT be used as the property method for the hydroformylation reaction section. These models explicitly account for association and will most accurately simulate the thermodynamic properties of these components. The following diagram Figure C.4 illustrates the decision making process which were followed in choosing the property methods used in simulations. Dashed blocks

indicate decisions made (i.e. system and component characteristics and properties) and dark blocks specify the final options for possible property methods. Almost all the property methods available in Aspen Plus™ are illustrated in this diagram.

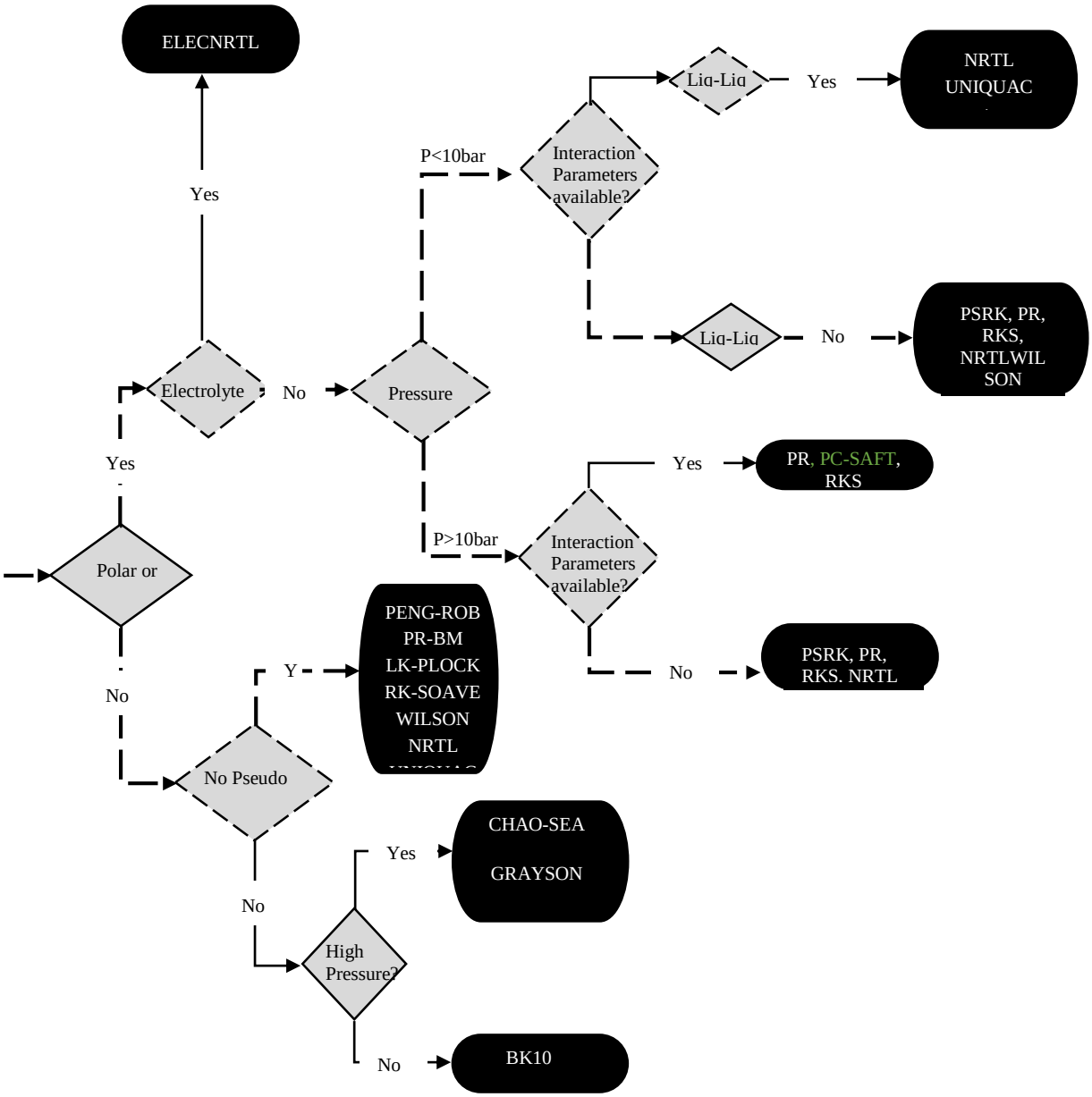

Figure C.5 Property method selection for the study

Methods that are based on Raoult's law, or that use activity coefficients, are not accurate at high pressure or when the temperature is above the critical temperature of a component. Henry's law is used when there are light gases in subcritical solvents (e.g. CO and H2, which

are above their critical temperatures in the simulations). The availability of pure-component and binary parameters is a very important factor for calculating pure-component or mixture properties. The choice of property method is highly dependent on the availability of binary parameters in ASPEN Plus, seeing that obtaining of experimental data and regression thereof are not in the scope of this project.

C.1.2 Design Specifications

The phase behaviour of microemulsions using 1-dodecene has been studied in detail and it is known from the literature that the general pattern observed with 1-dodecene can also be applied when using 7-tetradecene as alkene (Haumann et al., 2002). Hence, the following design specifications for 1-dodecene hydroformylation must also allow the determination of alkene/surfactant/water ratio during the hydroformylation 7-tetradecene.

$$\alpha = \frac{m_{olefin}}{m_{olefin} + m_{water}} = 50\ \%$$

$$\gamma = \frac{m_{surfactant}}{m_{olefin} + m_{water} + m_{surfactant}} = 8\ \%$$

This design specification made sure that the catalyst loss in the product stream lies to a minimum (lower than 1 ppm) ensure economic feasibility according to Muller et al. (2013) and Muller et al. (2015)

C1.1.3 Section AREA-A100 simulation flowsheet

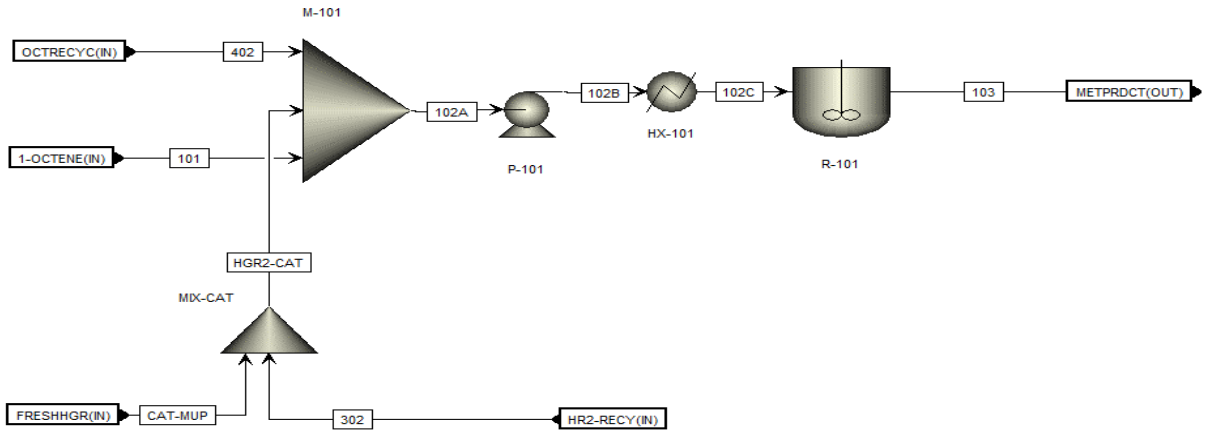

Figure C.6 Section AREA-A100 Aspen Plus™ flowsheet

Table C.2 stream Table Section AREA-A100

Stream	Units	101	101A	101B	101C	103	302	402	CAT-MUP	HGR-2 CAT
Mass flow	tonne/yr									
1-OCT-01	tonne/yr.	14159.64	31100.76	31100.76	31100.76	16941.12	10050.09	6891.03	0.00	10050.09
7-TET-01	tonne/yr.	0.00	18586.20	18586.20	18586.20	30977.03	18586.08	0.12	0.00	18586.08
ETHYL-01	tonne/yr.	0.00	73.75	73.75	73.75	1843.70	44.25	29.50	0.00	44.25
2-OCT-01	tonne/yr.	0.00	0.00	0.00	0.00	5.46	0.00	0.00	0.00	0.00
6-TRIDEC	tonne/yr.	0.00	0.80	0.80	0.80	0.80	0.48	0.32	0.00	0.48
PROPYLEN	tonne/yr.	0.00	0.00	0.00	0.00	0.00	0.00	0.00	0.00	0.00
HYDRO-01	tonne/yr.	0.00	0.00	0.00	0.00	0.00	0.00	0.00	0.00	0.00
CARB-01	tonne/yr.	0.00	0.00	0.00	0.00	0.00	0.00	0.00	0.00	0.00
MARLIPAL	tonne/yr.	0.00	0.00	0.00	0.00	0.00	0.00	0.00	0.00	0.00
WATER	tonne/yr.	0.00	0.00	0.00	0.00	0.00	0.00	0.00	0.00	0.00
2-HEXYLNO	tonne/yr.	0.00	0.00	0.00	0.00	0.00	0.00	0.00	0.00	0.00
ISO-ALDEH	tonne/yr.	0.00	0.00	0.00	0.00	0.00	0.00	0.00	0.00	0.00
HGR-2-CATA	tonne/yr.	0.00	11.86	11.86	11.86	11.86	11.86	0.00	0.00	11.86
RHO-CAT	tonne/yr.	0.00	0.00	0.00	0.00	0.00	0.00	0.00	0.00	0.00
Total flow	tonne/yr.	14159.64	49773.37	49773.37	49773.37	49773.37	28692.76	6920.97	0.00	28692.76
Temperature	°C	30.00	36.10	36.10	50.00	50.00	30.00	157.00	30.00	30.00
Pressure	bar	1.00	1.06	2.00	2.00	2.00	1.00	1.00	1.00	1.00
Vapour fraction			0	0	0	0	0	0	0	0

C.1.1.4 Aspen Plus™ Section AREA-A200

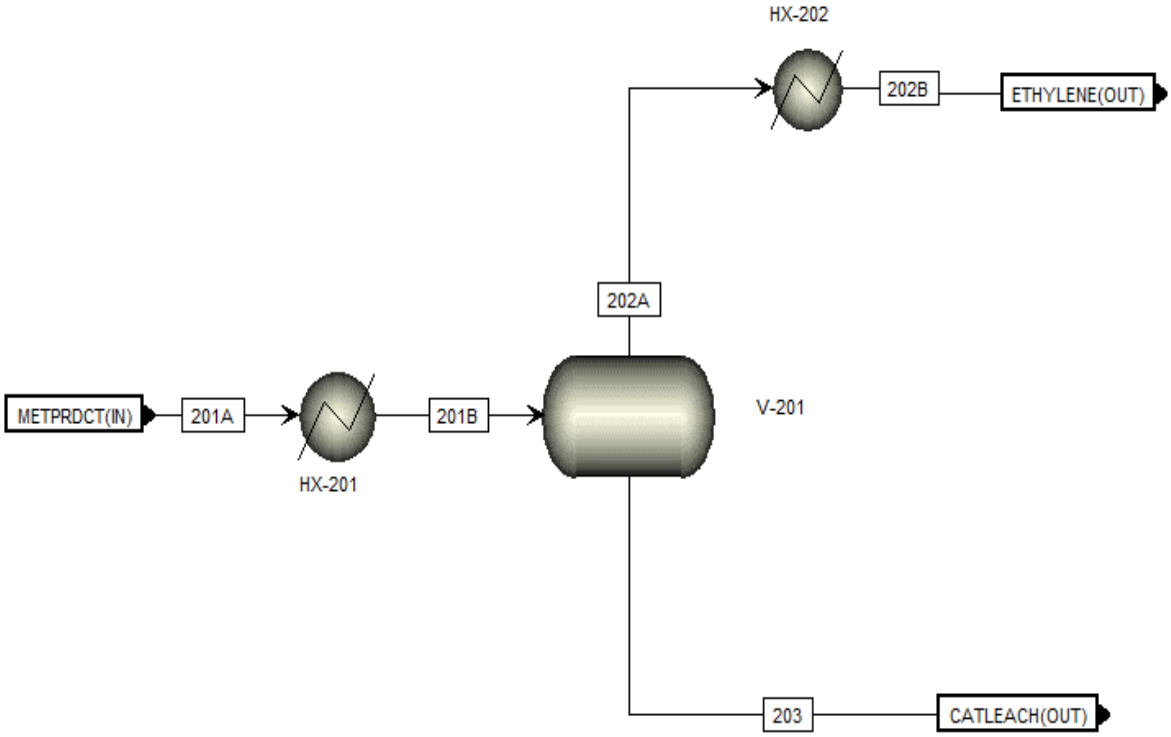

Figure C.7 Section AREA-A200 Aspen Plus™ flowsheet

Table C.3 Stream Table Section AREA-A200

Stream	Units	201A	201B	202A	202B	203
Mass flow	tonne/yr					
1-OCT-01	tonne/yr	16941.1166	16941.12	190.97	190.971836	16750.14
7-TET-01	tonne/yr	30977.0256	30977.03	0.228607	0.228607	30976.797
ETHYL-01	tonne/yr	1843.70319	1843.703	1769.95506	1769.95506	73.7481275
2-OCT-01	tonne/yr	5.46123	5.46123	5.46	5.46	0
6-TRIDEC	tonne/yr	0.8	0.8	0	0	0.8
PROPYLEN	tonne/yr	0	0	0	0	0
HYDRO-01	tonne/yr	0	0			
CARB-01	tonne/yr	0	0			
MARLIPAL	tonne/yr	0	0			
WATER	tonne/yr	0	0			
2-HEXYLNO	tonne/yr	0	0			
ISO-ALDEH	tonne/yr	0	0			
HGR-2-CATA	tonne/yr	11.861917	11.86192	0	0	11.861917
RHO-CAT	tonne/yr	0	0			
Total flow	tonne/yr	49779.9686	49779.97	1966.61673	1966.61673	47813.35
Temperature	°C	50	33	33	33	33
Pressure	bar	2	2	1	1	1
Vapour fraction		0	0	0	0	0

C.1.1.4 Aspen Plus™ Section AREA-A300

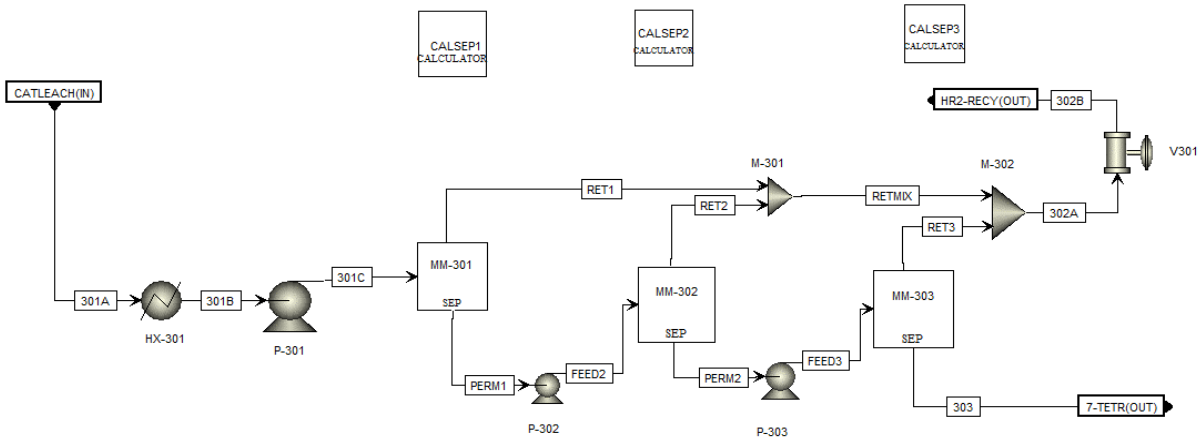

Figure C.8 Section AREA-A300 Aspen Plus™ flowsheet

Table C.4 Stream Table Section AREA-A200

Stream	Units	301A	301B	301C	302A	302B	303
Mass flow	tonne/yr						
1-OCT-01	tonne/yr	16750.14	16750.14	16750.14	10050.087	10050.0869	6700.06
7-TET-01	tonne/yr	30976.80	30976.80	30976.80	18586.078	18586.0782	12390.95
ETHYL-01	tonne/yr	73.75	73.75	73.75	44.248877	44.2488765	29.50
2-OCT-01	tonne/yr	0.00	0.00	0.00	0	0	0.00
6-TRIDEC	tonne/yr	0.80	0.80	0.80	0.48	0.48	0.32
PROPYLEN	tonne/yr	0.00	0.00	0.00	0	0	0.00
HYDRO-01	tonne/yr	0.00	0.00	0.00	0	0	0.00
CARB-01	tonne/yr	0.00	0.00	0.00	0	0	0.00
MARLIPAL	tonne/yr	0.00	0.00	0.00	0	0	0.00
WATER	tonne/yr	0.00	0.00	0.00	0	0	0.00
2-HEXYLNO	tonne/yr	0.00	0.00	0.00	0	0	0.00
ISO-ALDEH	tonne/yr	0.00	0.00	0.00	0	0	0.00
HGR-2-CATA	tonne/yr	11.86	11.86	11.86	11.86	11.861917	0.00
RHO-CAT	tonne/yr	0.00	0.00	0.00	0	0	0.00
Total flow	tonne/yr	47813.35	47813.35	47813.35	28692.56	28692.7559	19120.82
Temperature	°C	33	30	30	30	30	30
Pressure	bar	1	1	40	40	40	40
Vapour fraction		0	0	0	0	0	0

C.1.1.5 Aspen Plus™ Section AREA-A400

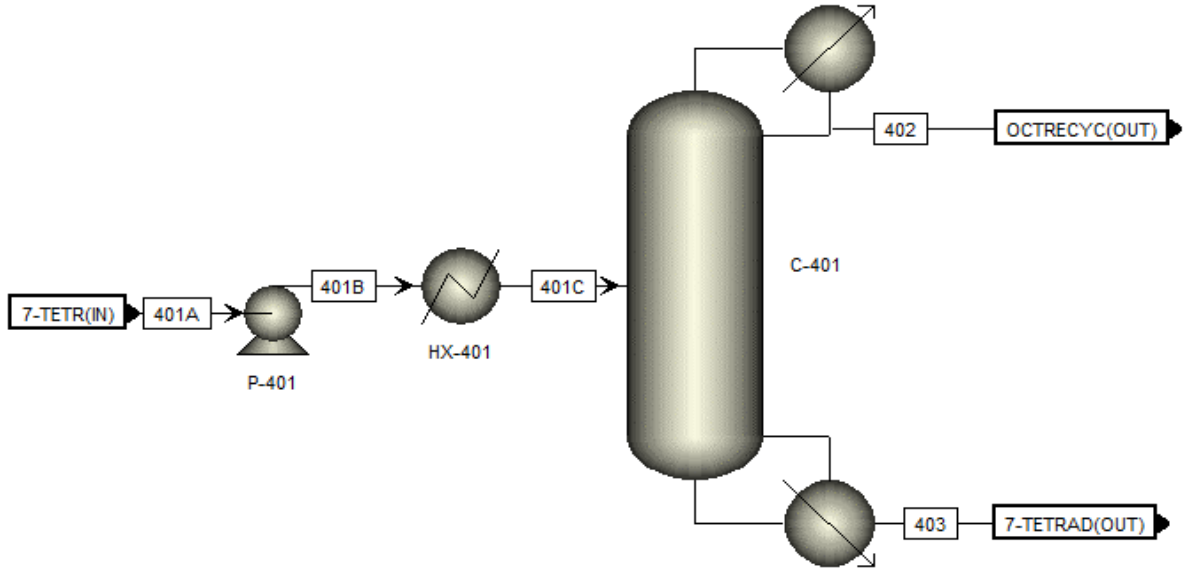

Figure C.9 Section AREA-A400 Aspen Plus™ flowsheet

Table C.5 Stream Table Section AREA-A400

Stream	Units	401A	401B	401C	402	403
Mass flow	tonne/yr					
1-OCT-01	tonne/yr	6700.06	6700.06	6891.02976	6891.03	0
7-TET-01	tonne/yr	12390.95	12390.95	12390.95	0.123909	12390.8235
ETHYL-01	tonne/yr	29.50	29.50	29.50	29.50	0.00
2-OCT-01	tonne/yr	0.00	0.00	0.00	0.00	0.00
6-TRIDEC	tonne/yr	0.32	0.32	0.32	0.32	0.32
PROPYLEN	tonne/yr	0.00	0.00	0.00	0.00	0.00
HYDRO-01	tonne/yr	0.00	0.00	0.00	0.00	0.00
CARB-01	tonne/yr	0.00	0.00	0.00	0.00	0.00
MARLIPAL	tonne/yr	0.00	0.00	0.00	0.00	0.00
WATER	tonne/yr	0.00	0.00	0.00	0.00	0.00
2-HEXYLNO	tonne/yr	0.00	0.00	0.00	0.00	0.00
ISO-ALDEH	tonne/yr	0.00	0.00	0.00	0.00	0.00
HGR-2-CATA	tonne/yr	0.00	0.00	0.00	0.00	0.00
RHO-CAT	tonne/yr	0.00	0.00	0.00	0.00	0.00
Total flow	tonne/yr	19120.82	19120.82	19120.82	6920.973	12199.85
Temperature	°C	30	30	120	150	171
Pressure	bar	1	1	1	1	1.5
Vapour fraction		0	0	0	0	0

C.1.1.6 Aspen Plus™ Section AREA-A500

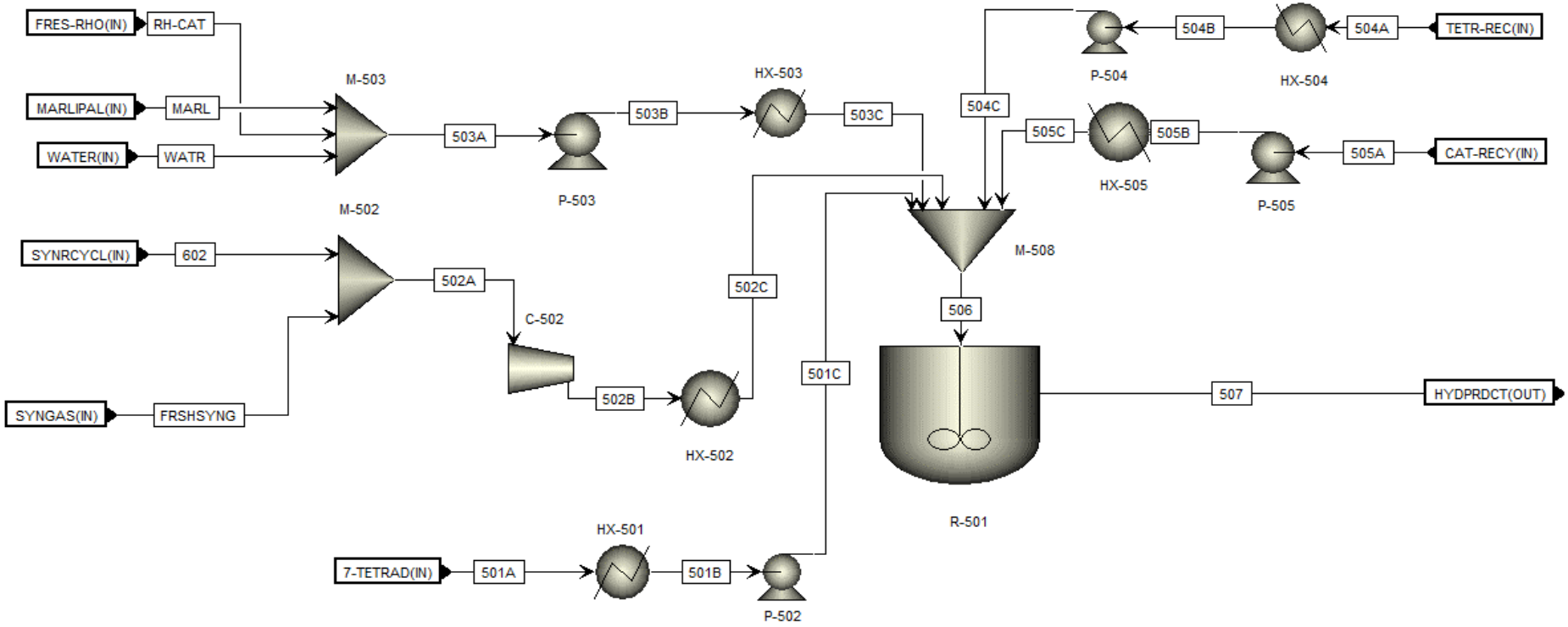

Figure C.10 Section AREA-A500 Aspen Plus™ flowsheet

Table C.6 Stream Table Section AREA-A500

Stream	Units	501A	501B	501C	502A	502B	502C	503A	503B	503C	504A
Mass flow	tonne/yr										
1-OCT-01	tonne/yr	0	0	0	0	0	0	0	0	0	0
7-TET-01	tonne/yr	12390.8235	12390.8235	12390.82	0	0	0	0	0	0	15044.16
ETHYL-01	tonne/yr	0	0	0	0	0	0	0	0	0	0
2-OCT-01	tonne/yr	0	0	0	0	0	0	0	0	0	0
6-TRIDEC	tonne/yr	0.32	0.32	0.32	0	0	0	0	0	0	67.75789
PROPYLEN	tonne/yr	0	0	0	0	0	0	0	0	0	0
HYDRO-01	tonne/yr	0	0	0	2809.759	2809.759	2809.759	0	0	0	141.117
CARB-01	tonne/yr	0	0	0	3855.337	3855.337	3855.337	0	0	0	59.44621
MARLIPAL	tonne/yr	0	0	0	0	0	0	495.63294	495.6329	495.6329	346.8043
WATER	tonne/yr	0	0	0	2022.378	0	0	12.056	12.056	12.056	3008.832
2-HEXYLNO	tonne/yr	0	0	0	0	0	0	0	0	0	15.04416
ISO-ALDEH	tonne/yr	0	0	0	0	0	0	0	0	0	5.01472
HGR-2-CATA	tonne/yr	0	0	0	0	0	0	0	0	0	0
RHO-CAT	tonne/yr	0	0	0	0	0	0	0	0	0	21.92605
Total flow	tonne/yr	12391.1435	12391.1435	12391.14	8687.474	6665.096	6665.096	507.68894	507.6889	507.6889	18710.1
Temperature	°C	175	160	160	30	120	160	30	30	160	180
Pressure	bar	1.5	1.5	40	15	40	40	1	40	40	0.01
Vapour fraction		0	0	0	1	0	0	0	0	0	0

Table C.7 Continued Stream Table Section AREA-A500

Stream	Units	504B	504C	505A	505B	505C	506	507	RH-CAT	MARL	WATR	602	FRSHSYNG
Mass flow	tonne/yr												
1-OCT-01	tonne/yr	0	0	0	0	0	0	0	0	0	0	0	0
7-TET-01	tonne/yr	15044.16	15044.16	0.01074	0.01074	0.01074	27434.99	15063.18	0	0	0	12.99926	0
ETHYL-01	tonne/yr	0	0	0	0	0	0	0	0	0	0	0	0
2-OCT-01	tonne/yr	0	0	0	0	0	0	0	0	0	0	0	0
6-TRIDEC	tonne/yr	67.75789	67.75789	0.006	0.006	0.006	68.08389	68.08389	0	0	0	0.098	0
PROPYLEN	tonne/yr	0	0	0	0	0	0	0	0	0	0	0	0
HYDRO-01	tonne/yr	141.117	141.117	118.3335	118.3335	118.3335	3069.209	2823.47	0	0	0	2682.297	127.462
CARB-01	tonne/yr	59.44621	59.44621	59.47	59.47	59.47	3974.254	2147.37	0	0	0	2087.9	1767.437
MARLIPAL	tonne/yr	346.8043	346.8043	283.9431	283.9431	283.9431	1126.38	1126.38	0	0.138777	0	148.6899	0
WATER	tonne/yr	3008.832	3008.832	25170.42	25170.42	25170.42	27434.99	30213.69	0	0	0.1	2022.38	0
2-HEXYLNO	tonne/yr	15.04416	15.04416	10544	10544	10544	10559.04	21533.04	0	0	0	0.77	0
ISO-ALDEH	tonne/yr	5.01472	5.01472	43.717	43.717	43.717	48.73172	3669.727	0	0	0	0.32	0
HGR-2-CATA	tonne/yr	0	0	0	0	0	0	0	0	0	0	0	0
RHO-CAT	tonne/yr	21.92605	21.92605	21.93483	21.93483	21.93483	43.86088	43.86088	21.93483	0	0	0	0
Total flow	tonne/yr	18710.1	18710.1	36241.84	36241.84	36241.84	76538.25	76538.24	21.93483	0.138777	0.1	6955.454	1894.899
Temperature	°C	176	160	75	75	160	160	160	30	30	30	75	30
Pressure	bar	0.01	0.01	15	40	40	40	40	1	1	1	15	15
Vapour fraction		0	0	0	0	0	0	0	0	0	0	1	1

C.1.1.7 Aspen Plus™ Section AREA-A600

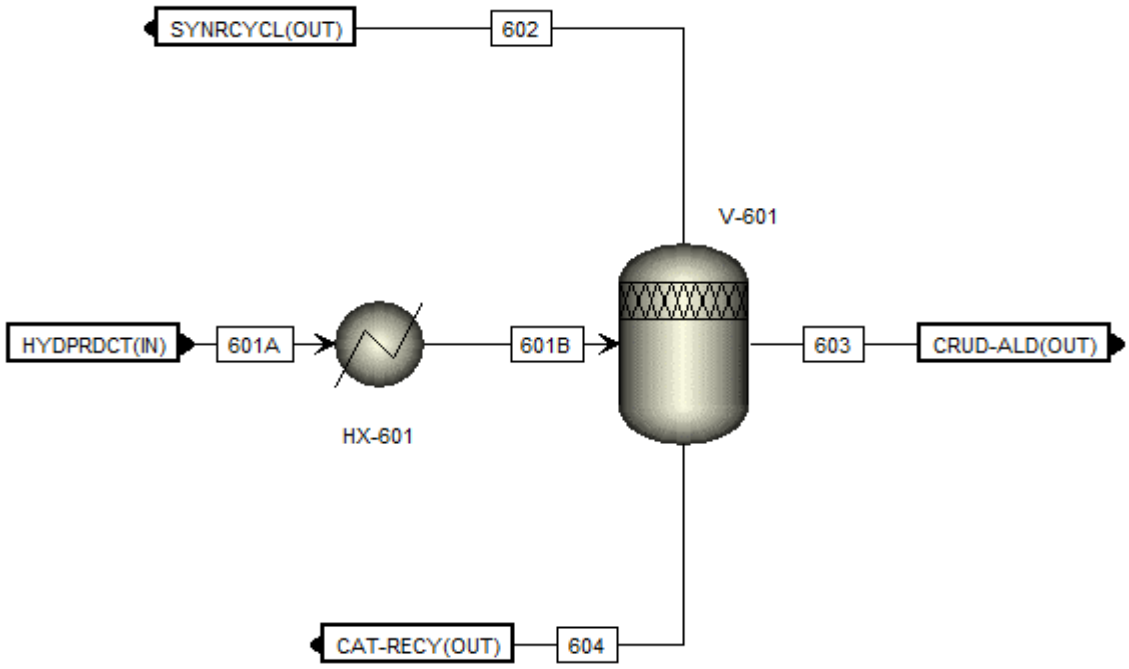

Figure C.11: Section AREA-A600 Aspen Plus™ flowsheet

Table C.8 Stream Table Section AREA-A600

Stream	Units	601A	601B	602	603	604
Mass flow	tonne/yr					
1-OCT-01	tonne/yr	0	0	0	0	0
7-TET-01	tonne/yr	15063.18	15063.18	12.99926	15050.17	0.01074
ETHYL-01	tonne/yr	0	0	0	0	0
2-OCT-01	tonne/yr	0	0	0	0	0
6-TRIDEC	tonne/yr	67.883	67.883	0.098	67.779	0.006
PROPYLEN	tonne/yr	0	0	0	0	0
HYDRO-01	tonne/yr	2823.47	2823.47	2682.297	22.84	118.3335
CARB-01	tonne/yr	2147.37	2147.37	2087.9	0	59.47
MARLIPAL	tonne/yr	495.63294	495.63294	148.6899	63	283.9431
WATER	tonne/yr	27454.0035	27454.0035	2105.38	261.2	25170.42
2-HEXYLNO	tonne/yr	21533.0421	21533.0421	0.77	10905	10544
ISO-ALDEH	tonne/yr	3669.727	3669.727	0.32	3625.69	43.717
HGR-2-CATA	tonne/yr	0	0	0	0	0
RHO-CAT	tonne/yr	21.9436063	21.9436063	0	0.029996	21.91361
Total flow	tonne/yr	73276.2522	73276.2522	6955.454	29995.71	36241.82
Total flow	tonne/yr	75624.4665	75624.4665	7187.144	29995.69	38524.63
Temperature	°C	160	75	75	75	75
Pressure	bar	40	40	15	15	15
Vapour fraction		0	0	1	0	0

C.1.1.8 Aspen Plus™ Section AREA-A700

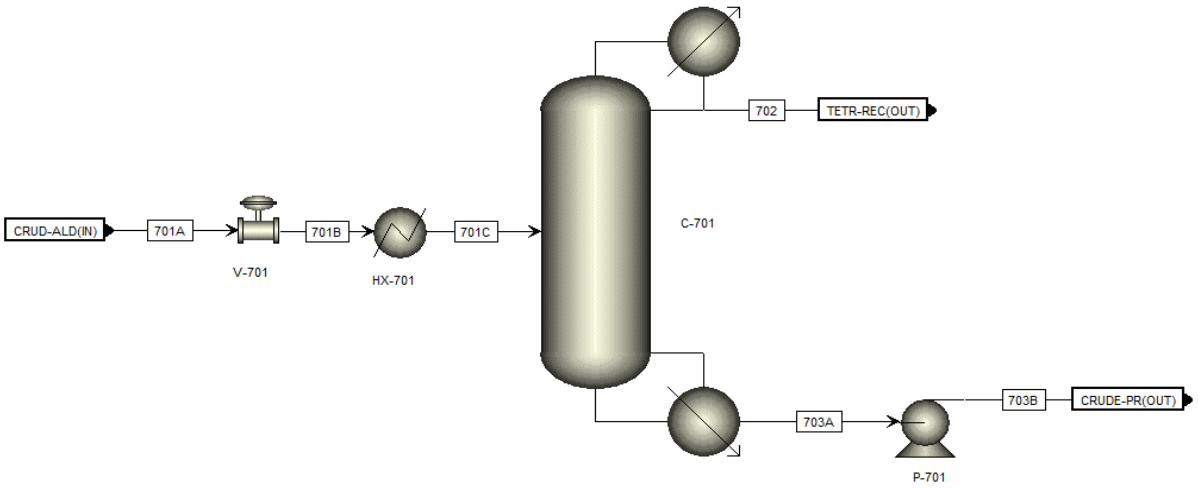

Figure C.12: Section AREA-A700 Aspen Plus™ flowsheet

Table C.9 Stream Table Section AREA-A700

Stream	Units	701A	701B	702	703
Mass flow	tonne/yr				
1-OCT-01	tonne/yr	0	0	0	0
7-TET-01	tonne/yr	15050.17	15050.17	15044.15	6.020068
ETHYL-01	tonne/yr	0	0	0	0
2-OCT-01	tonne/yr	0	0	0	0
6-TRIDEC	tonne/yr	67.779	67.779	67.75189	0.027112
PROPYLEN	tonne/yr	0	0	0	0
HYDRO-01	tonne/yr	22.84	22.84	22.83086	0.009136
CARB-01	tonne/yr	0	0	0	0
MARLIPAL	tonne/yr	63	63	0.0252	62.9748
WATER	tonne/yr	261.2	261.2	261.0955	0.10448
2-HEXYLNO	tonne/yr	10905	10905	449	10456
ISO-ALDEH	tonne/yr	3625.69	3625.69	1.450276	3624.24
HGR-2-CATA	tonne/yr	0	0	0	0
RHO-CAT	tonne/yr	0.029996	0.029996	0.029984	1.2E-05
Total flow	tonne/yr	29995.71	29995.71	15846.33	14149.38
Temperature	°C	30	121	150	171
Pressure	bar	1	1	0.01	0.015
Vapour fraction		0	0	0	0

C.1.1.9 Aspen Plus™ Section AREA-A800

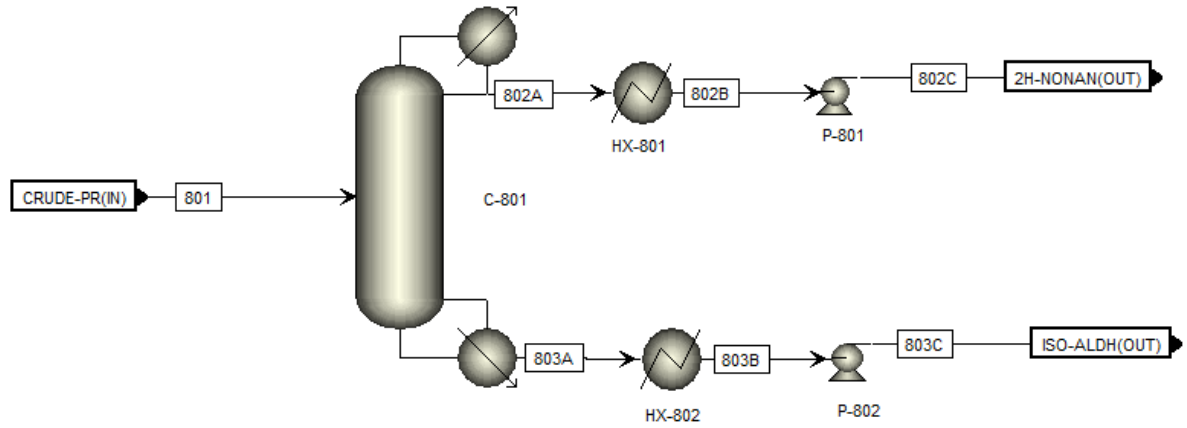

Figure C.13 Section AREA-A800 Aspen Plus™ flowsheet

Table C.10 Stream Table Section AREA-A800

Stream	Units	801	802A	802B	803A	803B
Mass flow	tonne/yr					
1-OCT-01	tonne/yr	0	0	0	0	0
7-TET-01	tonne/yr	6.020068	6.020068	0	0	0
ETHYL-01	tonne/yr	0	0	0	0	0
2-OCT-01	tonne/yr	0	0	0	0	0
6-TRIDEC	tonne/yr	0.027112	0.027112	0	0	0
PROPYLEN	tonne/yr	0	0	0	0	0
HYDRO-01	tonne/yr	0.009136	0.009136	0	0	0
CARB-01	tonne/yr	0	0	0	0	0
MARLIPAL	tonne/yr	62.9748	0	0	63	63
WATER	tonne/yr	0.10448	0.10448	261.2	0	0
2-HEXYLNO	tonne/yr	10456	10309.62	10309.62	146.384	146.384
ISO-ALDEH	tonne/yr	3624.24	50.73936	50.73936	3573.5	3573.5
HGR-2-CATA	tonne/yr	0	0	0	0	0
RHO-CAT	tonne/yr	1.2E-05	1.2E-05	0	0	0
Total flow	tonne/yr	14149.38	10366.52	10621.56	3782.884	3782.884
Stream	Units	801	802A	802B	803A	803B
Temperature	oC	171	171	30	175	30
Pressure	bar	0.01	0.01	0.01	0.01	0.01
Vapour fraction		0	0	0	0	0

Scenario B hydroformylation section

C.1.1.20 Aspen Plus™ Section AREA-B600

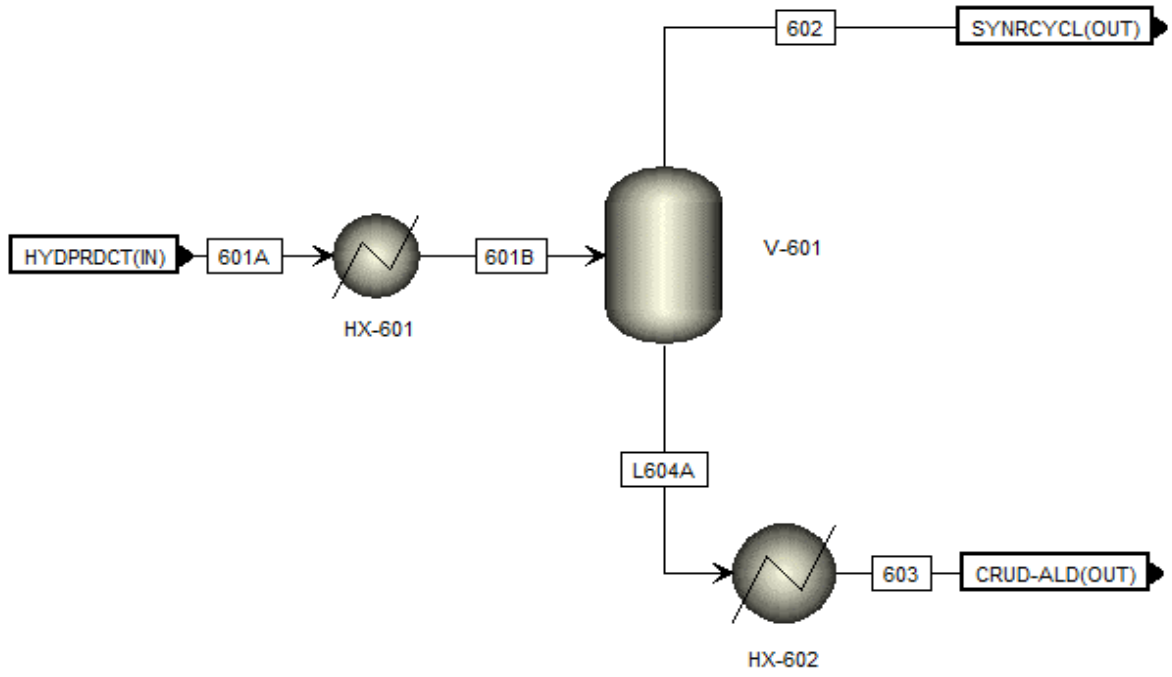

Figure C.14 Section AREA-AB60 Aspen Plus™ flowsheet

Table C.11 Stream Table Section AREA-B600

Stream	Units	601A	601B	602	603
Stream	Units	601A	601B	602	603
Mass flow	tonne/yr				
1-OCT-01	tonne/yr	0	0	0	0
7-TET-01	tonne/yr	15063.18	15063.18	12.99926	15050.18
ETHYL-01	tonne/yr	0	0	0	0
2-OCT-01	tonne/yr	0	0	0	0
6-TRIDEC	tonne/yr	67.883	67.883	0.098	67.785
PROPYLEN	tonne/yr	0	0	0	0
HYDRO-01	tonne/yr	2823.47	2823.47	2682.297	141.1735
CARB-01	tonne/yr	2147.37	2147.37	2087.9	59.47
MARLIPAL	tonne/yr	495.6329	495.6329	148.6899	346.9431
WATER	tonne/yr	27454	27454	2022.38	25431.62
2-HEXYLNO	tonne/yr	21533.04	21533.04	0.77	21449
ISO-ALDEH	tonne/yr	3669.727	3669.727	0.32	3669.407
HGR-2-CATA	tonne/yr	0	0	0	0
RHO-CAT	tonne/yr	21.94361	21.94361	0	21.94361
Total flow	tonne/yr	73192.45	73192.45	6955.454	66237.53
Temperature	°C	160	71	71	71
Pressure	bar	40	40	15	15
Vapour fraction		0	0	1	0

C.1.1.21 Aspen Plus™ Section AREA-B700

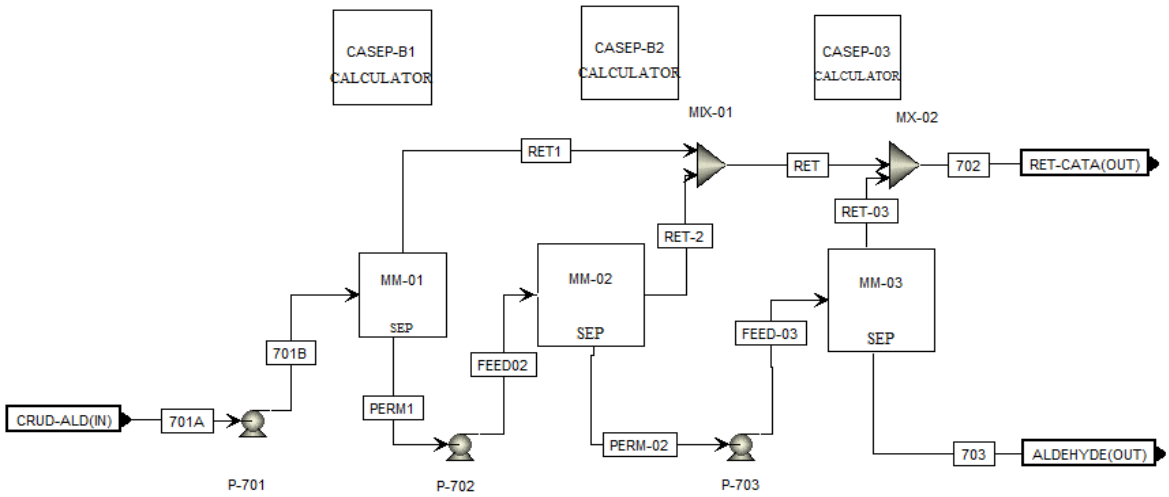

Figure C.15 Section AREA-B700 Aspen Plus™ flowsheet

Table C.12 Stream Table Section AREA-B700

Stream	Units	701A	701B	702	703
Mass flow	tonne/yr				
1-OCT-01	tonne/yr	0	0	0	0
7-TET-01	tonne/yr	15050.18	15050.18	15044.16	6.020072
ETHYL-01	tonne/yr	0	0	0	0
2-OCT-01	tonne/yr	0	0	0	0
6-TRIDEC	tonne/yr	67.785	67.785	67.75789	0.027114
PROPYLEN	tonne/yr	0	0	0	0
HYDRO-01	tonne/yr	141.1735	141.1735	141.117	0.056469
CARB-01	tonne/yr	59.47	59.47	59.44621	0.023788
MARLIPAL	tonne/yr	346.9431	346.9431	0.138777	346.8043
WATER	tonne/yr	25431.62	25431.62	25421.45	10.17265
2-HEXYLNO	tonne/yr	21449	21449	10993	10456
ISO-ALDEH	tonne/yr	3669.407	3669.407	1.467763	3667.939
HGR-2-CATA	tonne/yr	0	0	0	0
RHO-CAT	tonne/yr	21.94361	21.94361	21.93483	0.008777
Total flow	tonne/yr	66237.53	66237.53	51750.47	14487.05
Temperature	°C	30	30	30	30
Pressure	bar	15	40	40	1
Vapour fraction		0	0	0	00

C.1.1.22 Aspen Plus™ Section AREA-B800

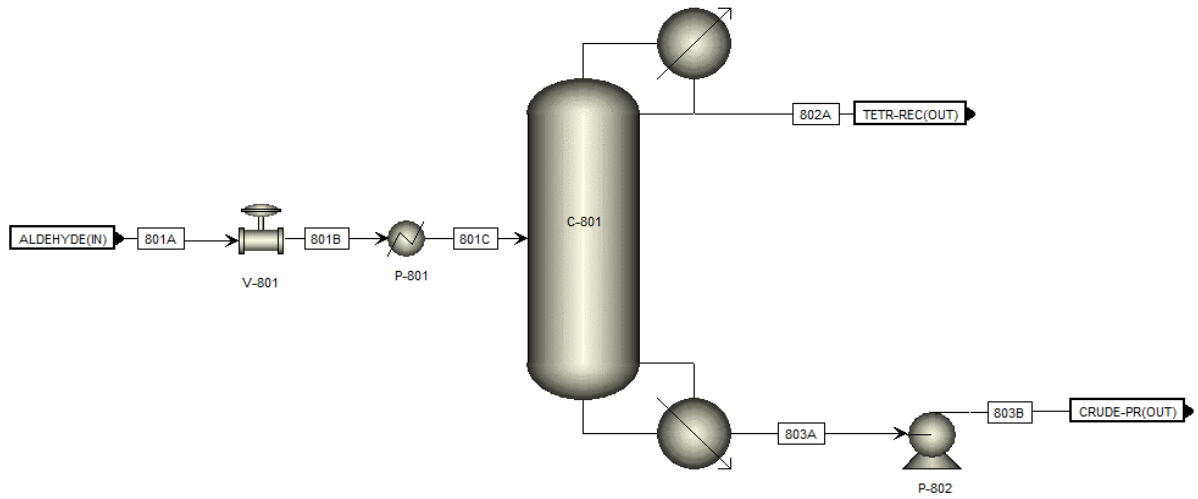

Figure C.16 Section AREA-B800 Aspen Plus™ flowsheet

Table C.13 Stream Table Section AREA-B800

Stream	Units	801A	801B	802	803
Mass flow	tonne/yr				
1-OCT-01	tonne/yr	0	0	0	0
7-TET-01	tonne/yr	15050.18	15050.18	15044.16	6.020072
ETHYL-01	tonne/yr	0	0	0	0
2-OCT-01	tonne/yr	0	0	0	0
6-TRIDEC	tonne/yr	67.785	67.785	67.75789	0.027114
PROPYLEN	tonne/yr	0	0	0	0
HYDRO-01	tonne/yr	141.1735	141.1735	141.117	0.056469
CARB-01	tonne/yr	59.47	59.47	59.44621	0.023788
MARLIPAL	tonne/yr	346.9431	346.9431	0.138777	346.8043
WATER	tonne/yr	25431.62	25431.62	25421.45	10.17265
2-HEXYLNO	tonne/yr	10905	10905	449	10456
ISO-ALDEH	tonne/yr	3669.407	3669.407	1.467763	3667.939
HGR-2-CATA	tonne/yr	0	0	0	0
RHO-CAT	tonne/yr	21.94361	21.94361	21.93483	0.008777
Total flow	tonne/yr	55693.53	55693.53	41206.47	14487.05
Temperature	°C	30	121	150	171
Pressure	bar	1	1	0.01	0.015
Vapour fraction		0	0	0	0

C.1.1.23 Aspen Plus™ Section AREA-B900

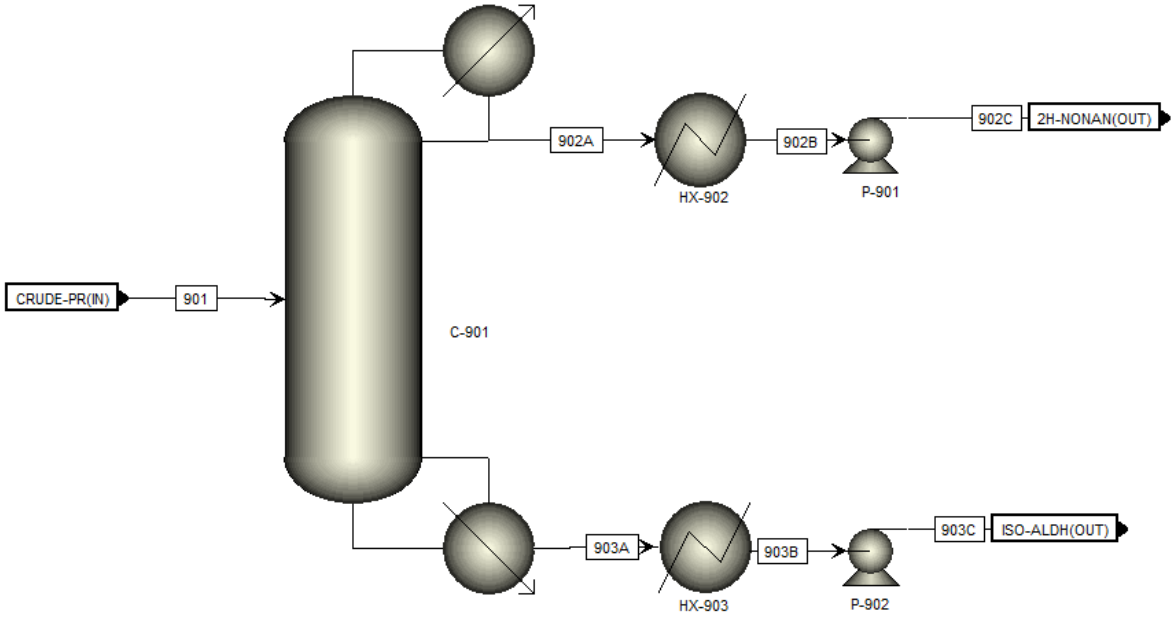

Figure C.17 Section AREA-B900 Aspen Plus™ flowsheet

Table C.14 Stream Table Section AREA-B900

Stream	Units	901	902A	902B	903A	903B
Mass flow	tonne/yr					
1-OCT-01	tonne/yr	0	0	0	0	0
7-TET-01	tonne/yr	6.020072	6.020072	0	0	0
ETHYL-01	tonne/yr	0	0	0	0	0
2-OCT-01	tonne/yr	0	0	0	0	0
6-TRIDEC	tonne/yr	0.027114	0.027114	0	0	0
PROPYLEN	tonne/yr	0	0	0	0	0
HYDRO-01	tonne/yr	0.056469	0.056469	0	0	0
CARB-01	tonne/yr	0.023788	0.023788	0	0	0
MARLIPAL	tonne/yr	346.8043	0	0	63	63
WATER	tonne/yr	10.17265	10.17265	261.2	0	0
2-HEXYLNO	tonne/yr	10456	10309.62	10309.62	146.384	146.384
ISO-ALDEH	tonne/yr	3667.939	51.35115	51.35115	3616.588	3616.588
HGR-2-CATA	tonne/yr	0	0	0	0	0
RHO-CAT	tonne/yr	0.008777	0.008777	0	0	0
Total flow	tonne/yr	14487.05	10377.28	10622.17	3825.972	3825.972
Temperature	oC	171	171	30	175	30
Pressure	bar	0.01	0.01	0.01	0.01	0.01
Vapour fraction		0	0	0	0	0

C.1.1.24 Aspen Plus™ Custom HGr-2 separation model FORTRAN codes

```
NUMTUBES=5000
    DIAM=0.0635
    LENG=1.06157
    AREA=3.14*DIAM*LENG*NUMTUBES
    REJCOE=0.99
    CF=MFRACCAT
    CP=CF*(1-REJCOE)
    C1C8=TOTCONC*MOLFRC8
    C14=TOTCONC*MOLFRC14
    CHN=TOTCONC*MOLFRCHN
    CPD=TOTCONC*MOLFRCPD
    CWA=TOTCONC*MOLFRCWA
    CMA=TOTCONC*MOLFRCMA
    MOLARVOL=VOL*3600/NTOTAL
    VC8=MOLARVOL*MOLFRC8
    VC14=MOLARVOL*MOLFRC14
    VHN=MOLARVOL*MOLFRCHN
    VPD=MOLARVOL*MOLFRCPD
    VWA=MOLARVOL*MOLFRCWA
    VMA=MOLARVOL*MOLFRCMA
    PEMC8=0.6851*10^-15
    PEMC14=0.1311*10^-15
    PEMHN=0.31469*10^-16
    PEMPD=0.31469*10^-16
    PEMWA=0.6434*10^-16
    PEMMA=0.1254*10^-15
    PEMAVG1=C1C8*VC8*PEMC8+C14*VC14*PEMC14
    PEMAVG2=CHN*VHN*PEMHN+CPD*VPD*PEMPD
    PEMAVG3=CWA*VWA*PEMWA+CMA*VMWA*PEMMA
    PEMAVG=PEMAVG1+PEMAVG2+PEMAVG3
    JTOTAL=TMP*PEMAVG*DENSFEED*100000*3600/VISC
    J1C8=JTOTAL*MFRAC1C8
    FP1C8=J1C8*AREA
    J2C8=JTOTAL*MFRAC2C8
    FP2C8=J2C8*AREA
    JC14=JTOTAL*MFRACC14
    FPC14=JC14*AREA
    JC13=JTOTAL*MFRACC13
    FPC13=JC13*AREA
    JHN=JTOTAL*MFRAC2HN
    FPHN=JHN*AREA
    NHNPERM=FPHN/MWHN
    JPD=JTOTAL*MFRACPD
    FPPD=JPD*AREA
    NPDPERM=FPPD/MWPD
    JWA=JTOTAL*MFRACWA
    FPWA=JWA*AREA
    NWAPERM=FPWA/MWWA
    JMA=JTOTAL*MFRACMA
    FPMA=JMA*AREA
    NMAPERM=FPMA/MWMA
    JCO=JTOTAL*MFRACCO
    FPCO=JCO*AREA
    NCOPERM=FPCO/MWCO
    JH2=JTOTAL*MFRACH2
    FPH2=JH2*AREA
    NH2PERM=FPH2/MWH2
    JHGR=JTOTAL*MFRACHG
    FPHG=JHGR*AREA
    NHGRPERM=FPHG/MWHG
    N1C8PERM=FP1C8/MW1C8
    N2C8PERM=FP2C8/MW2C8
    NC13PERM=FPC13/MWC13
    NC14PERM=FPC14/MWC14
    JCAT=JTOTAL*CP
    FPCAT=JCAT*AREA
    NCATPERM=FPCAT/MWCAT
    NCATRET=NCATFEED-NCATPERM
    N1C8RET=N1C8FEED-N1C8PERM
    N2C8RET=N2C8FEED-N2C8PERM
    NC13RET=NC13FEED-NC13PERM
    NC14RET=NC14FEED-NC14PERM
    NHNRET=NHNFEED-NHNPERM
    NPDRET=NPDFEED-NPDPERM
    NWARET=NWAFEED-NWAPERM
    NMARET=NMAFEED-NMAPERM
    NCORET=NCOFEED-NCOPERM
    NH2RET=NH2FEED-NH2PERM
    NHGRET=NHGFEED-NHGPERM
```

C1.1.25 Aspen Plus™ Custom Rh-TPPTS membrane custom model FORTRAN codes

```
NUMTUBES=6400
DIAM=0.0635
LENG=1.06157
AREA=3.14*DIAM*LENG*NUMTUBES
REJCOE=0.90
CF=MFRACCAT
CP=CF*(1-REJCOE)
C1C8=TOTCONC*MOLFRC8
C14=TOTCONC*MOLFRC14
MOLARVOL=VOL*3600/NTOTAL
VC8=MOLARVOL*MOLFRC8
VC14=MOLARVOL*MOLFRC14
PEMC8=0.6851*10^-15
PEMC14=0.1311*10^-15
PEMAVG=C1C8*VC8*PEMC8+C14*VC14*PEMC14
JTOTAL=TMP*PEMAVG*DENSFEED*100000*3600/VISC
J1C8=JTOTAL*MFRAC1C8
FP1C8=J1C8*AREA
J2C8=JTOTAL*MFRAC2C8
FP2C8=J2C8*AREA
JC14=JTOTAL*MFRACC14
FPC14=JC14*AREA
JC13=JTOTAL*MFRACC13
FPC13=JC13*AREA
JC2=JTOTAL*MFRACC2
FPC2=JC2*AREA
NC2PERM=FPC2/MWC2
JC3=JTOTAL*MFRACC3
FPC3=JC3*AREA
NC3PERM=FPC3/MWC3
N1C8PERM=FP1C8/MW1C8
N2C8PERM=FP2C8/MW2C8
NC13PERM=FPC13/MWC13
NC14PERM=FPC14/MWC14
JCAT=JTOTAL*CP
FPCAT=JCAT*AREA
NCATPERM=FPCAT/MWHG2
NCATRET=NCATFEED-NCATPERM
NC2RET=NC2FEED-NC2PERM
N1C8RET=N1C8FEED-N1C8PERM
N2C8RET=N2C8FEED-N2C8PERM
NC13RET=NC13FEED-NC13PERM
NC3RET=NC3FEED-NC3PERM
NC14RET=NC14FEED-NC14PERM
```

Appendix D: Chapter 6: Economic evauation

D.1.1 Energy requirements

Energy requirements have an influence on the profitability of the process; hence, it is a requirement to compare the two process scenarios in terms of energy utilization. In this section, the overall energy requirements for the two process scenarios are evaluated. A comparison of the theoretical to the simulation energy requirements was also carried out in order to check the accuracy of results of the simulations.

D.1.1.1 Process scenario A simulation

Thermodynamic balances were carried out to determine the energy requirements of each processing step. The overall balances were obtained by carrying out heat balances for each of the reaction steps in the process. Tables D.1-D.4 are a record of the heat balances for the steps considered for the upgrading of low value 1-octene from Fischer-Tropsch's Synthol product stream to 2-hexyl-nonanal a Guebert-type aldehyde.

Table D.1 Heat balance for the metathesis reaction

Heat input	Heat output
• Heat required to raise temperature of reactants to reaction temperature • $\int_{30}^{50} Cp_{(C8)} dT$	• Heat released by cooling ethylene product • $-\int_{30}^{50} Cp_{(C2)} dT$
• Heat required for endothermic metathesis reaction	

Table D.2 Heat balance for the hydroformylation reaction

Heat input	Heat output
• Heat required to raise temperature of reactants to reaction temperature	• Heat released by cooling the product
$\int_{30}^{160} Cp_{(C14)}dT + \int_{30}^{160} Cp_{(H2O)}dT + \int_{30}^{160} Cp_{(Marlipal)}dT + \int_{30}^{160} Cp_{(H2)}dT + \int_{30}^{160} Cp_{(CO)}dT$	• $-\int_{30}^{171} Cp_{(C15O)}dT - \int_{30}^{171} Cp_{(Iso-C15O)}dT$
	• Heat released by exothermic reaction

By evaluating all the energy balances for each individual step from Tables D.1- D.2, the overall balance can be obtained as summarized in Table and Table . Our analysis comprises an energy analysis that quantifies the difference in energy content between all process inputs and the products of the process at standard conditions (303.15 K and 1 bar). The individual processes are studied as black boxes, i.e., the flows between the various unit operations (reactors, separation equipment, etc.) and the actual temperature and pressures of these flows are not considered. In this work, the European Union average of 72 % was assumed as overall theoretical energy recovery efficiency (Neelis et al., 2007).

Table D.3 Overall heat balance for process scenario A

Heat input		Heat output	
Step description	*Energy (kJ/mol 2-HN)*	*Step description*	*Energy (kJ/mol 2-HN)*
1-octene preheating for metathesis reaction (30-50 °C)	13.53337	Ethylene product cooling (50-30 °C)	1.69
Metathesis heat of reaction	0.30427	2-HN product cooling (160-30 °C)	80.62

Table D.4 *Overall heat balance for process scenario* continoued

Heat input		Heat output	
7-tetradecene preheating for hydroformylation reaction (120-150 °C)	21.23952	Hydroformylation heat of reaction	0.13100
Water preheating for hydroformylation reaction (30-160 °C)	0.00178	iso-Aldehy product cooling (157 °C -30 °C)	38.04112
Marlipal preheating for hydroformylation reaction (30-160 °C)	0.00468	*Total heat output*	120.47783
CO preheating for hydroformylation reaction (30-160 °C)	5.37114	*Recoverable heat % (Neelis et al., 2007)*	72
H2 preheating for hydroformylation reaction (30-160 °C)	6.37076	*Total recoverable*	*86.74*
Total heat input	46.83		
Net heat			**39.91**

Table 6.3 shows that the process theoretically has a heat excess of 39.91 kJ/mol 2-HN. The auxiliary work energy that includes pumping and separation energy, also not included in the balance is 43.45 kJ/mol 2-HN. Adding the thermal energies and auxiliary work process scenario A theoretically requires 3.24 kJ/mol 2-HN.

D.1.1.2 Process Scenario B simulation

The energy requirement for scenario B were done in a similar manner to scenario A. Table A.20 is a summary of the energy requirements calculation considered in the balance.

Table D.5 Overall heat balance for process scenario B

Heat input		**Heat output**	
Step description	*Energy (kJ/mol 2-HN)*	*Step description*	*Energy (kJ/mol 2-HN)*
1-octene preheating for metathesis reaction (30-50 °C)	14.81763	Ethylene product cooling (50-30 °C)	1.84559
Metathesis heat of reaction	0.33314	Hydroformylation product cooling (160-30 °C)	80.99557
7-tetradecene preheating for hydroformylation reaction (120-150 °C)	23.25506	Hydroformylation heat of reaction	0.13100
Water preheating for hydroformylation reaction (30-160 °C)	0.00000	Iso-product cooling (160 -30 °C)	39.62501
Marlipal preheating for hydroformylation reaction (30-160 °C)	0.00512	Total heat output	122.59717
CO preheating for hydroformylation reaction (30-160 °C)	5.88084	Recoverable heat %	72
H2 preheating for hydroformylation reaction (30-160 °C)	6.97531	Total recoverable	88.27
Total heat input	51.26710	*Max recoverable output*	
Net heat			**37.00**

Table A.20 shows that the process theoretically has a heat excess of 37.00 kJ/mol 2-HN. The auxiliary work energy that includes pumping and separation energy, also not included in the balance is 40.45 kJ/mol 2-HN. Adding the thermal energies and auxiliary work process scenario A theoretically requires 6.45 kJ/mol 2-HN.

D.1.1.3 Simulation and energy requirement

The simulation energy requirement was calculated as the sum of the duties of all individual blocks in the flowsheet and the net energy requirement for the heat exchanger network. The operating unit block duties were extracted from Aspen Plus™ and heat exchanger network heat requirements were optimized with the aid of Aspen Plus Energy Analyser™ v8.2 Table D.7. Compares energy requirement to the expected values.

Table D.6: Comparison of simulated to theoretical energy requirements

Process	Energy requirement	
	Calculated (kJ/mol 2-HN)	Simulated (kJ/mol 2-HN)
Scenario A	3.24	5.43
Scenario B	3.19	5.17

Table D.6 summarizes the expected energy requirements and the actual from simulation. From Table D.6, the process scenario B shows large deviations between the calculated values and the obtained values. In both cases, the expected heat recovery was much more than the actual recovered heat. Some of the low-grade heat, which could not be re-used elsewhere in the process, was accounted as recoverable in the theoretical calculations. The highest contributor of this low grade unrecoverable energy was the low temperature flash process for the ethylene recovery section.

Figure D.1 shows the HEN for process Scenario A

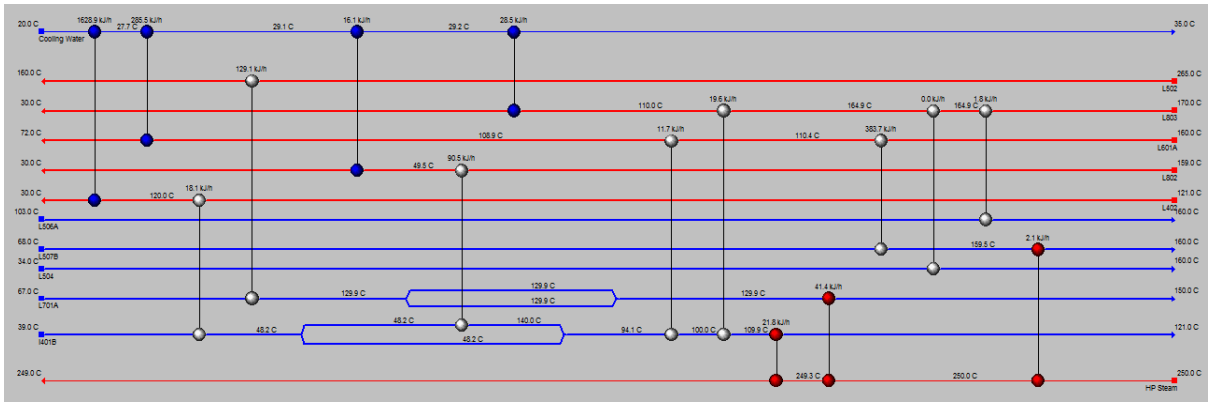

Figure D.1 HEN for process Scenario A

Figure D.2 shows the HEN for process Scenario B

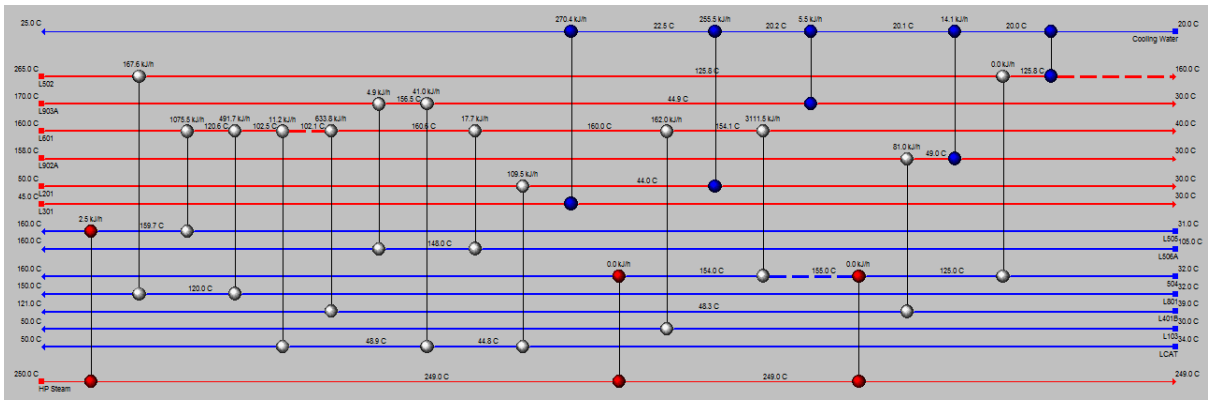

Figure D.2 HEN for process Scenario A

D.2 Economic evaluation

D.2.1 Capital expenses estimation

For some pieces of equipment such OSN membrane, scaling law equations relating the cost to size was used.

$$\text{Cost(C2016)} = \text{Cost(C0)}\left(\frac{\text{Capacity(S2016)}}{\text{Capacity(S0)}}\right)^{\text{n}} \quad \text{(D.1)}$$

Where,

Cost (C2016) is the new estimated cost in current year

Capacity (SS2016) is the new estimation variable in year 2016,

Cost (C0) is the initial equipment cost with in the base year

Capacity (S0) is the capacity in base year, and

n, is the scaling factor.

As a demonstrative calculation, the purchased cost of an OSN membrane separator of feed rate 26,40 ton/hr can be calculated using the installed cost of an OSN reported by Evonik industry of 35 ton/hr purchased in 2015 at $ 1700 000,00. Using the scaling method in Eq. 6.1 Reference capacity= 35 ton/r, New Capacity=26.4 ton/hr, Reference cost=$78400, from data tables n=0.6 (Turton et al. 2012). Using these data:

$$\text{Installed Cost(IC)} = \$1700000\left(\frac{26.4}{35.0}\right)^{0.6} = \$1435391{,}77$$

The capital costs were adjusted with the Chemical Engineering Plant Cost Index (CEPCI) to a common basis period April 2016 (Chemical Engineering, 2016) according to Eq. (6.2).

$$\text{Cost (C2016)} = \text{Cost (C0)}\left(\frac{\text{CEPCI2016}}{\text{CEPCI0}}\right) \quad \text{(D.2)}$$

Where,

Cost (C2016) is the new estimated cost in current year 2016,

Cost (C0) is the cost in base year,

CEPCI (2016) is the most recent index in Q1,

CEPCI (0) is the cost index in base year,

CEPCI (2016) is the index during that year the equipment was supplied.

As a demonstrative calculation, the installed cost of a carbon steel metathesis reactor purchased in 2012 at $ 44 523 702,46. Using the scaling method in Equation. D.2 CEPCI2012=584.60 and CEPCI2016= 568,70. Using these data;

$$\text{Cost (2016)} = \$\,44\,523\,702.46\left(\frac{568.7}{584.6}\right) = \$\,43\,312\,743{,}06$$

Table D.7 Comparison between Fixed operating Costs for the Project Scenarios A and B

		SCENARIO A	SCENARIO B
	Remark	**CASE A**	**CASE B**
Installed Cost (IC)		90811173.71	93087244.80
Purchased Cost	IC/2,262	40146407.48	41152628.12
Direct Capital Cost	% of PC		
(a) Freight	3 % of PC	1204392.22	1234578.84
(b) Yard Improvements	11 % PC	4416104.82	4526789.09
(c) Environmemntal	0 % PC	0.00	
(d) Buildings	43 % PC	1726295.52	1769563.01
Total direct Cost (DC)	(IC + above)	**18162234.74**	**18617448.96**
Indirect capital cost			
(a) Engineering	16% of DC	2905957.56	297879.18
(b) construction	26 % of DC	4722181.03	484053.67
(d) contractor fees	17% of DC	3087579.91	316496.63
(e) contingency	23 % of DC	3632446.95	372348.98
Total indirect cost (IDC)	20 % of DC	18162234.74	18617448.96
PC	31% of DC	18162234.74	18617448.96
Fixed Capital Investment, FCI	DC + IDC + AO	145297877.94	148939591.67
Working Capital, WC	20% of TCI	36324469.49	37234897.92
Total Capital Investment, TCI	FCI/0.8	**181622347.43**	**186174489.59**

D.2.1.1 Installed costs for membrane modules

Table D.2 is a summary of the membrane modules for the two process scenarios.

Table D.8 Comparison of membrane modules for scenario A and B

		Scenario A		Scenario B	
		No. Modules	Cost ($M)	No. Modules	Cost ($M)
HGr-2 OSN	Stage 1	13	2.79	13	2.79
	Stage 2	12	2.16	12	2.16
	Stage 3	12	1.80	12	1.8
Rh OSN	Stage 1	-	-	13	2.61
	Stage 2	-	-	13	2.01
	Stage 3	-	-	12	1.75
Total		**37**	**6.75**	**37**	**13.12**

D.2.3 Operating Costs

Operating Labour

The cost of operating labour is calculated according to the number of operators required per shift and that is calculated according to Eq. (5.3) (Turton et al., 2012),

$$N_{OL} = (6{,}29 + 31{,}7P^2 + 0{,}23N_{np})^{0{,}5} \quad \text{(D.4)}$$

Where, P is the number of solid handling stages and N_{np} is the total number of major process equipment, which includes compressors, towers, reactors, heaters and exchangers.

Total operating costs

A summary of the operating costs is listed in Table D.3.

Table D.9: Calculation of capital investment for project Scenarios A and B

Utility	Prize	Unit	Source
Hoveyda-Grubbs 2	267,622,64	$/kg	www.alibaba.com
Rh catalyst	120,000,00	$/kg	www.Kitco.com, (2015)
1-octene	1,60	$/kg	Sasol Olefins, (2015)
H2	0,03	$/kg	Piet *et al*. (2014)
CO	0,03	$/kg	Piet *et al*. (2014)
Water	0,20	$/kg	www.randwater.com
Marlipal	3,96	$/kg	www.zauba.com/import
Electricity	0.052	$/KW	www.eskom.co.za/ (2016)
Steam	0.3-0.76	$/kg	Hentschel et al. (2014)
Cooling water	0.05	$/kg	Hentschel et al. (2014)
Membrane price/stability factor	500	$/m^{2}yr	Schmidt et al. (2014)
Rhodium concentration	50	ppm	Schmidt et al. (2014)
HGr-2 concentration	200	ppm	Van der Gryp et al. (2012)

Table D.10 Manufacturing costs comparison between Scenarios A and B

		SCENARIO A	SCENARIO B
COST ITEM	**Typical range**	**Value Used**	**value Used**
1. Direct/ Variable Manufacturing costs			
(a) Raw Materials			
1-octene	input	29108697.39	29108697.39
H2	input	57255.86	59830.52
CO	input	1779758.00	17779587.00
Direct Operating Labour, DOL	(6,29+31,7P2+0,23Np)^2	**3234598.00**	**3844433.00**
Supervisory and clerical labour, SCL	15 % of DOL	**485189.70**	**72778.46**
(b) solvents			
Marlipal	input	441.60	441.25
H20	input	128.25	128.15
(c) Catalysts			
HGr-2	input	231847309.41	231847309.41
Rh-catalyst	input	627302594.32	623568000.00
	TOTAL RAW MATERIALS	**888320811.83**	**884584406.71**
(d) Utilities			
Electricity		3673552.48	3173552.48
Steam		902263.11	902263.11
Cooling water		139599.50	139599.50
	TOTAL UTILITIES	**4715415.09**	**4215415.09**
(e) Other			
Plant Maintenance and Repairs, PMR	7 % of FCI	1017085.15	1042577.14
Operating Supplies	15 % of PMR	15256.28	15638.66
Laboratory Charges	15 % of DOL	48518.97	57666.50
Patents and Royalties	4 % of TPC	5208862.90	5192003.95
Membranes Replacement		546575.00	1153262.00
Subtotal: Variable Production Costs, VPC		**899872525.21**	**896260970.04**
2. Fixed Charges, $ FCh			
(a) Depreciation	w/o		
(b) Taxes (property)	0,02*FCI	2905957.56	2978791.83
(c) Financing (interest)	1% of FCI	1452978.78	1489395.92
(d) Insurance	8 % of FCI	11623830.24	11915167.33
(e) Rent	5 % of FCI	7264893.90	7446979.58
(f) Contingency	10% FCI	1452978.78	1489395.92
Subtotal: Fixed Charges, FCH		**24700639.25**	**25319730.58**
3. Plant Overhead Costs, $ POC			
(a) General Plant Overhead			
Subtotal: Plant Overhead Costs, POC of TPC	10 % of TPC	**130221572.46**	**129800098.68**
Total Operating Costs	VPC+FCh+POC	**1054794736.92**	**1051380799.30**
4. General expenses, GE			
(a) Administration costs	4 % TPC	52088628.98	51920039.47
(b) Distribution and Marketing Costs	10 % TPC	130221572.46	129800098.68
(c) Research And Developmnent	5 %of TPC	65110786.23	64900049.34
Total General Expenses, TGE		247420987.67	246620187.49
Total production Costs		**1302215724.60**	**1298000986.79**

Table D.11: Cash flow projections for scenario B (Notes: FCI- Fixed Capital Investment, COM- Cost of manufacturing, DCF- Discounted cash flow)

Fixed Capital Investment	$145 297 877.94		**Operating Labour**	3917211.45500	**Revenue**	**2-HEXYL-NONANAL**	$1 500 000 000.00
Raw Materials	$884 584 406.71		**Utilities**	4215415.08900			
Periodic Expenses	$53 031 521.40						
Total Installed Cost	$186 174 490		**discount rate**	15%		**TOTAL**	$1 500 000 000.00
COM	$1 298 000 986.79		**Taxation**	28.00%			
Year	**Depreciation**	**FCI-depreciation**	**Revenue**	**COM**	**Cashflow**	**Discounted Cash Flow**	**Cummulative Discounted Cash Flow**
1.00	-	145297877.94	-	-	(111704693.76)	**(97134516.31)**	(97134516.31)
2.00	-	145297877.94	-	-	(74469795.84)	**(56309864.53)**	(153444380.84)
3.00	72648938.97	72648938.97	1500000000.00	1298000986.79	165780992.42	**109003693.54**	(44440687.29)
3.00	29059575.59	116238302.35	1500000000.00	1298000986.79	153575970.67	**100978693.63**	56538006.34
4.00	14529787.79	130768090.15	1500000000.00	1298000986.79	149507630.09	**85481472.74**	142019479.08
5.00	14529787.79	130768090.15	1500000000.00	1298000986.79	149507630.09	**74331715.43**	216351194.51
6.00	14529787.79	130768090.15	1500000000.00	1298000986.79	149507630.09	**64636274.29**	280987468.80
7.00	-	145297877.94	1500000000.00	1298000986.79	145439289.51	**54676015.99**	335663484.79
8.00	-	145297877.94	1500000000.00	1298000986.79	145439289.51	**47544361.73**	383207846.51
9.00	-	145297877.94	1500000000.00	1298000986.79	145439289.51	**41342923.24**	424550769.75
10.00	-	145297877.94	1500000000.00	1298000986.79	145439289.51	**35950368.04**	460501137.79
11.00	-	145297877.94	1500000000.00	1298000986.79	145439289.51	**31261189.60**	491762327.39
12.00	-	145297877.94	1500000000.00	1298000986.79	145439289.51	**27183643.13**	518945970.51
13.00	-	145297877.94	1500000000.00	1298000986.79	145439289.51	**23637950.55**	542583921.06
14.00	-	145297877.94	1500000000.00	1298000986.79	145439289.51	**20554739.60**	563138660.66
15.00	-	145297877.94	1500000000.00	1298000986.79	145439289.51	**17873686.61**	**583693400.27**

Table D.12: Cash flow projections for scenario A (Notes: FCI- Fixed Capital Investment, COM- Cost of manufacturing, DCF- Discounted cash flow)

Total Installed Cost	$181 622 347					**Revenue From products**	
Fixed Capital Investment	$145 297 877.94		Operating Labour	$3 719 787.70000		**2-HEXYL-NONANAL**	$1 500 000 000.00
Raw Materials	$888 320 811.83		Utilities	$4 715 415.08900			
Periodic Expenses	$11 735 983.12		Discount rate	15 %			
COM	$1 313 951 707.72		Tax rate	28 %		**TOTAL**	$1 500 000 000.00
Year	**Depreciation**	**FCI-depreciation**	**Revenue**	**COM**	**Cashflow**	**Discounted Cash Flow**	**Cummulative Discounted Cash Flow**
0.00							0.00
1.00	-	145297877.94	-	108973408.46	(108973408.46)	**(94759485.61)**	(94759485.61)
2.00	-	145297877.94	-	72648938.97	(72648938.97)	**(54933035.14)**	(149692520.75)
3.00	72648938.97	72648938.97	1500000000.00	1313951707.72	154296473.35	**101452435.84**	(48240084.91)
4.00	29059575.59	116238302.35	1500000000.00	1313951707.72	142091451.61	**81241248.63**	33001163.71
5.00	14529787.79	130768090.15	1500000000.00	1313951707.72	138023111.03	**68621879.74**	101623043.45
6.00	14529787.79	130768090.15	1500000000.00	1313951707.72	138023111.03	**59671199.77**	161294243.22
7.00	14529787.79	130768090.15	1500000000.00	1313951707.72	138023111.03	**51887999.80**	213182243.02
8.00	0.00	145297877.94	1500000000.00	1313951707.72	133954770.44	**43790052.07**	256972295.09
9.00	0.00	145297877.94	1500000000.00	1313951707.72	133954770.44	**38078306.15**	295050601.24
10.00	0.00	145297877.94	1500000000.00	1313951707.72	133954770.44	**33111570.57**	328162171.81
11.00	0.00	145297877.94	1500000000.00	1313951707.72	133954770.44	**28792670.06**	356954841.86
12.00	0.00	145297877.94	1500000000.00	1313951707.72	133954770.44	**25037104.40**	381991946.26
13.00	0.00	145297877.94	1500000000.00	1313951707.72	133954770.44	**21771395.13**	403763341.39
14.00	0.00	145297877.94	1500000000.00	1313951707.72	133954770.44	**18931647.94**	422694989.33
15.00	0.00	145297877.94	1500000000.00	1313951707.72	133954770.44	**16462302.55**	**439157291.88**

Appendix A: Indices

Marshal and Smith Index

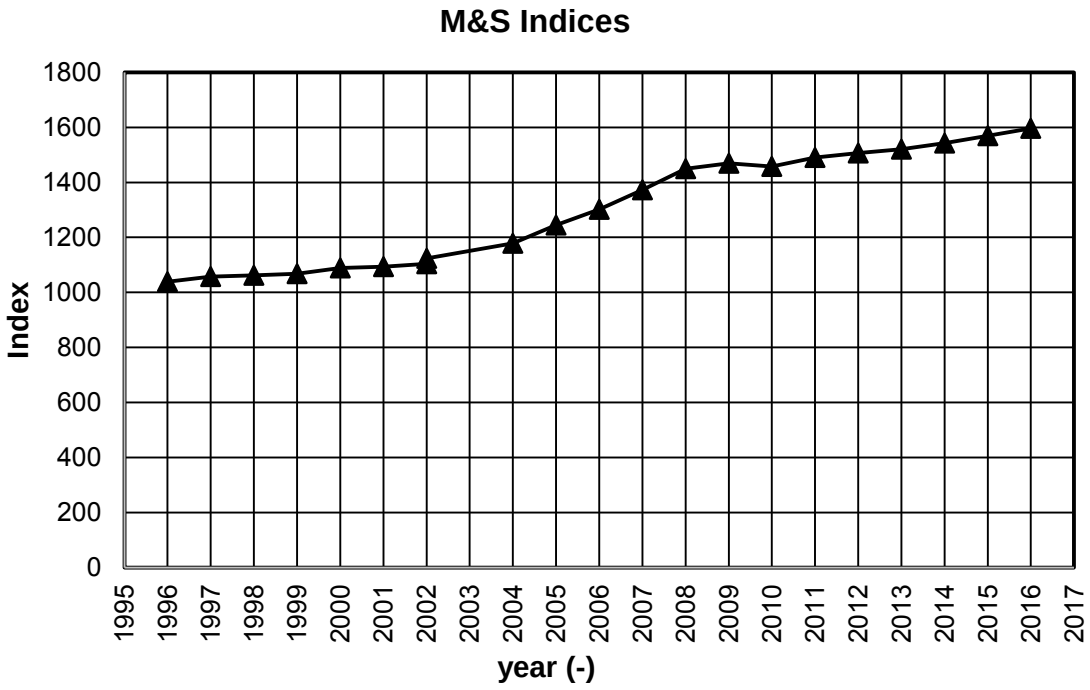

Figure E.2 M& S indices estimation

Chemical Engineering Plant Cost Index

Marshall & Swift/Boeckh, LLC, (2013) http://www.equipment-cost-index.com/eci/Downloads (extrapolated for years 2013-2016 using projected increases)

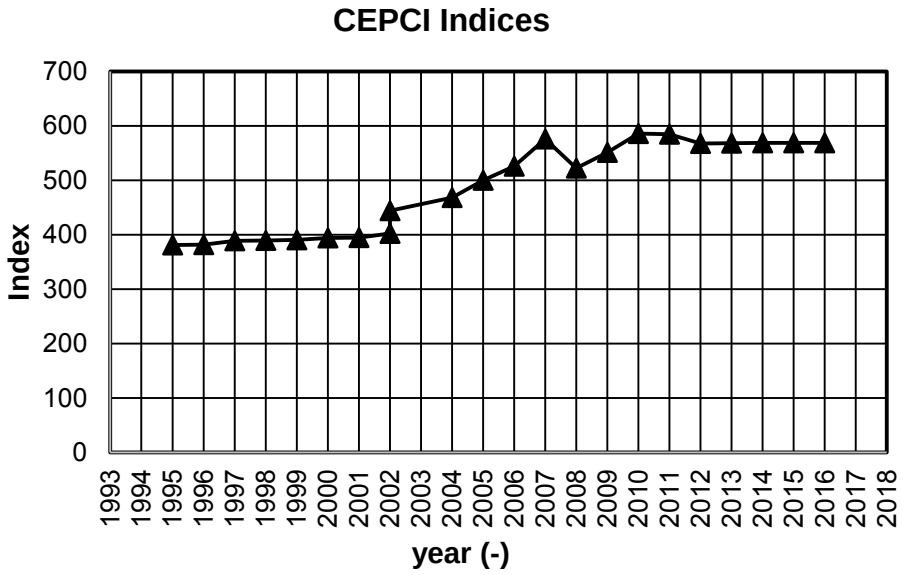

Chemical Engineering Cost Index January 2015
http://www.isr.umd.edu/~adomaiti/chbe446/literature/ChECostIndexJan2015.pdf